PHYSICAL, GEOCHEMICAL AND MICROBIAL PARAMETERS DRIVING THE IMPROVEMENT OF WATER QUALITY IN MANAGED AQUIFER RECHARGE

Ph.D. Thesis

Carme Barba Ferrer

Advisors: Dr. Albert Folch Sancho

Dr. Xavier Sanchez-Vila

UNIVERSITAT POLITÈCNICA DE CATALUNYA

Department of Civil and Environmental Engineering

Hydrogeology Group (UPC-CSIC)

Physical, geochemical and microbial parameters driving the improvement of water quality in Managed Aquifer Recharge

by

Carme Barba Ferrer

Advised by Dr. Albert Folch Sancho and Dr. Xavier Sanchez-Vila

External Reviewers:

1. *Dr. Daniele Pedretti (Geological Survey of Finland)*
2. *Dr. Fulvio Boano (Politecnico di Torino)*

September 2018

This thesis has been financially supported by Generalitat de Catalunya via FI scholarship program (FI-DGR 2014), the European Union project MARSOL grant agreement no. 619120, FP7-ENV-2013-WATER-INNO-DEMO, the Spanish Government and EU (project ACWAPUR PCIN-2015-239), and the Spanish Government project REMEDIATION (CGL2014-57215-C4-2-R).

Carme Barba Ferrer
Physical, geochemical and microbial parameters driving the improvement of water quality in Managed Aquifer Recharge
Ph.D. Thesis, September 2018
Reviewers: Dr. Daniele Pedretti and Dr. Fulvio Boano
Advisors: Dr. Albert Folch Sancho and Dr. Xavier Sanchez-Vila

Universitat Politècnica de Catalunya
Hydrogeology Group (UPC-CSIC)
Department of Civil and Environmental Engineering
C/Jordi Girona 1-3, Edifici D2, despatx 005
08034 Barcelona

Summary

Water demand around the world has been continuously increasing over time, mainly due to population growth and development. In addition, climate change is causing a significant alteration of the periodicity and intensity of precipitation and climate-related events. All this implies significant challenges in water management, especially in arid and semi-arid regions (the Mediterranean amongst others), where the integral management of water (including both surface water and groundwater) is crucial to ensure water supply. The management of quality and quantity aspects are essential, not only for the prevention of threats to those resources but also to ensure a sustainable exploitation. In this context of management, the work undertaken in this thesis is framed in the management of groundwater resources due to the possibility of exploitation of those during surface water scarcity periods.

Therefore, Managed Aquifer Recharge (MAR) represents a feasible solution to deal with future water management challenges promoting the storage of available water in aquifers improving the recharged water quality.

The present dissertation is focused on the study of microbial, biogeochemical and physical processes related to MAR ponds, regarding both quantity and quality aspects. The knowledge about these processes has allowed identifying key issues affecting the correct operation of infiltration ponds, laying the foundations for the optimization of quantity and quality targets.

Two different sites in the Llobregat River Basin were chosen as a frame for the investigations.

The first part of this thesis was developed in Sant Vicenç MAR system (Barcelona), where an innovative treatment for emerging contaminants had been proved successfully. A reactive layer was put in the bottom of the infiltration pond, promoting different redox conditions below the pond and enhancing the removal of dissolved organic matter as well as emergent organic contaminants. In this thesis, further work has been carried out, by investigating the role of the microbial community in this removal, by means of a microbial fingerprinting study between two different scenarios. Which were (1) when no-recharge was present and (2) during a long recharge period. The microbial fingerprinting study confirmed that microbial diversity during recharge period fitted in Intermediate Disturbance Hypothesis approach. Furthermore, sequencing of prominent bands evidenced the presence of

principally degradative-like microorganisms during recharge. A multivariate statistical analysis including hydrochemical, soil grain-size distribution, operational and microbial variables was also performed. Most relevant variables affecting microbial populations were identified. Likewise, the correlations between some microbial prints in the system revealed the presence of some classes and species involved in denitrification as well as methanotrophic pathways.

The second investigation was focused on the study of redox processes from the infiltration pond to the aquifer, passing through the vadose zone. The study was placed in Castellbisbal MAR system (Barcelona). This facility has a conventional surface infiltration pond without the effect of the reactive layer. The infiltration path was widely monitored and four sampling campaigns were carried out in four different moments along a one-year study. Results from *in situ* redox potential measurements, temperature evolution, operating conditions (water levels, flow rate, and infiltration rate), characterization of the organic matter and hydrochemical composition of water were collected and analyzed. Especially, operating conditions and redox potential, where it was observed that evolution in the first meter of the infiltration profile had been related to clogging development in the pond bottom.

Finally, results from monitoring tasks were used as the basis to construct a flow and heat transport model simulating the recharge process. The flow model included the decrease of hydraulic conductivity caused by clogging periods. In addition, a heat transport model was capable to calculate the modifications of hydraulic conductivity due to temporal temperature evolution. Taking into account the results of heat transport model, two batch-type biogeochemical models were suggested to explain redox processes in winter and summer scenarios. Furthermore, models were capable to explain the fate of different fractions of dissolved organic matter, i.e. labile, recalcitrant and immobile, and the corresponding change of degradation rates due to temperature changes amongst different scenarios.

Resum

La demanda d'aigua arreu del món es preveu que continuarà augmentant a causa de l'increment de la població i el seu desenvolupament. El canvi climàtic, a més, suposarà un agreujant d'aquesta problemàtica, ja que es preveu que alterarà la periodicitat i intensitat de les precipitacions arreu. La gestió de l'aigua s'enfronta, doncs, a grans reptes, especialment a les regions àrides i semiàrides (la mediterrània d'entre altres), on caldrà gestionar de manera integrada aigües superficials i subterrànies. La bona qualitat de les masses d'aigua, tant a nivell quantitatiu com qualitatiu, serà clau per afrontar els reptes de futur i per garantir que es faci un aprofitament sostenible d'aquest recurs. En aquest context de gestió, el paper de l'aigua subterrània és, doncs, clau, ja que permet ser explotada fins i tot en moments d'escassetat hídrica.

Partint d'aquest marc, la recàrrega artificial d'aqüífers representa una solució vàlida per afrontar els reptes de futur que presenta la gestió de l'aigua. La recàrrega induïda promou l'emmagatzematge d'aigua en el subsol millorant-ne la qualitat.

La present tesi doctoral té com a objectiu l'estudi de processos microbiològics, biogeoquímics i físics relacionats amb les basses de recàrrega. Tot aquest coneixement ha permès detectar molts dels aspectes que afecten el correcte funcionament d'aquestes infraestructures, construint les bases per a poder optimitzar-ne el funcionament.

Per poder abordar els objectius plantejats, s'han dut a terme diferents investigacions a dos emplaçaments de la conca del riu Llobregat destinats a recarregar el seu aqüífer.

El primer estudi de la present tesi ha estat desenvolupat al sistema de recàrrega de Sant Vicenç (Barcelona). Aquest sistema contenia un tractament innovador basat en una barrera reactiva permeable instal·lada al llit de la bassa. La barrera, amb un alt contingut de matèria orgànica, promovia diferents condicions redox sota la bassa i millorava la degradació de matèria orgànica dissolta així com també de contaminants orgànics emergents.

En aquesta tesi s'ha volgut anar un pas més enllà, i s'ha investigat el paper de les comunitats microbianes mitjançant un estudi de patrons microbiològics comparant dos escenaris diferents. S'ha avaluat la contribució de les comunitats microbianes

sota els efectes prolongats de la recàrrega i amb la bassa parada. Aquest estudi confirma que els efectes de la recàrrega sobre la diversitat microbiana es podrien assimilar als predits per la Hipòtesi de la Pertorbació Intermèdia. Així mateix, la seqüenciació de les bandes més prominents ha revelat que les espècies principals de microorganismes que es trobaven sota els efectes de la recàrrega tenien capacitats degradatives.

A continuació s'ha efectuat un estudi estadístic multivariant, englobant variables de tipus hidroquímic, de mida i distribució de gra en sòls, de tipus operacional i microbiològiques. S'han identificat doncs, les variables més rellevants que afecten les poblacions microbianes. A més, s'han detectat correlacions entre algunes variables hidroquímiques i espècies com ara desnitrificants o metanòtrofes.

La segona part de la tesi ha estat emmarcada en el sistema de recàrrega de Castellbisbal (Barcelona). Aquest sistema inclou també una bassa d'infiltració, però sense l'efecte d'una capa reactiva. A Castellbisbal s'han estudiat els processos redox en tot el perfil d'infiltració, des de l'aigua d'infiltració fins a la zona saturada de sota la bassa, passant per la zona no saturada. Tot aquest perfil es va monitoritzar i es van dur a terme quatre campanyes de mostreig durant l'any sencer que ha durat l'estudi. La monitorització ha permès obtenir resultats d'evolució de potencial redox a diferents profunditats, de la temperatura i de tots els paràmetres d'operació (nivells, cabals i taxa d'infiltració). Les campanyes de mostreig han permès caracteritzar hidroquímicament les mostres així com també caracteritzar l'origen de la matèria orgànica present. La integració de tots aquests resultats, especialment pel que fa a la monitorització del potencial redox en el primer metre de sòl ha permès evidenciar la relació que tenen tots ells amb la colmatació al llit de la bassa.

Finalment, la monitorització efectuada a la bassa ha servit per establir les bases per a construir un model de flux i transport de calor simulant l'acció de la recàrrega. El model inclou l'efecte de la colmatació sobre el descens de la conductivitat hidràulica. De la mateixa manera, el model de transport de calor pot calcular les modificacions en la conductivitat hidràulica que venen donades per les variacions temporals de la temperatura. El model evidencia la importància de la temperatura en els paràmetres hidràulics. Partint d'aquesta base, s'han desenvolupat dos models biogeoquímics de tipus *batch* amb l'objectiu d'explicar els processos redox en dos escenaris estiu-hivern. Els models, a més, inclouen diferents fraccions de matèria orgànica dissolta: de caràcter làbil, recalcitrant i una tercera, d'immòbil. S'avaluen, doncs, els canvis

en les taxes de degradació de la matèria orgànica a causa de les variacions de temperatura entre escenaris.

Resumen

A nivel mundial se prevé que la demanda de agua siga creciendo a causa del aumento de población y su desarrollo. El cambio climático, además, va a suponer un agravante a esta problemática, ya que se prevé que alterará la periodicidad e intensidad de las precipitaciones. La gestión del agua se enfrenta pues a grandes retos, especialmente en las regiones áridas y semiáridas (como por ejemplo la mediterránea), donde será necesaria una gestión integral de las aguas superficiales y subterráneas. La buena calidad de las masas de agua, tanto a lo que a cantidad y calidad se refiere, será clave para afrontar los retos de futuro y para garantizar un aprovechamiento sostenible de este recurso. En este contexto de gestión, el papel del agua subterránea es clave, ya que permite ser explotada incluso en periodos de escasez hídrica.

Partiendo de este contexto, la recarga artificial de acuíferos representa una solución válida para afrontar los retos de futuro que presenta la gestión del agua. La recarga artificial de acuíferos promueve el almacenamiento de agua en el subsuelo y mejora su calidad.

La presente tesis doctoral tiene como principal objetivo estudiar los procesos microbiológicos, biogeoquímicos y físicos relacionados con las balsas de recarga. Todo este conocimiento ha permitido detectar muchos aspectos que afectan el correcto funcionamiento de estas infraestructuras, sentado la base para poder optimizar su funcionamiento.

Para abordar los objetivos planteados, se han llevado a cabo diferentes investigaciones en dos emplazamientos de la cuenca del río Llobregat destinados a recargar su acuífero.

El primer estudio de la presente tesis ha sido desarrollado en el sistema de recarga de Sant Vicenç (Barcleona). Este sistema contenía un tratamiento innovador basado en una barrera reactiva permeable instalada en el lecho de la balsa. La barrera, con un alto contenido en materia orgánica, promovía diferentes condiciones redox debajo de la balsa y mejoraba la degradación de materia orgánica disuelta, así como también de contaminantes orgánicos emergentes.

En esta tesis se ha querido ir un paso más allá, y se ha investigado el papel de las comunidades microbianas mediante un estudio de patrones microbianos comparando diferentes escenarios. Se ha evaluado la contribución de las comunidades

microbianas bajo los efectos prolongados de la recarga y con la balsa parada. Este estudio confirma que los efectos de la recarga sobre la diversidad microbiana se podrían asimilar a los predichos por la Hipótesis de la Perturbación Intermedia. Asimismo, la secuenciación de las bandas más prominentes ha revelado que las especies principales de microorganismos que se encontraban bajo los efectos de la recarga tenían capacidades de degradación.

A continuación, se ha efectuado un estudio estadístico multivariante, englobando variables de tipo hidroquímico, de tamaño y distribución de grano en suelos, de tipo operacional y microbiológicas. Se han identificado, pues, las variables más relevantes que afectan a las poblaciones microbianas. Además, se han detectado correlaciones entre algunas variables hidroquímicas y especies desnitrificantes y metanótrofas (de entre otras).

La segunda parte de la tesis ha sido enmarcada en el sistema de recarga de Castellbisbal (Barcelona). Este sistema incluye también una balsa de infiltración, pero sin el efecto de una barrera reactiva. En Castellbisbal se han estudiado procesos redox en el perfil de infiltración, desde el agua de infiltración hasta la zona saturada, pasando por la zona no saturada. Todo este perfil se monitorizó y se llevaron a cabo cuatro campañas de muestreo durante un año. La monitorización ha permitido obtener resultados sobre la evolución del potencial redox en diferentes profundidades, de la temperatura y de todos los parámetros de operación (niveles, caudales y tasa de infiltración). Las campañas de muestreo han permitido caracterizar hidroquímicamente las muestras, así como también caracterizar el origen de la materia orgánica presente. La integración de todos estos resultados, especialmente los relacionados con la monitorización del potencial redox en el primer metro de suelo, ha permitido evidenciar la relación que tienen todos ellos con la colmatación en el lecho de la balsa.

Finalmente, la monitorización efectuada en la balsa ha servido para establecer las bases de construcción de un modelo de flujo y transporte de calor simulando la acción de la recarga. El modelo incluye el efecto de la colmatación sobre el descenso de la conductividad hidráulica. Asimismo, el modelo de transporte de calor puede calcular las modificaciones en la conductividad hidráulica que vienen dadas por las variaciones temporales de la temperatura. El modelo pone de relieve la importancia de la temperatura en los parámetros hidráulicos. Partiendo de esta base, se han desarrollado dos modeles biogeoquímicos de tipo *batch*, con el objetivo de explicar los

procesos redox en dos escenarios verano-invierno. Los modelos, además, incluyen diferentes fracciones de materia orgánica disuelta: de carácter lábil, recalcitrante y una tercera, inmóvil. Se evalúan, pues, cambios en las tasas de degradación de la materia orgánica a causa de variaciones de temperatura entre escenarios.

Acknowledgements

Malgrat sembli un tòpic, puc estar ben segura que aquesta tesi és del tot inconcebible sense el suport i participació d'una llarga llista de persones.

En primer lloc, he d'agrair al Xavier Sanchez i a l'Albert Folch l'oportunitat que m'han donat de fer la tesi al Grup d'Hidrologia Subterrània. Penso que la seva complementarietat com a directors ha estat clau en el resultat final d'aquest treball. Xavi, gràcies per donar-me l'oportunitat d'entrar a la gran família del GHS, on m'hi he sentit com si fos casa meva. Absolutament sempre m'has donat carta blanca a totes les iniciatives que he proposat. Per altra banda, és una evidència que la redacció de la tesi no tindria la mateixa qualitat sense la teva ajuda. Albert, gràcies per obrir-me les portes del món de la hidrogeologia i per la oportunitat que em vas donar de començar la tesi, per la infinita paciència que has tingut amb mi i el meu caràcter, per haver respectat sempre la meva estranya logística i els meus ritmes de treball, pel teu optimisme contagiós i per tota l'ajuda i suport que m'has donat durant tots aquests anys.

De tot cor, moltes gràcies a tots dos!

En segon lloc vull agrair molt especialment a la Núria Gaju, la Maira Martínez, el Rafa Marcé i la Paula Rodríguez la seva gran contribució en aquest treball. Tractant-se d'una tesi multidisciplinària, hagués estat impossible d'acabar amb èxit sense la seva expertesa i coneixements.

També agrair a tots els professors del Grup d'Hidrologia Subterrània que al llarg d'aquests anys m'han deixat "colar" a les seves classes. Al Maarten, el Jesús, l'Enric, la Nieves, el Carlos A i l'Ester T. Molt especialment he d'agrair al Dani la seva predisposició, ajuda i, després de tant de temps, també amistat.

I ja se sap que *lo meu* són les famílies grans, de manera que moltes gràcies a la família GHS, als de l'IDAEA i molt especialment als meus amics i companys d'aquí dalt l'UPC. Primer de tot a la Tere, per ajudar-me sempre amb els tiquets, factures, maldecaps amb la furgo, i tota la paperassa: Tere, tens solucions per a tot! També vull tenir un record especial per tots els que ja no hi són i en algun moment han estat al meu costat -el Joel, el Genís, la

Sona, l'Albert, la Carlota i la Perujo- ja sigui discutint resultats, fent *voltes a la poma*, fent intercanvis lingüístics o parlant dels fills i les aventures de ser pares. I també gràcies als que compartim el dia a dia, -l'Arnau, el Carni, el David, el Guillem, la Gumbi, el Jordi, la Jou, la Laura, la Lurdes, la Miki, la Mireia, l'Uri i el Yufei- i tots els integrants dels Esmorzars UPC, que sense vosaltres els àpats no serien ni de bon tros tan apassionants (ni llargs!). Vull agrair especialment tot el suport dels integrants del "Grup de Paddle", no pas per la nostra regularitat en el joc, sinó per tota l'ajuda durant aquests anys: gràcies perquè m'heu fet riure cada dia, m'heu animat en els moments difícils i heu fet que aquí m'hi senti com a casa. Gràcies pels acudits sense gràcia, pels poemes trobadorescos, pels detalls de tofu que tant m'agraden, per les calçotades a Can Sanchez, per les barbacoes a Can Fernàndez, pels bodorrios, per les teràpies, per les Juanis, per les bitlles, pels piti-breaks, pels sopars estiuencs, per les jornades padelsurferes a l'estiu, per deixar-me ser creativa als aniversaris. I el més important, moltes gràcies perquè tots, absolutament tots, m'heu ajudat d'alguna o altra manera amb la tesi. Especialment, gràcies a tots els qui m'heu ajudat al camp, ja sigui per la vostra generositat innata o per no haver d'aguantar els meus rotllos i xantatges. Amb Dockers, bikini, *traje* de pesca o *chándal*, és innegable que us hi heu deixat la pell (literalment). I parlant de camp, seria impossible no pensar en el Jordi Massana, l'Enric Queralt i molt especialment la Vinyet Solà que des de la CUADLL i la CUACSA sempre m'han facilitat la feina i m'han donat l'oportunitat de treballar a Sant Vicenç i Castellbisbal. També gràcies al Jordi Bellés, la Sara Insa i la Carmen Guitérrez per tota l'ajuda amb l'anàlisi de mostres i al laboratori. I a l'Alba Grau, la Giulia i l'Álvaro per la seva col·laboració al camp i en la interpretació de les dades.

I no puc acabar els agraïments sense esmentar la Nuri, la meva companya de viatge científic des de fa 11 anys (!!), per tants moments que hem compartit (i compartirem!), per ser-hi sempre i ajudar-me al camp, al despatx, amb els nens, i amb tot!

Per últim, vull donar les gràcies a la meva família i amics per tot el suport (directe o indirectament) que m'han donat. Als meus pares, germans i sogres especialment. Per cuidar els nens, pels *tuppers*, per tants "Tu pots!!".

I com no, res hagués estat possible sense el Miguel, l'Aina, l'Helena i el Miquel. Malgrat es podria pensar el contrari, els meus fills m'han facilitat el camí fins aquí; em donen llum els dies negres, em fan espavilar fins i tot els dies que no en tinc ganes, i m'omplen d'optimisme i ganes de viure tantes vegades. I gràcies al Miguel, per suplir les meves hores de mare absent, per compartir els èxits i aguantar estoicament els mals moments. No hi ha paraules d'agraïment suficients per explicar el que això representa per a mi.

Contents

List of Figures

Chapter 1

Chapter 2

Chapter 3

Chapter 4

Chapter 5

List of Tables

Abbreviations

BIX: Biological Index

BOD: Biological Oxygen Demand

CC: Coefficient of Curvature

CU: Uniformity Coefficient

DGGE: Denaturing Gradient Gel Electrophoresis

DOC: Dissolved Organic Carbon

DOC_{lab}: Labile Dissolved Organic Carbon

DOM: Dissolved Organic Matter

DOM_{imm}: Immobile Dissolved Organic Matter

DOM_{rec}: Recalcitrant Dissolved Organic Matter

EEM: Excitation-Emission Matrix

FI: Fluorescence Index

EOC: Emerging Organic Contaminant

HIX: Humification Index

IDH: Intermediate Disturbance Hypothesis

ORP: Oxidation Reduction Potential

PCA: Principal Component Analysis

PCR: Polymerase Chain Reaction

POC: Particulate Organic Carbon

SUVA: Ultra-Violet Absorbance

TOC: Total Organic Carbon

TIC: Total Inorganic Carbon

CHAPTER 1: INTRODUCTION

Nowadays, increasing water demand and the progressive pollution of water resources are some of the most alarming issues for human development. Furthermore, the context of climate change represents an additional problem in the management of hydric resources. In fact, anthropogenic pollution, i.e. the increase of greenhouse gas emissions, has a direct affection to climate global patterns. Concretely, the increase of average planet temperature (linked mainly to such emissions) is expected to significantly affect the hydrological cycle, changing the intensity and the patterns of precipitation events, the widespread melting of snow and ice, and the increase of evaporation and atmospheric water vapor. Therefore, changes in soil moisture and runoff are consequently induced. All these effects, directly or indirectly, affect the availability of water resources. Hence, arid and semi-arid zones (such as the Mediterranean Basin), which are exposed to a recurrent risk of scarcity, might be quite vulnerable to climate change effects. Furthermore, if the tendency in the increase of water withdrawals is maintained, the impact of droughts will be exacerbated. The gravity of the situation was exemplified by Turner et al. (1991) stating that withdrawals of water from natural circulation has been multiplied for almost 40 times in the past 300 years.

Indeed, the challenge of getting a sustainable exploitation of freshwater and other Earth resources are and will be a key factor for the development and well-being of future generations. The sustainable management should be capable to deal with the uncertain effects of climate change plus future scenarios of water demand.

Considering the available water resources, one can see that 97.5% of the water on Earth is salty. The 70% of the rest, i.e. freshwater, is frozen mostly in Antarctica and Greenland and almost the rest is not available remaining in soil moisture or inaccessible aquifers. Only less than 1% of freshwater is available for human uses, that is, water from lakes, rivers, reservoirs and accessible aquifers (Shiklomanov, 1997). A global assessment of water resources confirms that freshwater resources have been under high human pressure, both for the rising of demand as well as the negative impacts of pollution.

Despite patterns are changing, water had been traditionally used for waste disposal. Even now, water bodies suffer lots of impacts devaluating their quality. Major pollution problems include:

- Microbial pollution (bacteria, protozoa and viruses) from the pouring of untreated water or without an adequate treatment of freshwater bodies.

- Accelerate growth of algae in surface waters due to the high amounts of nitrogen and phosphorous present in many discharges.
- Presence of nitrates in groundwater from fertilizers.
- Release of heavy metals in soils and water by the industry and mining.
- Distribution of thousands of synthetized chemical compounds into the environment: fertilizers, personal care products, drugs, or pharmaceutical compounds among others, can reach the environment and become transported by rivers and be accountable of pollution of aquifers, coastal waters, and oceans. Furthermore, most of them and/or their by-products are toxic and highly persistent (recalcitrant) in the environment.

All of these pollution loads are causing worldwide public health problems, limiting economic and agricultural development, and harming a number of ecosystems. Therefore, it is necessary to increase the amount of water resources, not only by finding complementary resources but also by improving the quality of available freshwater.

1.1. Managed Aquifer Recharge as a component in the integrated water resources management

Water resources should be managed and used efficiently in order to ensure the long-term human population development. Managed Aquifer Recharge (MAR) was born as a solution to increase the availability of water in groundwater reservoirs. MAR is conceived as a local strategic management tool since it can use opportunistic water (e.g. wastewater, river water, or runoff waters among others) to replenish aquifers (San-Sebastián-Sauto et al., 2018). In this way, groundwater resources represent an advantage with respect to surface ones, since the larger residence time of water within the aquifers allows to consider them as reservoirs. Then, such reservoirs could be exploited in times of water shortages. Furthermore, the replenishment of aquifers helps to ensure the supply of water necessities of different sectors by means of a wide display of sources. So, MAR fits with the concept of integrated water resources management, adequately responding to a claim for the conjunctive use of surface water and groundwater.

1.2. Types of MAR techniques

MAR includes the group of all programmed techniques that induce the entrance of water into aquifers. In this way, both the availability and quality of water resources

can be increased. MAR facilities are divided into two main groups: filtration from the surface or direct injection into the aquifer. The first group is basically used in unconfined aquifers, whereas deep injection is mostly applied to semi-confined and confined aquifers. Taking into account both groups, Dillon (2005) describes the following MAR types:

- Aquifer storage and recovery (ASR): injection of water into a well and then extraction from the same well.
- Aquifer storage transfer and recovery (ASTR): injection of water into a well and then extraction from a different well to provide an additional treatment based on transport through the aquifer.
- Bank-filtration: extraction of groundwater to induce infiltration from the surface water body, therefore improving the quality of water.
- Dune filtration: infiltration of water from ponds constructed in dunes and recovery of water with higher quality downstream.
- Infiltration ponds: diverting of surface water that infiltrates into the aquifer through the vadose zone.
- Percolation tanks: water is detained and infiltrates through the base in ephemeral waddies. Water is then extracted down-valley to supply towns.
- Rainwater harvesting: use of runoff water from roofs to replenish wells or caissons filled with sand or gravel.
- Soil aquifer treatment (SAT): use of infiltration ponds to remove nutrients and pathogens during the passage through the vadose zone.
- Sand dams: accumulation of sand that traps sediment during flow, and accumulates water in successive floods that can be exploited in dry seasons.
- Underground dams: construction of trenches in the streambed of ephemeral streams to help the retaining flood flows.
- Recharge releases: construction of dams in ephemeral streams to retain flooding water and slow release water into the streambed downstream.

1.3. Quality targets of MAR: microbial community role in water quality improvement

Human impacts can affect water bodies. Pollutants can be removed from water; yet, eliminating some substances can be technically difficult and economically expensive. In this way, MAR is a quite common technique to take advantage of the potential of the soil as a biogeochemical reactor to enhance the quality of water infiltrating

through the vadose zone, especially in surface replenishment systems (Drewes et al., 2003; Nadav et al., 2012). In fact, MAR has been proven effective to remove pathogens (Bekele et al., 2011; Betancourt et al., 2014), dissolved organic carbon (DOC) (Maeng et al., 2011; Mermillod-Blondin et al., 2015), nitrate (Grau-Martínez et al., 2018), as well as some organic persistent contaminants (Hamann et al., 2016; Regnery et al., 2015; Valhondo et al., 2018). The feasibility of MAR as a water treatment technique is based on the capability of microorganisms to degrade water contaminants. The potentiality attenuation effect of microorganisms has been applied for example in landfill leakage affections (Röling et al., 2001; Staats et al., 2011), contaminant spills (Fahrenfeld et al., 2014; Haack et al., 2004; Martínez-Pascual et al., 2010; Nijenhuis and Kuntze, 2016) or nitrate polluted aquifers (Bellini et al., 2018, 2013).

Microbial growth and activity is conditioned by several environmental parameters such as DOC availability, dissolved oxygen content, redox conditions, temperature, nutrient concentrations or soil moisture (Alidina et al., 2015; Bekele et al., 2011; Dutta et al., 2015; Goren et al., 2014; Greskowiak et al., 2006, 2005b; Hellauer et al., 2017; Laws et al., 2011; Rezanezhad et al., 2014). All these parameters have a crucial role in the metabolic path of microorganisms and, consequently, in the removal efficiency of the targeted pollutants.

Studies testing the link between water quality and microbial communities in real MAR facilities are few, dealing with recharge wells (Ginige et al., 2013), riverbank areas (Schütz et al., 2009), or surface infiltration ponds (Reed et al., 2008; Regnery et al., 2016). However, there are no microbial fingerprinting studies that integrate results from infiltrating water, soil and groundwater samples comparing different operational periods in surface recharge systems. Furthermore, what species are favored under recharge conditions is not well known either.

On the other hand, intrinsic properties of the porous media (e.g., porosity and pore size distribution) determine the spatial and temporal distribution of microorganisms in soils (Chau et al., 2011). Physical and hydraulic characteristics of soils condition the availability of pore space and the access to nutrients, thus affecting in a distinct way the growth and activity of microorganisms (Perujo et al., 2018, 2017).

Subsequently, determining how much and to what extent physical, geochemical, biological and operational parameters influence the system functioning is useful for managing purposes (Dutta et al., 2015; Grau-Martínez et al., 2018; Hellauer et al.,

2017; Pedretti et al., 2012b; Rodríguez-Escales et al., 2017). Despite that, it is difficult to find multidisciplinary research dealing with integrated approaches to improve the understanding of MAR problems.

1.4. Motivation and objectives

The present dissertation is contextualized in the frame of the EU project MARSOL (Demonstrating Managed Aquifer Recharge as a Solution to Water Scarcity and Drought). The consortium involved different European partners, including the Universitat Politècnica de Catalunya in charge of the Sant Vicenç site, as well as managing a work package in water quality. The site involves a sedimentation pond followed by an infiltration pond. The latter included an innovative treatment based on a reactive layer placed at the bottom to enhance degradation of emerging organic contaminants (EOCs). The investigations performed there, allowed concluding that redox conditions occurring below the infiltration pond induced the depletion of some EOCs. Then, it was demonstrated that the existence of a reactive layer enhanced some contaminant attenuation processes. But several questions remained unanswered: Which were the microbial populations driving such quality processes? What are the dominant microbial populations and their dynamics under recharge and non-recharge scenarios? Which is the ecological behavior of MAR microbial communities? Are they diverse? Are there some microbial key-species?

Very little is known about the sensitivity of microbial populations to MAR-linked environmental (external) factors that affect water quality, such as hydrochemical composition, temperature, redox potential, organic matter, and nutrients concentration.

In order to monitor and study processes related to water quality improvement under "natural" conditions, the Castellbisbal MAR system (again surface ponding) allowed to analyze them without the influence of the reactive layer. Biodegradation processes are highly dependent on redox conditions (Burke et al., 2014; Regnery et al., 2017; Rodríguez-Escales et al., 2017), and both, in turn, are very influenced by temperature (Henzler et al., 2016; Prommer and Stuyfzand, 2005).

Temperature also can modify water intrinsic properties, mainly viscosity. This may have important implications in the saturated hydraulic conductivity, especially in MAR surface systems with drastic seasonal climatic situations (Braga et al., 2007; Lin et al., 2003; Vandenbohede and Van Houtte, 2012). However, temperature not

only affects water properties; bio-mediated processes will be also influenced (Maeng et al., 2011; D Or et al., 2007; Zhang et al., 2015). The extent in which temperature changes may affect the infiltration rate and in turn biodegradation rates is an unknown issue related to MAR ponds management.

The principal aim of this thesis is:

> To understand and characterize in detail the biogeochemical process occurring during MAR in infiltration ponds, as well as the dynamic of local microbial populations under different recharge conditions

To accomplish this objective, a number of studies were carried out in two different recharge ponds in the Llobregat alluvial aquifer, targeting specific goals:

- Perform a microbial fingerprinting study between two opposite scenarios of recharge.
- Identify key microbial species linked to the recharge process.
- Evaluate the ecological implications of MAR.
- Associate microbial community distribution tendencies related to changes in hydrochemistry, management, and soil properties.
- Monitor biological activity through the infiltration system (infiltration water, vadose zone, and aquifer) with annual redox potential evolution.
- Determine the role of redox potential in the carbon cycle through the infiltration system.
- Quantify the effect of temperature in redox reactions rates.
- Quantify variations in hydraulic saturated conductivity due to seasonal temperature fluctuations.
- Plan management measures in order to optimize both quantity and quality targets pursued by recharge.

1.5. Managed Aquifer Recharge in Llobregat River Basin: study sites

1.5.1. Background

Barcelona Conurbation encompasses a population over 3.5 million inhabitants. The water supply for this area is mainly based on surface water resources, from rivers Ter and Llobregat. Only a small portion for human supply is covered by groundwater withdrawals, mainly from the Llobregat Lower Valley and Delta. However, there are some industrial and agricultural zones supplied mainly by groundwater, resulting in 11% of the total supply on average. There is thus, a management in an integrated way considering both surface and sub-surface as a unique water body unit. In fact, the strategies performed in the Llobregat River were pioneers in the Spanish water management system; noticeably the Water User's Community created in 1981, as a union of different water users.

In the context of the Barcelona Conurbation, aquifers are considered strategic reservoirs to be exploited in high shortage periods, capable of partially supplying the population living in the area. Scarcity periods are quite frequent in the context of Mediterranean climate conditions. Furthermore, the climate change perspective and the effects of population growth that are forecasted in the area increase the risk of a future lack of water, so that groundwater should be properly managed within an integrated framework.

The sedimentary basin of the Llobregat River is formed by two detritic levels, separated by an intercalation of silty materials that lose continuity towards the valley and boundaries. The upper part of the aquifer is formed by sands of a delta front, about 15 m thick. The deep aquifer is formed by a combination of sands and gravels. This, is considered the main aquifer with values of transmissivity in the range between 1000 to 5000 m^2/day. A silty wedge acts hydrogeologically as a semiconfining unit.

Several groundwater models have been developed in the area, the last one performed by the Hydrogeology Group (UPC-CSIC) in 2006. The model confirmed the clear deficit of groundwater in the area, claiming the need for induced recharge actions, to be distributed all along the lower course of the River. Accordingly, managed aquifer recharge practices were recommended in the delta region and in the lower valley. In short, it was established that a sustainable exploitation could not be guaranteed only due natural recharge, especially during drought events.

For this reason, the Water Catalan Agency (ACA) and the water supply operator (Aigües de Barcelona –Agbar) have been promoting strategies to recover the aquifer in the lower course of Llobregat. These consist of:

- Riverbed scarification in the Lower Valley: consists on removing the fine materials settled in the riverbed. This activity has been performed since the 1950s, contributing in an infiltration rate that has been estimated in 40000 m^3/d, although this figure is questioned.

- Deep injection: this technique has been intermittently applied since 1969, taking advantage of drinking water quality excess production at some periods. It was the first deep recharge system built in Spain and it is composed of 12 wells that allow decreasing the regional head gradient. The recharge capacity of this technique has been calculated in 75000 m^3/d, but it is used only intermittently.

- Seawater positive barrier in Llobregat Delta: seawater intrusion in the deep delta aquifer has progressively deteriorated the groundwater quality since the 1960s. For this reason, in 2007 a seawater positive barrier was put into operation. Water for injection is tertiary-treated water (UV-disinfected, ultra-filtered and treated with reverse osmosis). Wells are located 1 km inland from the coast, displaying a line parallel to the coast about 6 km long. The total injected flow was 15000 m^3/d during operation, that was discontinued in 2010 due to financial problems of the funding agency.

More information about recharge practices in the Llobregat Basin can be found in Sanchez-Vila et al. (2012) and in Deliverable 6.1 of MARSOL project (www.marsol.eu).

1.5.2. Study site 1: Sant Vicenç MAR system

The Sant Vicenç MAR system is located 15 km inland from the Mediterranean Sea, close to Barcelona city (Figure 1.1). It feeds the Lower Valley Aquifer, with 10-15 m of thickness in the vicinity. The aquifer presents alternate sands and gravels with non-continuous fine-grained sediments (Pedretti et al., 2012b). The water supplied to the system is diverted from upstream the river to a pre-sedimentation basin. After 2-4 days of residence time, it is diverted to an infiltration basin of 6500 m^2. The

infiltration capacity has been estimated at 1 $m^3m^{-2}d^{-1}$ on average, and the local transmissivity of the aquifer is estimated as 14000 m^2d^{-1} (unpublished).

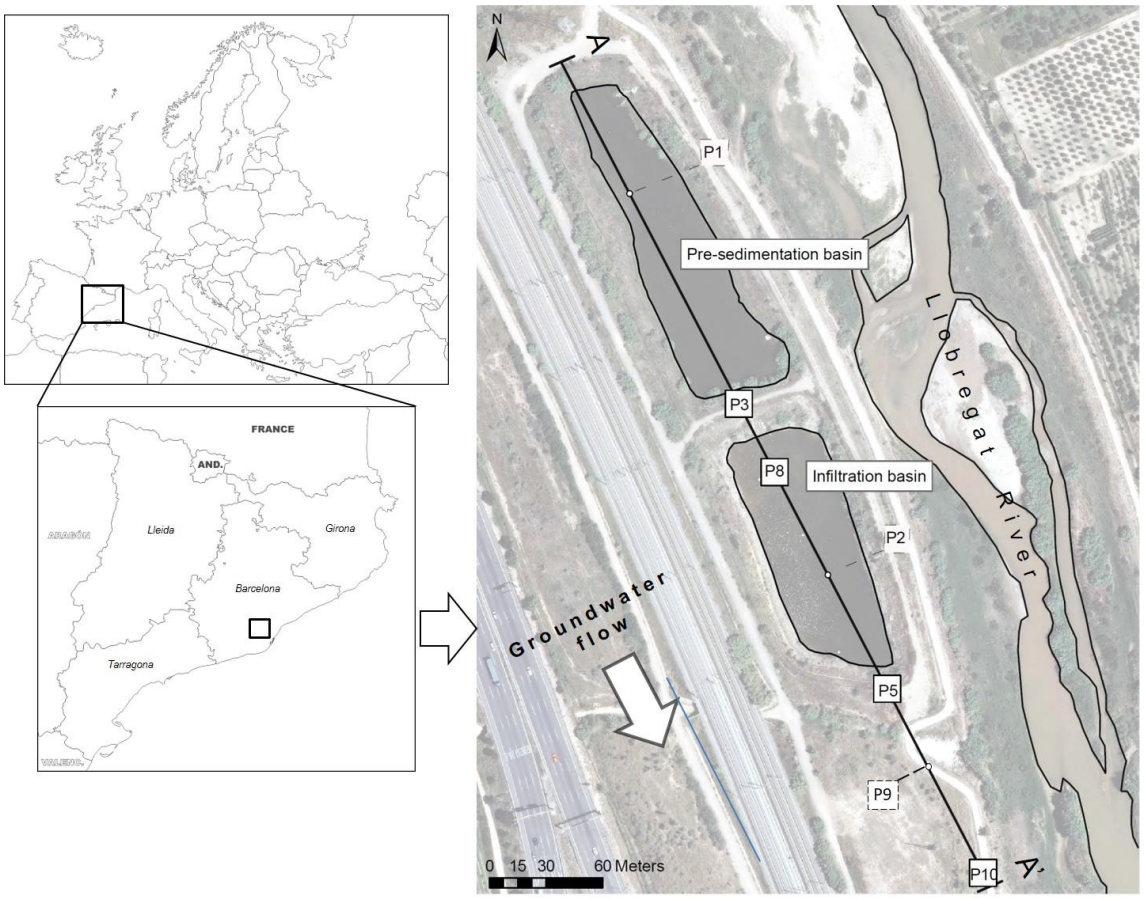

Figure 1.1 Geographical location of the Sant Vicenç MAR System and piezometers' network

Since the construction of the ponds in 2009, many studies have been carried out in the Sant Vicenç MAR System. The two first projects emplaced there were GABARDINE (2005-2008) and RASA (2008-2010). Thanks to the RASA project, the site was instrumented, a network of piezometers was constructed, pumping and tracer tests performed, and a hydrologic model was developed. In 2010, the EU project LIFE-ENSAT started, including the installation of a reactive layer at the bottom of the infiltration pond to enhance the removal of emergent organic contaminants. The idea of the reactive layer was to increase the organic load of the infiltration water, promoting biological processes through the soil and the vadose zone. The barrier was composed of organic compost (50% in volume) mixed with local sand and gravel. Small amounts of clay and iron oxides were added to foster adsorption and ion exchange, respectively.

Finally, the MARSOL project funded by the UE, dealing with quality and risk issues related to artificial recharge, took place during 2014-2017.

Several Ph.D. thesis were developed based partially on these four projects: Barbieri (2011), Pedretti (2012), Barahona-Palomo (2014), Valhondo (2016) and Grau-Martínez (2018). Barbieri (2011) studied the potential effect of redox conditions on the biodegradation of some selected micropollutants. Batch experiments were performed with reactive barrier material from the site, simulating the conditions during recharge. Results showed removal rates similar to those of conventional wastewater treatments for ideal redox conditions. It was concluded that infiltration ponds can be a suitable complement to traditional wastewater treatments.

Pedretti (2012) focused on the development of tools to map recharge affected by the heterogeneity of the topsoil porous media. The combination of satellite imaging with field data allowed modeling the spatial variability of infiltration capacity in the site. The model considered the development of the clogging process in a probabilistic risk assessment framework during recharge events.

Barahona-Palomo (2014) studied the effect of temperature fluctuations in the vertical hydraulic conductivity behavior below the pond. Field data were compared with a 1D model results.

The Ph.D. dissertations of Valhondo (2016) and Grau Martínez (2018) dealt with quality aspects related to MAR. The former analyzed the efficiency of the reactive layer to remove selected EOCs. A local reactive transport model explaining the behavior of pond recharge was also presented. On the other hand, the latter focused on denitrification processes occurring below the pond.

Overall, the published work provides a good hydrogeological characterization of the site. Additionally, the four mentioned projects resulted in site equipment and a significant monitoring network. So, it represents an excellent starting point to develop the objectives introduced before.

1.5.3. Study site 2: Castellbisbal MAR system: site description and previous studies

The Castellbisbal MAR system is located NW of the Barcelona Metropolitan Area (Figure 1.2) The pond feeds the Cubeta de Sant Andreu's aquifer that is constituted by Quaternary detritic materials associated to the evolution of the Llobregat River. The aquifer is composed of different levels of stepped alluvial terraces. The study zone is located in a river meander, on a terrace sitting on Cenozoic red mudstones (Martín and López, 2001). The aquifer depth under the pond is around 10 m. The

lithology under the pond is composed by gravels in a sand matrix. The associated transmissivity in the vicinity is estimated around 4100 m^2/d while the porosity was estimated in 0.2-0.3 (Martín and López, 2001). Groundwater from the Cubeta de Sant Andreu supplies the cities of Sant Andreu de la Barca, Castellbisbal and Corbera, as well as industrial and agricultural activities in the area.

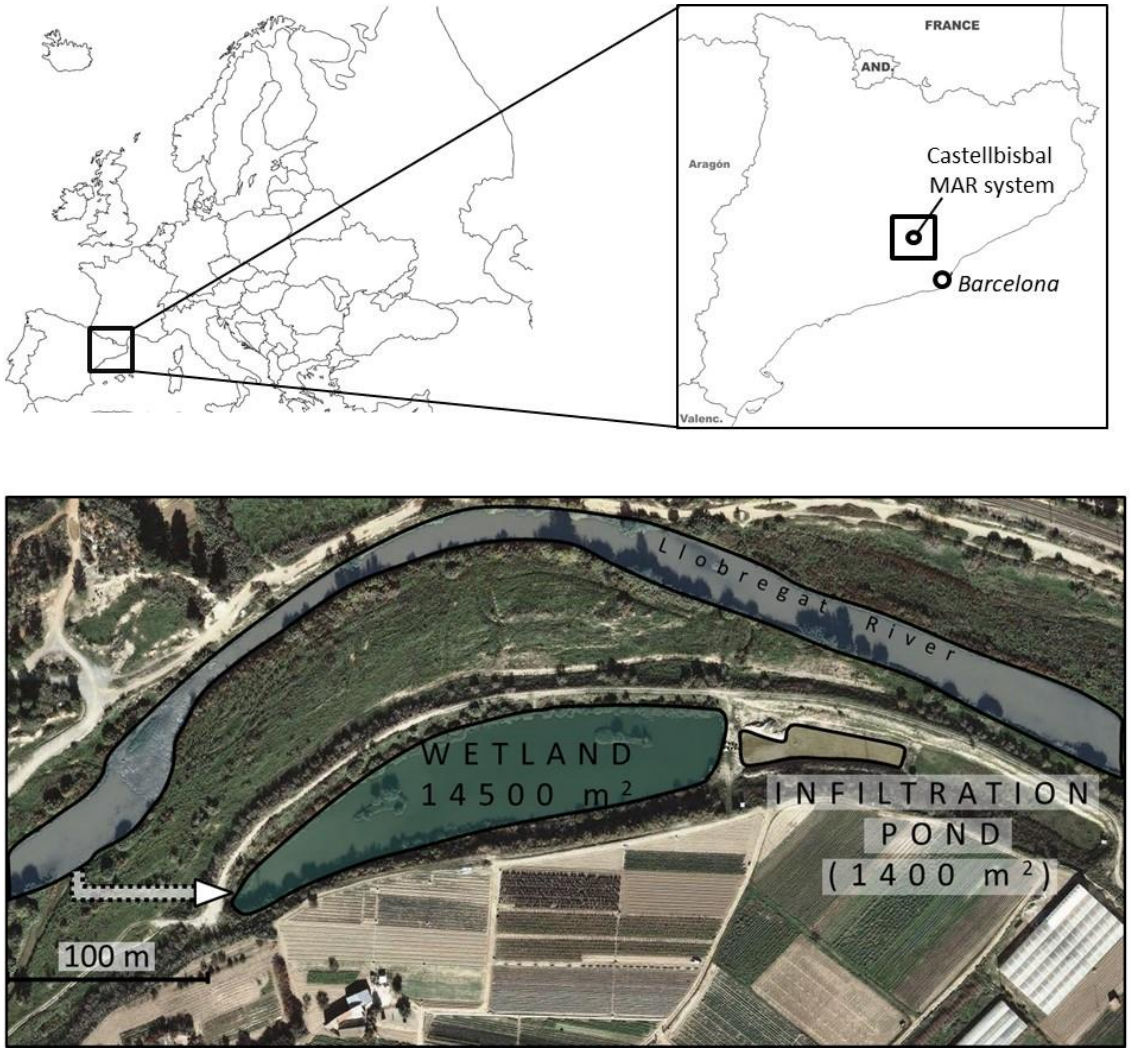

Figure 1.2 Geographical location and disposition of the Castellbisbal surface infiltration system

The MAR system exists since the 1980's. However, it was fully reconstructed in 2007 after a complete damage due to flooding in 1998. Water for recharge purposes is collected from the Llobregat River some 300 m upstream the study zone. Firstly, water passes through a permanent-regime wetland (14500 m^2), with a residence time of about 3 days. Then, water is diverted to the infiltration pond (1400 m^2). In principle, recharge is continuous over the year, closing the interconnection between ponds when the turbidity in the Llobregat River reaches 150 NTUs. Maintenance operations (scrapping) in the infiltration is carried out approximately once a year.

Compared to the Sant Vicenç MAR site, the recharge system of Castellbisbal has been much less studied, with no reactive layer installed. The work of Rodríguez Vicente (2013) evaluated the availability of MAR at this location in terms of Llobregat River average flow rate and water quality. Sendrós Brea-Iglesias (2016) in his dissertation proposed geophysical prospection as a non-invasive technique to characterize the infiltrating medium. The main monitoring point is a piezometer drilled inside the infiltration pond, crossing the vadose zone and penetrating the aquifer (PJ) (Sendrós Brea-Iglesias, 2016).

1.6. Outline of the thesis

This dissertation is organized into six main chapters.

Apart from this introduction (Chapter 1), Chapter 2 and Chapter 3 correspond to the investigations carried out in the Sant Vicenç MAR system. Chapter 2 shows a microbial fingerprinting comparing recharge and non-recharge scenarios. The goal of this chapter is to link the conceptual flow model -mapping different groundwater zones according to the influence of recharge- with microbial community behavior in both scenarios. Chapter 2 also provides a wide discussion about ecological implications of MAR ponds related to these two operation extremes.

In Chapter 3, all the data obtained in the latter study is compiled and subjected to a statistical analysis. Compilation of microbial community composition data for soil and water samples, diversity indices, the hydrochemical composition of water at different depths, and grain-size distribution of soil samples allowed treating the variables by means of PCA analysis. The objective of this chapter is to bring forth strong correlations about non-biological and biological variables. Likewise, all analyses have been framed in the two scenarios studied in the previous chapter.

Chapter 4 and Chapter 5 have been carried out in the context of the Castellbisbal MAR system, where the reactive layer is not present.

In Chapter 4, several sampling surveys with analytical methods distributed along one year are presented; this allowed to characterize redox species, the origin of organic matter in water samples, and to quantify the amount of carbon in sediments of the infiltration pond bed. Results from continuous monitoring of the hydrological regime (water table in the infiltration pond, infiltration flow rate, and groundwater level below the pond); temperature and redox potential in infiltration water, soil and groundwater are also presented. The aim of this chapter is to understand clogging

development and redox processes induced by infiltration to improve MAR management.

Chapter 5 focuses on modeling flow and heat transport of the Castellbisbal MAR system in order to know and quantify (1) reduction of hydraulic conductivity caused by clogging, (2) changes in hydraulic conductivity due to temperature fluctuations in space and time. Furthermore, two reactive biogeochemical models are implemented in order to test the impact of temperature on redox processes, i.e. on degradation rates. The last section of this chapter presents some suggestions in order to couple reactive transport with flow and heat transport.

Finally, Chapter 6 presents the conclusions of the overall performed research along the Ph.D. dissertation.

The Appendix includes two parts. The first one provides some hydrochemical data obtained in the Sant Vicenç MAR sampling campaigns; the second includes two scientific papers, one with a content similar to Chapter 2, and another one is a paper that I coauthor dealing with denitrification processes occurring in the Sant Vicenç MAR system.

CHAPTER 2: PARAMETERS AFFECTING MICROBIAL COMMUNITY COMPOSITION IN SURFACE INFILTRATION PONDS

2.1. Introduction

As the Intergovernmental Panel on Climate Change has stated for years, climate change is affecting and will continue to affect the availability and quality of freshwater resources, with severe consequences to humans and ecosystems. In particular, the Mediterranean Basin is expected to become warmer and drier (Bates et al., 2008). Therefore, among other actions, claiming a secure water supply should increase groundwater storage of quality water as a strategic management tool in times of scarcity. Managed Aquifer Recharge (MAR) is a globally used, worldwide extended technology based on refilling aquifers with water from different sources (e.g., river, reclaimed, or opportunity water). MAR facilities are usually intended to recover groundwater levels, to become water reservoirs or as a means for improving water quality during infiltration (Drewes et al., 2003; Nadav et al., 2012).

The Llobregat River (Catalonia, NE Spain) is fed by about a hundred Waste Water Treatment Plants. While nitrogen, phosphorous and organic matter (DOC) are eliminated below the legal limits before treated wastewater is discharged to the river, emerging organic contaminants (EOCs) are not fully removed (Loos et al., 2013). Consequently, significant concentrations of many EOCs have been detected in the Llobregat River (López-Serna et al., 2012) and its associated groundwater bodies (Jurado et al., 2012).

Biodegradation of EOCs strongly depends on redox conditions (Barbieri et al., 2011; Maeng et al., 2010). In this regard, it has been shown that MAR is a feasible technique capable of partially degrading some of these contaminants (Hellauer et al., 2017; Massmann et al., 2008), particularly when bioprocesses are enhanced (Grau-Martínez et al., 2018; Schaffer et al., 2015). Infiltration through the soil intrinsically leads to two main consequences in groundwater recharge:

1. Development of different vertical and temporal redox zonations responding to organic matter availability as electron acceptors are consumed (Greskowiak et al., 2006).

2. Development of microbial communities according to the flow paths. Fingering below the surface of the recharge systems and preferential flow paths in the saturated zone can create anaerobic microsites Bridgham et al. (2013) in which oxygen is consumed faster than it can be diffused from oxic zones.

Indeed, MAR implies groundwater quality modifications when compared to natural flow conditions. This includes several parameters such as organic matter, dissolved oxygen content, temperature, pH, electrical conductivity, and nutrients (Rivett et al., 2008; Zhang et al., 2016). Such disturbances have ecological implications, as all these parameters affect the growth and activity of microorganisms and the corresponding degradation of emerging contaminants (Barbieri et al., 2012; Regnery et al., 2017; Valhondo et al., 2018).

Microbial studies linked to MAR practices involve mostly laboratory experiments (Alidina et al., 2014c; Freixa et al., 2015; Li et al., 2013; Rubol et al., 2014). As for microbial MAR field studies, most relevant research is limited to well injection systems (Ginige et al., 2013; Reed et al., 2008; Zhang et al., 2016) or riverbank filtration conditions (Huang et al., 2015). Onesios-Barry et al. (2014) compared results from a column experiment and soil samples in a MAR site in the US, focusing on the microbial populations linked to pharmaceutical and personal care products removal, and concluded that microbial composition and structure of both systems were comparable. Regnery et al. (2016) went one step further by relating the relative abundance of functional genes involved in xenobiotic pathways with attenuation of some trace organic chemicals and their byproducts in a combination of laboratory experiments and a full-scale MAR facility. However, in our knowledge, there are no microbial fingerprinting studies of MAR surface infiltration basins, that integrate results from surface water, groundwater, and soil samples and comparing them in two different operational periods.

The main goal of this chapter is to determine how MAR activities induce changes in the microbial communities in Sant Vicenç recharge system. Here, changes on diversity indices are evaluated and we incorporate results of the DNA sequence analysis of excised DGGE band patterns for samples taken from different environments and locations within the site and under conditions of recharge and non-recharge. Additionally, results are linked with ecological principles and potential biogeochemical processes (i.e. pollutants degradation) occurring due to MAR activities.

2.2. Methodology

This second chapter is framed in Sant Vicenç MAR facility (see Chapter 1, section 2.3.1.).

2.2.1. Monitoring network and hydrochemistry sampling surveys

Two recharge situations were compared to evaluate the effect of MAR on groundwater chemical signature. After six months of continuous recharge operation, a sampling campaign took place in July 2014 (wet campaign). Samples were collected from surface water in both basins and in the existing piezometers at different depths (from -5 to 3 masl, see Figure 1.1 and Figure 2.1).

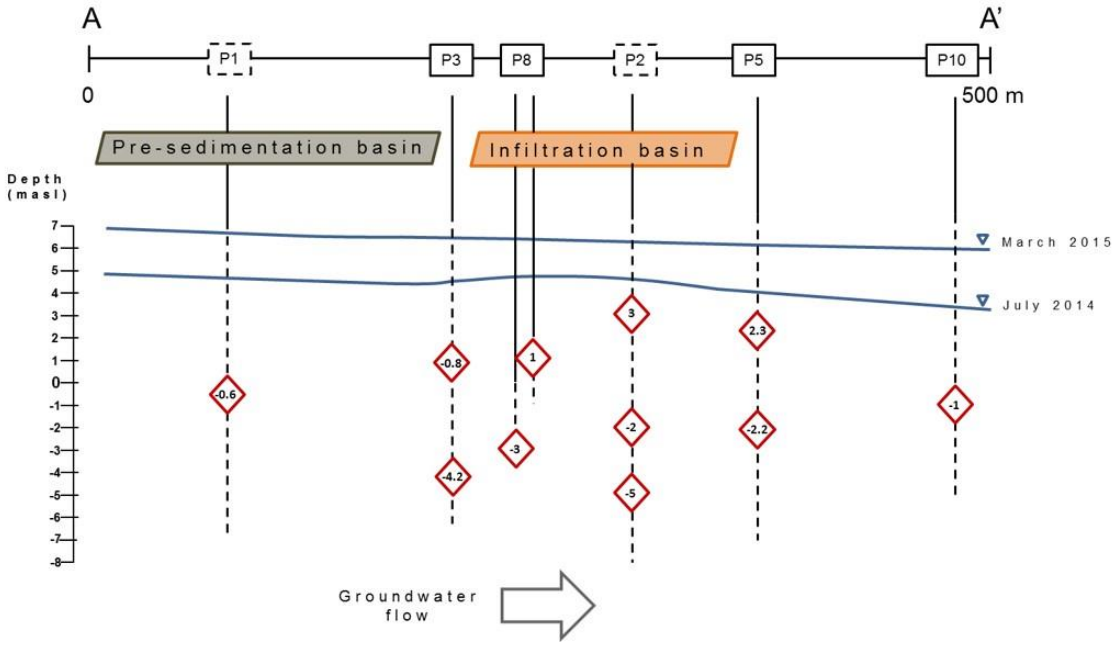

Figure 2.1 Transect section studied with piezometers (P1 and P2 are projected) and displaying sampling depths (red diamonds). Water from piezometer P1 represents background conditions (not affected by recharge. The blue line shows the groundwater level in July 2014 (active recharge scenario) and March 2015 (non-recharge scenario)

A second sampling campaign was performed in March 2015 after recharge had been discontinued for four months. In this case, groundwater was also sampled. Water was analyzed for cations, anions (Cl^-, NO_3^-, SO_4^{-2}, HCO_3^-), DOC and TOC. Samples for Cl^-, NO_3^-, $SO_4^{-2,}$ and HCO_3^- analysis were filtered through 0.2-µm nylon filters, stored at 4ºC and analyzed using high-performance liquid chromatography (HPLC) with a WATERS 515 HPLC pump, IC-PAC anion columns, and a WATERS 432 detector. Samples for the determination of cations were filtered through a 0.2-µm filter, acidified in the field with 1% HNO_3^- and stored at 4ºC. Cations were analyzed using inductively coupled plasma-optical emission spectrometry (ICP-OES, Perkin-Elmer Optima 3200 RL). Samples for DOC analysis were filtered through a 0.45-µm nylon filter and collected in muffled (450ºC, 4.30 h) glass bottles, acidified and stored

at 4ºC. In addition, water for TOC determination was sampled and stored at 4ºC. TOC and DOC were analyzed with an infrared detector using the NPOC method (Shimadzu TOC-Vcsh).

In both campaigns, temperature and electrical conductivity vertical profiles were mapped along the transect from data obtained at 50 cm intervals (MPS-D8, SEBA Hydrometrie).

2.2.2. Microbial community characterization

Water samples were extracted from the pre-sedimentation and infiltration basins at three locations (entrance, middle, and end) during recharge conditions (from now on, wet scenario). On the contrary, 3 soil samples were extracted at the same locations in the infiltration basin under non-recharge conditions (termed dry scenario). Soil samples were obtained from around 10 to 50 cm in depth. The sampling procedure for soil was done taking into account Lombard et al. (2011) recommendations, especially regarding the variability of microbial communities along a field transect. Soil samples were taken by means of cores, individually disassembled and kept in a sterile bag. Groundwater samples were taken from -5 to 3 masl depending on the piezometers (10 samples for wet scenario and 7 for dry). All soil and groundwater samples were taken in duplicate, kept in sterile conditions, and preserved in dark at 4ºC until being taken to the laboratory for molecular analyses.

Liquid samples were filtered through 0.22-µm GV Durapore® membrane filters (Merck 14 Millipore, USA) and stored at -80ºC. Soil samples were centrifuged at 14.000 rpm and the liquid fraction was discarded before pellets were cold-stored at -80ºC. Total DNA extraction was conducted using PowerWater® and PowerSoil® DNA Isolation Kits (MoBio Laboratories, USA) for water (100 mL) and soil (200 mg) samples, respectively. For bacterial analyses, a 550-bp DNA fragment in the 16S region of the small-subunit ribosomal RNA gene was amplified using the primer set 341f/907r (Muyzer et al., 1993) a with a GC clamp added at the 5' end of the forward primer. Final concentrations of the PCR reactions consisted of 1x PCR buffer, 2 mM of $MgCl_2$, 200 µM of each deoxynucleoside triphosphate, 500 nM of each primer, 2.5 U of Taq DNA polymerase (Invitrogen, ThermoFisher Scientific, USA) and 10 ng of template DNA. The amplification protocol consisted of 94ºC for 5 min; 20 cycles of 94ºC for 1 min, 65ºC for 1 min (-0.5ºC/cycle), 72ºC for 3 min; 15 cycles of 94ºC for 1 min, 55ºC for 1 min, 72ºC for 3 min; and a single final extension of 72ºC for 7 min.

Denaturing gradient gel electrophoresis (DGGE) was performed using the Dcode Universal Mutation Detection System (Bio-Rad, Spain). First, 900 ng of DNA from PCR products were loaded onto 6% (w/v) polyacrylamide gels (acrylamide/bis solution 37.5:1) containing linear chemical gradients of 30-70% denaturant. The 100% denaturing solution contained 7 M urea and 40% (v/v) deionized formamide. Gels were run in 1X Tris acetate-EDTA (TAE) for 16 h at 75 V and 60ºC, stained with 1 µg/mL ethidium bromide solution for 25 min, washed with deionized water for 25 min and photographed with Universal Hood II (Bio-Rad, Spain). DGGE images were analyzed using InfoQuest™ FP software. Dice's coefficient and the unweighted pair group method with arithmetic averages (UPGMA) were employed for the clustering of DGGE gel profiles. Non-metric Multidimensional Scaling (NMD) was performed using the Vegan package (Oksanen et al., 2017). Prominent bands from the DGGE were excised, re-amplified and sequenced by Macrogen (South Korea). The obtained sequences were trimmed with FinchTV software and checked for chimeras using the UCHIME algorithm (Edgar et al., 2011) integrated into Mothur version 1.38 (Schloss et al., 2009). Each 16S rRNA sequence was assigned to its closest neighbor according to the Basic Local Alignment Search Tool (BLAST) results (Altschul et al., 1997). Curated sequences were deposited in the National Center for Biotechnology Information (NCBI) GenBank database under accession numbers MF471641-MF471667.

Once the main microbial communities were characterized, three diversity indices were calculated. The first one is Richness (S), defined as the proportional number of microbial species present in a sample, i.e., equal to the total number of bands; the other two, Shannon (H), and Evenness (E), were calculated for each sample as follows:

$$H = -\sum_{i=1}^{S} p_i \cdot ln(p_i) \qquad (2.1.)$$

$$E = \frac{H}{H_{max}}; \quad \text{with } H_{max}=ln\, S \qquad (2.2)$$

where H_{max}=lnS and p_i is the relative intensity of each band of the sample. Values reported correspond to the average of the two replicas.

2.2.3. Physical characterization of soil

To complement the soil microbial community's characterization, particle size measurements of soil samples were taken according to the ASTM guidelines. The soil was sampled in the pre-sedimentation basin and at the entrance, middle, and end of infiltration basin. Soil sampling was performed close to the location where samples were taken for microbial analyses.

2.3. Results

2.3.1. Clustering of recharge influenced zones according to temperature and conductivity changes

Understanding the flow pattern in MAR basins is essential to explain microbial community dynamics. In this regard, 2D transects of temperature and conductivity alterations obtained at the time of the sampling campaigns (Figure 2.2 and Figure 2.3) based on vertical profiles indicate that: 1) the vertical flow gradient pushes the existing groundwater downwards and forms a shallow front that travels approximately 120 m downstream, eventually mixing with the background water; 2) the background water is mostly found near the recharge pond and at the deepest sampling points below the pond.

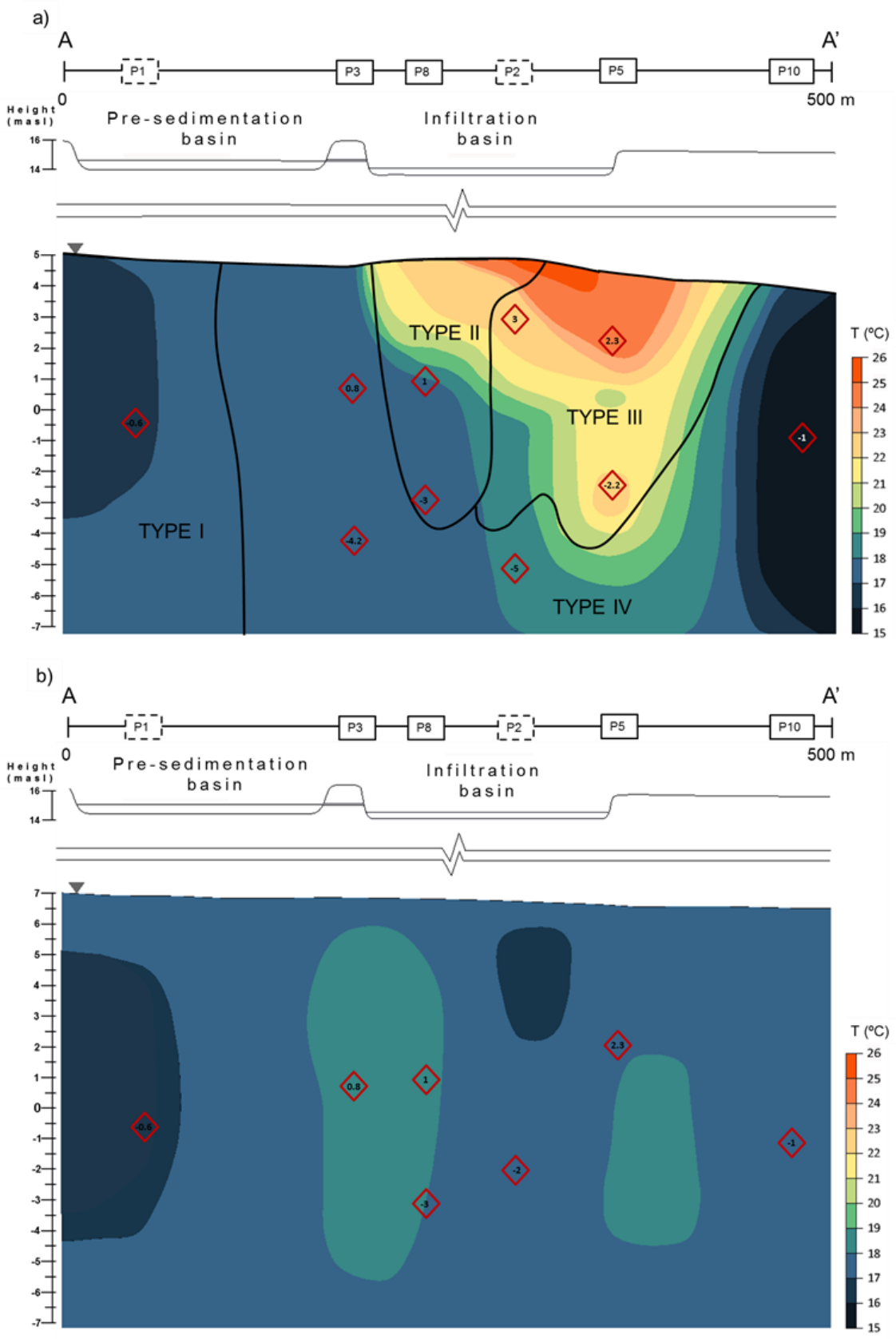

Figure 2.2 Temperature distribution at the local scale in (a) July 2014 (wet), and (b) March 2015 (dry). Red diamonds indicate sampling points for microbial and water analysis in each campaign

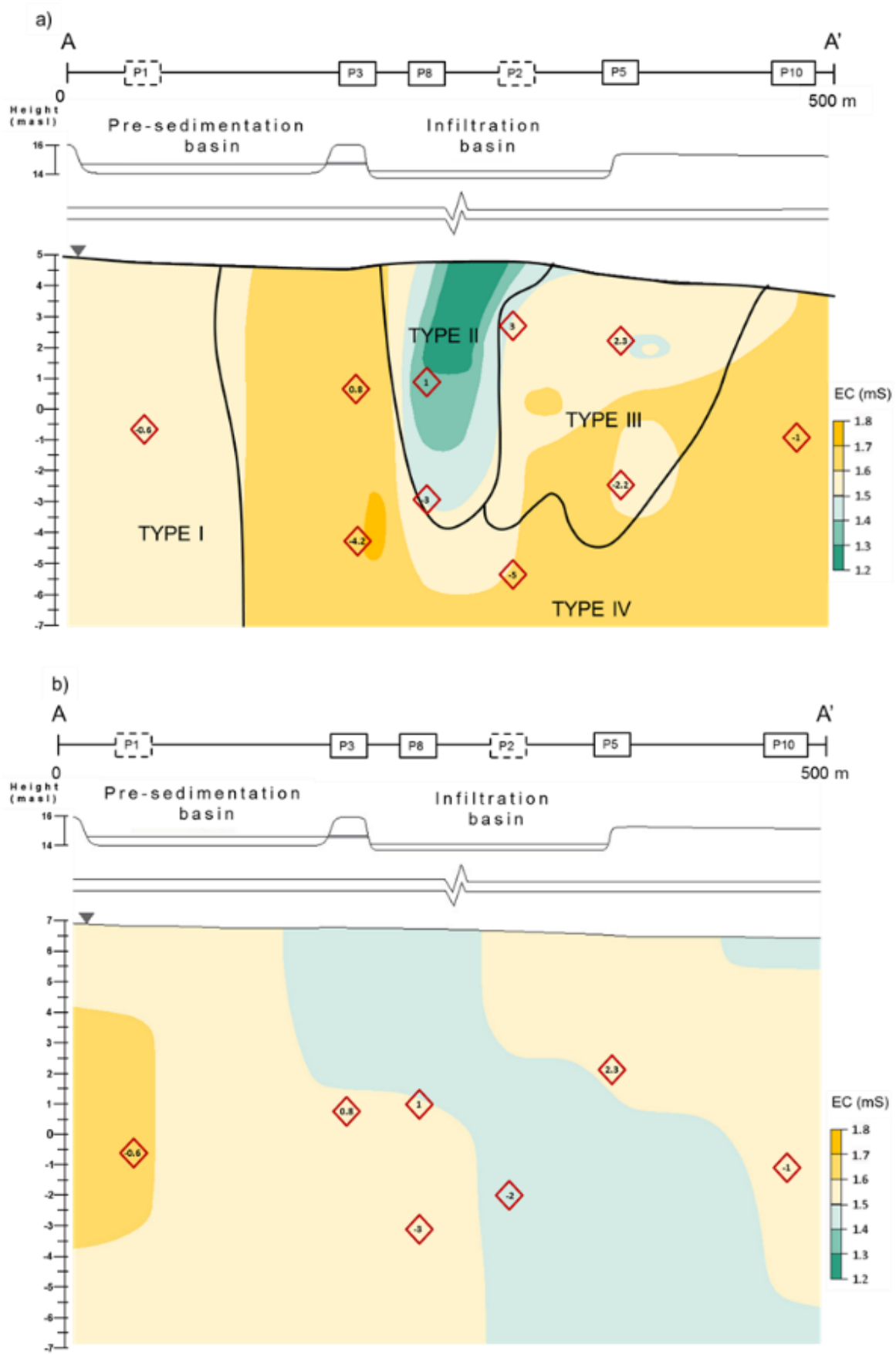

Figure 2.3 Electrical Conductivity distribution at the local scale in (a) July 2014 (wet), and (b) March 2015 (dry)

From this conceptual model, four main groups of groundwater can be defined under recharge conditions:

- Type I water represents the background environment of the aquifer, unaffected by MAR activities. Water sampled in P1 is an example of this type.
- Type II water is the infiltrating one (best observed in P8 at both sampling depths). It flows vertically through the vadose zone to the aquifer, creating a small water mound that pushes down the Type I water.
- Type III water, characteristic of points P2(3), P5(2.3) and P5(-2.2), is a mixture between Types I and II waters, with a high proportion of the latter.
- Type IV is again a mixture but with a lower proportion of Type II water. It is present in piezometers P3(0.8), P3(-4.2), P2(-5) and P10(-1).

  Apart from temperature and conductivity, major ions composition does not show any significant trend related with groundwater zonation below the pond (see Table A1.1 in Appendix A). The role of nitrate and DOC in microbial community patterns is discussed further below.

2.3.2. Fitting groundwater microbial communities in the conceptual flow model

To characterize differences in microbial communities due to recharge, groundwater samples were subjected to molecular analysis. Post-processing of DGGE gels allowed for Non-Metric Multidimensional Scaling (NMDS), showing similarities among band patterns (Figure 2.4) and strong clustering of microbial communities. Samples from both scenarios were completely separated; blue squares (dry) and triangles (wet) represent groundwater samples and are clearly clustered in top and bottom halves of the plot, respectively. Moreover, samples from the wet scenario grouped according to water types. Types I and II are displayed on opposite sides; Types III and IV (mixed) are displayed in between. The two green triangles in the center of the plot correspond to groundwater samples from P10.

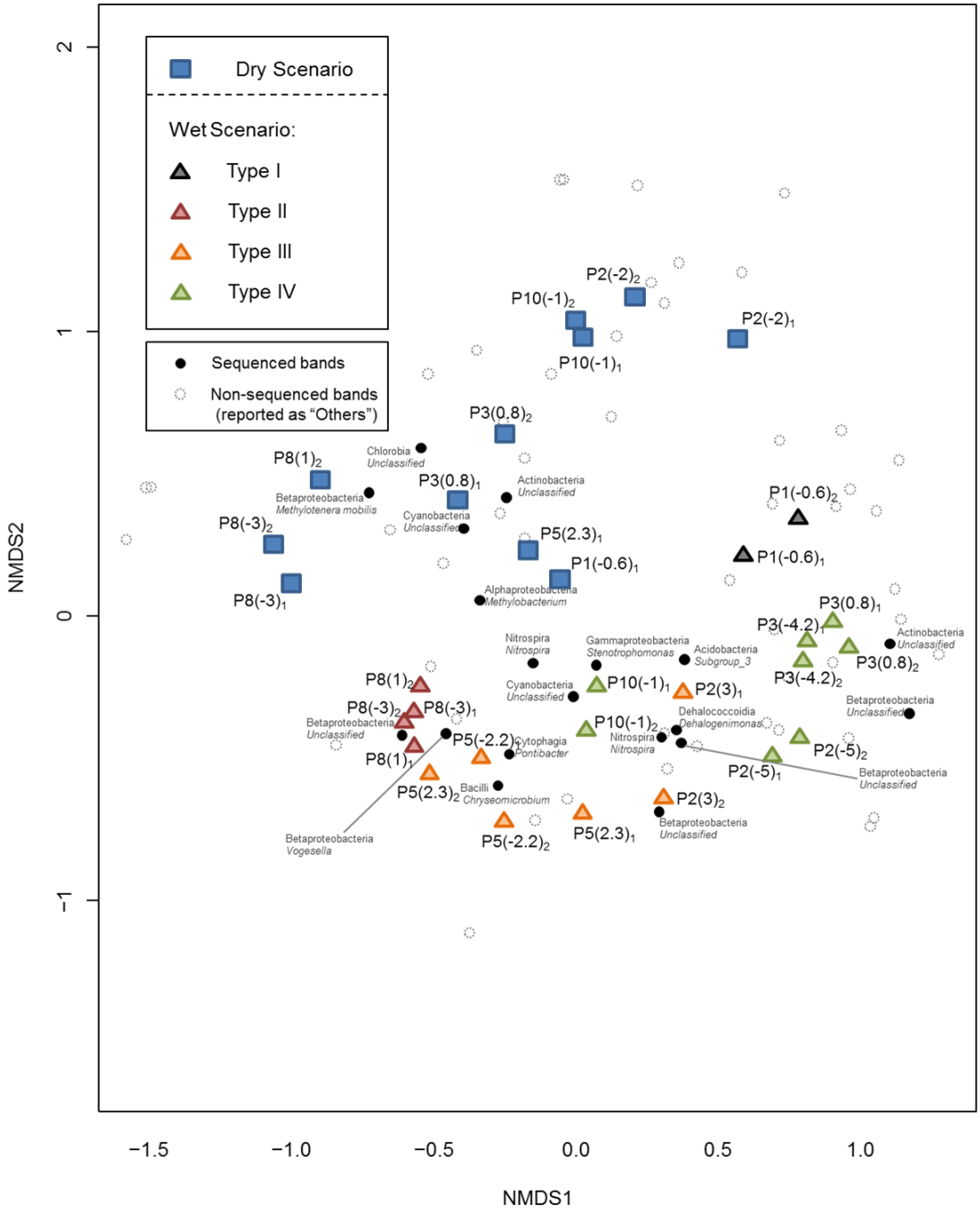

Figure 2.4 Non-metric Multidimensional Scaling clustering for all groundwater samples. Blue squares and triangles represent samples in dry and wet scenarios, respectively. Colors in triangles represent water types. Black circles correspond to band migration numbers in DGGE gels that were sequenced (phylogenetic affiliation corresponding to each black circle). Non-sequenced bands are also portrayed (empty circles). Discrete bands are also portrayed (circles), allowing linkage of the bands' contribution to sample assemblages. Filled circles report the class and genus of the sequenced bands, whereas empty circles symbolize non-sequenced bands

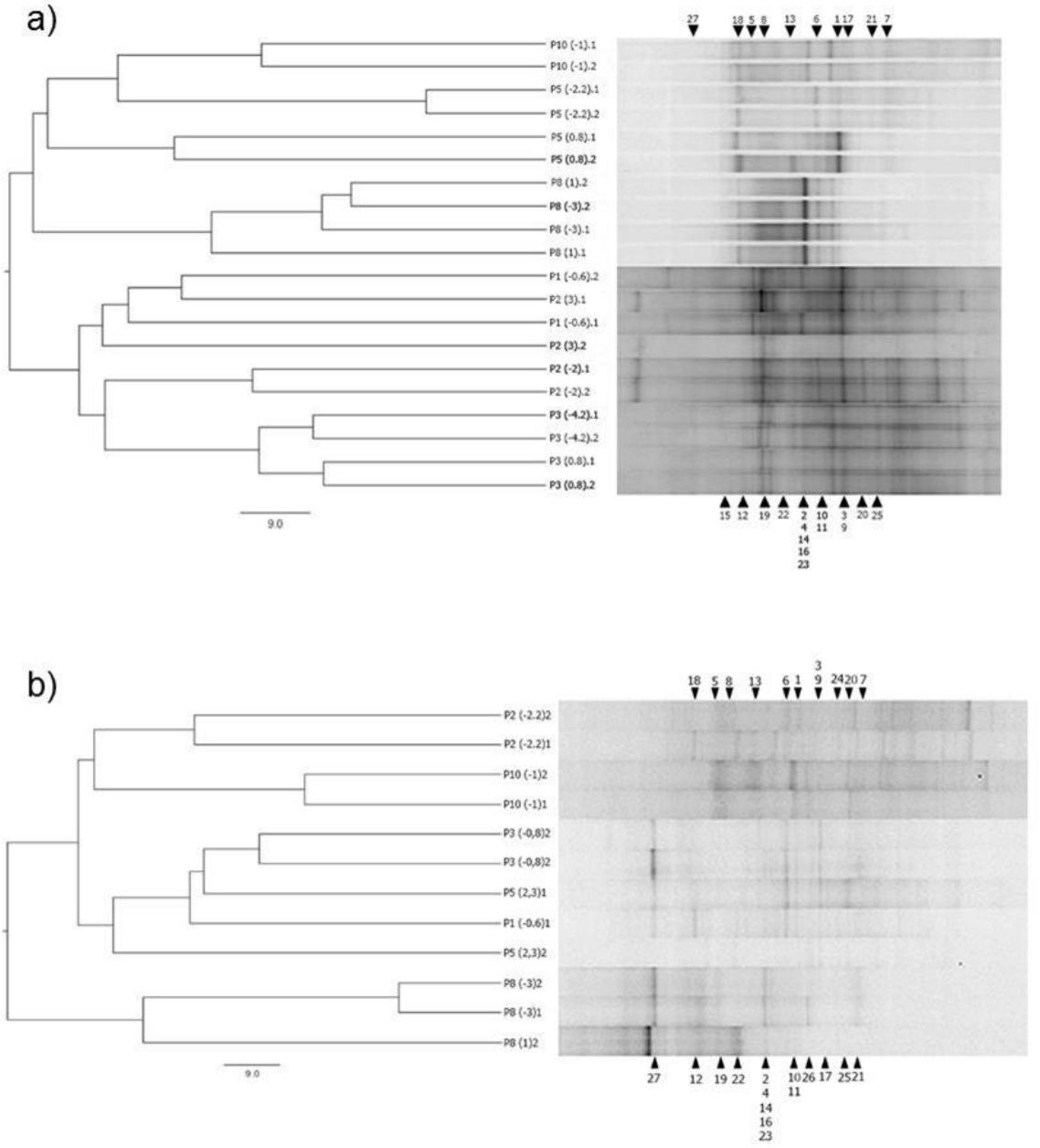

Figure 2.5 DGGE band patterns of bacterial 16S rRNA gene fragments and UPGMA cluster analysis for fingerprints obtained from wet (July 2014) (a) and dry (March 2015) (b) periods. Bar indicates 9% divergence. Each sample is defined by a code indicating piezometer number and sampling depth (see table 1). Black triangles indicate the position of bands recovered and sequenced, and numbers correspond to their phylogenetic affiliation (see table A1.2 in Annex A)

Figure 2.5 shows DGGE profiles and UPGMA clustering analysis of groundwater samples. The genetic fingerprints revealed high dissimilarities in the bacterial assemblage of about 70% and 80% during the active recharge period and the dry campaign, respectively (Figure 2.5). Moreover, most replicas grouped together, indicating sampling quality. Under active recharge (wet) conditions (Figure 2.5a), the dendrogram reproduces quite well the water types postulated by the conceptual flow model: in the first group, we can include four out of the five samples that were

strongly influenced by recharge (P5(-2.2), P5(2.3), P8(1) and P8(-3)); while in the second group, P2(3), P3(-4.2) and P3(0.8) clustered together with P1 (non-affected by recharge). In the dry campaign (Figure 2.5b), although no infiltration occurred, P8 appears separated from the other piezometers, indicating the still marked influence of the water infiltrated during the wet period, which occurred over four months earlier.

2.3.3. Spatial and temporal variations in microbial diversity indices in groundwater

The structure and processes of ecosystems change when a disturbance occurs (Grimm, 1994). Such changes in microbial communities have been quantified and described by means of diversity indices. Such indices, grouped according to water types during wet conditions, were ordered along an imaginary line from low to highly perturbed as a consequence of water infiltration (

Figure 2.6). The lowest diversity indices were obtained for the recharging water (Type II), indicating low species richness and a highly dissimilar proportion. In contrast, Type IV water, only slightly affected by water infiltration, displayed higher Shannon and Evenness indices, similar to Type I (unaffected by recharge).

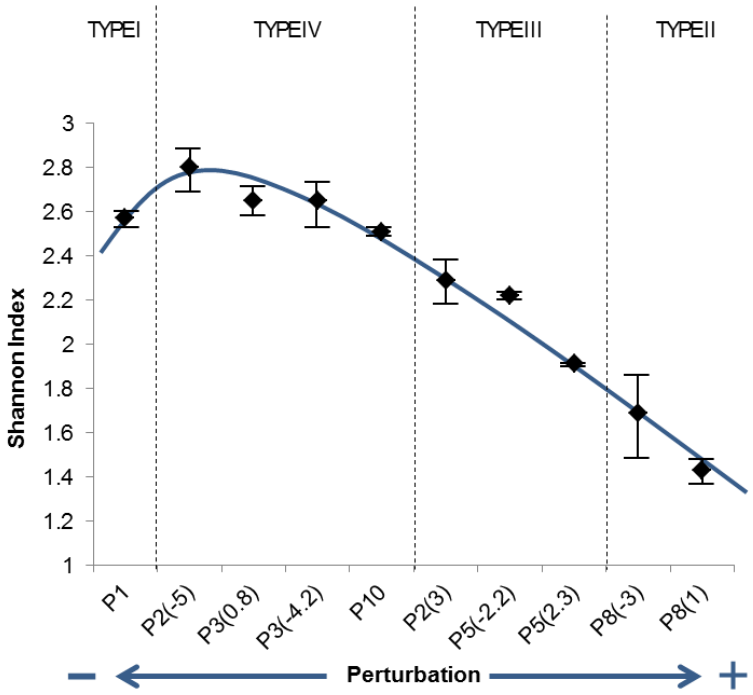

Figure 2.6 Average of Shannon Indices in piezometer samples under wet conditions. Standard deviation is shown in error bars. Horizontal axis reflects the degree of perturbation of original groundwater due to recharge

Table 2.1 Summary of Diversity Indices at the Llobregat MAR site in the different scenarios

Environment		Sampling location (**depth-***masl*-)	*Shannon (SD)**		*Richness (SD)**		*Evenness (SD)**	
			WET	**DRY**	**WET**	**DRY**	**WET**	**DRY**
Groundwater	T.I	P1-*BG* (**-0.6**)	2.57*(0.04)*	2.73	22 *(4.1)*	19	0.61*(0.01)*	0.64
	T.II	P8 (**1**)	1.43*(0.05)*	1.73	10 *(2.0)*	11	0.34*(0.01)*	0.41
		P8 (**-3**)	1.69*(0.20)*	2.03*(0.14)*	11	10 *(2.0)*	0.40*(0.05)*	0.48*(0.03)*
	T.III	P2 (**3**)	2.29*(0.13)*		18.5 *(7.2)*		0.54*(0.03)*	
		P2 (**-2**)		2.67*(0.13)*		18 *(2.0)*		0.63*(0.03)*
		P5 (**2.3**)	1.91*(0.01)*	2.41	14.5 *(1.0)*	14	0.45*(1·10-3)*	0.56
		P5 (**-2.2**)	2.22*(0.01)*		12.5 *(1.0)*		0.52*(2·10-3)*	
	T.IV	P3 (**0.8**)	2.65*(0.09)*	2.01*(0.28)*	21	10.5 *(3.07)*	0.63*(0.02)*	0.48*(0.07)*
		P3 (**-4.2**)	2.65*(0.13)*		20		0.63*(0.03)*	
		P2 (**-5**)	2.80*(0.12)*		23 *(4.1)*		0.66*(0.03)*	
		P10 (**-1**)	2.51*(0.20)*	2.49*(0.09)*	17	16 *(4.1)*	0.59*(0.01)*	0.59*(0.02)*
Water of basins		Pre-sedimentation	2.93*(0.28)*		29 *(14.3)*		0.69*(0.07)*	
		Infiltration entrance	2.78*(0.53)*		28.5 *(17.4)*		0.66*(0.12)*	
		Infiltration midfield	2.66*(0.14)*		25.5 *(3.1)*		0.63*(0.03)*	
		Infiltration end	2.58*(0.08)*		24 *(2.0)*		0.61*(0.02)*	
Soil of basins		Pre-sedimentation	2.89*(0.16)*		*25.5 (7.2)*		0.68*(0.04)*	
		Infiltration entrance	3.22*(0.09)*	2.93*(0.21)*	35.5 *(1.0)*	25 *(7.6)*	0.76*(0.02)*	0.69*(0.08)*
		Infiltration midfield	3.36*(0.14)*	2.90*(0.05)*	30.5 *(3.1)*	21	0.79*(0.03)*	0.68*(0.01)*
		Infiltration end	3.29*(0.05)*	2.40*(0.07)*	34 *(2.0)*	16	0.78*(0.01)*	0.57*(0.02)*

* Numbers in parenthesis after each index value indicate standard deviation, not reported whenever when the replica was damaged

2.3.4. Role of MAR activities for the microbial community structure

Prominent bands were recovered from the DGGE gels (Figure 2.5) and sequenced. Table A1.2 (Appendix A) shows the sequenced bands, their similarity values compared to the closest related GenBank sequences, and their phylogenetic affiliations. Overall, sequences fell into nine different bacterial phyla and eleven classes: Proteobacteria (Alphaproteobacteria, Betaproteobacteria, and Gammaproteobacteria), Cyanobacteria, Chloroflexi (Dehalococcoidia), Chlorobi (Chlorobia), Nitrospirae (Nitrospira), Acidobacteria, Actinobacteria, Firmicutes (Bacilli) and Bacteroidetes (Cytophagia) (Figure 2.7). The group designated as "Others" includes unclassified and non-sequenced fine bands.

The two main classes displaying the largest differences between the two scenarios are Betaproteobacteria and Dehalococcoidia, which were favored under recharge conditions. In particular, Dehalococcoidia is present in medium- and low-influenced waters, and it is absent from the high recharge-influenced groundwater (P8(1) and P8(-3)). This phylotype was identified at the genus level as *Dehalogenimonas sp* (Table A1.2). Similar behavior was found in the Nitrospira class, appearing in low-influenced groundwater in the wet scenario.

Patterns in the structure of microbial populations correlated with water types. For Type I, differences in the bacterial assemblage between both campaigns were attributed to seasonal changes (Table A1.2). Dehalococcoidia and Chlorobia were only detected in the wet scenario, while Cytophagia and Nitrospira could only be detected under dry conditions.

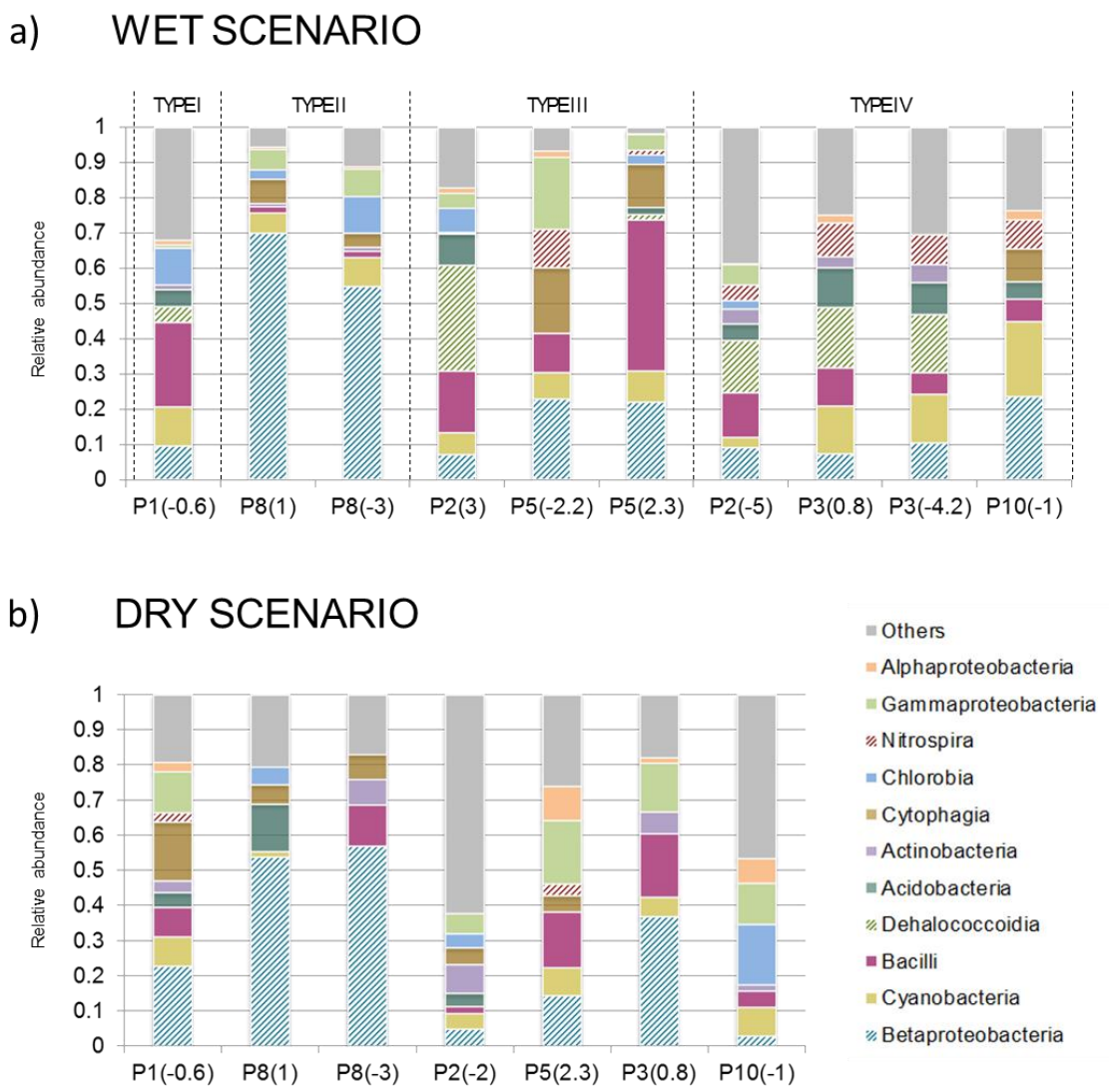

Figure 2.7 Bacterial community structure of groundwater samples. Class relative abundances calculated for wet (a) and dry (b) scenarios

During the active recharge period and for Type IV water, Dehalococcoidia was found in three out of four sampling points and was the most abundant phylotype. For Type III water, significant differences were observed among in the samples analyzed. Populations with the highest relative abundance in P5 (2.3) were Betaproteobacteria and Bacilli. The former was also prominent in P5(–2.2), together with Cytophagia, while Dehalococcoidia were dominant in P2(3). Finally, in the case of groundwater Type II (recharge water), the bacterial assemblage was dominated by members of the Betaproteobacteria class. During the dry period, no clear distribution patterns in the bacterial relative abundances at the phylum and class level were observed, in part due to the DGGE profiles, mainly composed by fine bands (Figure 2.5); these were difficult to recover and purify, and thus could not be characterized. However, it

should be mentioned that Betaproteobacteria were dominant in both P8 samples, contributing more than 50% to the relative abundance.

2.3.5. Microbial community indicators of MAR in soil and surface water

To study the impact of MAR on microbial community structure, recharge water from pre-sedimentation and infiltration basins, as well as soils, were analyzed. Figure 2.8 and Figure 2.9 show the relative abundance of bacterial phylotypes at the taxonomical level of classes for surface water and soil samples. The results are displayed according to the distance to the recharge basin inlet. Microbial richness in soil samples was controlled by water content. Non-recharge conditions had a primarily negative effect on the populations of Dehalococcoidia, Acidobacteria, and Chlorobia, but favored the presence of Nitrospira, Cytophagia and Actinobacteria (Figure 2.8). Shannon and Evenness indices demonstrated that soils were more diverse under wet conditions than under dry ones (**Table 2.1**).

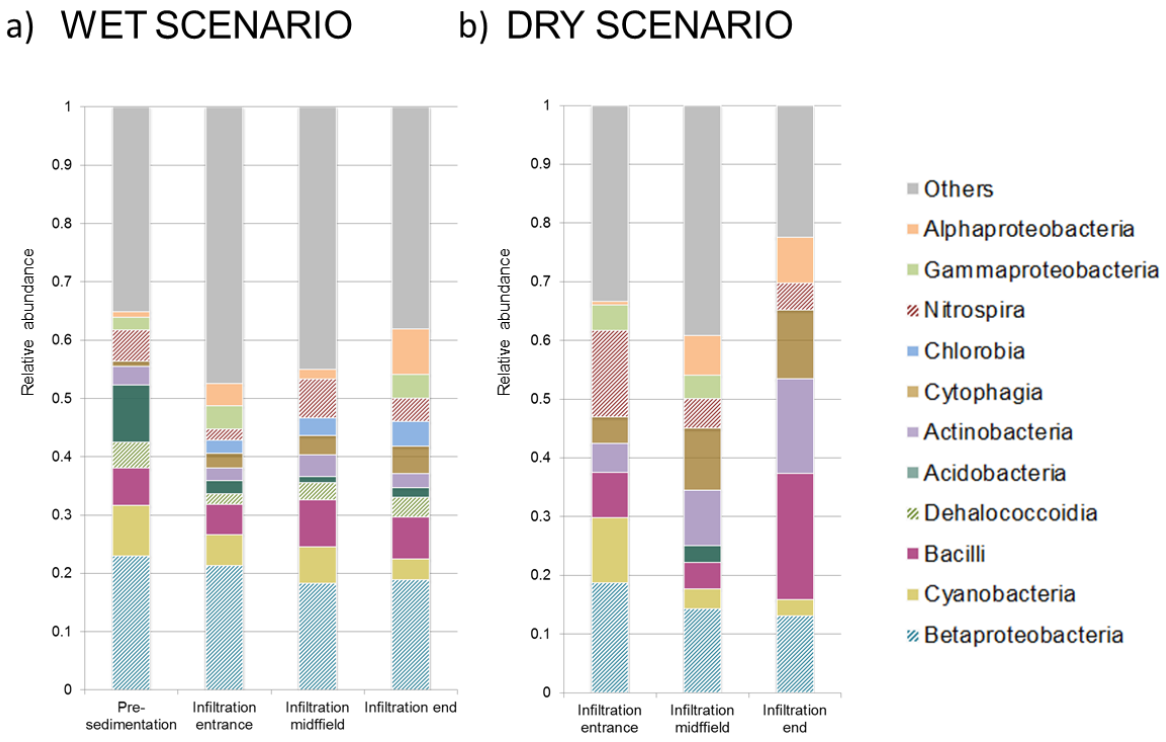

Figure 2.8 Bacterial community structure of soil samples from pre-sedimentation and infiltration basins. Class relative abundances calculated for wet (a) and dry (b) scenarios

For surface water samples (Figure 2.9), there was a decreasing gradient in community complexity along the ponds. Acidobacteria, Betaproteobacteria, and Cyanobacteria were the main phylotypes present.

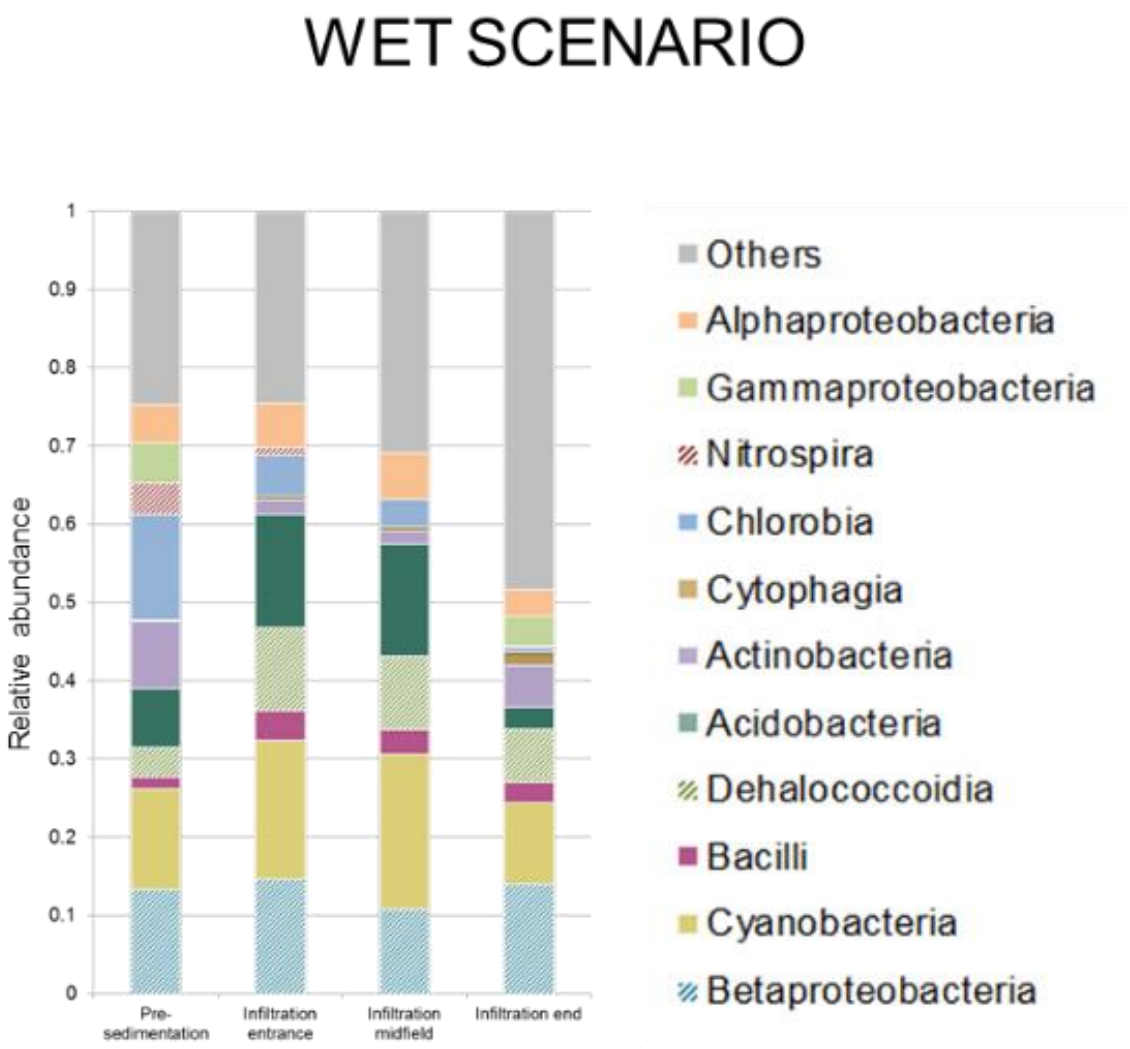

Figure 2.9 Bacterial community structure from water samples of pre-sedimentation and infiltration basins. Class relative abundance calculated for wet scenario

2.4. Discussion

2.4.1. Matching groundwater model, ecological disturbance principle and microbial community composition

Groundwater is a quite stable aquatic environment (Griebler and Lueders, 2009) as it is shown by the low variability in the hydrochemical data (Table A1.1). One could expect that microbial communities in groundwater should also display low variability that could be reflected in the diversity indices. In this way, piezometer P1, which is unaffected by recharge, showed stable diversity indices regardless of the sampling campaign. However, disturbances produced by recharge, evidenced by temperature and conductivity gradients below the pond (Figure 2.2 and Figure 2.3), favor the highest Shannon values for the intermediate-disturbed samples. As a

result, the average of diversity indices remains constant between both scenarios but with higher standard deviation during the wet scenario. These two facts combined, suggest that perturbations caused by recharge influence much more the composition of microbial communities in groundwater than the natural variability of the background aquifer water between scenarios.

MAR is a passive treatment technique that can provide simultaneously oxic and anoxic conditions (Maeng et al., 2011). This has wide implications for the potential biological removal of selected emerging contaminants, as each micropollutant is most efficiently removed under specific redox conditions (Schmidt et al., 2007). Some can even be degraded by co-metabolism, involving different redox states in the process (Rodriguez-Escales and Sanchez-Vila, 2016). In this sense, MAR is an efficient remediation system. In addition, many sequenced phylotypes, such as *Nitrospira sp*, *Stenotrophomonas sp,* and *Methylobacterium sp* have been associated with degradation capabilities (Cycoń et al., 2017; Daims et al., 2001; Wang et al., 2015). In short, the MAR microbial ecosystem studied in this work presents many more phylotypes than previous studies reported in groundwater systems (Logue et al., 2015), and thus, MAR can be considered an efficient remediation system.

We further tested the Intermediate Disturbance Hypothesis (IDH) for microbial communities in groundwater (Figure 2.4) related to MAR activities. IDH was originally proposed for tropical rainforests and coral reefs (Connell, 1978) and supports the idea that small perturbations create new access to resources for species which have overlapping niches, allowing their coexistence. This mechanism, known as a competition-colonization trade-off, can explain IDH in local communities, leading to an increase in diversity. However, when the degree of disturbance rises, only eurytolerant populations can survive and grow. Thus, an inverse correlation between diversity and the degree of disturbance (reflected in the temperature and conductivity profiles) was expected (see Table 2.1). Such correlations have also been reported in recharge wells and snowmelt-influenced aquifers (Ginige et al., 2013; Zhou et al., 2012).

In Sant Vicenç MAR system, the initial diversity in the microbial community increased with perturbation caused by recharge (

Figure 2.6), with maximum diversity associated with Type IV water, and lowest for the most disturbed water (Type II). In ecological terms, Type III and Type IV waters represent different proportions of perturbation.

In the most altered groundwater zone (represented by P8 samples), Betaproteobacteria grew above 50% of the relative abundance (Figure 2.7). The main phylogenetic affiliation of this phylotype at the genus level is *Vogesella*. Strains of this genus are able to catabolize monosaccharides under aerobic conditions, but not under low-oxygen conditions. Furthermore, all *Vogesella* strains are denitrifiers (Grimes et al., 1997). Indeed, P8, located below the pond, receives oxygen-rich water during the recharge process, driven by fingering in the vadose zone. Although dissolved oxygen was not measured in the present study, data from other campaigns confirm this behavior for oxygen in P8 samples (data not shown). Moreover, nitrate concentration in the surface water was low (Table A1.1), and thus most denitrification is expected to occur under the pond. Grau-Martínez et al. (2018) recently confirmed that nitrate was consumed via denitrification pathway under the infiltration pond in Sant Vicenç MAR system, supporting the idea that *Vogesella sp* could be one of the genera involved in nitrate consumption. Likely, depending on the oxygen content, *Vogesella sp* will adapt its metabolic function in favor of aerobic oxidation of organic matter or by means of denitrification, thus becoming a good indicator of highly-disturbed MAR environments.

For Type III and Type IV waters, *Dehalogenimonas sp*, within the Dehalococcoidia class, is characteristic of medium-disturbance groundwater (Figure 2.4 and Figure 2.7). Dehalogenimonas sp has been studied in recent years because some strains are associated with dechlorination in contaminated sites. This genus is strictly anaerobic and mesophilic, and some species can reductively dehalogenate polychlorinated aliphatic alkanes (Martín-González et al., 2015; Moe et al., 2009). As a result, recharge creates reducing conditions, likely indicating the existence of microzones or microsites (Bridgham et al., 2013; Hamersley and Howes, 2002), defined as local anoxic areas that coexist with fast-traveling oxygen-rich paths. Thus, microbial analysis can be used to unmask the apparent mishap of water samples that are oxic and display some typical anaerobic species. Moreover, some species of Dehalogenimonas can dechlorinate some Trichloroethane isomers (Dillehay et al., 2014), a pollutant reported in the Llobregat Lower Valley at levels as high as 300µg/L

(Valhondo et al., 2014), thus opening the door for the development of enhanced remediation activities.

The Evenness index is an indicator of the equity of a community and can be quite informative for observing perturbations to microbial communities. In the wet scenario, the lowest values of E were obtained for the samples most affected by recharge (Table 2.1), indicating that some species developed into predominant members of the microbial assemblage. Groundwater samples displayed the highest evenness values in the area less affected by recharge and in the dry scenario. In the latter case, values indicate the recovery of microbial communities from the disruption caused by recharge. In fact, P8(1) samples in the dry scenario were not fully consistent with this conceptual model, with low evenness index and very low nitrate concentration. Furthermore, the presence of *Methylotenera mobilis* (Betaproteobacteria class) in both P8 sampling points was more than 40%, on average, of the relative abundance. *Methylotenera mobilis* is a methylotroph species with denitrification abilities (Chistoserdova, 2011). These results suggest that P8 denitrification processes occur below the basin even when it is empty, indicating that four months is not enough time to revert back to natural conditions at this sampling point. This assumption is consistent with nitrate isotopic data presented in Grau-Martínez et al. (2018) and is also in agreement with the study of Rodriguez-Escales et al. (2016) in which biomass decay acted as an endogenous carbon source for respiration once the input carbon was reduced, maintaining denitrification rates.

2.4.2. Role of microbial populations in soil and surface water

We analyzed the heterogeneity of the microbial community structure in soil and surface water in terms of the distance to the infiltration basin entry point (Figure 2.8 and Figure 2.9) Patterns in surface water microbial composition are linked to sequential sedimentation processes as revealed by granulometric analyses of soil samples (Table A1.3 in Appendix 1). The result was that surface water became poorer in terms of the presence of microbial communities between the pre-sedimentation basin and the end of the infiltration basin. The main reason could be the decrease in solids suspended throughout the system due to the sequential decantation of particles and their attached biomass. Furthermore, surface water displays relatively higher values of Cyanobacteria and Acidobacteria classes compared to groundwater. Cyanobacteria constitute the largest, most diverse, and most widely distributed group of photosynthetic prokaryotes, which are capable of

conducting N fixation (Stanier and Cohen-Bazire, 1977). However, members of the phylum Acidobacteria are physiologically diverse and ubiquitous in soils, degrade a wide range of carbon sources (from substances with a wide range of complexity), and are capable of reducing nitrates and nitrites (Kielak et al., 2016). This heterogeneous effect with distance to the entry point of the basin is also observed in the diversity indices, which lose diversity with distance and are inversely correlated to the proportion of fine particles. Similar behavior for richness correlated to soil texture was reported elsewhere (Chau et al., 2011).

Differences in the microbial communities in soils between the two basins were concentrated in the large organic matter content provided by the reactive barrier present in the latter, being a source for the growth of bacterial communities and enhanced diversity under recharge conditions. The role of the humidity on microbial diversity is also significant, as was previously reported in horizontal subsurface constructed wetlands (Nurk et al., 2005). Furthermore, phylotypes distribution changes among scenarios. Whereas Dehaloccocoidia and Chlorobia classes appear in wet soils, Nitrospira, Cytophagia, and Actinobacteria are favored under dry conditions.

The role of the reactive layer at the infiltration pond could be extrapolated as a system fed with a considerable organic carbon load. Laboratory experiments and constructed wetlands demonstrate that concentration of microbial activity and TOC degradation is concentrated in the first centimeters of the filter material (Ragusa et al., 2004; Sleytr et al., 2007; Tietz et al., 2007) in response to oxygen concentration vertical distribution. Although rapid oxygen depletion and consequent denitrification conditions have been evidenced in lab-scale MAR experiments (Alidina et al., 2014a; Dutta et al., 2015), this effect may not happen rapidly under real infiltration conditions, where entrapped gas (Heilweil et al., 2004) or fingering processes (Kung, 1990) may provide higher oxygen concentrations than in lower dimension systems (e.g., columns). Lab-experiments are doubtlessly useful to elucidate the behavior of microbial communities under controlled conditions. However, sometimes it could exist a difficulty of transferring conclusions obtained from lab samples to real sites.

2.4.3. Transferability of results

The results of the present work are from a field experiment. This intrinsically means that is not performed under controlled conditions. Field studies are indeed realistic, but their transferability to other areas becomes challenging. However, some microbial and ecological approaches are comparable between experimental studies. In this way, the diversity indices are common calculations performed to assess the ecological state of a microbial community which allows comparing different communities (samples under different operational conditions in our case). Following an ecological argument, this study evidences that Intermediate Disturbance Hypothesis has been accomplished in Sant Vicenç MAR site. Therefore, we could expect the same behavior in other impacted areas under similar recharge conditions. Another information that could be useful for other scientific works is the role of some microbial species in the organic matter degradation and denitrification processes, such as the role of *Vogesella sp* and other key species discussed previously. The sequences of all species found were deposited into GenBank, so it represents a contribution to the genetic database and to the overall scientific knowledge.

2.5. Conclusions

This study aims at integrating different fields such as hydrogeology, ecology and microbiology applied to a real MAR facility, relating flow (infiltration) conditions, physicochemical water parameters, and microbial changes induced by managed recharge along the vertical transect. We observed that infiltration ponds modify the hydrochemistry and ecology of the groundwater environment, especially in terms of microbial communities. Comparing recharge and non-recharge scenarios, we found that microbial diversity indices (Shannon) correlate inversely with the degree of perturbation caused by the induced recharge, substantiating an Intermediate Disturbance Hypothesis distribution. In fact, MAR (surface) basins operation can promote different levels of disturbance at the same time, and microbial community structures change accordingly. From the microbial fingerprinting analysis, we observed the boosting of Betaproteobacteria and Dehalococcoidia classes correlate to recharge practices. Furthermore, genera such as *Dehalogenimonas*, *Nitrospira*, *Stenotrophomonas*, *Methylobacterium* were also detected, indicating a wide spectrum of biodegradation capabilities. Likewise, sequencing tasks revealed characteristic phylotypes from each water type, particularly *Vogesella sp* for highly perturbed water or *Dehalogenimonas sp* for medium-perturbed water. Microbial

populations in the soil are quite diverse when comparing wet with dry scenarios. Soil moisture and sediment grain size appear to be the key factors explaining diversity patterns. Furthermore, variation in recharge conditions does not translate immediately to changes in communities. All these results combined confirm the difficulty of extending laboratory experiment results to the field scale.

CHAPTER 3: THE ROLE OF WATER QUALITY AND SOIL CHARACTERISTICS IN SOME DOMINANT MICROBIAL SUB-SURFACE POPULATIONS

3.1. Introduction

Groundwater systems are perceived as relatively stable environments as compared to most aquatic ecosystems (Zhou et al., 2012). Despite that, investigations have shown that soil-aquifer systems support a wide diversity of organisms (e.g. Griebler and Lueders, 2009). Actually, the unsaturated zone, and more specifically the topsoil, supports the highest microbial activity and biomass of all compartments within the subsurface environment (Lapworth et al., 2012). Likewise, microorganisms are responsible of most biological processes in aquifers (Stein et al., 2010).

Several studies evidence microbial adaptation to groundwater extreme environments (thermal or hypersaline) (e.g. Rothschild and Mancinelli, 2001) or disturbed by human activities (Meckenstock et al., 2015). Human activities have caused disruption in aquifer dynamics to some extent (Griebler and Lueders, 2009; Zhu et al., 2017), with biological implications as indigenous microorganisms can acclimate (Pett-Ridge and Firestone, 2005) or even take advantage (Rezanezhad et al., 2014) to these environmental disturbances.

In fact, the water treatment industry has taken advantage of the adaptability and metabolic capabilities of microorganisms to maximize the improvement of water quality. Several laboratory studies and engineering applications have tested the effectiveness of microbial engineered techniques for water reclaim purposes. Laboratory experiments have been conducted aiming at (1) describing specific targets, such as metabolic rates and degradation pathways of specific pollutants, and quantifying degradation rates (Greskowiak et al., 2017; Regnery et al., 2015; Rodriguez-Escales and Sanchez-Vila, 2016), (2) determining the physical and hydrochemical conditions that can govern the behavior of specific microbial groups (Alidina et al., 2014b; Drewes et al., 2014; Freixa et al., 2015; Kolehmainen et al., 2008; Perujo et al., 2017) or (3) understanding the role of organic matter (i.e., dissolved organic carbon -DOC- or micropollutants), on the growth of microbial communities (Li et al., 2013, 2012). Regarding the engineered applications of microbial ecology designed to improve the quality of reclaimed water, some examples are constructed wetlands (Faulwetter et al., 2009; Truu et al., 2009; Zhang et al., 2018) and sand filters (D'Alessio et al., 2015).

Natural and induced microbial attenuation have been studied and applied at the field scale concerning groundwater related environmental issues. This includes, e.g.,

landfill leakage affections (Röling et al., 2001; Staats et al., 2011), contaminant spills (Fahrenfeld et al., 2014; Haack et al., 2004; Martínez-Pascual et al., 2010; Nijenhuis and Kuntze, 2016), or nitrate polluted aquifers (Bellini et al., 2018, 2013).

In the recent years, soil aquifer treatment (SAT) facilities are increasing in number worldwide. These MAR techniques combine the replenishment of groundwater bodies with the treatment of water during infiltration, by taking advantage of the potential of the subsurface microbial communities degradation potential (Bouwer, 2002). Studies testing the link between water quality and microbial communities in MAR systems can be separated depending on the system type, whether recharge wells (Ginige et al., 2013), riverbank areas (Schütz et al., 2009), or surface infiltration ponds (Reed et al., 2008; Regnery et al., 2016). Infiltration ponds are low-cost, low-tech, passive facilities compared to advanced water treatment methods (Drewes et al., 2003; San-Sebastián-Sauto et al., 2018); for these reasons, they are widely implemented, mostly in arid or semi-arid environments (Goren et al., 2014; Greskowiak et al., 2006; Rodríguez-Escales et al., 2018).

Biodegradation processes linked to surface infiltration ponds include aerobic oxidation of DOC (Maeng et al., 2011; Mermillod-Blondin et al., 2015), denitrification (Grau-Martínez et al., 2018), and fate of selected emerging organic contaminants (Hamann et al., 2016; Valhondo et al., 2015). Parameters modifying bioprocesses, such as DOC availability, dissolved oxygen content, redox conditions, temperature, nutrient concentrations, or soil moisture have been widely studied (Alidina et al., 2015; Bekele et al., 2011; Dutta et al., 2015; Goren et al., 2014; Greskowiak et al., 2005a; Hellauer et al., 2017; Laws et al., 2011; Massmann et al., 2006; Rezanezhad et al., 2014). Apart from environmental parameters, intrinsic properties of the porous media (e.g., porosity and pore size distribution), determine the spatial and temporal distributions of microorganisms in soils (Chau et al., 2011). Physical and hydraulic characteristics of soils condition the availability of pore space and the access to nutrients, thus affecting in a distinct way the growth and activity of microorganisms (Perujo et al., 2018, 2017).

Subsequently, determining how much and to what extent physical, geochemical, biological and operational parameters influence the system functioning is useful for managing purposes (Dutta et al., 2015; Grau-Martínez et al., 2018; Hellauer et al., 2017; Pedretti et al., 2012a; Rodríguez-Escales et al., 2017). Despite of that, it is difficult to find multidisciplinary research dealing with integrated approaches to

improve understanding of infiltration problems. We contend that a full analysis of processes occurring at the surface recharge system should involve the simultaneous use of physical, hydraulic, geochemical, microbial structure, and metabolic potential; therefore, the problem involves the simultaneous analysis of continuous, discrete and categorical data, with different resolution windows. A rigorous analysis to combine datasets with different variable types and various available data for each individual variable involves the use of multivariate statistical techniques. Such techniques have been widely used in hydrogeology to understand and to accompany stochastic numeric and conceptual groundwater models (e.g. El Alfy et al., 2017; Menció et al., 2012). In the case of microbial ecology, the development of molecular analyses allowed the generation of large data sets that are best treated using multivariate (MV) statistical techniques. As an example, Paliy and Shankar (2016) reviewed the different existing applications and provided some examples of the use of MV techniques in microbial ecology.

In this work, we aim at combining both the ecological and hydrological approaches to understand sub-surface microbial community distribution under the recharge changing conditions of Sant Vicenç MAR system. For this purpose, we compiled a physical-bio-geochemical dataset (data from Chapter 2). We then applied Principal Component Analysis (PCA), aiming at statistically discriminate the relationships among microbial community structure and geochemical variables, grain size distribution of soil samples, or operational conditions (recharge/no recharge). The specific objectives were to provide the most relevant microbial indicators present in the system and to correlate them with soil and groundwater local characteristics. Furthermore, the existing data between microbial clades both in water and soil were also analyzed separately to obtain further relevant inter-clade correlations.

3.2. Methodology

The present chapter is built on the dataset provided in Chapter 2. Therefore, the methodology to obtain raw data for the statistical analysis is also explained in section 2.2 of Chapter 2. In this section is provided only the essential information to contextualize the statistical analysis.

3.2.1. Input data for the multivariate statistical approach

As presented in the previous chapter, water and soil samples were taken in two different periods, July 2014 and March 2015, representing different recharge

operation conditions. Figure 3.1 shows again the conformation of the piezometric network and adding P9 and soil samples location with respect to the previous study.

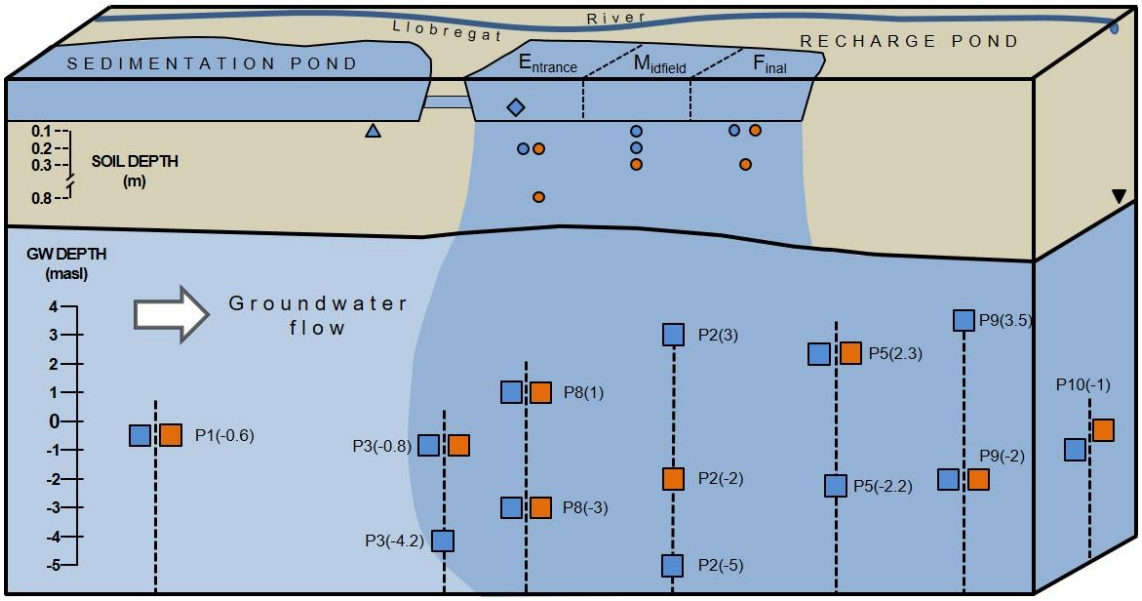

Figure 3.1 Cross-section of Sant Vicenç MAR system. Triangle and circles represent the location of soil samples. Diamond and squares represent those of water and groundwater samples, respectively. Blue symbols indicate samples taken in July 2014, after six months of continuous uninterrupted recharge. Orange samples were taken after recharge was discontinued for 4 months in March 2015

In total, 21 water samples (20 for groundwater and 1 for recharge water) and 10 soil samples were subjected to molecular analyses, in duplicate (only average values are presented in this work). Furthermore, water samples were hydrochemically characterized, while granulometric curves were obtained for the soil samples. The sampling and analysis methodologies for chemistry, granulometry, DNA extraction, PCR, DGGE, diversity indices and relative abundances of the microbial clades, are reported in Chapter 2.

The statistical analyses performed in this chapter, grouped samples according to their nature and their associated variables. Soil as in water samples is studied separately, as different variables are included in each case. In the case of the water samples, the statistical analysis took into account (1) microbial diversity indexes, (2) relative microbial abundances at the taxonomical rank level of class and species, and (3) hydrochemical characterization of samples (major, minor and trace elements). While statistical analyses of soil samples contained (1) microbial diversity indexes, (2) relative microbial abundances at the taxonomical rank level of class and species, (3) grain-size distribution representative parameters, (4) depth, and (5) an operational binary variable indicating the sampling campaign. Finally, a general statistical analysis was performed for all soil and water samples (31 in total) and

their variables in common, that is, (1) microbial diversity indexes, (2) relative microbial abundances at the taxonomical rank level of class and species and (3) a binary variable indicating the nature of the sample (soil or water).

3.2.2. Rationale for the multivariate statistical approach: requirements for PCA

Multivariate statistics is a useful technique to treat large datasets involving different types of variables, from quantitative to categorical. In short, PCA transforms a set of data values of variables that in principle are correlated into a set of values of linearly uncorrelated variables called principal components. Principal components are defined such that the first one accounts for as much of the variability in the data as possible, and each succeeding component, in turn, has the highest variance possible under the constraint that it is orthogonal to the preceding components. Thus, a multidimensional system in terms of variables is projected into a low dimensional map of components. Solutions were subjected to a varimax rotation. This implies the rotation of the original system corresponding to the directions of the largest variance in the dataset. Statistical analysis was done using software SPSS (IBM SPSS Statistics 24).

3.2.3. Selecting variables for the statistical analysis of water samples

Statistical parametric methods perform best when data follows a unimodal symmetric distribution (Paliy and Shankar, 2016). For this reason, some variables from the initial dataset were eliminated, grouped and/or transformed in order to conform better to the assumptions of PCA analysis.

For example, hydrochemical variables with most values below the detection limit were eliminated (this is the case of Al, B, Cd, Co, Fe, Pb, and P). Also, Ba concentration values were rejected for data inconsistency. Second, non-Gaussian hydrochemical variables were transformed to log concentrations (Cu, DOC, Ni, S, and V). Contrarily, depth, electrical conductivity (EC), temperature, and the concentrations of HCO_3, Ca, Cl, Li, Mg, Mn, Na, NO_3, pH, Si, SO_4, and Zn were added to the analysis as raw data without any transformation.

With reference to variables of microbial abundances, they were all transformed into new variables. For ecological data, displaying a large number of zero values, (Legendre and Gallagher, 2001) recommend applying either the Chord or the

Hellinger transformations to data values. In our case, we applied the latter one, because, after some preliminary analyses, the transformed variables presented higher correlation coefficients (r^2) than the non-transformed ones. Hellinger transformation (x'_{ij}) of a datum x_{ij} pertaining to the i -class and j -object, is:

$$x'_{ij} = \sqrt{\frac{x_{ij}}{\sum x_{i+}}} \tag{3.1}$$

where $i+$ denotes all i's.

Finally, in the case of microbial diversity indices, the input data for the PCA were directly the Shannon, Richness and Evenness index values for each sample.

Once established the variables for the analysis, the next step was to perform a bivariate correlation analysis with all variables taken two by two, including hydrochemical variables (both raw and log-transformed; actually this was the way of selecting whether the log-transformation was finally applied or not) and Hellinger-transformed microbial variables in order to select the ones that would be used in the final analysis. Since the aim of the statistical analysis was to emphasize the correlations with the microbial data, most redundant geochemical variables, as well as those which displayed very low values of the r^2 coefficient to the biological ones, were removed. This was the case of As, HCO_3, Ca, Li, Mg, Mn, Si, Zn, and also depth, pH, and temperature. In the case of microbial phylotypes, some of them were eliminated because they did not show significant correlations with other variables; this is the case of Bacilli, Acidobacteria, Actinobacteria, Chlorobia, Nitrospira, Gammaproteobacteria, Alphaproteobacteria, *Subgroup3 sp* (Acidobacteria), *Stenotrophomonas sp, Chryseomicrobium sp, Nitrospira1 sp, Methylobacterium sp,* and *Nitrospira2 sp*.

The selected variables could not be incorporated all together in a single PCA because the total variance was too high to allow proper discrimination of components. Then, different PCAs (each one involving a different subset of parameters) were performed, trying to maximize the amount of explained information. We performed two PCAs for microbial abundances at the class level and two more at the species level; each of these four included all the variables that were (even if mildly) correlated. The most informative set of variables were selected as the subset that maximized the measure of sampling adequacy reported by Kaiser-Meyer-Olkin test (KMO); the variables included in each analysis are provided in **Table 3.1**.

3.2.4. Selecting variables for the statistical analysis of soil samples

Soil samples described in the previous chapter were subjected to sieve analysis, obtaining grain-size distribution curves. For each sample, the uniformity coefficient (*CU*) and the coefficient of curvature (*CC*) were calculated as Terzaghi et al. (1996): $CU=\frac{D_{60}}{D_{10}}$, $CC=\frac{(D_{30})^2}{D_{60}\cdot D_{10}}$, where D_{60}, D_{30} and D_{10} are the diameters so that 60%, 30% and 10% of the material (in weight) pass the corresponding sieve. D_{10} has also been used as one of the variables in the statistical analysis. Another variable incorporated in the analysis was the proportion (in weight) of fine material (<0.074 mm) for each sample. Soil samples depth and sampling campaign (operation) were also included.

The same procedure as that performed for the water samples followed, stated with the bivariate correlation analyses. However, here Hellinger transformation was not applied to relative abundances of microbial species, because correlations were high already for the raw relative abundances. Some microbial variables were removed for the final analyses, based on the low bivariate r^2 coefficients obtained (this was the case of Cyanobacteria, Nitrospira, Gammaproteobacteria, Alphaproteobacteria, *Stenotrophomonas sp, Chryseomicrobium sp,* and *Nitrospira1 sp).*

Here, the optimization between the number of PCAs, the measurement of sampling adequacy (KMO) and the number of considered variables was done following the same criteria as indicated in the statistical analysis of the water samples.

3.2.5. PCA for microbial print in water and soil samples

Taking advantage of the shared variables by water and soil samples, a third statistical analysis was performed, now including all 31 samples (soil and water) together. Microbial classes and microbial species were treated separately and were Hellinger transformed. In addition to microbial data, the type of sample was also included as a binary variable. From the bivariate correlation analysis, some variables were removed from the final statistical analysis: Cyanobacteria, Gammaproteobacteria, Alphaproteobacteria, *Methylotenera mobilis, Vogesella indigofera, Stenotrophomonas sp, Chryseomicrobium sp, Methylobacterium sp,* and *Nitrospira2 sp*. The optimization criteria were the same as indicated in the two previous sections.

3.3. Results

As a consequence of the preliminary analysis, PCAs of water samples considered 10 hydrochemical variables, 2 diversity indices and 10 microbial variables (5 classes and 5 species). PCAs of soil samples took into account 1 operational variable, depth, 4 grain-size soil parameters, 3 diversity indices and 14 microbial variables (7 classes and 7 species). Finally, the statistical approach for the total of 31 samples (soil and water) included 3 diversity indices, the type of sample and 13 microbial variables (9 classes and 4 species).

We present firstly global results of the eleven PCAs performed (**Table 3.1**). We indicate, in the same table and for each statistical analysis performed, the extracted components with their variables and the proportion of variance represented for each component. Also, the measure of sampling adequacy (KMO test value) is reported for each analysis.

3.3.1. Key parameters influencing microbial classes in surface water and groundwater

Two PCAs were developed; the first one (PCA1 in **Table 3.1**) included Shannon and Richness indices, Cl, EC, Na, the log transformations of S, Cu, and V, as well as Betaproteobacteria$_H$, Dehalococcoidia$_H$, Nitrospira$_H$, and Others$_H$ classes. The group "Others" includes microbial classes that could not be classified. Results of this PCA show that these twelve variables could be well explained with only two principal components (that combined explained 74% of the total variance). The strength of the analysis is supported by a value of 0.744 in the KMO test. Results of a 2D representation of varifactors and components (Figure 3.2) show the significance of hydrochemistry beyond microbial variables. All the chemical variables included in the analysis are grouped in the first component, showing a high correlation amongst them; Na, Cl, EC and Cu-log ("-log" indicates log-transformed) are positively correlated, whereas V-log and S-log are situated in the opposite side of the plot (negative correlation).

Table 3.1 Relation to main correlations among variables obtained by PCA analysis (inverse correlations in bold). Subscript "H" in microbial variables indicates that Hellinger transformation was applied to the data. –log in geochemical variables indicates that log transformation was performed

Type of sample	Microbial clade data treated	PCAs performed	PCA number	Extracted components	% of variance	KMO Test value
Water	Classes	2	PCA_1	C1: **V-log**, Cu-log, Cl, EC, **S-log**, Na, **Others$_H$**	46.9	0.744
				C2: Shannon, **Betaproteobacteria$_H$**, Dehalococcoidia$_H$, Richness	27.2	
			PCA_2	C1: Cyanobacteria$_H$, EC, Cl, Cu-log, Ni-log	52.6	0.701
				C2: **Cytophagia$_H$**, Richness	24.4	
	Species	2	PCA_3	C1: *Methylotenera_mobilis*$_H$, NO_3, SO_4, **DOC-log**	61.5	0.797
				C2: *Nitrospira_sp2*$_H$, EC, Na, **V-log**, Cu-log, Cl	15.4	
			PCA_4	C1: ***Pontibacter_sp*$_H$**, *Dehalogenimonas_sp*$_H$, Richness	52.9	0.635
				C2: *Vogesella_indigofera*$_H$, Shannon, DOC-log	24.3	
Soil	Classes	2	PCA_5	C1: **Betaproteobacteria$_H$**, Actinobacteria$_H$, Dryness, Depth, Cytophagia$_H$	62.5	0.750
				C2: CU, % Fine, Acidobacteria$_H$	22.1	
			PCA_6	C1: Richness, Dehalococcoidia$_H$, Chlorobia$_H$	75.5	0.727
				C2: Shannon, Evenness, **Actinobacteria$_H$**, **Bacilli$_H$**	12.3	
	Species	2	PCA_7	C1: *Nitrospira_2sp*, Dryness, **Shannon**, *Pontibacter_sp*,	64.6	0.758
				C2: % Fine, *Subgroup3_sp*, CU	27.6	
			PCA_8	C1: CC, D10, *Methylotenera_mobilis*, *Methylobacterium sp*,	59.5	0.640
				C2: % Fine, CU, *Dehalogenimonas_sp*, *Vogesella indigofera*	23.9	
Water and soil	Classes	2	PCA_9	C1: Shannon, Richness, Actinobacteria$_H$, Type, Evenness	53.8	0.692
				C2: Others$_H$, **Betaproteobacteira$_H$**	16.4	
				C3: Bacilli$_H$	12.5	
			PCA_{10}	C1: Shannon, Evenness, Richness	44.0	0.696
				C2: Dehalococcoides$_H$, **Cytophagia$_H$**, Acidobacteria$_H$	26.4	
				C3: Nitrospira$_H$, **Chlorobia$_H$**	14.4	
	Species	1	PCA_{11}	C1: Shannon, Richness, Evenness, Type, *Nitrospira_sp1*$_H$	48.8	0.705
				C2: ***Pontibacter_sp*$_H$**, *Dehalogenimonas_sp*$_H$, *Subgroup3_sp*$_H$	25.5	

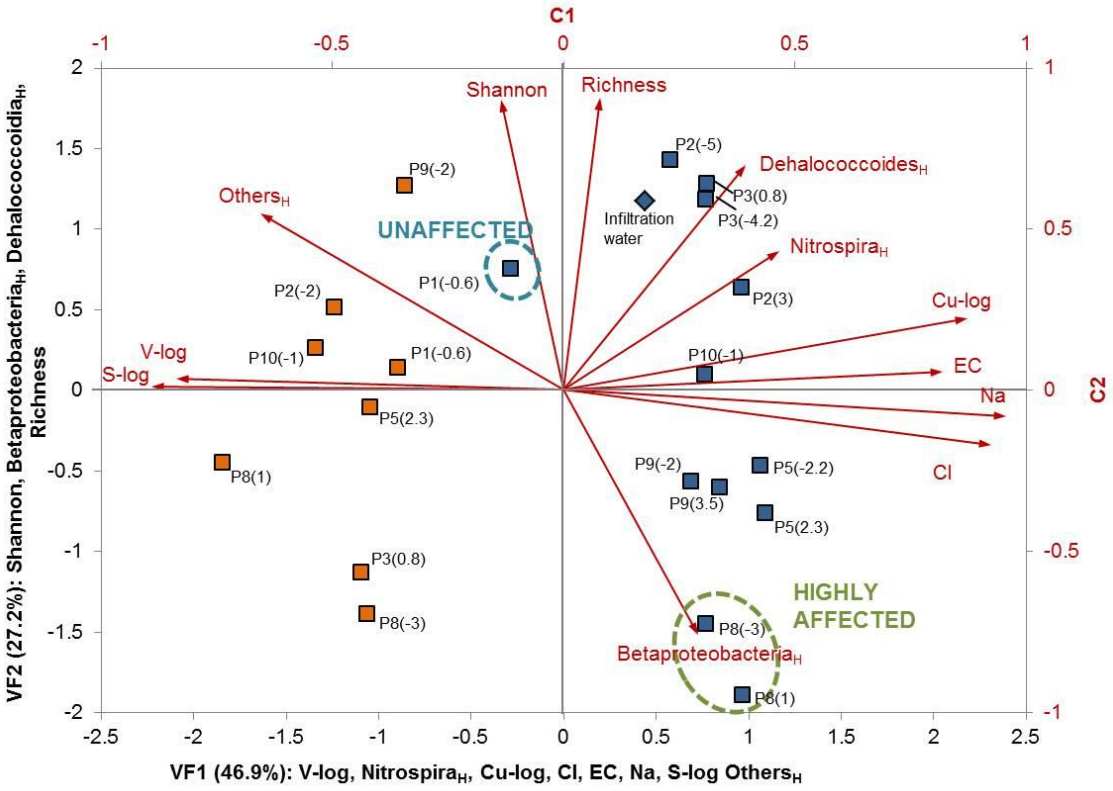

Figure 3.2 PCA$_1$ analysis including diversity indices, microbial classes and hydrochemical data from groundwater samples (squares) and one infiltration water sample (diamond) during the recharge period (blue) and no-recharge period (orange). The position of samples is scaled in VF1 and VF2 axes for visualization purposes. Red arrows represent the contribution of each variable projected into the varifactor plane. Samples are labeled corresponding to the sampling point and the height (meters above sea level, or masl) indicated in brackets. The symbols assignment follows the same criteria in all PCA plots.

The second component relates inversely the presence of Betaproteobacteria$_H$ to the Shannon and Richness indices. Furthermore, Betaproteobacteria$_H$ has a particular importance in the samples most affected by recharge (piezometer P8, located directly below the infiltration pond). Finally, the projection of sample data in the plane composed of the two varifactors (VF1, VF2) clearly separate data according to the operational period (recharge/no-recharge). Moreover, the sample not affected by recharge (P1, placed upstream) is displayed in between the samples corresponding to the no-recharge and recharge periods.

The second PCA (Figure 3.3, PCA$_2$ in Table 3.1) also separates data corresponding to operational periods in the VF1-VF2 plane. Furthermore, two groups of variables can be distinguished. The first one relates Cyanobacteria$_H$, Cl, EC, Cu-log, and Ni-log. Apart from hydrochemical differences that force the separation of samples between operational periods, Cyanobacteria are more abundant in the groundwater

samples in the recharge period. Component 2 shows an inverse correlation between Richness and Cytophagia$_H$.

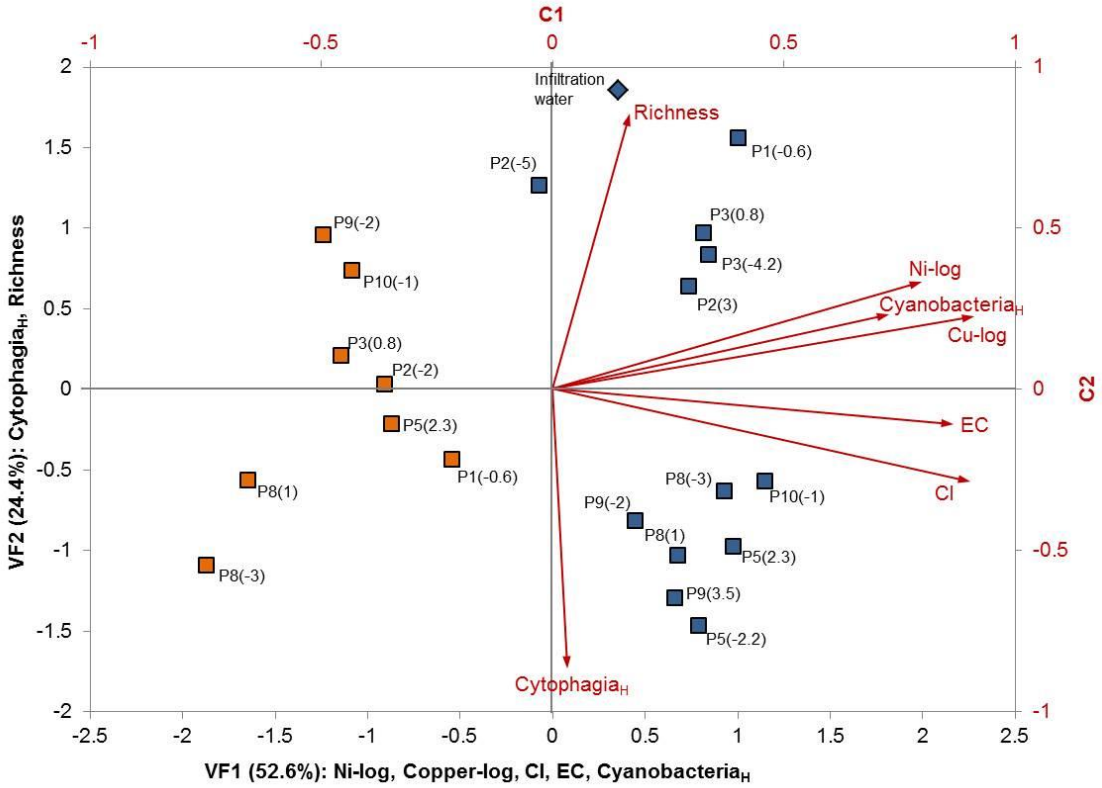

Figure 3.3 PCA$_2$ analysis with microbial classes and hydrochemical data from groundwater samples (squares) and the infiltration water sample (diamond) during the recharge period (blue) and during the no-recharge period (orange). The position of samples is scaled in VF1 and VF2 axes. Red arrows represent the contribution of each variable in both Varifactors

3.3.2. Key parameters influencing microbial species in water samples

PCA$_3$ analysis (Table 3.1) included variables EC, Na, Cl, V-log, Cu-log, NO_3, SO_4, DOC-log, and two microbial species (as opposed to microbial classes, that were the objective of PCA$_1$ and PCA$_2$): *Methylotenera mobilis$_H$* and *Nitrospira sp2$_H$*. From the projection on the varifactor plane (Figure 3.4), samples corresponding to operational conditions clearly display on different areas within the plot. Furthermore, samples taken during active operation display a disturbance degree caused by recharge (indicated in qualitative terms by the blue arrow). On the other hand, the sample representing background conditions (P1) is located separated from the rest, indicating that in no recharge periods the areas that were recharged kept some memory of the events, i.e., the microbial communities did not go back to the pre-recharge conditions.

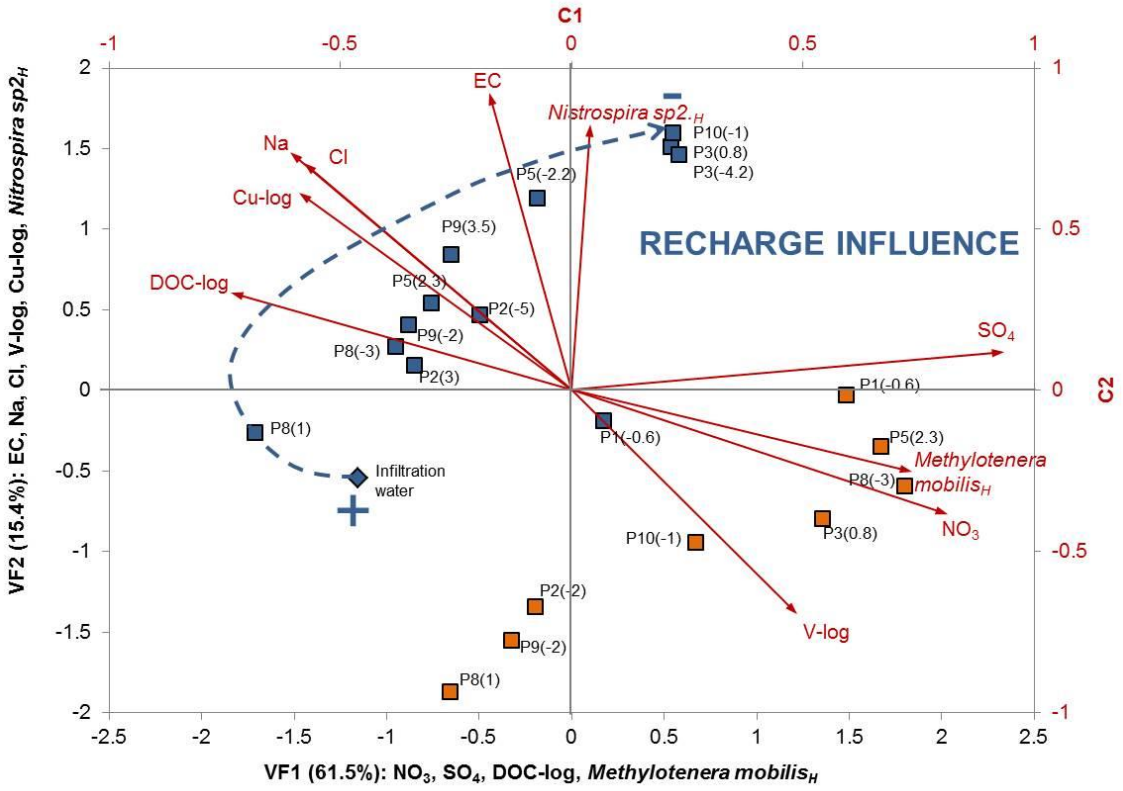

Figure 3.4 PCA$_3$ analysis including diversity indices, microbial species and hydrochemical data from groundwater samples (squares) and one infiltration water sample (diamond). The discontinuous blue arrow indicates disturbance degree caused by recharge.

Figure 3.4 also shows the main relations amongst variables. The first component groups mainly SO_4, NO_3 and DOC-log (inversely) with *Methylotenera mobilis*$_H$. The behavior of *Nitrospira sp2*$_H$ and its high correlation with conductivity were explained by the second component.

PCA$_4$ indicated a relationship between *Dehalogenimonas sp.*$_H$, *Pontibacter sp.*$_H$ and *Vogesella indigofera*$_H$ with some hydrochemical and biological indicators (Figure 3.5). *Dehalogenimonas sp.*$_H$ appears to be a key contributor to Richness and Diversity indices and in turn, is inversely correlated with *Pontibacter sp.*$_H$. However, *Vogesella indigofera*$_H$ *is* correlated with DOC-log (Figure 3.5), placed in the vicinity of the P8 samples projection, indicating the effect of recharge on both variables.

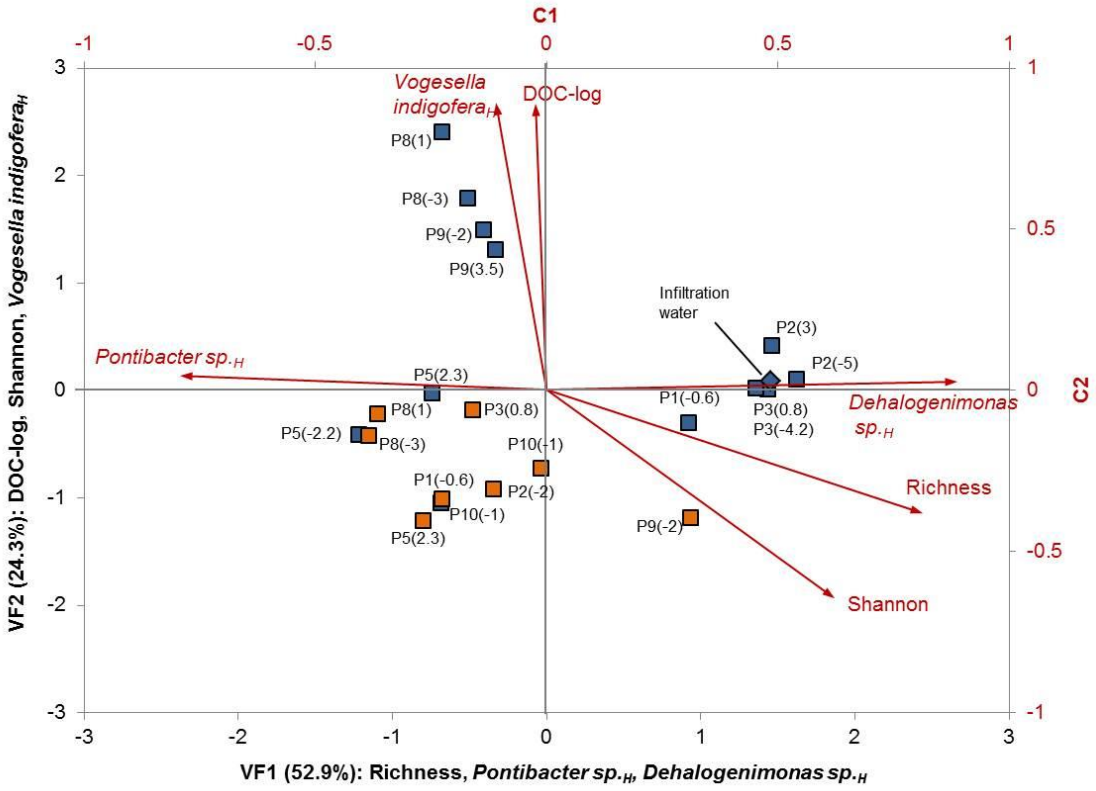

Figure 3.5 PCA$_4$ analysis with microbial species and hydrochemical data from groundwater samples (squares) and the infiltration water sample (diamond) during the recharge period (blue) and during the no-recharge period (orange). The position of samples is scaled in VF1 and VF2 axes. Red arrows represent the contribution of each variable in both Varifactors

3.3.3. Key parameters influencing microbial classes in MAR soils

PCA$_5$ to PCA$_8$ provide statistical analyses for samples taken from soils. Here, the parameters extracted from the grain-size distribution curves are included, together with microbial variables, depth, and the operational variable. In all cases, the position of samples is scaled in VF1 and VF2 axes. Red arrows represent the contribution of each variable projected into the plane defined by the two varifactors.

PCA$_5$ involved microbial soil classes (Acidobacteria$_H$, Betaproteobacteria$_H$, Actinobacteria$_H$, Cytophagia$_H$), Uniformity Coefficient (*CU*), fine material content (% Fine), Dryness (operation condition dry-wet) and Depth (**Table 3.1**). From Figure 3.6, Betaproteobacteria$_H$ displays oppositely to Depth, Actinobacteria$_H$, Cytophagia$_H$, and Dryness, suggesting that Betaproteobacteria$_H$ is more favorable to live in wet and shallow soils, while Actinobacteria$_H$ and Cytophagia$_H$ are preferably found in dry and deep soils. It should also be noted that when projected over the first two varifactors plane, wet samples (blue circles) are clustered, whereas dry samples (orange circles) are more scattered in space, indicating that they are affected by

depth gradients. Finally, Acidobacteria$_H$ is correlated positively with *CU* and the proportion of fines, well represented by the sample taken in the sedimentation pond (blue triangle).

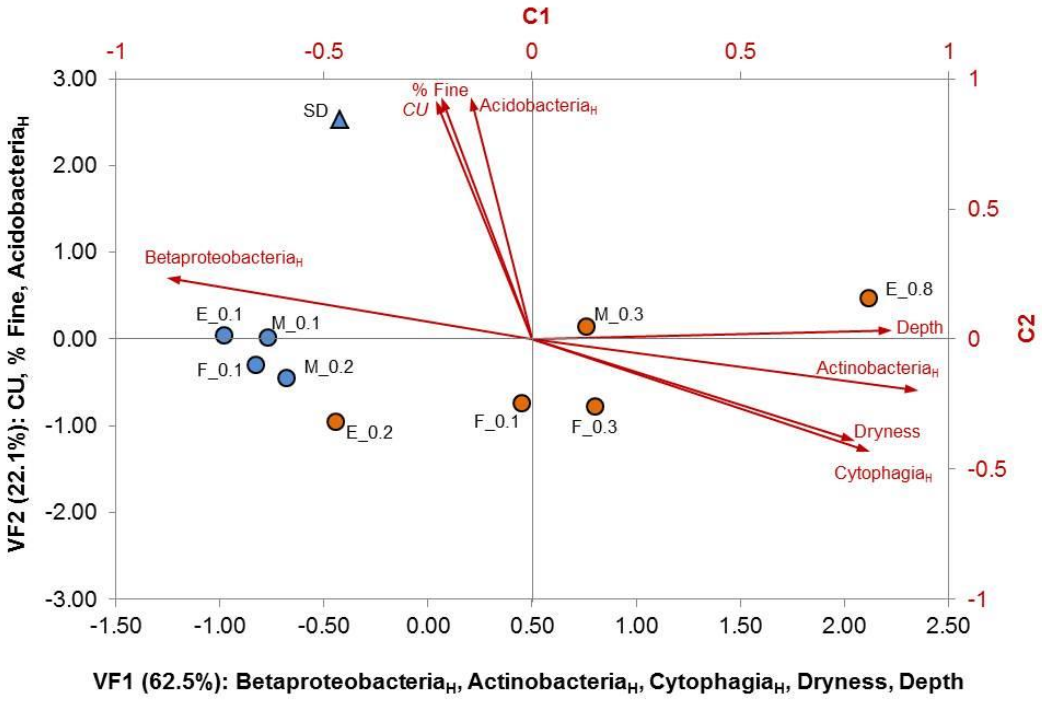

Figure 3.6 PCA5 analysis including microbial classes, grain-size distribution curve parameters and depth from soil samples during the recharge period (blue) and no-recharge period (orange). Circles are related to the infiltration pond samples (E-Entrance, M-Midfield, and F-Final stretch). Numbers indicate the depth the sample was taken (in m below surface). Triangle corresponds to the sedimentation pond sample. Symbols follow the same criteria in the following PCA charts

PCA$_6$ clusters microbial classes with diversity indices (Shannon, Richness, and Evenness), Actinobacteria$_H$, Dehalococcoidia$_H$, Chlorobia$_H$, Bacilli$_H$ and Others$_H$ (Figure 3.7). Whereas Bacilli$_H$ behavior is explained basically by the second component, Shannon, Evenness, and Actinobacteria$_H$ are partially included in both components. Same as shown in a previous analysis, Actinobacteria$_H$ is negatively correlated with Shannon and Evenness indices. Chlorobia$_H$ and Dehalococoidia$_H$ are explained by the first component and contribute visibly to the microbial print of the wet soil samples.

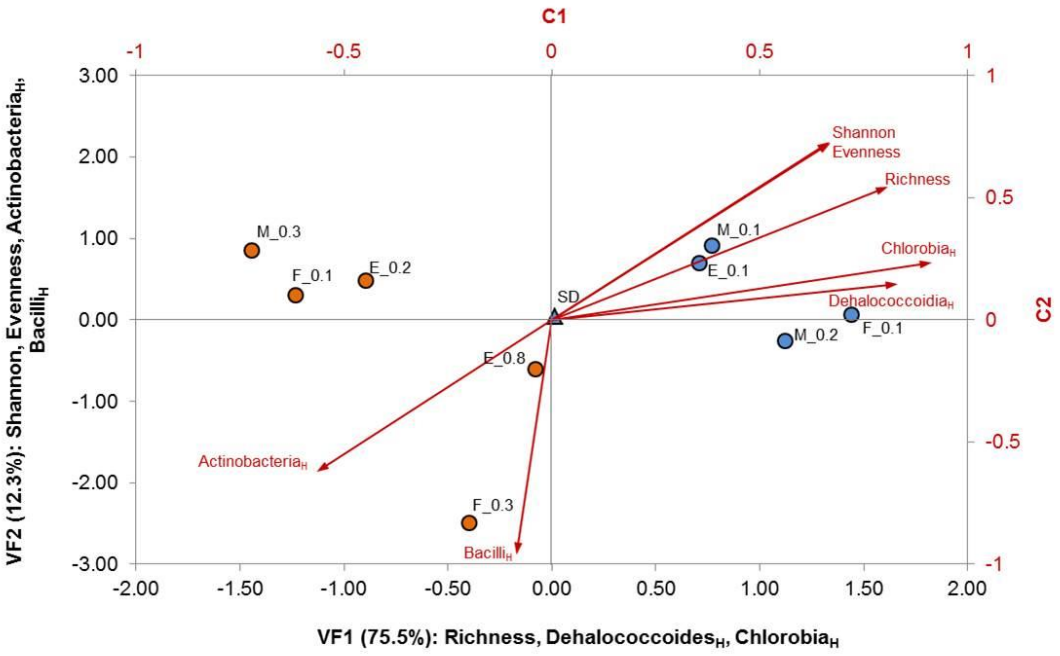

Figure 3.7 PCA6 analysis with microbial class data from soil samples during the recharge period (blue) and during the no-recharge period (orange). Circles are related to the infiltration pond samples (Entrance, Midfield and Final stretch according to the capital letter close to each symbol). Triangle is referred to the sedimentation pond sample. The position of samples is scaled in VF1 and VF2 axes. Red arrows represent the contribution of each variable in both Varifactors scaled by components

3.3.4. Key parameters influencing microbial species in MAR soils

In PCA$_7$ (Figure 3.8 and **Table 3.1**), the first two components explain 92% of the total variance. Projection of samples on varifactor space provides a clear separation of samples according to the operational period (during recharge and no-recharge periods), while the sample from the sedimentation pond remains separated. This last sample (SD in Figure 3.8) is explained mainly by the proportion of fines, *CU* and notably, the presence of Subgroup_3 Acidobacteria. Moreover, Shannon Index and Dryness are displayed in opposite sides of the plot, while the latter is placed in the same side as *Pontibacter sp* and *Nitrospira sp2*, highlighting that both species have a high affinity to dry conditions.

PCA$_8$ indicates the affinity of *Vogesella indigofera* to silty soils (Figure 3.9). Despite *Dehalogenimonas sp.* behavior is explained by the second component, this species does not show correlation with *V. indigofera* or *CU*. However, the bivariate correlations matrix (not showed) revealed the correlation of *Dehalogenimonas sp.* with fine particles proportion. On the other hand, both *Methylotenera mobilis* and *Methylobacterium sp.* are correlated positively with two other soil characteristics, *CC* and D10.

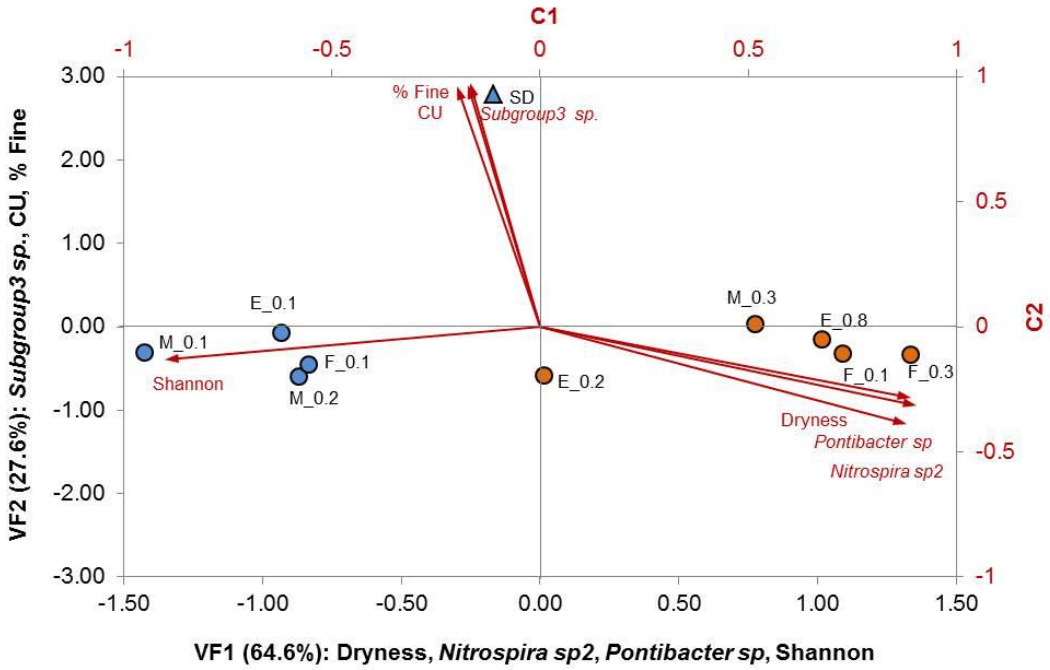

Figure 3.8 PCA7 analysis including microbial species, grain-size distribution curve parameters and the operational period from sediment samples during the recharge period (blue) and no-recharge period (orange)

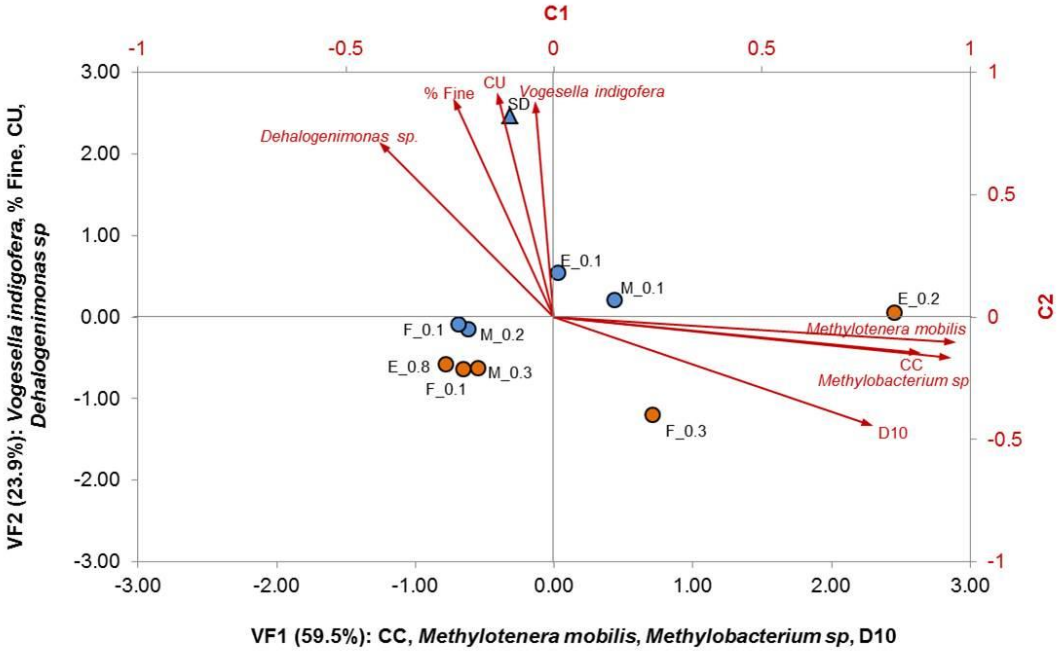

Figure 3.9 PCA8 analysis including microbial species and grain-size distribution curve parameters from sediment samples during the recharge period (blue) and no-recharge period (orange)

3.3.5. Interclass and interspecies relationships

PCA9 – PCA11 involves the statistical analysis of all 31 samples together. In PCA9, soil and water samples are distinctly located in the varifactor plane involving the first two components (explaining 70% of the total variance, Figure 3.10). From the

analysis, soil samples are the most diverse, equally-distributed and rich environments sustaining microbial growth. On the other hand, Betaproteobacteria$_H$ shows higher affinity for water samples. Bacilli$_H$ becomes an independent third component explaining 13% of the total variance (Table 3.1).

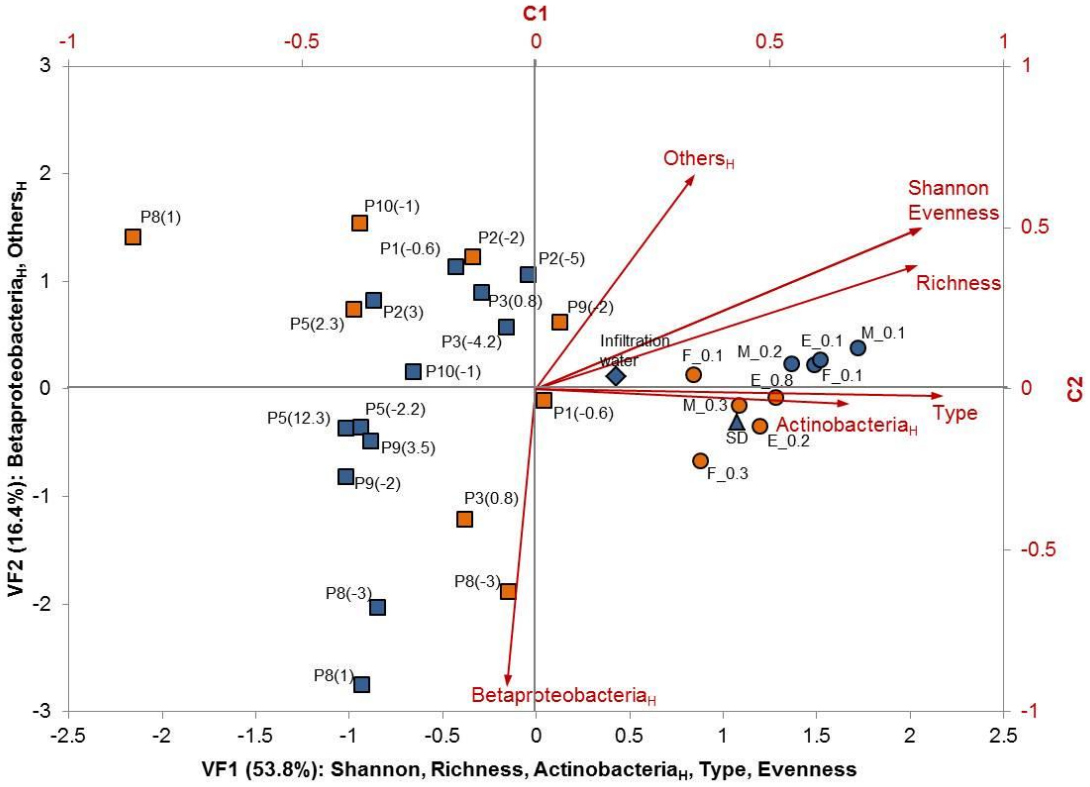

Figure 3.10 PCA$_9$ analysis including diversity indices, microbial classes and sample type from soil and water samples during the recharge period (blue) and no-recharge period (orange)

PCA$_{10}$ was performed to analyze the intra-relationships among microbial classes. Three components were needed to explain 85% of the total variance. The first one clusters the three microbial diversity indices. The second one explains the positive correlation between Dehalococcoidia$_H$ and Acidobacteria$_H$ and the negative one with Cytophagia$_H$. Finally, the third component showed a negative correlation between Nitrospira$_H$ and Chlorobia$_H$. Samples distribution in VF axes did not show any relevant association among samples (Figure 3.11).

Finally, PCA$_{11}$ emphasizes microbial species. Similar to PCA$_{10}$, the first component groups all three diversity indices, and is representative of soil samples in the varifactor plane (Figure 3.12). *Nitrospira sp1*$_H$ was also positively correlated with Shannon and Evenness indices. Regarding the second component, *Pontibacter sp.*$_H$ is inversely correlated with *Dehalogenimonas sp.*$_H$ and in turn, the latter correlated

positively with *Subgroup3 sp*$_H$, pointing out that these two species seem to be more associated to water and groundwater samples during active recharge period.

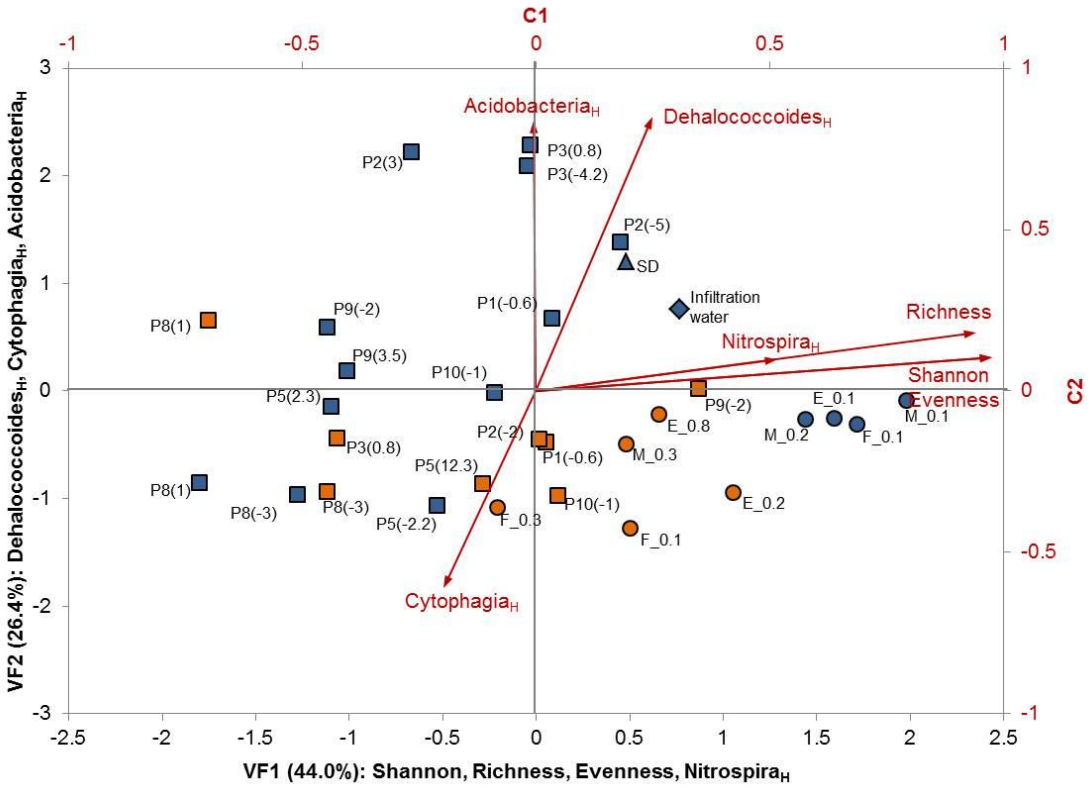

Figure 3.11 PCA$_{10}$ analysis including diversity indices and microbial classes from soil and water samples during the recharge period (blue) and no-recharge period (orange)

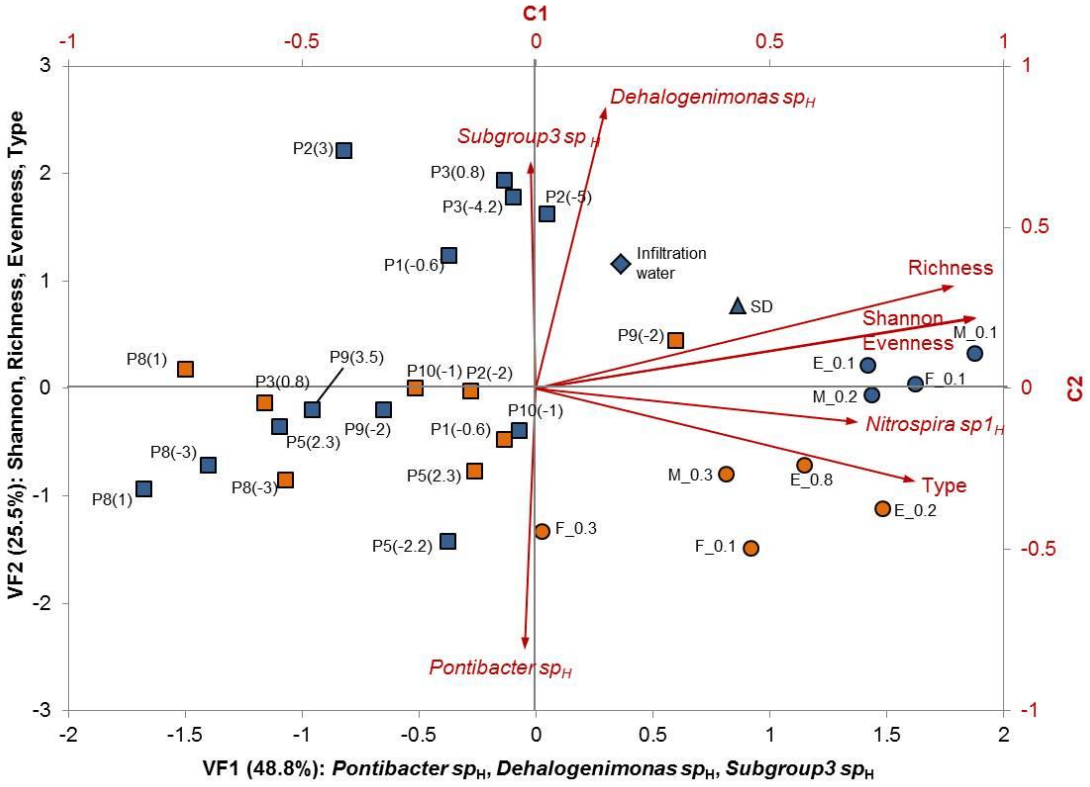

Figure 3.12 PCA$_{11}$ analysis including diversity indices, microbial species, and type of sample from sediment and water samples during the recharge period (blue) and no-recharge period (orange)

3.4. Discussion

The most significant result from the statistical analysis is that the projection of samples on the planes defined by the principal components shows a clear influence of the operational conditions. This implies that recharge operation drives significant changes in microbial communities. Recharge results in shifts in the microbial community structure, in terms of abundance and composition of dominant taxonomic groups.

Cyanobacteria, the only diazotrophs that produce oxygen as a by-product of the photosynthetic process, were found most abundantly in the surface water, and the measured concentrations correlated with several hydrogeochemical variables (EC, Cl, Cu-log, and Ni-log) (recall Figure 3.3). Correlations among EC and cyanobacteria abundance were already reported, for example, in a Neotropical urban lake (Frau et al., 2018) or in a eutrophicated reservoir in Brazil (Chellappa and Mederios Costa, 2003). Cu-log is positively correlated with cyanobacteria; this follows Dwivedi et al. (2006), who associated the presence of cyanobacteria with some metals (including copper) in river water samples enriched by fly-ash originated in a coal thermal power

station. Indeed, some cyanobacterial species have the ability to immobilize metals, thus used in some water treatment industries (de-Bashan and Bashan, 2010).

The highest relative abundance of Betaproteobacteria was found in the groundwater samples most affected by recharge, e.g., P8, located directly below the infiltration pond. The fact that this microbial group correlates inversely with Richness and Shannon indices (recall Figure 3.2) suggests that members of the Betaproteobacteria class could have an opportunistic behavior, displacing other microbial populations when recharge is active, and becoming the leading microorganisms degrading organic matter using different electron acceptors such as nitrate.

We also evaluated the role of DOC, nitrate, and sulfate on the abundance of *Methylotenera mobilis* in surface and subsurface water environments (see PCA_3). *M. mobilis* may carry out heterotrophic denitrification by using different substrates, such as methanol (Kalyuhznaya et al., 2009; Sun et al., 2016) or methylamine (Kalyuzhnaya et al., 2006) in an aerobic environment. In fact, *M. mobilis* is the first methylotroph using nitrate as an electron acceptor, thus being a potential explanation of the positive correlation observed between *M. mobilis* abundance with nitrate concentration in water. Denitrification is an anaerobic process but in some cases occurs in the presence of oxygen. In these situations, anoxic microenvironments (called microsites) would be created, and denitrification could take place (Knowles, 2005; Modin et al., 2007).

On the other hand, it is not surprising that abundance of *M. mobilis* correlates with *Methylobacterium sp.* presence in the soil environment (see PCA_8) since they belong to different proteobacterial classes, they are both obligate methylotrophs (Kumaresan et al., 2018). Indeed, correlations between both species of methylotrophs have been reported by Wright et al. (2017) in a groundwater dichloromethane contaminated site in the United States. Unlike *M. mobilis*, *Methylobacterium sp.* is a dichloromethane degrader (Gisi et al., 1998; Vuilleumier et al., 2009), capable to dechlorinate in aerobic conditions. Following Wright et al. (2017), this suggests that *M. mobilis* could take advantage by using the byproducts of dichloromethane degradation carried out by *Methylobacterium sp.* However, methane has not been measured at the site, so we are not assuming its presence *via* dichloromethane degradation.

In any case, it is not clear whether *M. mobilis* abundance correlates with some redox species; on one hand, the bivariate correlation coefficients with DOC-log and SO_4 were not significant (data not shown), but on the other hand, *M. mobilis* grouped in the same component with NO_3 and SO_4. Regarding this last point, there is no evidence that SO_4 might be part of the metabolic pathway of *M. mobilis*.

Vogesella indigofera positively correlates with DOC-log (PCA_5). Members of this genus are important denitrifiers in groundwater systems (Bellini et al., 2018), capable of oxidizing few monosaccharides in low-oxygen concentration conditions (Grimes et al., 1997). Contrarily, DOC-log was negatively correlated with NO_3 concentration (PCA_3). In fact, the isotopic study performed by Grau-Martínez et al. (2018) at the same facility and on the same dates confirmed that recharge induced denitrification.

Dryness (a binary dry = 0 / wet = 1 variable) is the most significant one controlling the distribution of microbial communities in soils. Similar to what was observed in water samples, soil samples during recharge periods displayed the largest diversity and highest Betaproteobacteria abundance. Recharge of river water ensured the continuous supply of nutrients and DOC to the system, favoring Betaproteobacteria growth, as it is one of the main bacterial groups biodegrading DOC (Li et al., 2013). In fact, in the work of Li et al. (2012), carried out in column models, Betaproteobacterias were found mainly close to the inlet, in response to the high DOC concentrations fed. On the other hand, they also found that water content (saturated and unsaturated, in our case equivalent to wet/dry) is also a key factor for the microbial community structure in soils. Therefore, we could expect that recharge conditions contribute to microbial diversity in soils. In this regard, decreasing proportions of Betaproteobacteria were found in dried soils respect to the wet ones in an experiment performed with streambed fresh sediments (Pohlon et al., 2013).

Distribution of microbial populations in soils is also strongly affected by granulometry (PCA_8). *M. mobilis* and *Methylobacterium sp.* correlated with *CC* and D_{10}. There is not much literature on this subject. The work performed by Madhaiyan et al. (2007) associated the variability in the distribution of pink-pigmented facultative metylotrophs, such as *Methylobacterium sp*, with soil type and moisture among other environmental variables. In fact, soil texture conditions is of paramount importance for nutrient transference into flooded soils (Perujo et al., 2017), also

influence methane consumption rates (Jäckel et al., 2001). In the same way, the presence of *Vogesella indigofera* and *Subgroup3 sp* (Acidobacteria) in soils is linked to *CU* (an indicator of grain-size heterogeneity) and proportion of fine particles, resulting in these two populations being most abundant in sandy-clay soils.

Members of the phylum Acidobacteria, such as *Subgroup 3 sp* are widespread abundant in soils and sediments, and capable to tolerate moisture fluctuations (Ward et al., 2009). This tolerance can be related to the capability to form biofilms, highly hydrated structures (Kielak et al., 2016), which allows them to survive under stressful dryness conditions (Ward et al., 2009); this could be the reason to find it regardless the operational period. Moreover, it is also important to know the interactions of this group with other microbial classes present in the soil. In this regard, we found a significant statistical positive correlation between *Subgroup3 sp* (Acidobacteria) and *Dehalogenimonas sp* (Dehalococcoidia class); both groups are environmentally important as they are involved in different contaminant degradation processes (Chen et al., 2018; Song et al., 2016), and this could be the reason of the correlation observed.

In the soil samples, the concentration of Actinobacteria was directly correlated with dry conditions (PCA_5), similar to the observations already reported by Pohlon et al. (2013). Different members of this phylum have the ability to grow developing mycelia structures and forming spores (Bhatti et al., 2017), providing them an advantage in the colonization of soil with limited water availability. Moreover, the combined analysis of soil and water samples showed the widespread presence of this phylum, especially abundant in soil samples, and could be associated to their important role in the cycling of organic matter due to their decomposition capabilities (Bhatti et al., 2017; Polkade et al., 2016). This behavior is consistent with results observed in our system (PCA_9), where Actinobacteria is linked to microbial diversity indexes and dryness conditions. These last results are not surprising since soils probably are one of the most diverse and rich environments supporting microbial life in the world (Curtis et al., 2002; Dani Or et al., 2007; Torsvik et al., 2002; Young and Crawford, 2004).

3.5. Conclusions

Managed Aquifer Recharge influences significantly microbial communities in soil, surface and subsurface water. Therefore, they can be used to assess the area of the

soil and the volume of the aquifer influenced by recharge. Microbial communities are directly influenced by a combination of physical, chemical and biological processes. Aquifer recharge *via* infiltration ponds has a significant importance in carbon and nitrogen cycles in the topsoil since most of the species detected in this study have a role in the aerobic degradation of organic matter and/linked to denitrification. In this way, the statistical analysis has shown the correlation between hydrochemical compounds and some microbial communities not only in the soil but also in groundwater; an example is the correlation between *Vogesella indigofera* with DOC and *Methylotenera mobilis* with NO_3.

The analysis of both groundwater and soil samples clearly discriminate operational conditions. Recharge drives several distinct populations to become dominant (Betaproteobacteria, Dehalococcoidia, and Nitrospira), reducing ecological diversity; once recharge is discontinued, other communities take over, with none becoming dominant; that is, increasing diversity (measured by entropy indices). In any case, when the operation is discontinued, the system does not go back to the initial non-perturbed conditions.

In the case of soil samples, there are two most significant variables affecting the distribution of communities. On one hand, microbial communities are affected by the grain-size distribution (*Vogesella indigofera* and *Subgroup3 sp* (Acidobacteria)), indicating that these microorganisms are preferentially found in the most heterogeneous clayey sediments. However, the most important factor is operation conditions in which wet soils contain more microbial diversity than dry ones. However, there are some classes (e.g., Acidobacteria) that are less affected by recharge conditions. In the future, this could provide ideas for the affection of the climate change consequences in stream-flows, wetlands, and other drought-vulnerable aquatic systems.

Multivariate statistical analysis indicates that DOC was a determinant factor shaping microbial community structure. Among them, members of Betaproteobacteria, Dehalococcoidia and Acidobacteria are involved in pollutant bioremediation and can be considered as potential bioindicators for recharge monitoring.

CHAPTER 4: MONITORING OF REDOX PROCESSES TO IMPROVE MAR MANAGEMENT

4.1. Introduction

Surface infiltration systems are widely implemented around the world, and several studies have been reported demonstrating their efficacy regarding different quantitative and qualitative targets (San-Sebastián-Sauto et al., 2018; Sprenger et al., 2017). Regarding water quality improvements, recharge ponds are particularly useful to remove organic matter, such as dissolved organic carbon (Bekele et al., 2011; Maeng et al., 2011) or emerging organic compounds (EOCs) (Alidina et al., 2014c; Rauch-Williams et al., 2010; Valhondo et al., 2018). In fact, redox conditions and the availability of electron acceptors have a key role in the fate of these organic substances (Greskowiak et al., 2006; Rodríguez-Escales et al., 2017).

In freshwater systems, such as surface infiltration ponds, the main process driving organic matter degradation is via microbial respiration (Greskowiak et al., 2017; Li et al., 2008; Regnery et al., 2015). During respiration, microorganisms catalyze the transfer of electrons between compounds during organic matter consumption; organic carbon is oxidized while releasing electrons to an oxidant molecule. While oxygen is present, it becomes the main oxidant element, because microorganisms take the most energetic advantage. On the other hand, when oxygen is completely or almost completely consumed, microorganisms use other electron acceptors to degrade organic matter. In fact, according to the energetic benefit that they can extract, they will use either nitrate, manganese, iron, sulfate or CH_4/CO_2 as electron acceptors, depending on availability, and following the redox chain indicated in Figure 4.1. For example, it has been estimated that a depletion between 30 and 80% of the total organic carbon can be reached by means of redox reactions during riverbank filtration (Kedziorek et al., 2008).

While labile organic carbon can be rapidly removed when oxygenic conditions are maintained, some recalcitrant organic molecules can be transformed or removed under more reductive conditions or co-metabolism processes needing different redox states (Ghattas et al., 2017; Rodriguez-Escales and Sanchez-Vila, 2016).

Tracing the fate of the organic carbon is also quite important to understand redox dynamics. Organic carbon reaches the recharge facility under different forms (labile carbon and different degrees of recalcitrant carbon), and from different pools (recharge water, generation within the system). Besides this, organic carbon is also transformed into biomass, or as inorganic carbon (e.g., CO_2).

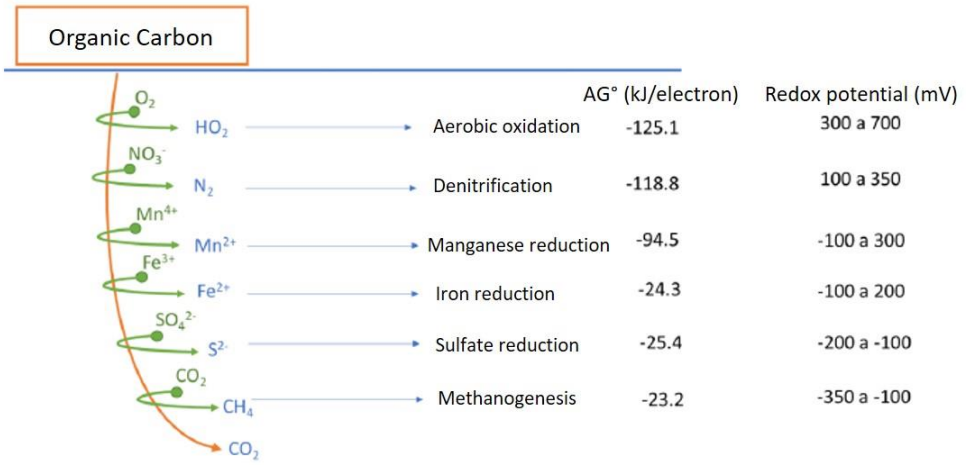

Figure 4.1 Electron acceptor sequence according to organic matter biodegradation process. Values of Free Gibbs Energy were provided by Faulwetter et al. (2009)

Although redox reactions govern microbial dynamics, redox monitoring has been traditionally a problem since most of the current instruments only provide discrete information, lumped at the scale of the instrument. Nevertheless, redox processes are quite dynamic both in time and in space (Alewell et al., 2008; Meckenstock et al., 2015). Furthermore, redox samples are quite sensitive to the presence of oxygen in the atmosphere, so monitoring should be done under strictly anaerobic conditions and/or with a flow cell.

Redox potential, thus, is an indicator of biological activity. Apart from bio-mediating several degradation processes, microorganisms have a key role in bioclogging development (Baveye et al., 1998; Hand et al., 2008). The polymeric structures and biological communities conforming biofilms have great implications on infiltration systems management (Baveye et al., 1998; Rubol et al., 2014). Characterizing the evolution of bioclogging might be a useful tool to optimize both the infiltration rate and to improve water quality. This bioclogging characterization can be carried out by means of e.g., redox potential monitoring, determination of organic carbon amount in the infiltration pond bed, characterizing redox species or characterizing dissolved organic matter origin by means of their fluorescence properties.

Clogging involves a combination of physical, chemical and biological processes (Pedretti et al., 2012a). Traditionally, processes affecting clogging are not differentiated, and so the usual approach is to (1) control it by means of a rotation of drying-wetting cycles, so that desiccation of the clogging layer would result in surface cracking; (2) in case this method would not work (infiltration rate were not restored), ploughing and/or mechanical removal of the topsoil would be carried out (Bouwer,

2002). The impacts of clogging imply changes in infiltration rate by the colonization of pores and throats resulting in changes in hydraulic conductivity and dispersivity (Carles Brangarí et al., 2017; Hand et al., 2008; Thullner et al., 2002). In a feedback process, changes in interstitial fluxes and redox potential also influence microbial dynamics in the subsurface (Perujo et al., 2017). Moreover, temperature plays a role in microorganism growth (Zhang et al., 2015). Altogether, understanding the microorganisms dynamics will facilitate the optimal management of the infiltration facilities.

4.2. Objectives

The objective of this chapter is to better understanding biogeochemical processes, occurring naturally in a MAR system, in order to suggest practices to optimize MAR facilities involving surface infiltration ponds. To reach this global objective, different specific objectives are included:

- Understanding the evolution of the infiltration rate linked to operating conditions in a real MAR facility.
- Evaluating temporal and spatial changes on redox potential using an intensive *in situ* monitoring network
- Linking redox potential evolution with:
    - Dissolved organic carbon and electron acceptors dynamics
    - Organic matter characterization due to their fluorescence properties
    - Biological clogging formation

4.3. Methodology

The study was framed in the Castellbisbal recharge system (see section 1.5.3. in Chapter 1). The period considered is of one year, from 25/10/2016 to 24/10/2017. During that period, continuous monitoring in addition to four sampling campaigns was carried out. According to the different criteria of recharge management, this period was divided into five sub-periods - Period I to Period V- (Table 4.1).

Table 4.1 Duration and characteristics of the five management periods stablished between 25th October 2016 and 24th October 2017

	Starting date	Duration (d)	Characteristics
PERIOD I	24th October 2016	64	Period after scrapping Maximum infiltration rate
PERIOD II	27th December 2016	83	Intermediate infiltration rate Period ends with a heavy rainfall event
PERIOD III	20th March 2017	75	Low infiltration rate Physical and biological clogging
PERIOD IV	3rd June 2017	27	Period after scrapping High infiltration rate
PERIOD V	30th June 2017	116	Fluctuation of infiltration rate Vacation period (stop) in the middle of the period

4.3.1. Monitoring operational conditions in the system

During the 365 days conforming the study, different information about the hydraulic regime in the system and in the vicinity was acquired from the network of pressure, temperature and redox sensors installed (Figure 4.2).

First of all, flow rate, turbidity, Total Organic Carbon (TOC), nitrate, nitrite, and ammonium were measured at the Llobregat River on a daily basis by the Water Supply Company (Aigües Ter-Llobregat - ATLL). These parameters were measured 10 km upstream from the facility. Precipitation was registered in the Castellbisbal meteorological station (UTM coordinates, X: 414461.00, Y: 4592431.00, located at a distance of 1.5 km from the facility), and it was available from RuralCat (www.ruralcat.gencat.cat).

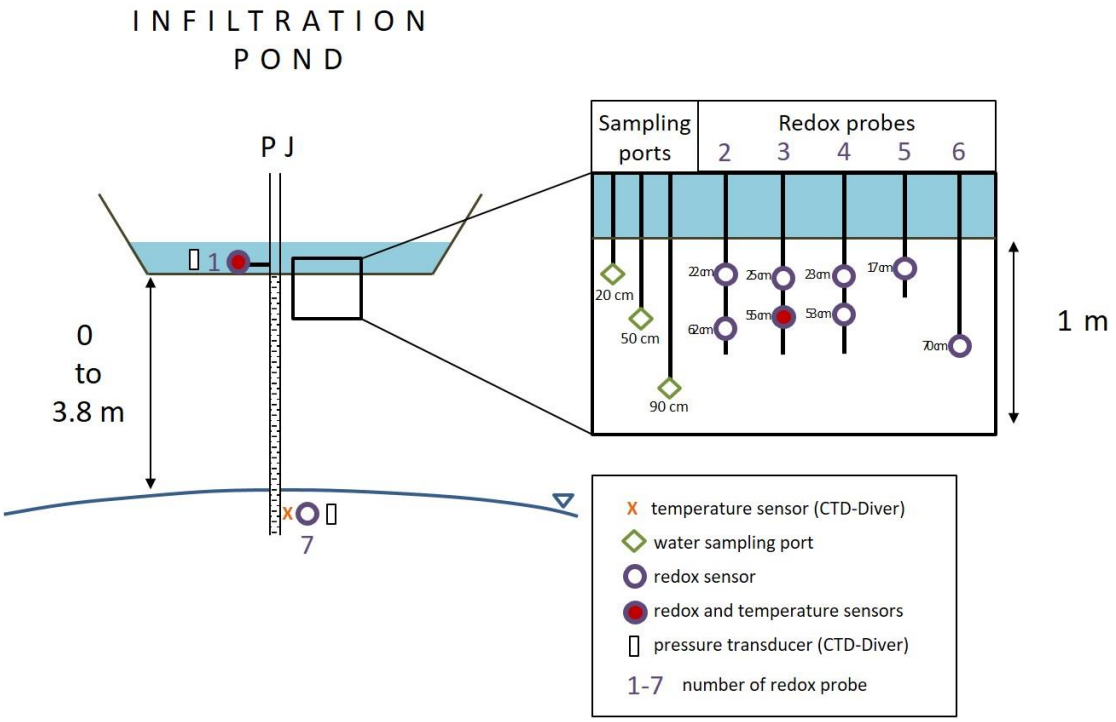

Figure 4.2 Instrumentation installed in the infiltration pond in the Castellbisbal MAR system.

On the other hand, the flow rate was measured daily at the interconnection between the wetland and infiltration ponds. This data was provided by the water user's community managers (CUACSA). Daily infiltration rate was calculated by balancing the inflow water entering the pond minus the storage accumulation in the pond (measured by the water level variation); evaporation is negligible compared to infiltration volumes.

The water table in the infiltration pond and groundwater level in the piezometer located in the center of infiltration pond (PJ) were monitored at time intervals of 30 minutes with pressure transducers (CTD Diver, Schlumberger). Transducers also provided measurements of temperature and electrical conductivity at the same level of temporal discretization. Barometric pressure was also measured (Baro-Diver, Schlumberger) in order to compensate water level measurements. Values of pressure were then daily averaged.

4.3.2. Sampling surveys

Apart from continuous monitoring, four sampling campaigns were performed during the one-year duration of the study. Campaigns were carried out taking into account different seasons and different operating conditions. The first campaign was in winter 2016 (12/12/16) with the lowest temperatures of the study period. The second

campaign was in April 2017 (20/04/17), when the pond was being dried because of clogging. The third sampling period took place in summer, after scrapping the bottom of the pond (22/06/17). Finally, the last sampling date was in July 2017 (21/07/17).

Water samples were taken at different locations: Infiltration pond, Vadose Zone at 20, 50 and 90cm and the aquifer just below the pond (PJ) (Figure 4.2). Vadose zone samples were extracted with a vacuum pump connected to three plastic fine sampling ports inserted at 20, 50 and 90 cm, respectively, and separated one meter and a half from each other. Groundwater samples were taken with a pump into PJ, purging since stable conditions were reached.

Dissolved oxygen, electrical conductivity, temperature, Oxidation Reduction Potential (ORP) and pH were measured *in situ* with a multiparameter meter (YSI Professional Plus). These field parameters were measured into a flow cell in the vadose zone and groundwater (PJ) in order to preserve the pressurization of the sample during the measurements. The CO_2 partial pressure in water samples was also measured in the field with an infrared gas analyzer (EGM-4, PP-Systems, USA) coupled to a membrane contactor (MiniModule, Liqui-Cel, USA). The measurement accuracy of the EGM-4/contactor system is estimated to be within 1% over the calibrated CO_2 range. For measurements, the water samples were circulated through the membrane contactor by gravity at a rate of 300 mL/min, while the internal pump of the EGM-4 recirculated a small volume of air between the contactor and the analyzer. The flow of water was kept constant until full gas equilibration with the recirculated air, which typically happened in less than 2 minutes.

After measuring field parameters, water samples were taken in order to analyze Biological Oxygen Demand (BOD), Total Organic Carbon (TOC), Dissolved Organic Carbon (DOC), Dissolved Organic Matter (DOM), major cations and anions, nutrients and metals.

Water samples for DOC determination were filtered in the field through pre-combusted and pre-rinsed 0.7 m glass fiber filters (GF/F; Whatman, UK). DOC and TOC concentrations were analyzed by high-temperature catalytic oxidation on a Shimadzu TOC-V CSH analyzer (Shimadzu Corporation, Japan). Samples for DOM characterization were filtered in situ in a similar way as those for DOC determination. DOM characterization was performed by absorbance-fluorescence

spectroscopy (AFS, Casas-Ruiz et al., 2016). AFS provides an Excitation-Emission Matrix (EEM) with fluorescence signals for each sample. EEM matrix allows identifying fluorophores by visual peak picking. The most common identified fluorophores are peaks A, C, M, T and B. Peaks A, C and M appear at the longer emissions and reflect humic-like compounds. A and C are considered to be terrestrially-derived (Hudson et al., 2007). Peak M has been related to humic-like compounds derived from microbial activity, and have a lower aromatic character (Romera-Castillo et al., 2010). On the contrary, peaks T (related to tryptophan) and B (related to tyrosine) correspond to the protein-like fraction of DOM, appearing at lower emission wavelengths (Yamashita and Tanoue, 2003).

Thanks to EEM, protein-like peaks (B and T) and humic-like peaks (C, A, and M) were determined for each sample in the four sampling surveys. Apart from fluorescence peaks, some optical indices were calculated as:

$$\mathrm{SUVA} = \frac{Abs_{254} \times ln(10)}{l} \times \frac{1}{[DOC]} \tag{4.1}$$

$$\mathrm{HIX} = \frac{\text{"H" range}}{\text{"L" range}} = \frac{\mathrm{Abs}\{\lambda ex_{254}, \lambda em_{235-480}\}}{\mathrm{Abs}\{\lambda ex_{254}, \lambda em_{330-345}\}} \tag{4.2}$$

$$\mathrm{BIX} = \frac{\mathrm{Abs}\{\lambda ex_{310}, \lambda em_{380}\}}{\mathrm{Abs}\{\lambda ex_{310}, \lambda em_{430}\}} \tag{4.3}$$

$$\mathrm{FI} = \frac{\mathrm{Abs}\{\lambda ex_{370}, \lambda em_{470}\}}{\mathrm{Abs}\{\lambda ex_{370}, \lambda em_{520}\}} \tag{4.4}$$

Specific Ultra-Violet Absorbance (SUVA) is a measurement of bulk DOM aromacity and the formulation was calculated according to Weishaar et al. (2003) (equation 4.1). Abs_{254} is the absorbance at 254 nm, l corresponds to the cuvette path length and [DOC] is the concentration of DOC.

The Humification Index (HIX, Zsolnay et al., 1999) was introduced in order to estimate the maturity of soil DOM. It is calculated as a ratio (equation 4.2) Abs{λex254,λem_(235-480) } corresponds to the sum of the emission signals between 325 and 480 nm for the excitation at 254 nm. Abs{λex254,λem_(330-345)} corresponds to the sum of the emission signals between 330 and 345 nm for the excitation at 254 nm.

The Biological Index (BIX) is calculated also as a ratio (Huguet et al., 2009) and defined in equation 4.3. In this case, the ratio is between Abs{λex310,λem380} and

Abs{λex310,λem430}, that is the points in EEM defined by the emission signal of 380 and 430 nm respectively, at 310 nm of emission. BIX is proportional to the recently produced organic matter.

Finally, Fluorescence Index (FI) (Cory et al., 2010; McKnight et al., 2001) is presented in equation 4.4. FI is defined by the ratio between Abs{λex370,λem470} and Abs{λex370,λem520} values in the EEM. FI is an indicator of DOC quality. That is, high values indicate that DOC is mainly composed of microbial-derived substances, while low values are representative of terrestrial-derived substances (McKnight et al., 2001).

Water for the determination of BOD_5, ammonia, phosphate, nitrate, nitrite, major anions and major cations was sampled and kept in dark at 4ºC until analysis. Samples were filtered, treated and analyzed directly in the laboratory in less than 24h. BOD_5 of water samples was determined using the respirometric method (WTW BOD OxiTop® OC 100). Nitrate, nitrite, major anions, and major cations were determined by liquid phase ionic chromatography (IC5000, Dionex, Thermo Fisher Scientific, USA). Phosphate was determined by spectrophotometry (Smartchem 140, AMS Alliance, Italy).

Samples for metal determination were filtered in the field through 0.2 μm nylon filters (Whatman, UK) and acidified with nitric acid since reaching a pH 2-3. They were preserved in dark at 4ºC. Samples were analyzed in the laboratory within 72 h by ICP- OES using a Perkin Elmer Optima 3200DV.

Finally, the organic carbon content in the surface of the sediments of the infiltration pond was estimated by measuring the Ash-Free-Dry Mass (AFDM) of a sample of sediment. A small plastic corer (volume=1mL) was used to sample the first two centimeters of the sediment, and the content transferred to a pre-combusted glass vial. Five replicates were collected at the pond during each sampling, randomly selecting the sediment locations in the infiltration pond. AFDM was calculated as the difference between the weight of the samples dried at 50ºC in an oven for 48h and after combustion of the samples at 450ºC for 4h.

4.3.3. Redox potential and temperature continuous monitoring

Three multilevel and four simple redox potential probes (Hypnos III, MVH Consult, The Netherlands) were installed from the infiltration pond water, along the first

meter of the vadose zone profile, to the groundwater below the pond (PJ) (Figure 4.2). The simple probes (one sensor per probe) monitored redox potential in the infiltration pond water (probe 1), at 17 cm (probe 5), at 70 cm (probe 6) and inside PJ (probe 7). The three multilevel probes measured redox potential at 22 and 62 cm (probe 2), 25 and 56 cm (probe 3) and at 23 and 53 cm (probe 4). Hypnos provided information of redox potential at the nine sensors of the seven different probes. Redox data was recorded every 12 minutes. Furthermore, two temperature sensors integrated into the redox probes allowed monitoring temperature in the water pond and at 55 cm depth of soil.

In order to calibrate redox probe measurements, values from the ORP probe (YSI Professional Plus) measured in each campaign were compared with the corresponding values of redox probes. Furthermore, ORP values from multiparametric meter were converted to the standard hydrogen electrode values (Eh). In this way, the resulting Eh corresponds to:

$$\mathrm{Eh\ (mV)} = \mathrm{ORP_{YSI}} + 220 + \mathrm{Eh_{probe}} \tag{4.5}$$

4.4. Results and discussion

4.4.1. Monitoring and field data

The present section presents the results of the monitoring network and the four sampling campaigns carried out in Castellbisbal MAR system during the period between October 2016 and October 2017. The study period includes different hydric regimes in the system as well as physical and biological clogging events, influencing in a different manner infiltration rates. In this way, sampling surveys allowed to go deeply into the characterization of the system under different seasonal and operational conditions.

Meteorological data and quality parameters of Llobregat River water

Thanks to Aigües Ter-Llobregat, it was possible to get a daily register of some quality parameters of the Llobregat River water, 10 km upstream of the recharge system location. Figure 4.3 displays the evolution of flow rate, Total Organic Carbon (TOC), concentrations of nitrate, nitrite, and ammonium, as well as turbidity monitored in the river water. Also, daily accumulated precipitation is showed.

Monitoring of quality parameters in the Llobregat River reflected a sinusoidal tendency of nitrate concentration, presenting higher concentrations in winter and spring and lower in summer and autumn (Figure 4.3a). In general, nitrate as well as TOC, ammonium, and nitrite, remained in low concentrations according to the legal constraints for the disposal of effluents from wastewater treatment plant to the natural media (rivers).

Actually, a correlation is visible between the three extreme rainfall events, flow rate and turbidity (Figure 4.3b). Moreover, the event occurred by the end of March generated flooding of the Llobregat River above the ponds. It is expected thus, an inevitable peak of turbidity in the infiltration water, resulting in enhanced clogging.

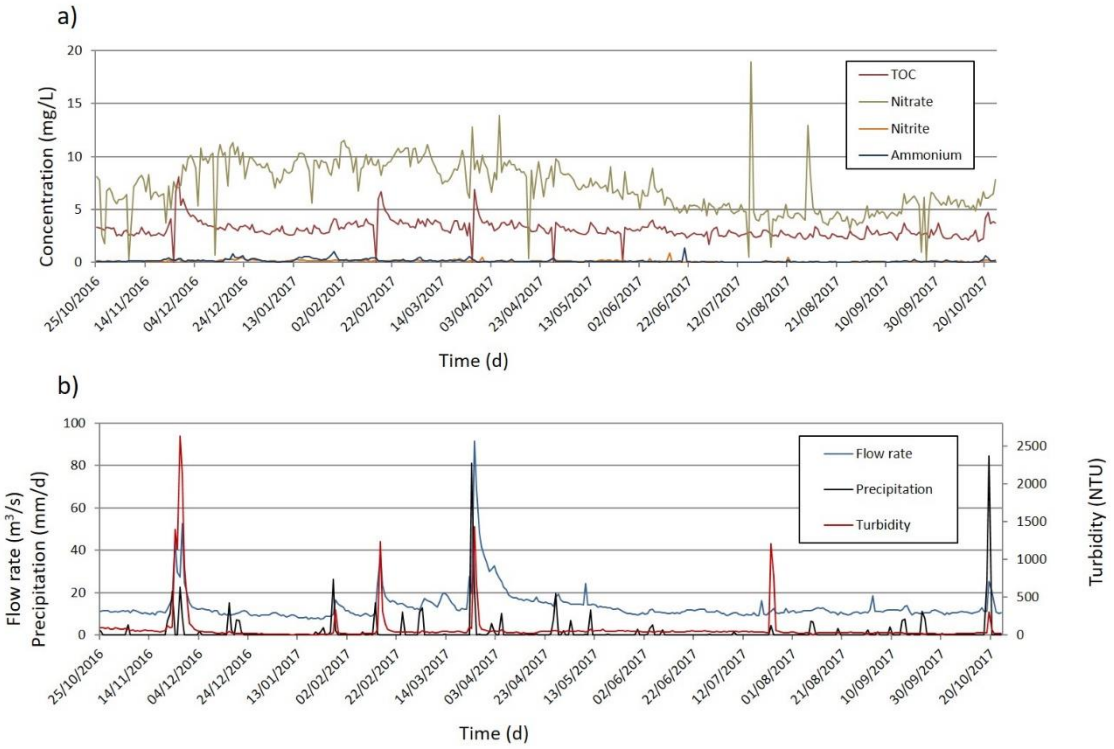

Figure 4.3 (a) Evolution of concentrations of TOC, nitrate, nitrite, ammonium and (b) values of turbidity, flow rate and precipitation in the Llobregat River water, measured 10 km upstream of the Castellbisbal MAR System.

Operating conditions in the Castellbisbal MAR system: flow rate, water table, infiltration rate, and groundwater table

The Castellbisbal MAR system is composed by an infiltration pond (1400 m^2) preceded by a natural wetland that acts as a sedimentation pond. The wetland receives water from the Llobregat River permanently, except during rainfall events, linked with high turbidity in the inlet water, when the sluice is closed. A floodgate

towards the river ensures the permanent movement of flow in the wetland. Furthermore, the wetland is connected with the infiltration pond through a pipe, where a flowmeter records daily the inflow rate.

The present study started in October 2016, after the infiltration pond had been emptied for the three previous months. Furthermore, during that period, the bottom of the infiltration pond was scrapped in order to remove the fine particles that settled during the previous operation. Therefore, the infiltration rate during Period I was the maximum (Figure 4.4). The flow rate and the water table level were not constant during this period since technical problems with the flowmeter and rain forecasts at different times forced often technical stops.

During Period II, it can be appreciated that the water table did not follow the same trend in infiltration rate as in the previous one, indicating that some kind of clogging was occurring. This tendency is even more evident in Period III, where the infiltration rate reduced drastically and the water table was maintained almost constant over the days, despite no water was flowing into the infiltration pond. Field observations evidenced that both biological (algae growing) and physical clogging were present during that period. Actually, Period III started after the flooding event that occurred at the end of March, probably causing the entrance of suspended solids from the river. At the end of Period III, the pond was totally dried and the surface was scrapped. In Period IV the infiltration capacity was recovered, confirmed by the high correlation between infiltration rates and water level in the pond. However, at the starting of July, this correlation was not observed anymore. During this period, physical clogging is discarded, since there was not any turbidity peak in the water sampled at the Llobregat River. High temperatures registered and the growth of bloom algae may indicate that bioclogging could occur. During August, the facility was stopped due to holidays period. After that, the water table rose slightly, while infiltration rate fluctuated drastically. This behavior was difficult to interpret, however, it could be a data monitoring problem, where flowmeter or pressure transducers malfunctioned due to the high temperatures.

Apart from the data obtained in the recharge ponds, the groundwater level was monitored just below the infiltration pond (Figure 4.2, piezometer PJ). In general, one would expect a local perturbation in the groundwater level due to the effect of enhanced recharge. In this particular case, the high transmissivities in the area (estimated in 4100 m^2/d from hydraulic tests(Martín and López, 2001)) buffer the

effect of mounding below the infiltration pond. The highest rising of aquifer phreatic level occurred by the end of March 2017 (beginning of Period III) during the mentioned flooding event, where the saturated zone reached the surface (Figure 4.5). In fact, groundwater level grew almost 4 meters in few hours, accordingly to the regional behavior of the whole aquifer levels (data not shown).

Comparing the water table in the pond and groundwater table during this flooding event, it can be seen that a vertical gradient existed through the profile. Since the groundwater level was above the surface and below the water table, it can be confirmed that clogging was present and acted as a semiconfining layer (Figure 4.4). According to such vertical gradient, infiltration occurred at low rates.

It should also be noted that the groundwater level remained almost constant during few months, just below the surface. Four months after the heavy rainfall at the end of March, groundwater level had dropt one meter. The scrapping of the pond surface (between Period III and IV) allowed the reestablishment of the initial infiltration rate.

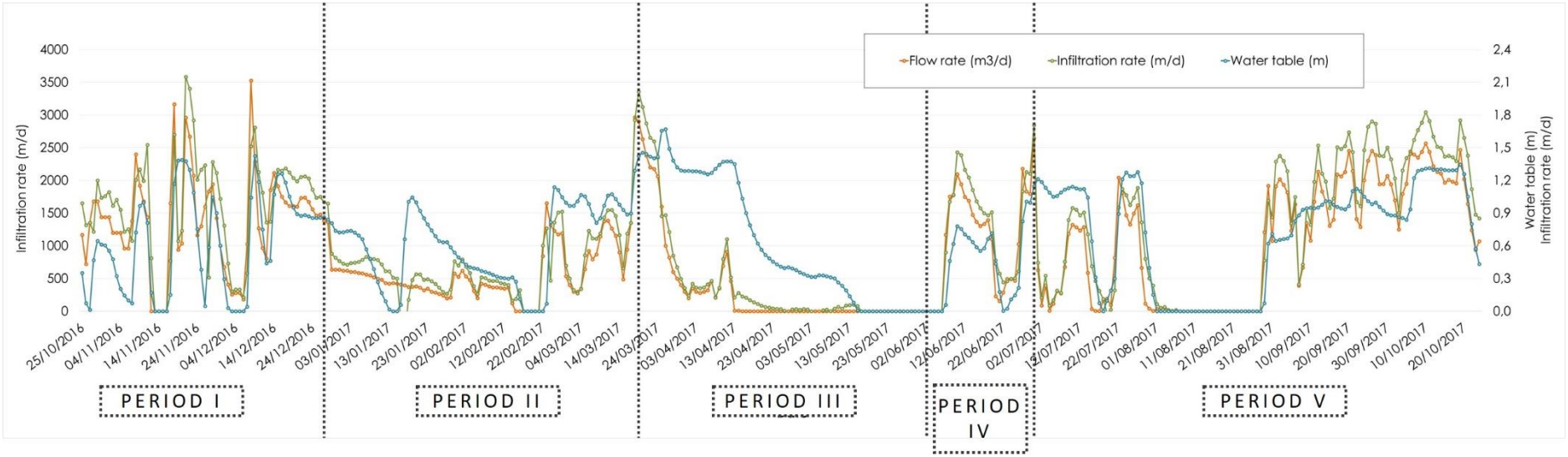

Figure 4.4 Evolution of flow rate (orange), infiltration rate (green) and water table (blue) in Castellbisbal MAR system from October 2016 to October 2017. Operational periods are emphasized according to infiltration rate variations

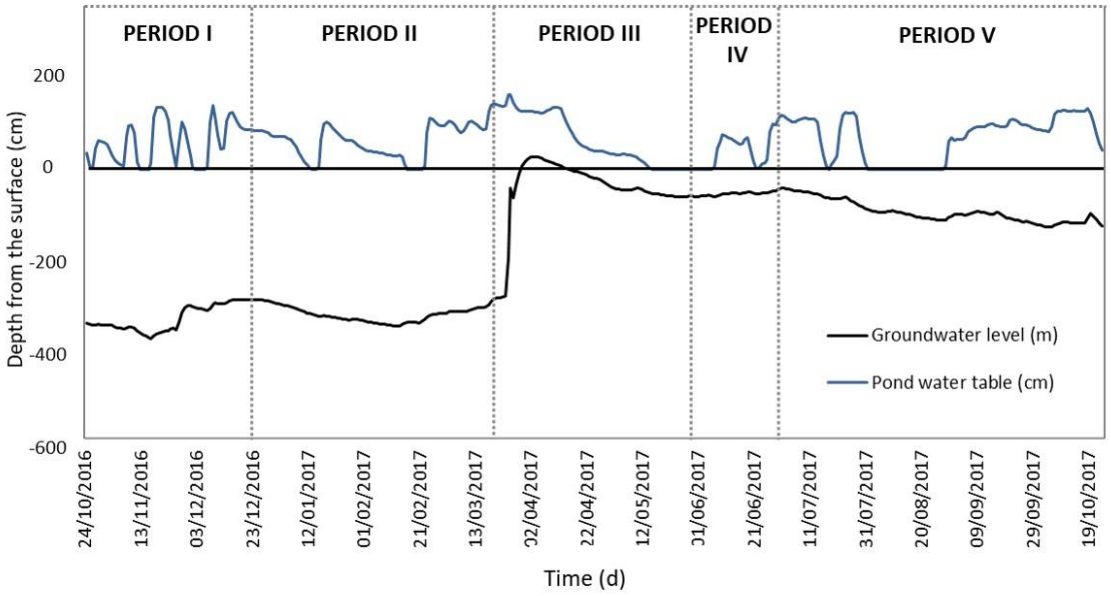

Figure 4.5 Evolution of groundwater level in PJ and water table in infiltration pond between October 2016 and October 2017

Discrete characterization: sampling surveys

Four sampling surveys were performed in the Castellbisbal recharge system. Water samples were taken in order to define physical, hydrochemical and organic matter composition characterization. For each campaign, samples were taken from the infiltration pond, vadose zone (at 20, 50 and 90 cm), and piezometer PJ. Sediment samples at the infiltration pond topsoil were taken to determine the amount of organic carbon.

a) Hydrochemistry

Hydrochemical characterization was made in order to understand redox reactions taking place through the system. Water samples of the infiltration pond, vadose zone (at three different depths) and groundwater just below the pond (PJ) were analyzed (Figure 4.6 and Figure 4.7). In general, there is a consistency between organic matter depletion and electron acceptors present in the water samples regardless of the sampling campaign. For example, the December campaign shows more stable concentrations of DOC and nitrate through the profile. Likewise, manganese and iron were not found in any of the two sampling points analyzed. BOD and O_2 concentrations in December were consistent with redox species behavior, overall evidencing lower activity of microorganisms in December compared to the rest of campaigns.

In fact, the April, June and July campaigns demonstrated highest variations in hydrochemistry. In general, O_2 depletion occurred in depth, while the partial pressure of CO_2 showed the opposite behavior, indicating the consumption of oxygen via microbial respiration and the consequent production of CO_2. ORP and manganese and iron concentrations were consistent with this assumption, indicating that both manganese and iron reduction were occurring, at least in the vadose zone (green area in the plots). The role of nitrate is not clear, as their concentration during the different surveys was very low in the three campaigns in all sampled points.

Comparing TOC and DOC concentration (first row in Figure 4.6), it seems that all the organic carbon in the system in the four campaigns was in dissolved form. However, samples were filtered by laboratory technicians in order to avoid the TOC analyzer damage. Consequently, Particulate Organic Carbon (POC) most probably was underestimated.

Despite in the April, June and July campaigns, there were evidence of redox processes in Castellbisbal MAR system according to major ions hydrochemistry, DOC concentrations were almost stable in time and space. The releasing of DOC via algae hydrolysis (or other POC sources) may be the reason why DOC concentrations remain constant despite biodegradation reactions occurring.

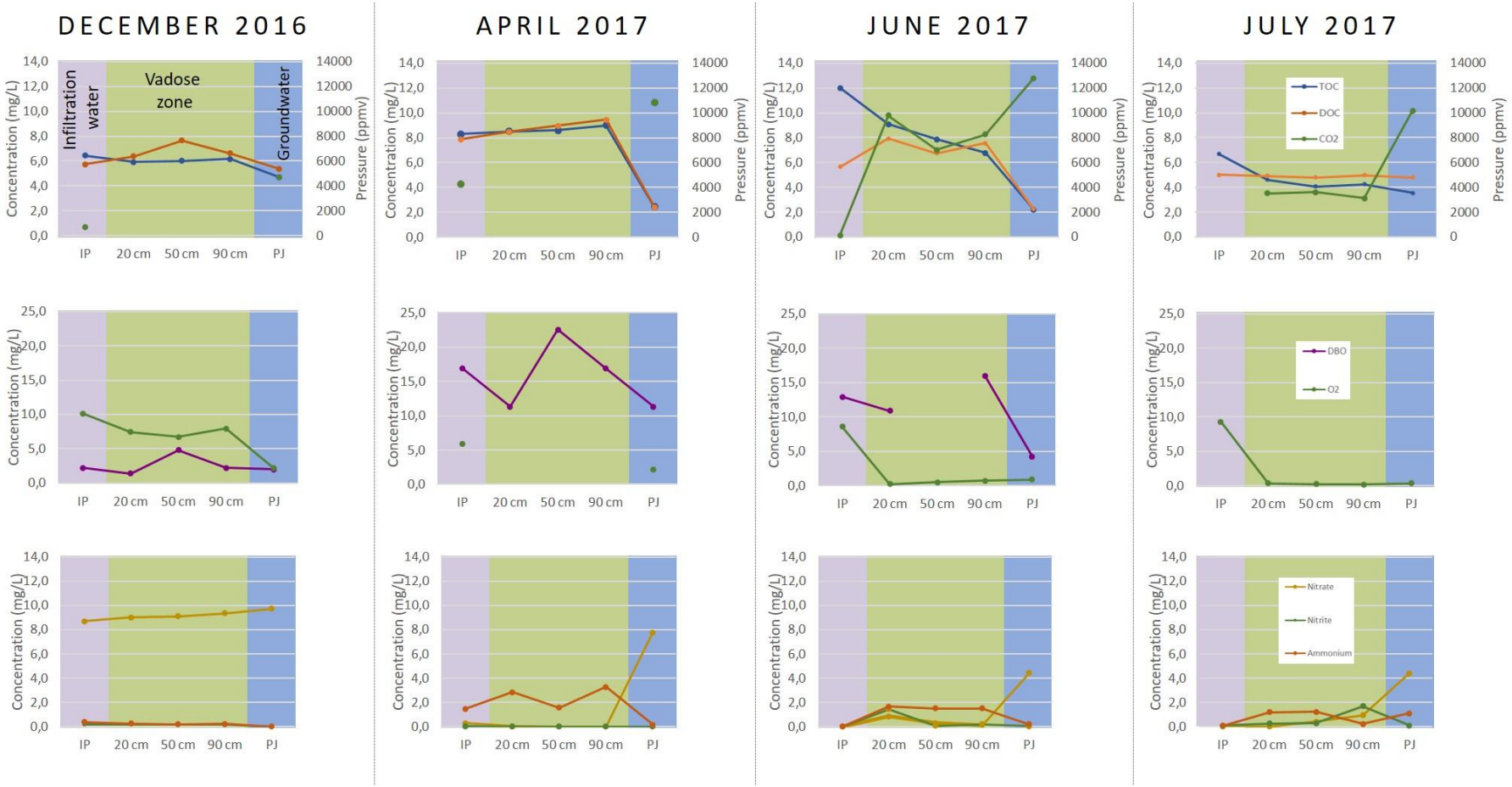

Figure 4.6 Evolution of TOC, DOC, CO_2, BOD, O_2, nitrate, nitrite and ammonium concentrations in four sampling campaigns performed in the Castellbisbal MAR system. Hydrochemical characterization of infiltration water (purple), vadose zone at three different depths (green) and saturated zone (blue) is represented. Missing values were samples that could not be measured/analyzed

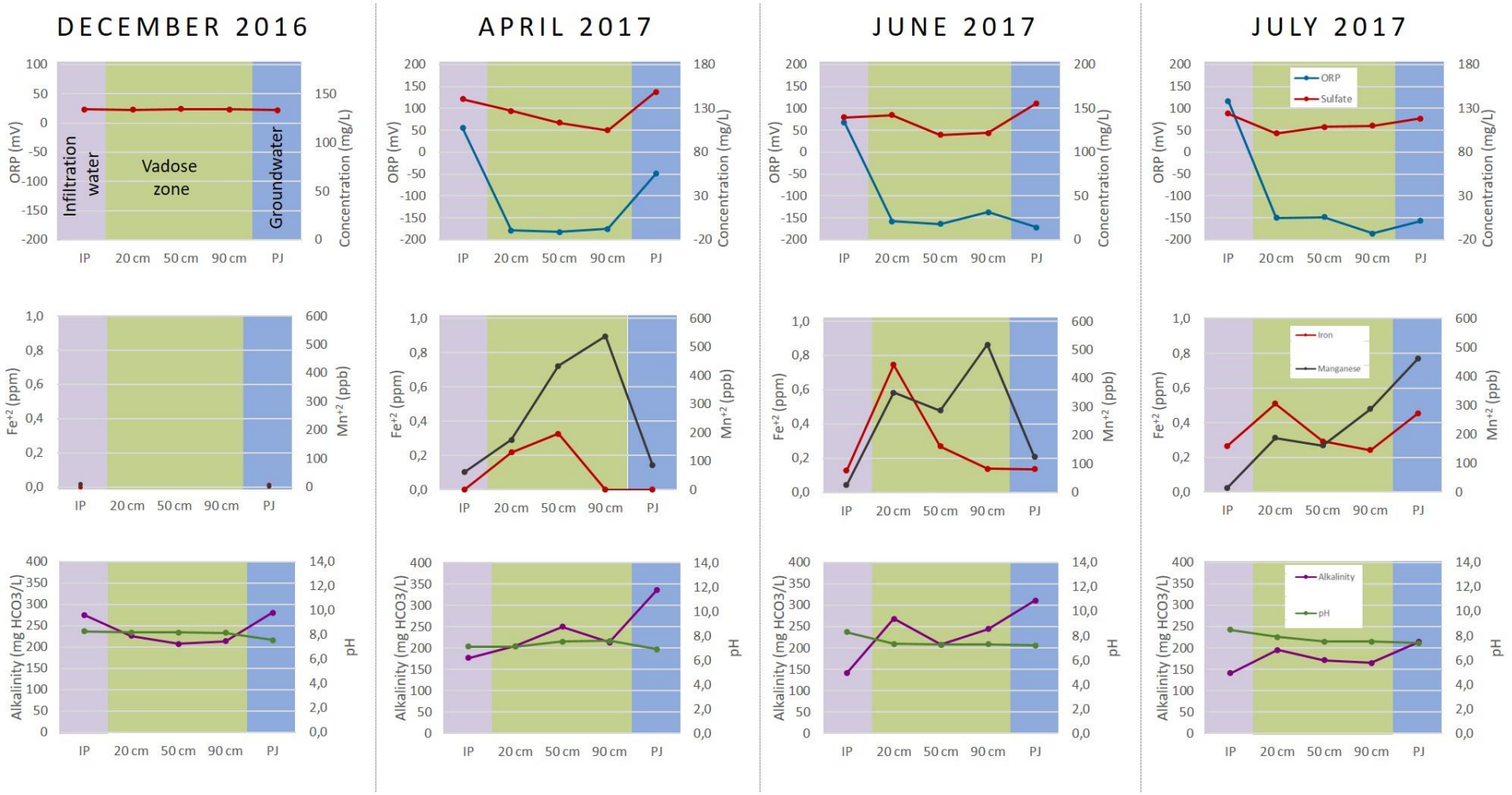

Figure 4.7 Evolution of Oxidation Reduction Potential (ORP), sulfate, iron, manganese concentrations, alkalinity and pH in four sampling campaigns performed in the Castellbisbal MAR system. Hydrochemical characterization of infiltration water (purple), vadose zone at three different depths (green) and saturated zone (blue) is represented. Missing values were samples that could not be measured/analyzed

b) Organic matter characterization in water, sediments, and stones

The origin of organic matter in water samples was determined by fluorescence. On the one hand, protein-like peaks (B and T) and humic-like peaks (C, A, and M) were determined (Figure 4.8). Protein-like peaks are indicators of organic matter that has been created recently, for example by means of photosynthesis. Humic-like peaks are typical of terrestrial organic matter, that is, organic matter not recently synthetized. On the other hand, SUVA, HIX, BIX and FI indices were calculated following Equations 4.1 to 4.4 (Figure 4.9). Comparing the results of the four sampling campaigns, infiltration pond water samples (IP, purple dots in Figure 4.9) showed the higher protein-like proportion, might indicating higher phototrophic activity with respect to other samples. However, December 2016 IP sample raised their proportion of humic-like peak compared with the rest of campaigns. A hypothesis of this behavior may be the drop of phototrophic processes in winter.

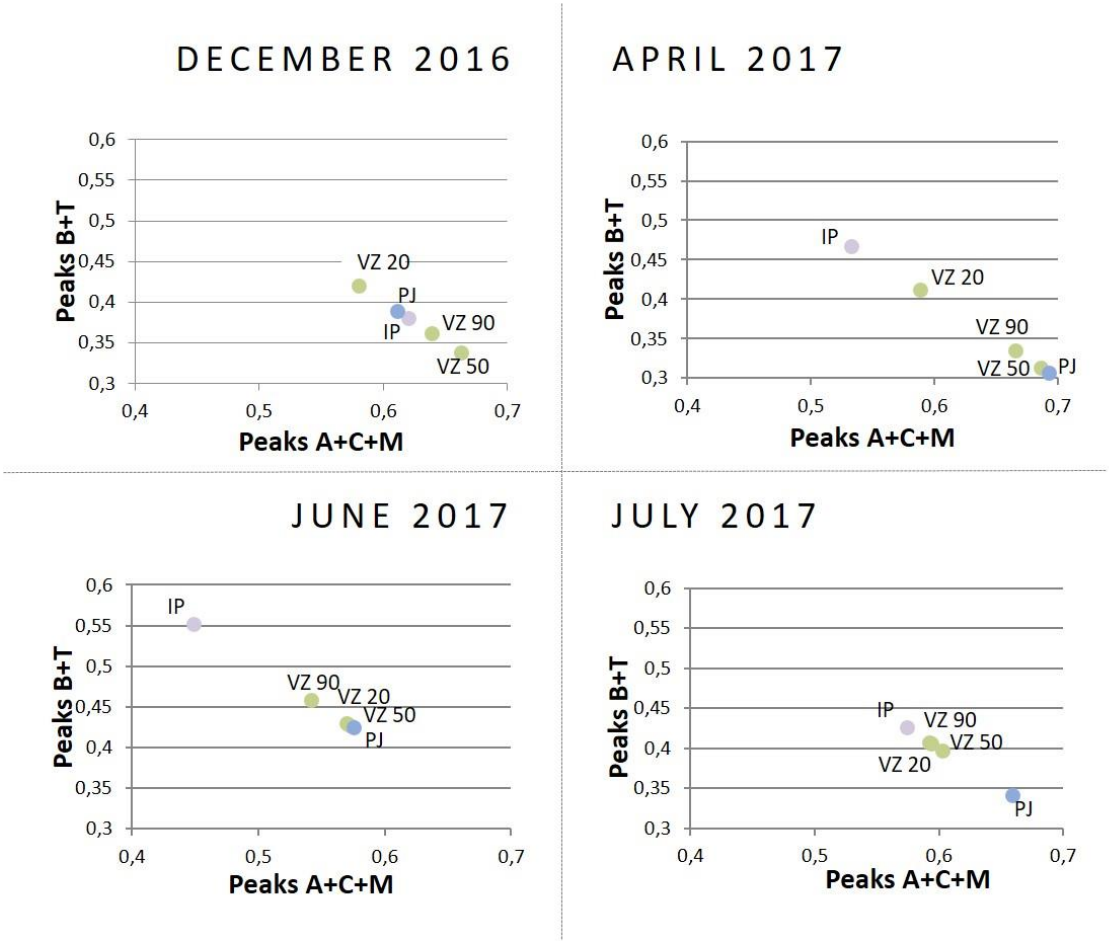

Figure 4.8 Relative contribution of the protein-like peak (B+T) and humic-like peak (A+C+M) intensities for Infiltration Pond (IP), vadose zone at three different depths (VZ – depth) and groundwater (PJ) water samples in the December 2016. April 2017, June 2017 and July 2017 sampling campaigns

IP sample in June (purple dot) showed the highest protein-like proportion of all data (55%). Despite bioclogging had been recently removed in June 2016, the protein-like proportion in the IP sample indicates probably the period with the highest primary production.

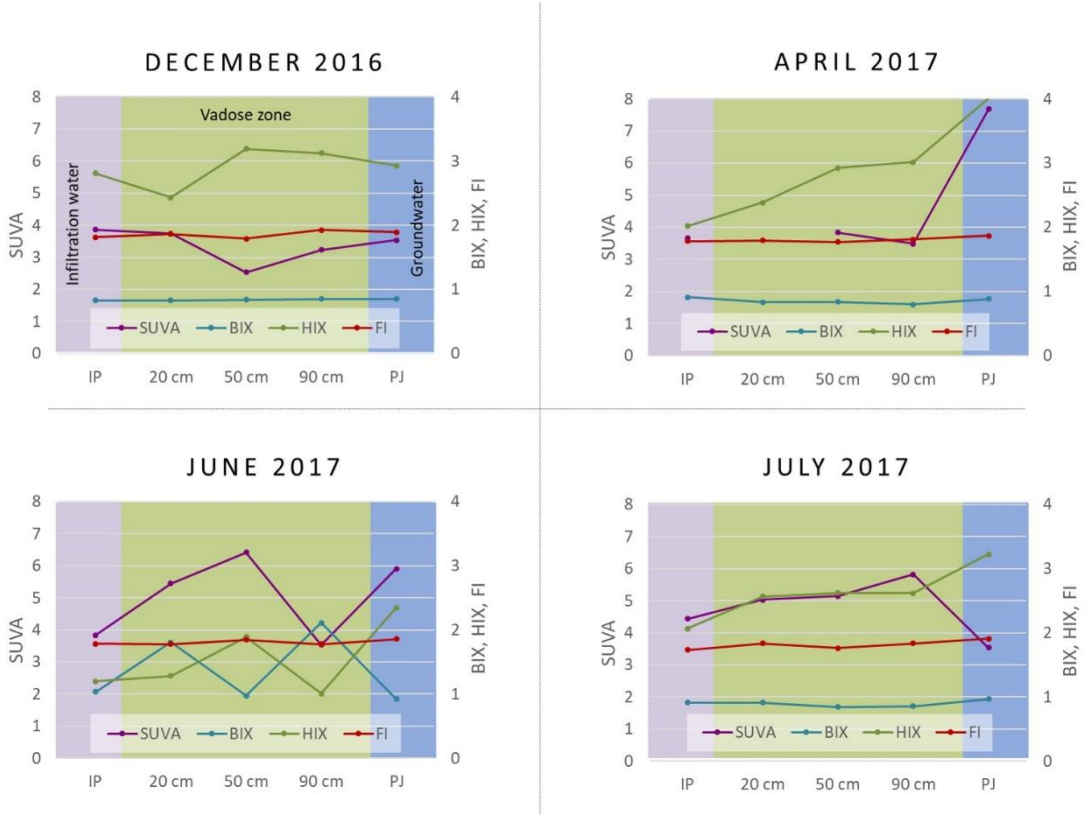

Figure 4.9 Evolution of fluorescence indices (SUVA, BIX, HIX, and FI) of water samples in the Castellbisbal MAR system for four different sampling campaigns

Samples taken at the vadose zone (green dots) had similar behavior between campaigns. The proportion of protein-like organic matter was relatively low for the three depths in December and April. Then, these proportions grew in June and decreased a little bit again in July. The main feature for these samples is the highest values of protein-like organic matter in June (see the IP sample). The difference between IP and vadose zone protein-peaks might give an idea about the proportion of labile DOM that has been oxidized by microorganisms in depth.

The PJ sample (blue dots) shows the opposite behavior of that of IP. In all campaigns, except that of December 2016, the former displayed higher humic-like organic matter proportion than the latter, indicating that higher consumption of labile DOM has been achieved. In the same way, values of TOC and DOC were almost always less in PJ than in the rest of the system, also suggesting that organic matter oxidation occurs into the soil profile before reaching PJ.

The evolution of fluorescence indices was apparently less informative than the proportion of humic and protein-like peaks. Concretely, Fluorescence Index (FI, red line) and Biological Index (BIX, blue line) remained constant in almost all campaigns and sampling points. Specific Ultra-Violet Absorbance index (SUVA, violet line) showed the most variability in time and space. SUVA in June 2017 was especially higher for the samples taken at 50 cm and PJ, indicating highest degree of aromaticity. Also, Humification Index (HIX, green line) was the highest for the PJ sample in June 2017; actually HIX in general raised in depth, indicating that organic matter maturity was proportional to travel time.

Organic matter amount in the infiltration pond sediment is presented in Figure 4.10. Results show for each campaign the average of the weight of carbon per surface unit for the five sediment samples analyzed. Also, error bars related to standard deviation are reported.

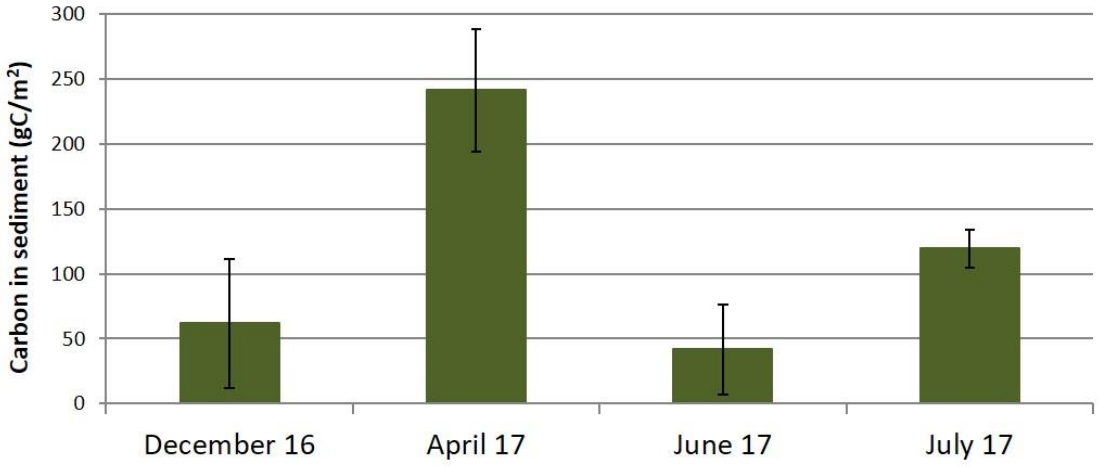

Figure 4.10 Evolution of the carbon content in the sediment of the Castellbisbal MAR infiltration pond

The evolution of carbon content per unit surface in the four sampling campaigns follows a tendency according to management practices. The highest rising of carbon content in the sediment took place between December 16 and April 17, coinciding with physical and biological clogging episode. The pronounced decreasing between April 17 and June 17 fits with the fact that the infiltration pond bottom was scrapped less than one month before the June campaign. The removal of infiltration pond sediment gives the reason for the losses of sediment carbon. After that, summer temperatures and the continuous operation of the MAR facility may be the reasons for the rising of carbon content in sediment in July 17.

Despite the general trend of organic carbon in sediment makes sense, the relatively high amounts of carbon in December are surprising since that campaign was performed one month and a half after scrapping. Likewise, hydrochemical data suggested that microbial activity in winter seemed not to be too high.

c) Continuous Redox potential measurements

In order to calibrate values from redox potential probes, ORP values (converted to Eh values) from sampling surveys were compared with redox fixed probes. ORP values of December campaign were not considered because electrode was damaged. Figure 4.11 shows the difference between campaigns values and soil redox probes. Values from infiltration water were not compared because the fixed sensor was collocated 30 cm above the bottom and in many campaigns was dry (infiltration pond had been dried in order to make possible the sampling). In all campaigns, the difference between both sensors was averaged in 320mV. Even groundwater sampled, representing a volume of water much greater than that surrounding the probe installed in the piezometer, give the same difference between both methods except in April.

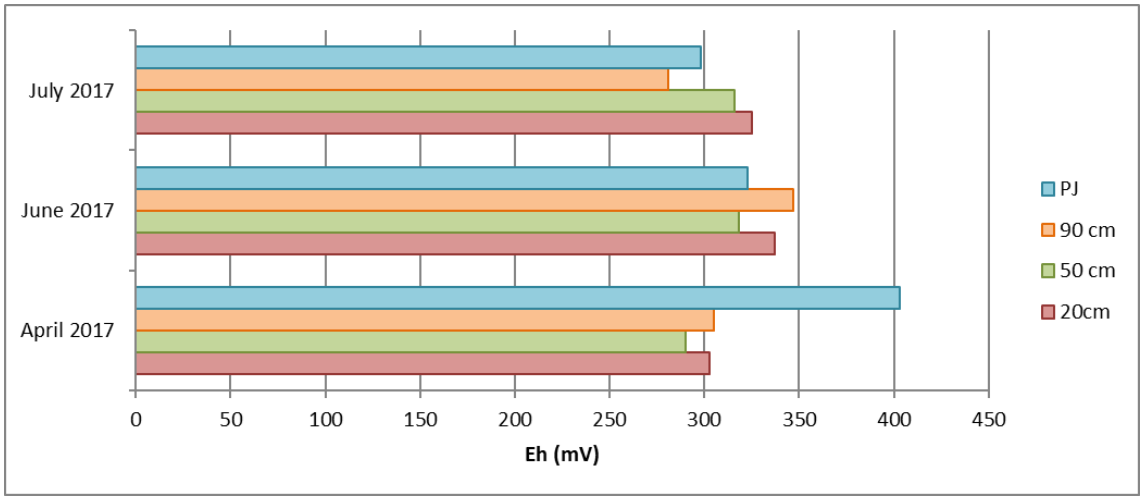

Figure 4.11 Difference between redox soil probes measurements and YSI Professional Plus values for the redox potential electrode in three sampling surveys. The averaged difference for all values is 320 mV (SD=32.2 mV)

Taking into account these differences, measurements of redox potential probes were corrected according to equation 4.6 and represented for the whole time studied (Figure 4.12 and Figure 4.13).

The redox potential of the infiltration water ranged between 0 and 1000 mV (Figure 4.12). However, the highest values and fluctuations are considered noise, because

correspond to measurements when the pond was empty, and the sensor was unstable. The temporal series of infiltration water redox potential shows oxic conditions over the whole year, showing the minimum values during the time period that groundwater reached the pond surface due to the flooding event at the end of March 2017 (beginning of Period III).

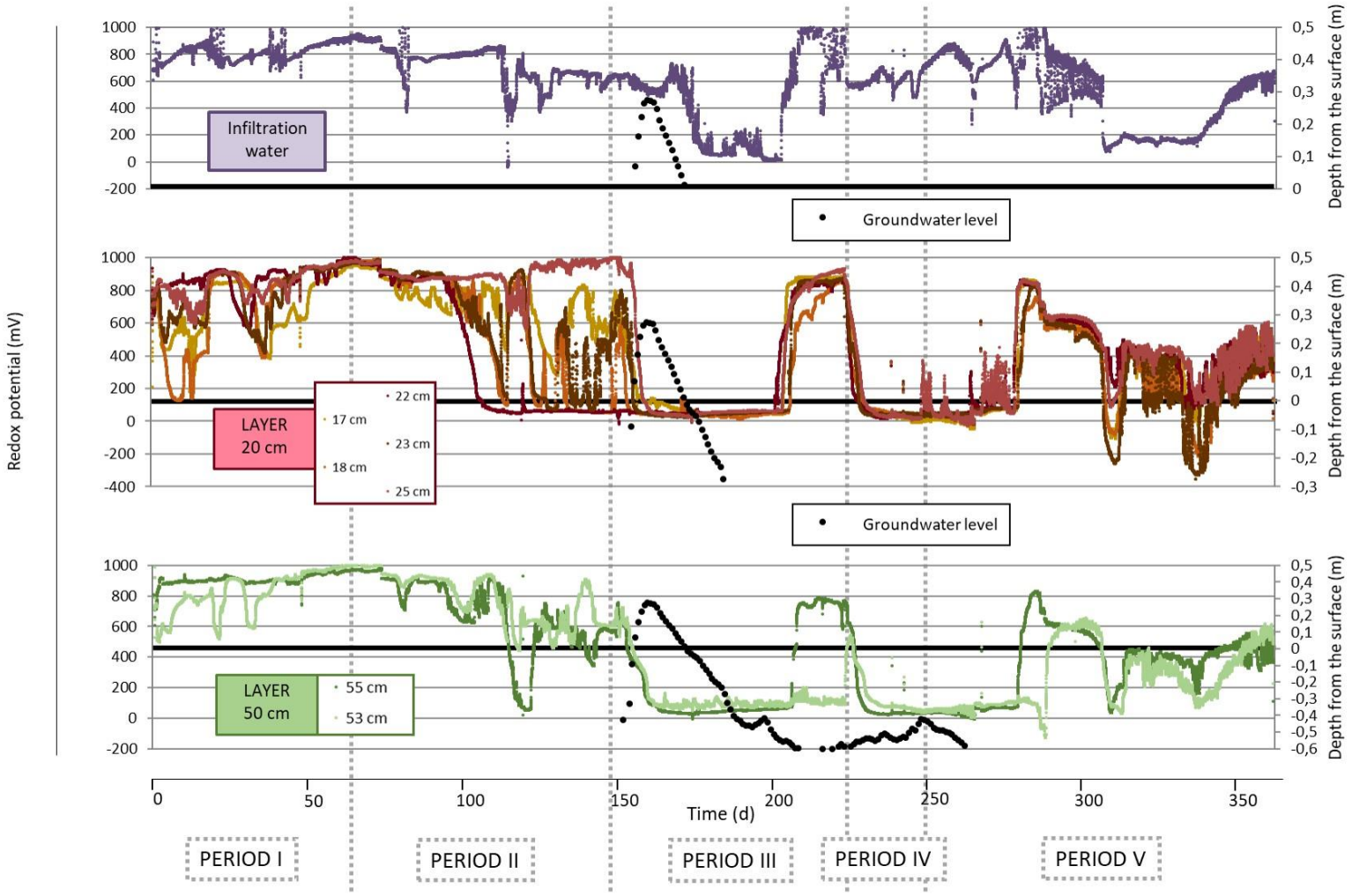

Figure 4.12 Redox potential measurements in the infiltration pond water (purple), in the 20 cm layer (brown ranges), and in the 50 cm layer (green ranges) between the October 24, 2016 and October 25, 2017. Groundwater level (black dots) is represented in reference to the surface level

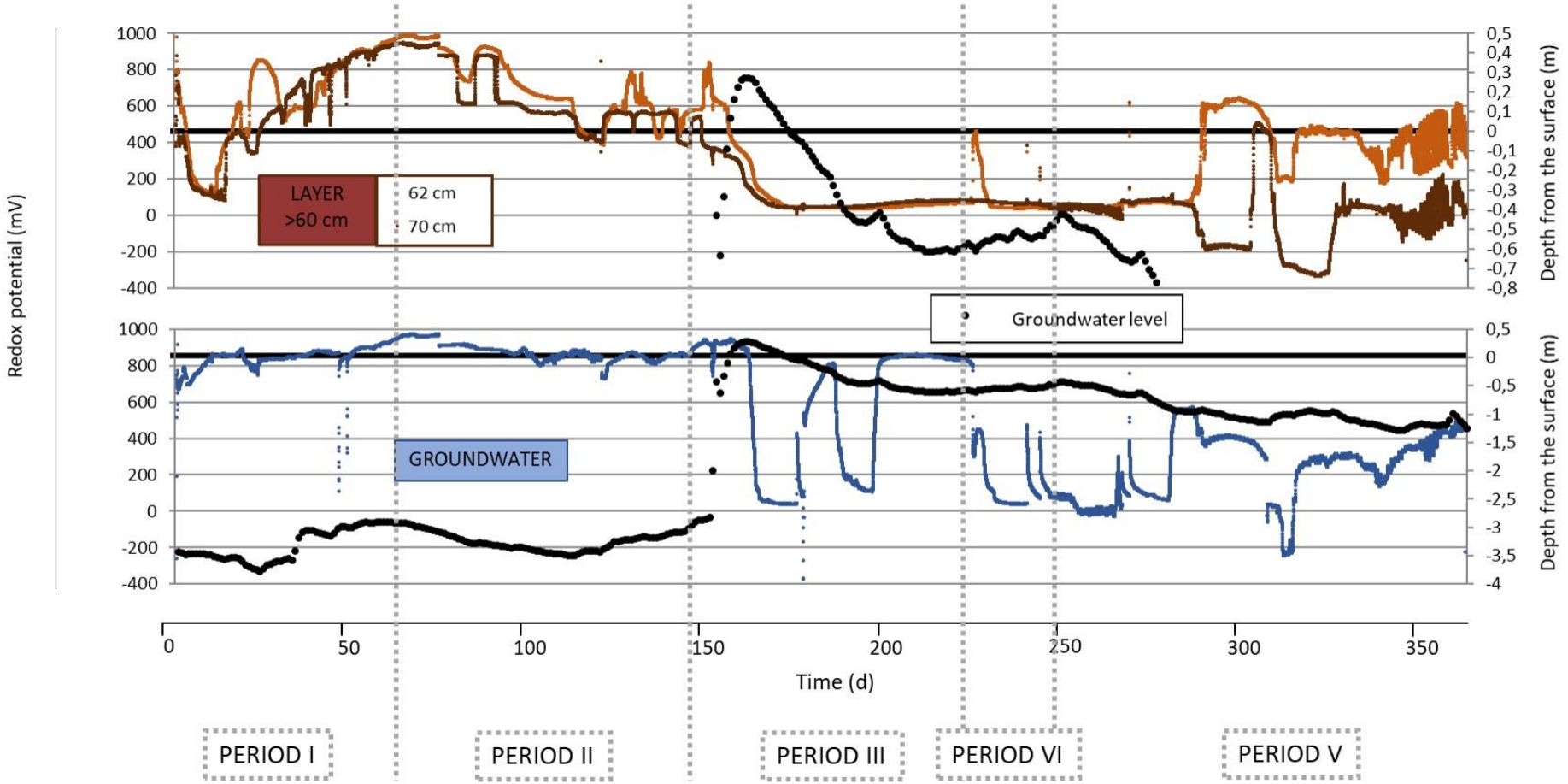

Figure 4.13 Redox potential measurements at 62 cm (orange) and 70 cm (brown) depths and in PJ (blue) at 4m depth below the surface. Groundwater level is represented in black dots

In general, all redox probes show very oxic conditions since the middle of the Period II, i.e. during the winter season. From the middle of Period II to the flooding event (beginning of Period III), soil redox potential was decreasing globally despite a large presence of fluctuations. However, redox potential in groundwater remained constant and highly oxic. The rising of groundwater level in March 2017 above the surface, caused the same behavior in all redox probes, from the infiltration pond to the aquifer, with a drastic fall in redox potentials, reaching almost 0 mV in all sensors. After the flooding event, redox potentials in all sensors of 20 cm layer and at 53 cm were rising at the same time that the groundwater level was falling. However, sensors at 55 cm, 62 cm, and 70 cm did not recover oxic conditions until Period V.

The variations in the groundwater level had in fact, a lot of consequences in the behavior of redox potential. During Periods III and IV, the groundwater level remained between the pond surface and 1m in depth. The redox potential was then negatively correlated with the depth of the sensors, becoming more oxidant in the shallow sensors. As the groundwater level was falling down, the shallow sensors were registering highest redox potentials. This also indicates that oxidant infiltration water was reaching the shallower sensors without the impact of groundwater.

Scrapping the bottom of the infiltration pond (by the end of Period III) had presumably some effects on all redox potentials measured by the sensors. It can be seen that oxic conditions, especially present in the shallow layers, were drastically altered in the Period III and IV transition, corresponding to the recovery of significant infiltration rates after scrapping.

In general, clogging episodes are related with more reductive conditions, while in periods with high infiltration rates (after scrapping and after summer stop), the redox potential raised.

Results from sampling campaigns are correlated with redox potentials measured in the field. Whereas redox conditions in winter (December sampling campaign) were oxidant (no nitrate depletion, nor iron and manganese presence), in the rest of sampling campaigns iron reduction conditions should had been reached (according to Figure 4.1 thresholds).

Finally, results of redox monitoring in PJ presented some drastic fluctuations. In many cases, the punctual extraction of sensors for monitoring purposes and pumping in some cases generated some unstable conditions, visible in Figure 4.13.

d) Evolution of temperature

Temperature sensors were installed to monitor infiltration water (30 cm above de bottom of the infiltration pond), at 55 cm, and inside PJ (Figure 4.14). Temperature measurements were daily averaged.

The evolution of temperature at three depths was almost the same during Period I and II (autumn and winter seasons). After the great flooding event (transition of Period II to III) and coinciding with the beginning of spring, the temperature of infiltration water and at 55 cm grew over the groundwater temperature. In fact, the temperature difference was about 10-15°C until the beginning of September. At the end of Period V, temperatures were linked again to the same behavior at the beginning of the study.

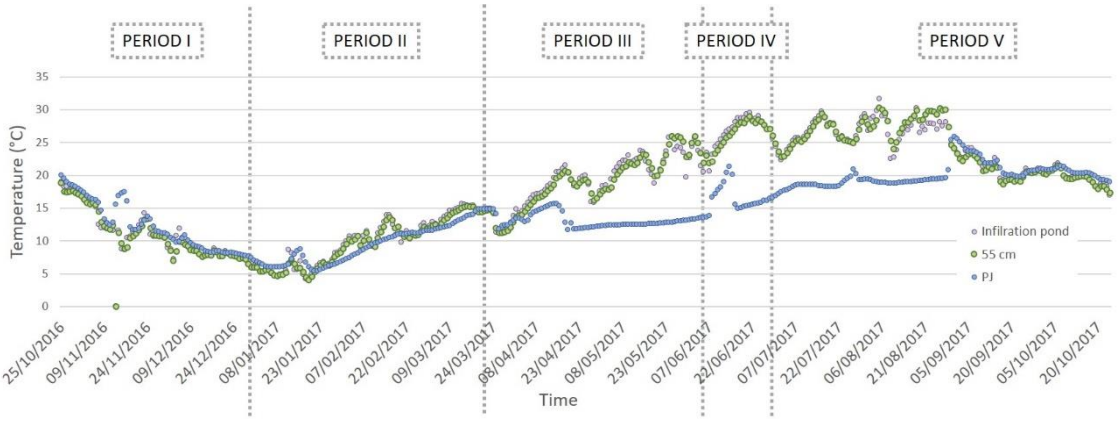

Figure 4.14 Temperature records in infiltration pond (in purple), 55 cm depth (green) and PJ (6 m below the surface) (blue) from October 2016 to October 2017 in Castellbisbal MAR system

Temporal evolution of redox potential and results for the four sampling campaigns performed suggest that temperature could be a determinant factor on biodegradation processes. Since microbial respiration has a strong temperature dependence (Or et al., 2007; Zhang et al., 2015), it is reasonable to think that microbial activity might be lower in cold periods than in the wet ones.

4.5. Conclusions

According to the wide monitoring control carried out in the Castellbisbal MAR system, different conclusions can be highlighted in order to improve the MAR system management:

- It is important to monitor the system in order to know and control processes occurring, i.e. monitoring groundwater levels just below the pond to avoid the excessive rise.
- Scrapping is a useful technique to revert the infiltration capacity of the system in terms of bioclogging and physical clogging removal.
- Physical clogging may accelerate bioclogging formation. The increase of residence time of water in an infiltration pond promotes photosynthetic activity, boosting particulate organic carbon for growth and respiration of organisms.
- Clogging processes are closed loops that can be interrupted and reverted with proper managing actions.
- Desiccation of the infiltration pond during the summer period had a favorable impact to mitigate bioclogging. Establishing drying-wetting hydric regimes might be a useful practice to avoid bioclogging effects, especially in the warmest periods.
- Data from sampling surveys and continuous monitoring support the idea that temperature is a key factor for redox processes and bioclogging development.
- MAR surface ponds can reach many different redox conditions in time and depth. This might have many consequences in order to improve water pollutants degradation.

CHAPTER 5: MODELING FLOW, TEMPERATURE AND BIOGEOCHEMICAL PROCESSES IN A SURFACE INFILTRATION SYSTEM

5.1. Introduction

Surface infiltration ponds are MAR facilities aimed at increasing groundwater resources, to store water and/or to improve the quality of water during the infiltration process (Bouwer, 2002).

Issues related to the operation of surface ponds are widely reported in the literature. Design aspects (Bouwer, 2002; Eusuff and Lansey, 2004; Hellauer et al., 2017), impacts on groundwater geochemistry (Goren et al., 2014), risk assessment (Pedretti et al., 2012a; Rodríguez-Escales et al., 2018); clogging issues and effects (Baveye et al., 1998; Dutta et al., 2015; Pedretti et al., 2012b); redox processes (Grau-Martínez et al., 2018; Greskowiak et al., 2006; Massmann et al., 2006; Rezanezhad et al., 2014; Schmidt et al., 2007); behavior of organic matter and pollutants (Alidina et al., 2014a; Regnery et al., 2015; Valhondo et al., 2018) and microbial community description (Alidina et al., 2014b; Li et al., 2013). Chapter 2 shows some examples of works concerning surface infiltration ponds. Most of these issues are dependent on temperature, and its role in infiltration facilities is often omitted. The temperature in the feeding water oscillates daily (Goren et al., 2014; Ronan et al., 1998) and seasonally (Braga et al., 2007; Greskowiak et al., 2006; Massmann et al., 2006); consequently, all the processes mentioned before are affected by it.

Temperature variations in the surface water of the Castellbisbal MAR system are not an exception; it shows a sinusoidal trend during the year (see Figure 4.14 in Chapter 4). The annual temperature cycle is characterized by a Mediterranean climate with moderate-low temperatures in winter (from 5ºC to 15ºC), tempered temperatures in autumn and spring (from 15ºC to 25ºC) and high temperatures at the end of spring and summer (from 25ºC to 45ºC). The maximum difference in environmental temperature registered in the facility between seasons was 46°C. Temperature variations have consequences for recharge facilities operation and management (Vandenbohede and Van Houtte, 2012). First, a large amount of intrinsic properties of fluids (mainly viscosity, density, and surface tension) are directly affected by temperature changes, thus, also changing hydraulic conductivity through:

$$f = \frac{\rho_w g}{\eta} = \frac{g}{\eta'} \tag{5.1}$$

where f is the fluidity of water [$L^{-1}T^{-1}$], ρ_w is water density [ML^{-3}], g is gravitational acceleration [LT^{-2}], η is viscosity [$ML^{-2}T^{-1}$] and η' is kinematic viscosity [L^2T^{-1}]. Lin et al. (2003) and Braga et al. (2007) estimated in 40% and 56% respectively the change of infiltration rate between the summer and winter months due to viscosity changes. The latter also predicted a cyclical pattern of high and low infiltration rates occurring across the year.

Another intrinsic property of water is surface tension at the air-water interface, decreasing with increasing temperature. However, its influence upon hydraulic conductivity is mild (Constantz, 1982; Lin et al., 2003; Ronan et al., 1998), and it is mostly neglected in experiments and studies evaluating infiltration yields (Lin et al., 2003).

Temperature also influences indirectly water quality in MAR systems, since it is one of the main factors catalyzing chemical reactions. As a consequence, microbial degradation rates depend on temperature evolution (Maeng et al., 2011). This fact is especially demonstrated in many field investigations, beyond laboratory studies (Greskowiak et al., 2017). For example, temperature affects pyrite oxidation (Prommer and Stuyfzand, 2005), aerobic oxidation of organic matter (Massmann et al., 2006), nitrogen reduction (Carrera et al., 2003; David et al., 1997; Massmann et al., 2006), and manganese reduction (Massmann et al., 2006). Many of these works are accompanied by biogeochemical models explaining the fate of redox-sensitive species in surface infiltration systems.

Taking into account the effect of temperature in reaction rates during MAR activities implies: 1) understanding multiphase flows in the unsaturated zone; 2) coupling temperature dynamics to flow models; and 3) coupling temperature dynamics and geochemical processes to multiphase systems. A model including temperature affections and their implication on redox reactions will help to improve the design, managing and operating MAR systems. With this information, both the infiltration rate and the quality of the recharged water could be optimized through, for example, a decision tool. Although some works have coupled all these processes (e.g. Greskowiak et al. 2006), to our knowledge, there is no work coupling flow in unsaturated and saturated media, heat transport, biogeochemical reactions, and managing actions (scraping, non-recharge periods, etc.).

Then, the main aim of this chapter is to assess and quantify with a numerical model the temperature impact on hydraulic conductivity and to evaluate its role in biodegradation processes (microbial degradation rates), in a real surface infiltration system during a year of operation. Improving knowledge about the influence of seasonal temperature changes on the infiltration rate would allow achieving optimal operation and maximum recharge efficiency in surface infiltration systems.

To achieve this goal, the first step was to develop a flow and heat transport model of the Castellbisbal recharge facility considering the temperature variations during one year and using the experimental information described in Chapter 4. After that, in order to test the impact of the temperature on the biogeochemistry of the system, a batch biogeochemical model was developed to:

- Test the role of temperature in biological clogging;
- Test the impacts of organic matter origin in redox processes; and
- Evaluate the effect of temperature on the redox processes occurring in the top-soil of the Castellbisbal infiltration pond.

This batch geochemical model was developed as an initial tool to quantify the relative importance of temperature in the system. It was done in order to set up the main biogeochemical processes involved in recharge and to evaluate the influence of temperature.

5.2. Methodology

A one-dimension flow and heat transport model of the Castellbisbal MAR system has been constructed. Two different biogeochemical scenarios were evaluated with batch simulations. The model was based on the field site of Castellbisbal (see section 1.5.3) and we used the experimental information collected during the period between October 2016 and October 2017, which is described in Chapter 4.

5.2.1. Flow and heat transport models

Governing equations

The flow between infiltration pond and groundwater was simulated with the software HYDRUS version 4.16.0110 (Jacques and Simunek, 2005). The code solves the Richards equation for water movement in a partially-saturated porous medium:

$$\frac{\partial \theta}{\partial t} = \frac{\partial}{\partial x}\left[K\left(\frac{\partial h}{\partial x} + \cos\alpha\right)\right] - S \tag{5.2.}$$

where h is the water pressure head [L], θ is the volumetric water content [$L^3\ L^{-3}$], t is time [T], x is the spatial coordinate [L] (positive upward), S is the sink term [$L^3\ L^{-3}T^{-1}$], α is the angle between the flow direction and the vertical axis ($\alpha = 0$ for vertical flow), and $K(h)$ is the unsaturated hydraulic conductivity [LT^{-1}] given by

$$K(h,x) = K_s(x)K_r(h,x) \tag{5.3.}$$

where Kr is the relative hydraulic conductivity [-] and Ks the saturated hydraulic conductivity [LT^{-1}].

A single porosity model was assumed based on the analytical solution of Van Genuchten (1980) (Eq 5.4 and 5.5) to estimate unsaturated hydraulic properties:

$$\theta(h) = \begin{cases} \frac{\theta_s - \theta_r}{[1+|\alpha h|^n]^m} & h < 0 \\ \theta_s & h \geq 0 \end{cases} \tag{5.4.}$$

$$K(h) = K_s S_e^l \left[1 - \left(1 - S_e^{\frac{l}{m}}\right)^m\right]^2 \tag{5.5.}$$

where θ_s is the saturated water content [-], θ_r is the residual water content [-], α, m, n are empirical parameters [1/L], [-], [-], and S_e is the effective water content[-].

Van Genuchten (1980) used the statistical pore-size distribution model of Mualem (1976) to obtain a predictive equation for the unsaturated hydraulic conductivity function in terms of soil water retention parameters.

Heat transport across the profile was considered following the solution described with a convection-dispersion equation of the form:

$$\frac{\partial C_p(\theta)T}{\partial t} = \frac{\partial}{\partial x}\left[\lambda(\theta)\frac{\partial T}{\partial x}\right] - C_w\frac{\partial qT}{\partial x} - C_w ST \tag{5.6.}$$

where $\lambda(\theta)$ is the coefficient of the apparent thermal conductivity of the soil [$MLT^{-3}K^{-1}$] and $C_p(\theta)$ and C_w are the volumetric heat capacities [$ML^{-1}T^{-2}K^{-1}$] of the porous medium and the liquid phase, respectively. The temperature for the inlet water (infiltration pond water) and outlet water (PJ) were set as thermal boundary conditions.

The definition of thermal conductivity proposed by Chung and Horton (1987) was used:

$$\lambda_0(\theta) = b_1 + b_2\theta + b_3\theta^{0.5} \quad (5.7)$$

where b_1, b_2, and b_3 are empirical parameters [$MLT^{-3}K^{-1}$] for a sandy material.

Since temperature may affect hydraulic parameters (mainly water viscosity), Ks changes as a function of temperature variations were calculated following the expression proposed by Constantz (1982):

$$K_T(\theta) = \frac{\mu_{ref}}{\mu_T}\frac{\rho_T}{\rho_{ref}}K_{ref}(\theta) \quad (5.8)$$

where K_{ref} and K_T denote hydraulic conductivities at the reference temperature T_{ref} and soil temperature T, respectively; μ_{ref} and μ_T (ρ_{ref} and ρ_T) represent the dynamic viscosity [$ML^{-1}T^{-1}$] (density of soil water [ML^{-3}]) at T_{ref} and T, respectively.

Model construction

A one-dimension model was constructed for the study zone of Castellbisbal. The model took into account the vertical profile constituted by the infiltration pond, the vadose zone, and the saturated zone. The total length of the model was 6 m. The domain was discretized with a regular mesh of 100 nodes (each one 6 cm long). Two layers were defined in the vadose zone (of lengths 20 cm and 580 cm) to consider the topsoil clogging effect as well as the corresponding maintenance practices of the infiltration pond along the modeled year (see Chapter 4).

In order to change hydraulic conductivity for the upper layer to simulate observed clogging, the whole model was divided into five different sub-models according to the periods presented in Chapter 4 and in Table 5.2. The lower layer (580 cm) was considered not affected by clogging and its hydraulic conductivity was assumed constant along the all modeled period. Soil hydraulic parameters for the sandy material of the two layers are presented in Table 5.1 and were set through pedotransfer functions provided by HYDRUS.

The total modeled time was 365 days and it was regularly discretized using a time step of 1 day. Both spatial and temporal discretizations were selected according to Péclet and Courant criteria in order to avoid numerical oscillations.

Table 5.1 Soil hydraulic parameters and geometry of the model

Layer	Layer 1	Layer 2
Depth [cm]	20	580
Qr [-]	0.045	
Qs [-]	0.28	
a [1/cm]	0.145	
n [-]	2.68	
l [-]	0.5	
***Ks* [cm/d]**	**calibrated**	**calibrated**

Qr Residual soil water content; *Qs* Saturated soil water content; *a, n* Parameters in the soil water retention curve; *l* Tortuosity factor in the conductivity function; *Ks* Saturated hydraulic conductivity

Table 5.2 Time periods for the model

Number of period	I	II	III	IV	V
Duration [d]	64	83	75	27	116

The water table of the pond and the groundwater pressure at 6 m depth (location of the pressure transducer in the piezometer) were set as upper and lower Dirichlet boundary conditions respectively during the modeling time of one year.

The initial conditions of the model were -20 cm of pressure head at the upper node linearly growing until node number 58 (depth 358 cm), where the groundwater level was set. From node 58 to the lower boundary (600 cm), saturated conditions were set at h=0 cm. The temperature was established for the upper node (19°C, infiltration water) and the lower node (20°C, aquifer). Values between both nodes were linearly interpolated.

Saturated hydraulic conductivity (K_s) was the calibrated parameter for both layers. Porosity (Q_s) value was defined according to different local studies (section 1.5.3 in Chapter 1). Calculated infiltration flow was compared to the real one, which was measured daily during the whole modeled period (see Chapter 4). The model was divided into five different sub-models considering the different periods. The outputs from each model were used as inputs for the subsequent one.

After flow model calibration, the heat transport model was carried out. Heat transport parameters were set to default values following the determination of Chung and Horton (1987) for a sandy material (Table 5.3). The temperature of the

infiltration water and at the aquifer were prescribed daily as upper and lower boundary conditions, respectively.

Table 5.3 Heat transport parameters for a sandy material according to Chung and Horton (1987)

S [-]	D_T [cm]	b_1 [kg·cm/d^3·°C]	b_2 [kg·cm/d^3·°C]	b_3 [kg·cm/d^3·°C]	C_n [kg·cm/d^2·°C]	C_w [kg·cm/d^2·°C]
0.72	5	$1.47054 \cdot 10^{16}$	$-1.5518 \cdot 10^{17}$	$3.16617 \cdot 10^{17}$	$1.43327 \cdot 10^{14}$	$3.12035 \cdot 10^{14}$

S Volume fraction of solid phase; D_T Longitudinal thermal dispersivity [cm]; b_1 Coefficient b_1 in the expression for the thermal conductivity function; b_2 Coefficient b_2 in the expression for the thermal conductivity function; b_3 Coefficient b_3 in the expression for the thermal conductivity function; C_n Volumetric heat capacity of the solid phase; C_w Volumetric heat capacity of the liquid phase.

The validity of the heat transport model was done comparing the fitting of temperature calculated at a depth of 55 cm with the data provided by the temperature sensor (Figure 4.14, Chapter 4).

5.2.2. Biogeochemical model: organic matter fate during managed aquifer recharge

The basis for the biogeochemical model: winter vs summer scenarios

The biogeochemical model at batch scale was developed using Phreeqc code (version 2.18.00) (Parkhurst and Appelo, 2013). In this model, the main processes of organic matter oxidation concerning the carbon and the nitrogen flow were considered. These are summarized in Figure 5.1.

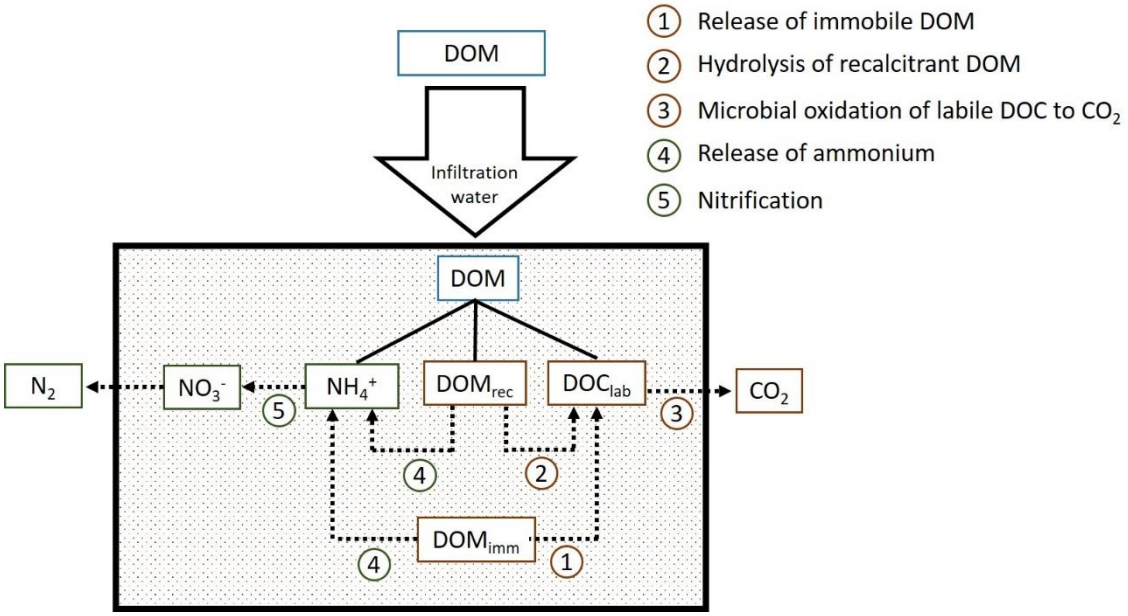

Figure 5.1 Conceptual biogeochemical model of DOM transformation and degradation via different paths (discontinuous arrows 1 to 5). DOM coming from infiltration water composition comprises a source of ammonium, DOM_{rec} (as the recalcitrant fraction of DOM), and DOC_{lab} (labile fraction of DOM). DOM_{imm} is the immobile form of DOM, as an endogenous source of organic matter synthetized in situ.

This model assumes that a fraction of dissolved organic matter (DOM) present in the soil profile comes from the infiltration water. DOM is divided into two different pools: recalcitrant organic matter and labile dissolved organic carbon (DOC_{lab}). Recalcitrant DOC can be converted to DOC_{lab} and ammonium (processes 2 and 4). The model also incorporates the carbon produced due to photosynthetic growth, it is called endogenous organic matter (DOM_{imm}). This endogenic production is assimilated as organic matter provided by bioclogging layer or settled algae on the bottom of the pond. DOM_{imm} can be also converted to labile DOC (process 1). DOC_{lab} is considered the unique species oxidized to CO_2 by microorganisms (process 3). This oxidation process takes into account the microbial use of different electron acceptors. Oxygen, nitrate, manganese, iron or sulfate will be used as electron acceptors according to their availability and their respective energy yield (Bethke et al., 2011; Ghattas et al., 2017).

The production of DOC_{lab} *via* demobilization of DOM_{imm} and hydrolysis of DOM_{rec} implies the release of ammonium (process 4), as a simplification of Dissolved Organic Nitrogen. If oxygen is present, ammonium is converted to nitrate through nitrification (process 5) and this can be reduced to nitrogen gas *via* denitrification path if anaerobic conditions are reached. Note that denitrification is also part of organic carbon oxidation (process 3).

Considering that nitrite was not significantly detected (Figure 4.6, Chapter 4), and in order to simplify the model, it was neglected. Besides, the model neither considers the growth nor the decay of biomass. Neither CO_2 autotrophic fixation by algae and cyanobacteria were considered in the model; they were assumed as part of bioclogging and as immobile DOM, setting an initial concentration. Photochemical and biological degradation of recalcitrant DOM was also omitted, considering that rates are much lower than those of oxidation of labile DOC.

Modeled reactions and governing equations

In Castellbisbal MAR system, aerobic, denitrifying, manganese and iron-reducing conditions were reached at different locations according to the results of Chapter 4. The simulation of labile organic matter described by the conceptual biogeochemical model described was carried out considering DOC_{lab} represented by the chemical formula CH_2O. The corresponding redox reactions for DOC_{lab} degradation are:

Aerobic respiration: $CH_2O + O_2 \rightarrow HCO_3^- + H^+$

Denitrification: $CH_2O + 0.8NO_3^- + 0.8H^+ \rightarrow HCO_3^- + 0.4N_2 + H^+ + 0.4H_2O$

Manganese reduction: $2CH_2O + 4MnO_2 + 6H^+ \rightarrow 2HCO_3^- + 4Mn^{2+} + 4H_2O$

Iron reduction: $CH_2O + 4Fe(OH) + 7H^+ \rightarrow HCO_3^- + 4Fe^{2+} + 6H_2O$

Sulfate reduction: $2CH_2O + SO_4^{-2} \rightarrow 2HCO_3^- + HS^- + H^+$

All these reactions were modeled grouped into the rates defined in Equation 5.11 in Table 5.4. In turn, DOC_{lab} comes from immobile and recalcitrant DOM, following 1:1 stoichiometry in the depletion of DOM in favor of the appearance of DOC_{lab}. The transformation of DOM_{imm} and DOM_{rec} into DOC_{lab} is modeled following rate definitions in equations 5.9 and 5.10 respectively in Table 5.4.

Table 5.4 Processes involved in DOM transformation and consumption in a shallow part of saturated soil

Number of process	Process	Rate definition
①	Release of immobile DOM	$\frac{dDOC_{lab}}{dt} = K_{imm} \times \frac{F(T)}{F(T_{opt})} \times [DOM_{imm}]$ (5.9)
②	Hydrolysis of recalcitrant DOM	$\frac{dDOC_{lab}}{dt} = K_{rec} \times \frac{F(T)}{F(T_{opt})} \times [DOM_{rec}]$ (5.10)
③	Microbial oxidation of labile DOC	$\frac{dDOC_{lab}}{dt} = \frac{F(T)}{F(T_{opt})} \times [DOC_{lab}] \times \sum_{i=1}^{n}\left(-k_i \frac{C_i}{C_i+K_i} \prod_{j=1}^{m} \frac{C_{j,i}+K_{inh,j,i}}{K_{inh,j,i}}\right)$ (5.11)
④	Release of ammonium	$\frac{dNH_4^+}{dt} = k_{imm} \times \frac{F(T)}{F(T_{opt})} \times [DOM_{imm}]$ (5.12) $\frac{dNH_4^+}{dt} = k_{rec} \times \frac{F(T)}{F(T_{opt})} \times [DOM_{rec}]$ (5.13)
⑤	Nitrification	$\mathbf{\frac{dNH_4^+}{dt} = -\frac{F(T)}{F(T_{opt})} \times k_{Amm} \times \frac{[O_2]}{K_{O_2}+[O_2]} \times \frac{[NH_4^+]}{K_{Amm}+[NH_4^+]}}$ (5.14)

K_{imm} [T^{-1}]is the first-order rate for the release of immobile DOM; *F(T)* [-] is the function of the temperature dependence of DOM transformation and mineralization; $F(T_{opt})$ [-] is the maximum value of *F(T)*; K_{rec} [T^{-1}] is the first-order rate for the hydrolysis of recalcitrant DOM; *n* is the number of the terminal electron acceptors; k_i [$M \cdot M^{-3} \cdot T^{-1}$] is the maximum rate for the DOC_{lab} degradation using *i* species as electron acceptor; C_i [$M \cdot M^{-3}$] is the concentration of the corresponding electron acceptor in the oxidation of DOC_{lab}; K_i [$M \cdot M^{-3}$] is the half-saturation constant of the corresponding electron acceptor in the oxidation of DOC_{lab}; $C_{j,i}$ [$M \cdot M^{-3}$] is the concentration of *j* inhibitor above the *i* species in the oxidation of DOC_{lab}; $K_{inh,j,i}$ [$M \cdot M^{-3}$] is the inhibition coefficient of the *j* inhibitor above the *i* species in the oxidation of DOC_{lab}; k_{Amm} [$M \cdot M^{-3} \cdot T^{-1}$] is the maximum nitrification rate; and K_{O_2} is the half-saturation constant for O_2 in nitrification; K_{Amm} is the half-saturation constant for ammonium in nitrification.

The release of ammonium (process 4, Table 4) during DOM_{imm} and DOM_{rec} transformations followed the equations 5.12 and 5.13 in Table 5.4. The stoichiometry of this transformation was set in 1:0.15 for the relation DOM:Ammonium. Finally, nitrification (process 5) was unified in order to group nitritation and nitratation in a single-step:

Nitritation: $2NH_4^+ + 3O_2 \rightarrow 2NO_2^- + 4H^+ + 2H_2O$

Nitratation: $2NO_2^- + O_2 \rightarrow 2NO_3^-$

Nitrification: $2NH_4^+ + 4O_2 \rightarrow 2NO_3^- + 4H^+ + 2H_2O$

Equation 5.14 defines the nitrification rate for the reduced organic nitrogen (ammonium) to the most oxidized form (nitrate). The stoichiometry of the reaction was set in 1:1 for ammonium:nitrate as it is shown in nitrification equation above. All values and sources of kinetic constants are summarized in Table 5.5.

The influence of temperature, F(T), in all defined processes is modeled according to Greskowiak et al. (2006), Kirschbaum (1995) and O'Connell (1990):

$$F(T) = exp\left[\alpha + \beta T\left(1 - 0.5\frac{T}{T_{opt}}\right)\right] \quad (5.15)$$

where α [-] and β [-] are fitting parameters and T_{opt} [Celsius] is the optimal temperature for the decomposition and transformation rates.

Table 5.5 Summary of parameters used in biogeochemical batch models: first order rates (K_{imm} and K_{rec}); maximum degradation rates (K); half-saturation constants (k); and inhibition constants (k_{inh}); T_{opt} and $F(T_{opt})$

Parameter	Units	Used value	Source	Values in literature
K_{imm}	d^{-1}	1	assumed	
K_{rec}	d^{-1}	0.01	assumed	
k_{O_2}	d^{-1}	0.15	a, b	0.08[b], 0.01[c]
$k_{NO_3^-}$	d^{-1}	0.12	a, b	0.01[b], 0.001[c]
$k_{Mn^{2+}}$	d^{-1}	0.1	a, b	0.011[b], 0.0002[c]
$k_{Fe^{2+}}$	d^{-1}	0.11	a, b	0.008[b]
$k_{SO_4^{2-}}$	d^{-1}	0.09	a, b	0.12[b], 0.01[c]
K_{O_2}	M	1.56e-05	a, b	1e-05[d], 3.1e-06[e], 2e-03[f]; 2.94e-04[g]
$K_{NO_3^-}$	M	8.06e-06	a, b	1e-05[d], 3.1e-06[e], 2e-03[f], 2.94e-04[g]
$K_{Mn^{2+}}$	M	5.62e-06	a	8.93e-06[b]
$K_{Fe^{2+}}$	M	5.75e-06	a	9.09e-06[b], 2.4e-04[e], 1e-04[g]
$K_{SO_4^{2-}}$	M	5.21e-06	a, b	1.6e-04[e], 1e-05[f],
K_{inh,O_2}	M	3.13e-07	a, b	1e-05[d], 3.1e-5[e]
K_{inh,NO_3^-}	M	1.61e-07	a, b	1.6e-5[e]
$K_{inh,Mn^{2+}}$	M	1.12e-07	a	1.79e-07[b]
$K_{inh,Fe^{2+}}$	M	1.15e-07	a	1.82e-07[b]
K_{amm}	M	5e-05	assumed	
k_{amm}	$M \cdot d^{-1}$	12.26	assumed	
T_{opt}	°C	35.0	d	36.9[h,i],33.1[j],33.8[j]
$F(T_{opt})$	-	5.20698	d	
α	-	-1.50	d	-3.432[h],-3.764[h], -1.16[j], -2.26[j]
β	-	0.18	d	0.19[h], 0.20[h], 0.21[j], 0.26[j], 0.15[i]

a Rodríguez-Escales et al. (2017); b Rolle et al. (2008); c Brun and Engesgaard (2002); d Greskowiak et al. (2006); e Mayer et al. (2001); f Prommer et al. (2002); g Prommer et al. (2006); h Kirschbaum (1995); i Kirschbaum (2000); j O'Connell (1990)

Model implementation in PHREEQC: input data

To compare the effect of temperature, the model was run using two different solutions representing water recharged in the facility of Castellbisbal: one

representative of winter and the other one representative of summer chemical signatures. The water of the infiltration pond and organic carbon in the sediment of December 2016 (winter scenario) and July 2017 (summer scenario) sampling surveys were taken as reference data for the two models.

In order to lay the hydrochemistry for the two models and considering the small differences between surveys, a typeset water was defined for the concentrations of sulfate, sodium, Total Inorganic Carbon (TIC), potassium, calcium, and chloride. Considering the four sampling campaigns (December 2016, April 2017, June 2017 and July 2017, see Chapter 4), the typeset water was established averaging the mentioned parameters of the infiltration water. Piper diagram was constructed to ensure the representability of the typeset water as an average of the four campaigns (Figure 5.2). Considering the same composition for both models allow also a better understanding of the organic carbon behavior and the corresponding redox processes involved.

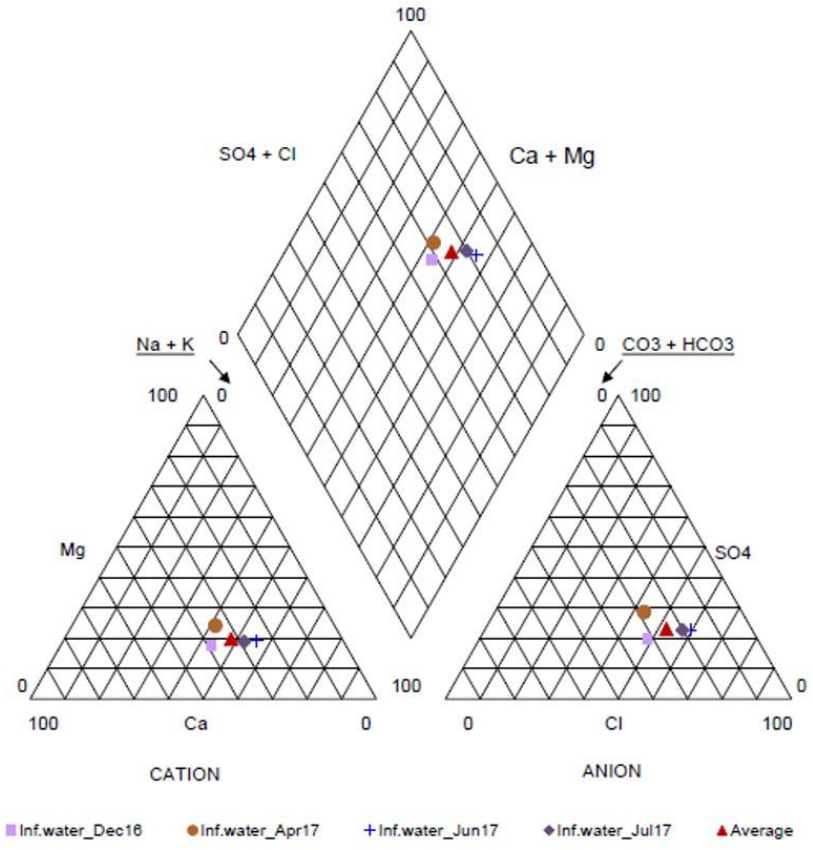

Figure 5.2 Piper diagram showing the relative position of infiltration water samples of the four sampling campaigns performed in the Castellbisbal MAR system. Red triangle represents the average values of water parameters for the four campaigns.

Nitrate, temperature, pH and dissolved oxygen in winter and summer models were set to the measurements in the infiltration water measured in December 2016 and July 2017, respectively. Value of pe was not specified.

These two sampling campaigns were the reference for DOC inputs as well. Recalcitrant DOM and labile DOC were determined using DOC concentration in infiltration water weighing the contribution of humic-like and protein-like peaks in each sample. These peaks were obtained from DOM fluorescence analysis (see section 4.4.1 in Chapter 4).

Organic carbon amount in the sediment was used as an indicator of immobile DOM. The maximum amount was observed in April 2017, because the pond was clogged, and field observations confirmed high algae growth and organic matter accumulation on the bottom of the pond. It was transformed to DOM_{imm} concentration considering a value of 10 mmol/kgw. This value is a reasonable concentration of immobile DOM (between 1 and 2 orders of magnitude above TOC annual concentration in the Llobregat River, Figure 4.3) for the most bioclogged period. Then, values of DOM_{imm} for summer and winter scenarios were predicted according to the amount of carbon in the sediment in July 2017 and December 16, respectively. DOM_{imm} species was considered immobile in PHREEQC.

Manganese and iron were considered in equilibrium with their mineral forms, pyrolusite and goethite, respectively. Equilibrium with both minerals allowed to ensure the availability of manganese and iron as electron acceptors in organic matter degradation. Values of initial concentrations of Mn^{4+} and Fe^{3+} as immobile species coming from pyrolusite and goethite minerals respectively were set comparing the experimental concentrations of their soluble forms (Mn^{+2} and Fe^{+2}) with model results.

The initial concentrations of all the components considered in solutions are summarized in Table 5.6.

Table 5.6 Input solutions defined in PHREEQC batch models for winter and summer scenarios

Parameter	Units	Winter	Summer
Temperature	°C	9.5	24.9
pH		8.27	8.49
DOC_{lab}*	mmol/kgw	0.18	0.18
DOM_{rec}*	mmol/kgw	0.30	0.24
$DOMi_{mm}$	mmol/kgw	2.56	4.90
O_2	mmol/kgw	0.32	0.20
NO_3^-	mmol/kgw	0.14	0.06
SO_4^{2-}	mmol/kgw	1.34	1.34
TIC**	mmol/kgw	4.12	4.12
Na^+	mmol/kgw	5.01	5.01
K^+	mmol/kgw	0.64	0.64
Ca^{2+}	mmol/kgw	2.19	2.19
Cl^-**	mmol/kgw	5.96	5.96
Mn^{4+}****	mmol/kgw	0.0164	0.0164
Fe^{3+}****	mmol/kgw	0.0429	0.0429

* The proportion of humic-like DOM and protein-like DOM was respectively 0.62 and 0.38 in winter and 0.57 and 0.43 in summer, according to December and July sampling campaigns. These proportions were applied to the infiltration water DOC, which was analyzed in the two mentioned campaigns. As a result, DOC_{lab} and DOM_{rec} were set. ** Total Inorganic Carbon (TIC) was set calculating the speciation with field alkalinity in the typeset water. ***Chloride was the species used to compensate ionic charges in the solution **** Mn^{4+} and Fe^{3+} were added as immobile species in their mineral form (goethite and pyrolusite)

5.3. Results and discussion

5.3.1. Flow and heat transport model: annual temperature and hydraulic conductivity evolution

The results of the flow model in the vertical profile of the infiltration pond of the Castellbisbal MAR system are presented in Figure 5.3. Calibration of hydraulic conductivity was carried out for the two set layers in the five modeling periods (Figure 5.4). Aquifer vertical hydraulic conductivity (5.80 m lower layer) was set in 600 cm/d for the whole year, while in the upper layer (20 cm) changed by periods. The calibration results for the upper layer explained quite well the development of clogging in the infiltration pond and maintenance practices. While Period IV recovered the hydraulic conductivity set for the aquifer layer because the topsoil was scrapped and removed, the rest of the periods showed values between 5 and 30 cm/d. Note that the hydraulic conductivity evolution follows the same dynamic as organic carbon in sediments presented in Chapter 4 (Figure 4.10). This indicates that hydraulic conductivity and organic carbon content are correlated parameters and indicate the presence of biological clogging. The model evidenced that clogging reduced between 95 and 99% the saturated hydraulic conductivity. Likewise, this reduction presented a drastic decrease only one month after scrapping (see Figure 5.4, values of hydraulic conductivity between Period IV and Period V).

Heat transport was added to the flow model showing a good fitting between the temperature simulated at 55 cm depth and the experimental one (Figure 5.5). The simulation of temperatures along the profile (600 cm) from October 2016 to October 2017 (Figure 5.5) showed that (1) the seasonal variations of temperature followed the climate behavior, and (2) the distribution of temperature was homogenously distributed in depth, showing similar temperatures for the infiltration water and that at 600 cm below the surface. The temperature dynamics shows that transit time in the non-saturated zone is relatively short because of both the model and the experimental results evidence that environmental temperature has an important influence on groundwater. However, during summertime, the aquifer temperature was about 10 degrees lower than that of the infiltration water. These differences are produced due to the static position of the pressure-temperature sensor as in summer, after the increase of levels of the spring, there are 3 m of saturated thickness above the sensor, then limiting the thermal effect of the infiltrated water.

Heat transport model revealed that apart from clogging, warmer temperatures in summer resulted in a reduction in hydraulic conductivity (from 600 to 480 cm/d) in the saturated zone, while colder temperatures in winter raised effective hydraulic conductivity (from 600 to 810 cm/d) (Figure 5.6 and Figure 5.7).

The distribution of hydraulic conductivity showed smaller values for the vadose zone, reflecting quite well the limit of the groundwater table. Saturated conditions resulted in 4.5 times the hydraulic conductivity of the unsaturated zone in the first 150 d of the simulation.

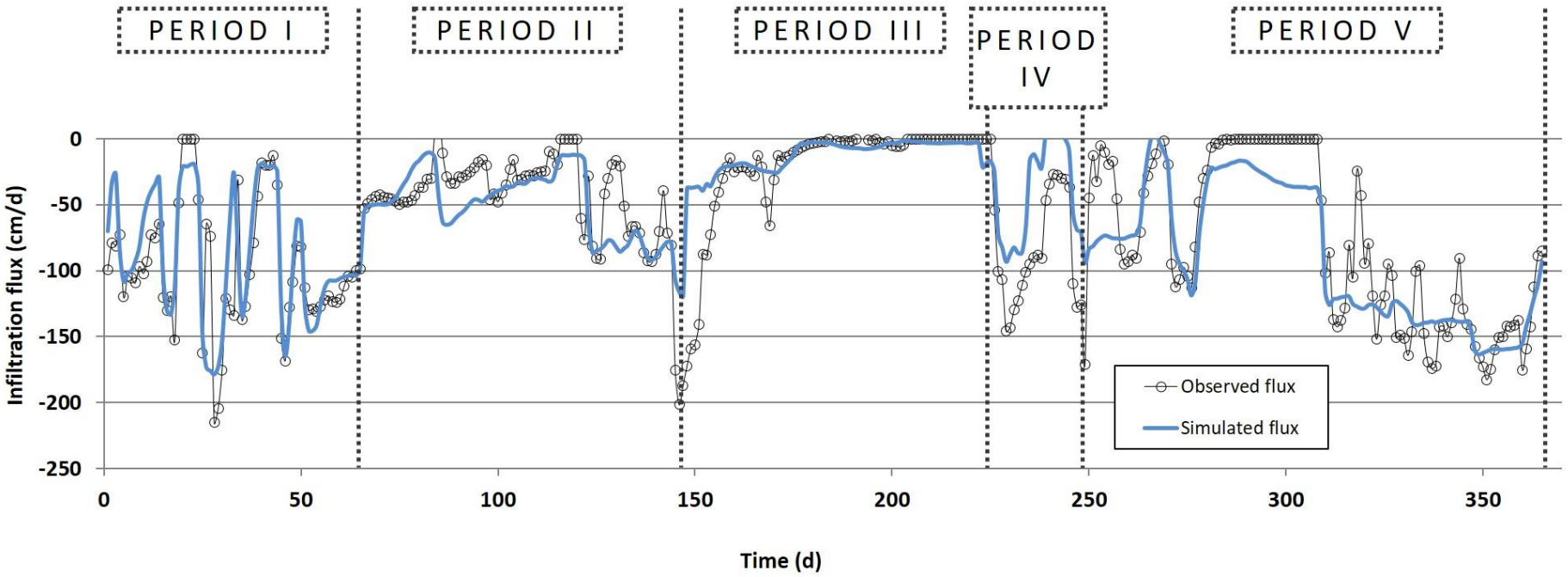

Figure 5.3 Results of the HYDRUS flow model of recharge in the infiltration pond of the Castellbisbal MAR system during the period from October 2016 to October 2017. Real daily infiltration flux (empty black circles) is compared with flux calculated by HYDRUS (blue line)

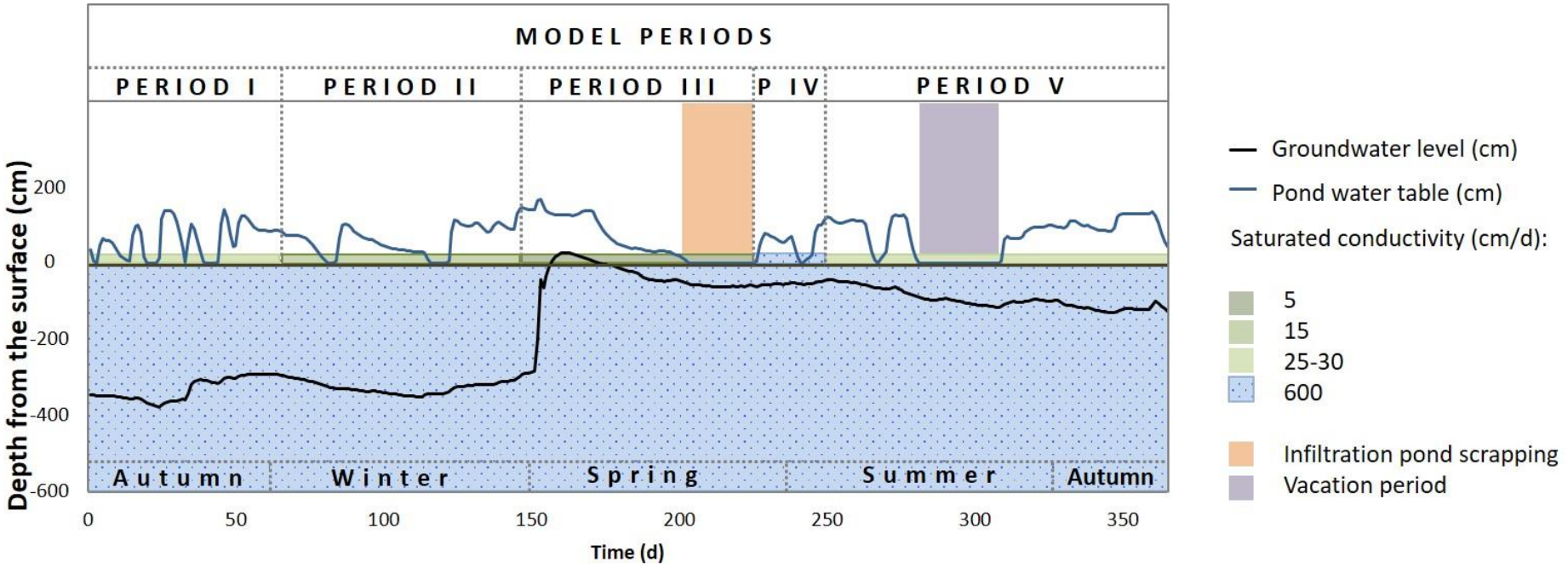

Figure 5.4 Summary of input parameters and calibrated parameters for the flow model. The 365 days-model was divided into 5 periods. Long-time non-recharge periods are displayed in orange (infiltration pond scrapping) and purple (vacation period). Time-boundary conditions are represented by a blue line (pond water table) and a black line (groundwater table). Calibrated parameters are showed for the upper and lower layers, fixed in 5 to 30 cm/d (green range) and 600 cm/d (blue pattern)

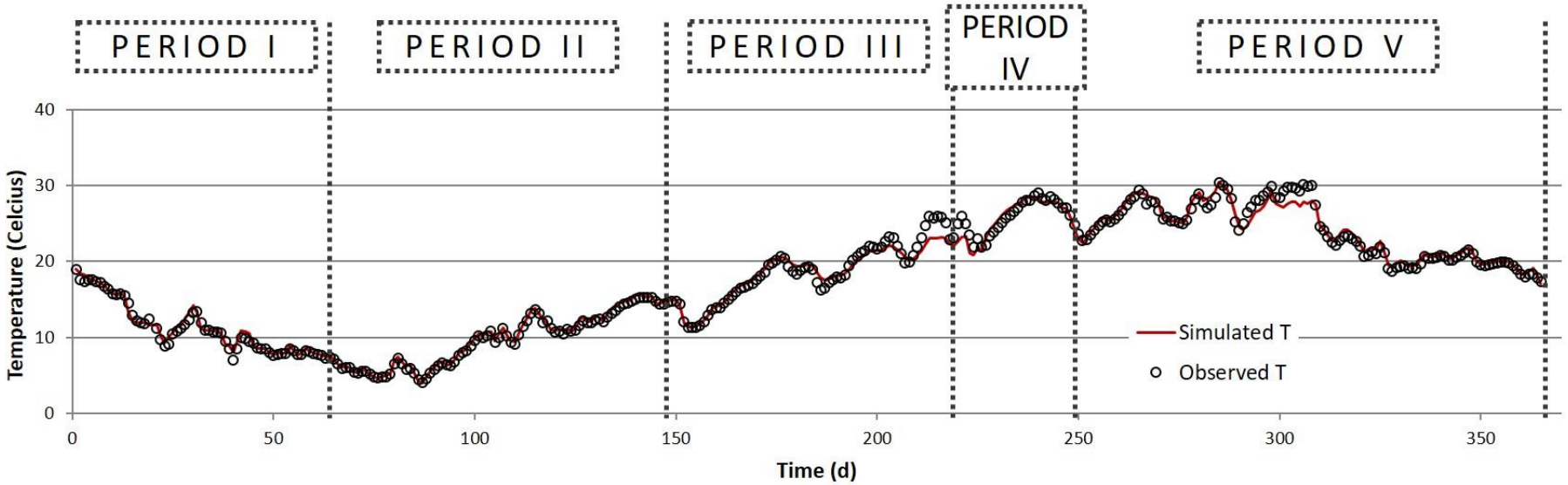

Figure 5.5 Results from the heat transport model at 55 cm depth. Empty black circles were the average of daily temperature measurements at 55 cm, while the red line shows the simulated temperature for the node at the same depth

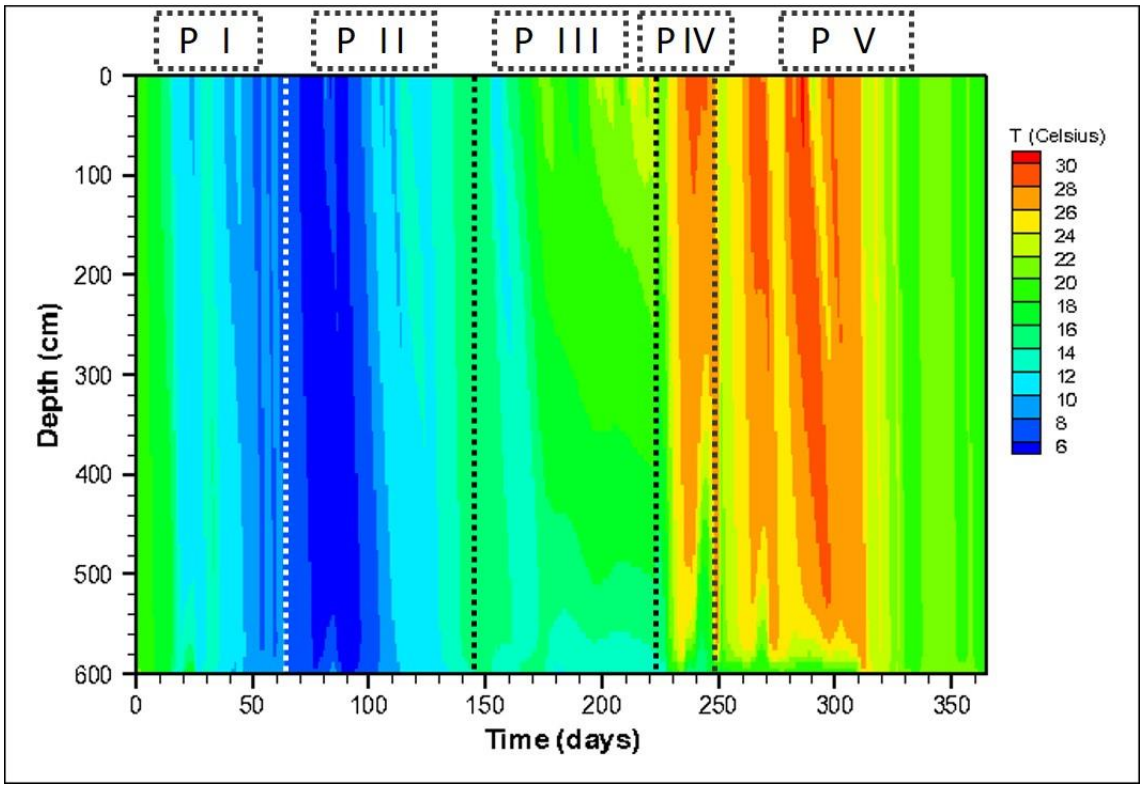

Figure 5.6 Spatial and temporal evolution of simulated temperature in the vadose zone and saturated zone below the infiltration pond of the Castellbisbal MAR system. Operational periods are delimited by discontinuous lines.

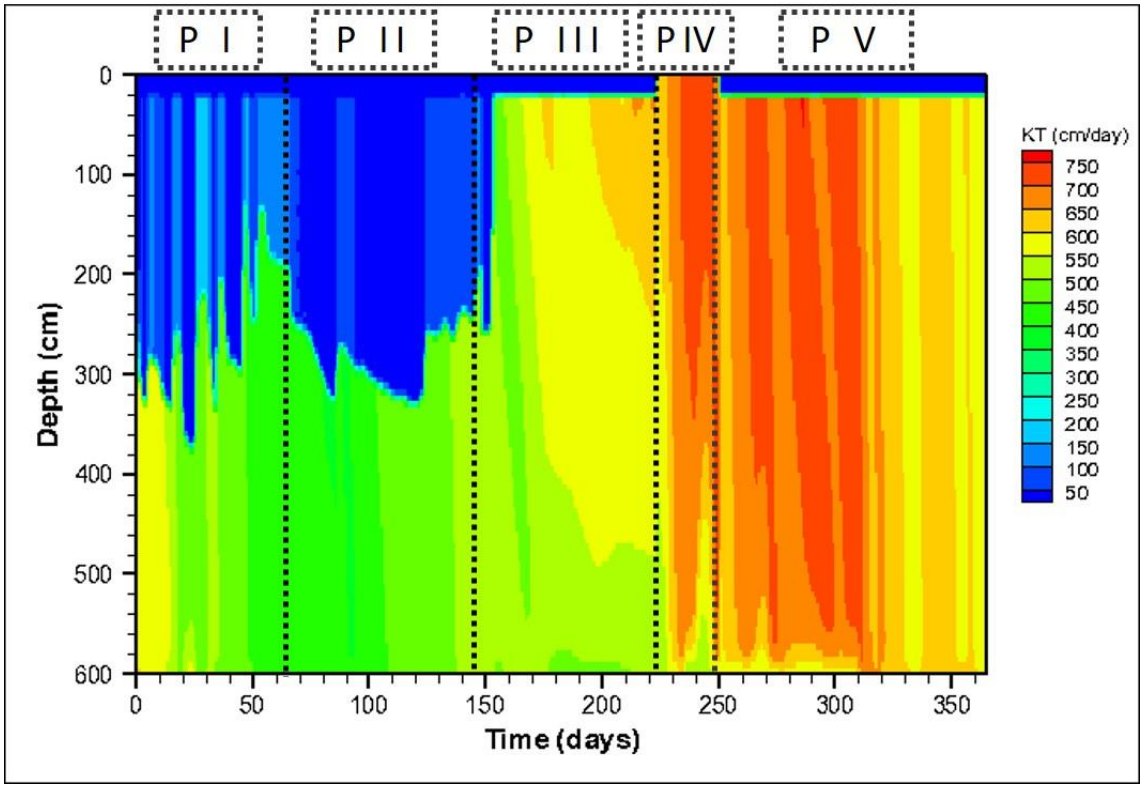

Figure 5.7 Spatial and temporal evolution of effective hydraulic conductivity in the vadose zone and saturated zone below the infiltration pond of the Castellbisbal MAR system. Operational periods are delimited by discontinuous lines.

In saturated conditions, the reduction of the hydraulic conductivity for thermal reasons was at most 35% in the coldest days and depths. On the contrary, for warmer periods, hydraulic conductivity reached more than 800 cm/d in some depths. This represents about 20% more than it was set in soil hydraulic parameters defined. The color map shows clearly that recharge would be more effective in warmer periods, that is, especially, in summer due to higher hydraulic conductivity during this period.

5.3.2. Biogeochemical models for winter and summer scenarios

Two batch models were constructed in order to test the role of temperature in the organic matter biodegradation during five days. The two basic differences between models were temperature and the amount of immobile organic matter. Whereas the winter model was at 9.5°C and had a DOM_{imm} concentration of 2.56 mmol/kgw, the summer model was at 24.9°C and DOM_{imm} was 4.90 mmol/kgw.

The first model explains the behavior of organic matter species in winter (Figure 5.8). Denitrification conditions were reached at the end of the second day when oxygen was totally consumed. As a consequence, pe dropped from 13.8 to 12.2. Despite the change in redox conditions, nitrate did not show many variations along the modeled period; thus, neither pyrolusite nor goethite were consumed. DOM dynamics were in accordance to the redox conditions. The concentration of DOC_{lab} was rising at the same time that DOM_{imm} concentration was decreasing. Little difference in the slope of both tendencies is explained by the slight amount of DOC_{lab} degraded *via* aerobic oxidation.

In the second batch plot (Figure 5.9), summer conditions were reproduced. Unlike during the winter model, denitrification conditions were reached in few hours, and then from the second day to the fifth, manganese reduction conditions were present. Electron acceptors consumption, pe, and pyrolusite concentration were consistent with the redox conditions. DOM_{imm} and DOC_{lab} showed again the opposite behavior but not in the same magnitude as in winter, with the highest slopes in this second case. Biodegradation of labile DOC and hydrolysis of immobile DOM in summer were in fact, higher than in winter. Most concretely, and according to plots, both rates were about 2.5 times faster in summer than in winter. The amount of labile DOC was higher due to the faster transformation of immobile DOM, and also the rates were higher.

The role of DOC_{rec} in the two scenarios was almost inappreciable, especially for the winter scenario. Despite the behavior of DOC_{rec} would be the expected, calibration of K_{rec} might be considered.

The fitting between pe in the model and pe in the field was compared taking values of Eh provided by the redox probe installed in the infiltration pond (see Chapter 4). Pe was calculated from the measurements recorded just before the sampling campaign. Those pe values were compared with an initial range of pe simulated in the model. For the winter model, calculated pe was 13.7 while the real pe according to redox probe was 14.2. In the summer model, calculated pe was 12.0 and the observed value was 11.7.

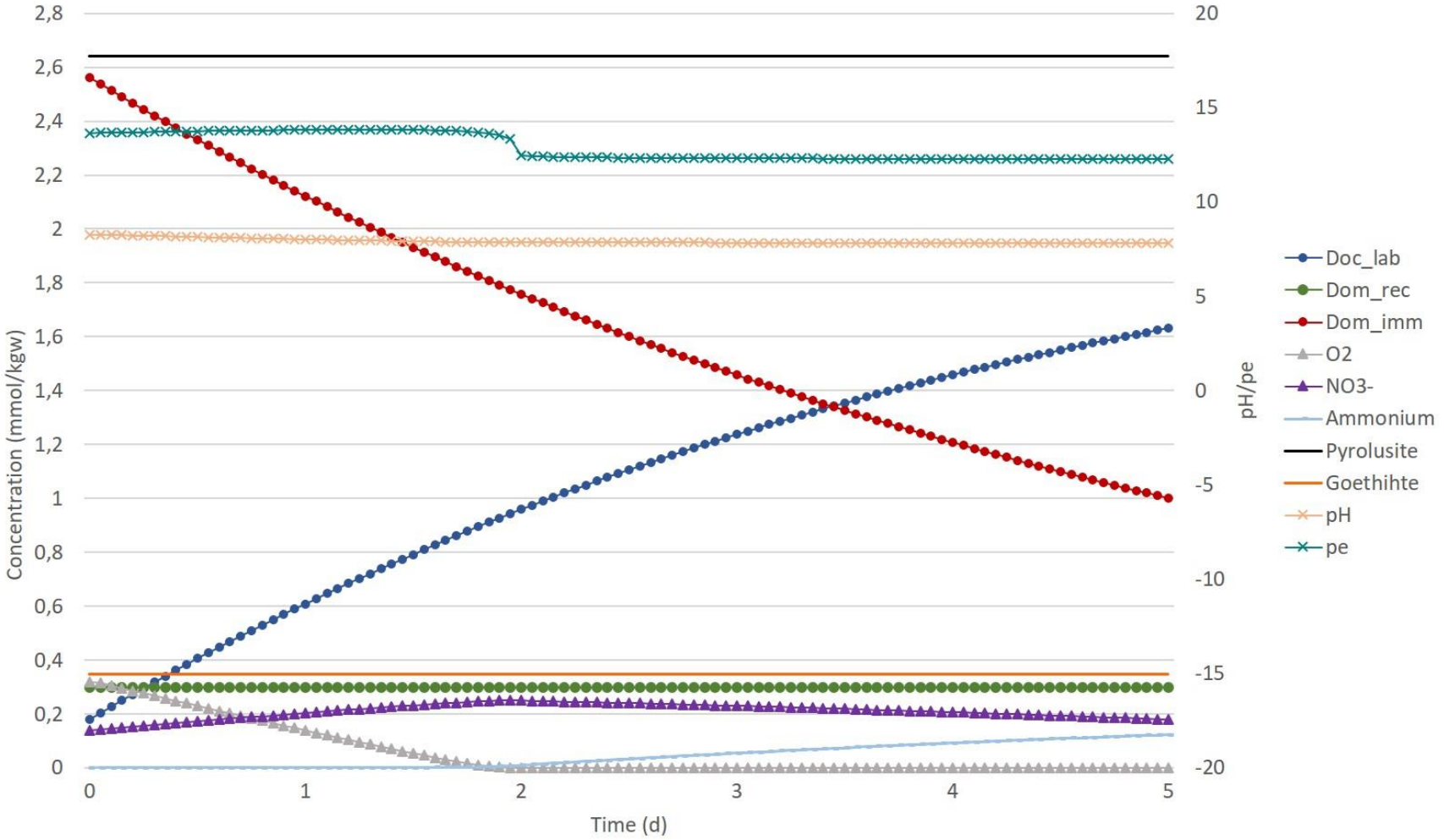

Figure 5.8 Five-days batch simulation of biodegradation of DOC_{lab} (blue dots), DOM_{rec} (green dots) and DOM_{imm} (red dots) species in winter. Electron acceptors consumed total or partially are represented with triangles, oxygen (grey) and nitrate (violet). Goethite (orange) and pyrolusite (black) consumption are represented by single lines. Secondary axis shows the evolution of pH (orange crosses) and pe (turquoise crosses)

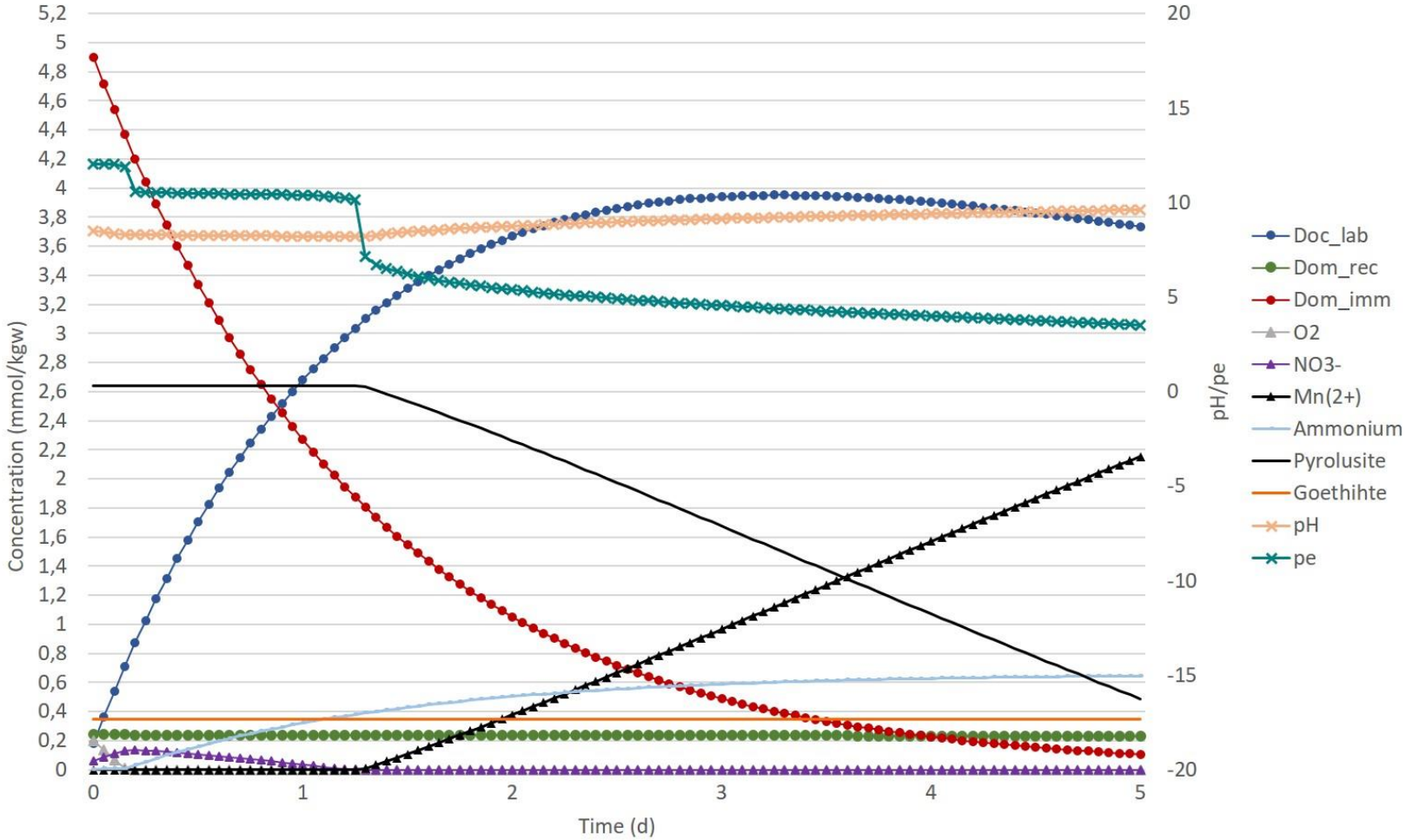

Figure 5.9 Five-days batch simulation of biodegradation of DOC_{lab} (blue dots), DOM_{rec} (green dots) and DOM_{imm} (red dots) species in summer. Electron acceptors consumed total or partially are represented with triangles, oxygen (grey), nitrate (violet) and manganese (purple). Goethite (orange) and pyrolusite (black) consumption are represented by single lines. Secondary axis shows the evolution of pH (orange crosses) and pe (turquoise crosses)

5.4. Conclusions

A flow and heat transport model has been constructed to simulate infiltration processes below a surface pond. Good fitting between simulated flux and temperature with the observed ones demonstrated the importance of the quality of data to construct the model. Therefore, the monitoring network of pressure transducers, temperature sensors, and data from the flow meter was crucial to construct a representative model of real infiltration conditions.

Heat transport model allowed predicting changes in hydraulic conductivity taking into account temperature fluctuations as well as unsaturated conditions. Carrying out recharge during summer would be more favorable than in winter since effective hydraulic conductivity is 20% higher than the theoretical one. The model, however, only predicts changes in hydraulic conductivity caused by viscosity modifications. Other indirect effects of temperature are not considered (isothermal vapor flux, changes in surface tension or in diffuse double-layer thickness). These other causes would underestimate the effects of temperature in hydraulic conductivity, and consequently, in infiltration rate.

Biogeochemical models evidenced that warmer conditions (25°C) increased degradation rates about 2.5 times compared with conditions in winter (10°C). Furthermore, production of labile DOC, as well as their consumption, were higher in the summer model.

Thus, the optimal scenario would be probably in autumn or spring, where intermediate temperatures would not allow too much clogging development, while microorganisms would still be active enough to remove DOM coming from the river while maintaining a good infiltration rate. Furthermore, lower temperatures would increase the infiltration rate with respect to the summer scenario. Thus, the optimization of the amount of water infiltrated and the improvement of its quality could be achieved.

Modeling temperature implications in infiltration ponds is and will be a powerful tool, especially important on the climate change context and their consequent alterations in temperature pattern behaviors.

CHAPTER 6: CONCLUSIONS

This thesis is aimed at improving our understanding of the operation and management of MAR systems. All the investigations carried out: field work, data analysis, and numerical model development, aimed at contributing to the sustainable management of water resources. In fact, the main novelty of this work is the integration of different interdisciplinary methodologies (microbial fingerprinting, multivariate statistical analysis, hydrochemical characterization, and numerical modeling) as well as monitoring tools (redox potential and hydrologic features) to better understanding processes in infiltration ponds.

The two first chapters of this work highlight the importance of microbial communities in the aquifer's water quality improvement during infiltration practices. Some denitrifiers, carbon fixators, and methanotrophs, among others, have been found associated with recharge practices. Recharge processes lead to the perturbation of the existing groundwater chemical signature, stimulating microbial activity and diversity. This tendency follows the Intermediate Disturbance Hypothesis, and it is evidenced in the Sant Vicenç site, as an example of MAR surface infiltration system. The increase of biological diversity due to intermediate disturbances implies the colonization of wide biological niches by microbial populations during MAR.

The relationship between microbial community composition, recharge operational conditions (whether recharge is active or discontinued), hydrochemistry (in water samples) and grain-size distribution properties (in soil samples) was further analyzed by means of Principal Component Analysis. This multivariate statistical analysis from data of the Sant Vicenç MAR system allowed distinguishing relevant variables for the development of microbial communities in different environments. For example, the presence of Cyanobacteria populations (mainly in surface water) might be linked to metals immobilization capability. Also, PCA allowed identifying in statistical terms key species related to biodegradation processes. For instance, the populations of *Methylotenera mobilis* and *Vogesella indigofera* can be used as denitrifying indicators in MAR environments, showing correlations with DOC (log) concentrations. The statistical analysis also highlighted (1) the importance of the grain-size distribution of soils in the development of microbial communities; and (2) moisture as a key parameter for the microbial diversity in soils. One could expect that these conclusions should be maintained when studying other MAR sites or freshwater environments.

Another innovative result of this thesis is the *in situ* continuous monitoring of redox potential in the infiltration water, the vadose zone, and in the aquifer. This allows studying the dynamics of redox processes in MAR systems, as an exponent of potential water quality improvement and bioclogging development, and could potentially have many implications for MAR ponds management.

Sampling surveys characterizing hydrochemistry and organic matter origin, as well as two biochemical reactive models, were also performed in order to complement the understanding of redox processes at the field scale. Redox potential measurements are relevant in several ways: (1) they give an idea of the redox state of the system; (2) they are indicative of the main redox processes that are occurring at each period (and their spatiotemporal evolution in depth). Indeed, there is an inverse relationship between water depth and redox potential, indicating that the thermodynamic chain in the consumption of electron acceptors is followed along the infiltration through the non-saturated zone. Furthermore, it was confirmed that redox potential measurements are indicators of clogging appearance. Comparing periods with clogging development with those after scrapping, we observed that oxic conditions recovered when recharge was restarted after clogging removal.

Measured redox potentials and biological activity indicators (partial pressure of CO_2, Biological Oxygen Demand -BOD- and Oxidation Reduction Potential -ORP-) suggest low biological activity during the cold months, when denitrification is not occurring. Oppositely, during the warm months at least iron reduction takes place. Last, dissolved organic matter, analyzed by fluorescence, was demonstrated as a useful tool to characterize the origin of the organic matter and the changes in concentrations along the year.

These results highlight that redox potential is dynamic during MAR activities, and therefore, potential bioclogging and/or biodegradation of pollutants/nutrients. Furthermore, it changes along the seasons and according to external managing measures (scrapping), with significant implications for the proper management and planning of MAR aims (quality and quantity). Developing a biogeochemical model and comparing two opposite scenarios (summer and winter) allowed making a first approximation of optimal practices. For example, during cold months microorganisms' activity is significantly low, so that it would not be reasonable to prioritize quality issues, especially those biodegradation processes needing redox reductive conditions.

The flow and heat transport models also showed that temperature changes during MAR activities have wide implications for the dynamics of hydraulic conductivity, which in turn might affect both water quality and quantity during recharge. Changes in viscosity in winter might involve a reduction of 35% of the hydraulic conductivity initially set in the model. Recharge in terms of quantity would be optimal during summer, with an increase of 20% in hydraulic conductivity.

Management of bioclogging takes special importance in the warm months, because it can directly affect the infiltration rate. Avoiding bioclogging in the summertime will result in the maximization of infiltration rate and the achievement of the target biogeochemical redox reactions occurring during recharge.

This dissertation has contributed to understanding the biogeochemical processes occurring in MAR infiltration ponds. It is expected that the results will help to improve their management according to the different targets of quantity and quality, but also according to the environmental conditions and MAR ponds design.

Future work

Finally, some more future work can be undertaken in order to improve the knowledge of processes involved in ponds functioning.

The microbial fingerprinting study performed in Sant Vicenç MAR system was the first approximation to determine if there were relevant microbial community differences between recharge and no-recharge operation conditions and at different locations along the flow path. Once these differences have been exposed, we target a broader study taking benefit of the advances in throughput sequencing; this technique allows getting a complete characterization of microbial communities, which can be applied under recharge and no-recharge conditions. This way, the less abundant populations could be classified and so, biological functions for the whole microbial community would be discriminated. Furthermore, a more detailed study, considering a wider area not affected by MAR, could be used to determine the relative importance of climate cycles in subsurface microbial ecosystems.

Regarding the statistical analysis of data from the Sant Vicenç MAR system, PCA allowed discriminating among relevant correlations between variables. However, soil and water samples had to be treated in separated analyses, since some of their

variables did not coincide. Therefore, performing a Redundancy Analysis would be useful to verify to which extent both environments are related.

Chapter 4 could be also extended, since sampling campaigns in the Castellbisbal system included more points than the ones shown in this work (Llobregat River, inflow and outflow of the wetland, one piezometer upstream and two piezometers downstream). It should be interesting to perform an organic carbon balance across and through the recharge system and taking into account its terrestrial or endogenous origin. Fluorescence data would be very helpful in order to distinguish the origin fractions of dissolved organic matter.

Regarding the modeling tasks, biogeochemical reactions should be implemented in flow and heat models for the whole year, in order to make it realistic. This could be done by means of reactive models HYDRUS-HPx (a model combining PHREEQC and HYDRUS). In this way, it would be possible to link temperature outputs from heat transport model with defined rates, which depend in turn to temperature by means of the function F(T) (Equation 5.15). Some improvements to the model could be performed, making an extended review about constant rates for the hydrolysis of DOM_{imm} and the release of DOC_{lab} from DOM_{rec}, linked to algae growth, a recurrent phenomenon observed in the Castellbisbal MAR system.

It is also predictable that photosynthesis may occur as a general rule in similar infiltration systems. It would be very interesting and also useful for management proposes, to study and quantify algae and cyanobacteria growth in the infiltration pond water, related to temperature changes. Likewise, organic matter conforming photosynthetic organisms could be analyzed in order to know their nature (degree of lability). All these information would be very interesting to include in the global biogeochemical model. It would be more realistic than our first approach of treating immobile DOM as a mineral with a hydrolysis rate.

Completing the flow and heat transport model with reactive transport for DOM degradation would allow testing the effect of temperature in an integrated way and would also be very useful for management purposes. Furthermore, some more simulations of different scenarios could be done, as a decisions benchmark, e.g, deciding the best moment to remove clogging, when to establish a drying period, finding the best moment to optimize both quantity and quality targets, etc.

Bibliography

Alewell, C., Paul, S., Lischeid, G., Storck, F.R., 2008. Co-regulation of redox processes in freshwater wetlands as a function of organic matter availability? Sci. Total Environ. 404, 335–342. https://doi.org/10.1016/j.scitotenv.2007.11.001

Alidina, M., Hoppe-Jones, C., Yoon, M., Hamadeh, A.F., Li, D., Drewes, J.E., 2014a. The occurrence of emerging trace organic chemicals in wastewater effluents in Saudi Arabia. Sci. Total Environ. 478, 152–62. https://doi.org/10.1016/j.scitotenv.2014.01.093

Alidina, M., Li, D., Drewes, J.E., 2014b. Investigating the role for adaptation of the microbial community to transform trace organic chemicals during managed aquifer recharge. Water Res. 56, 172–180. https://doi.org/http://dx.doi.org/10.1016/j.watres.2014.02.046

Alidina, M., Li, D., Ouf, M., Drewes, J.E., 2014c. Role of primary substrate composition and concentration on attenuation of trace organic chemicals in managed aquifer recharge systems. J. Environ. Manage. 144, 58–66. https://doi.org/10.1016/j.jenvman.2014.04.032

Alidina, M., Shewchuk, J., Drewes, J.E., 2015. Effect of temperature on removal of trace organic chemicals in managed aquifer recharge systems. Chemosphere 122, 23–31. https://doi.org/10.1016/j.chemosphere.2014.10.064

Altschul, S., Madden, T., Schaffer; AA, Zhang, J., Zhang, Z., Miller, W., Lipman, D., 1997. Gapped BLAST and PSI-BLAST: a new generation of protein database search programs. Nucleic Acids Res. 25, 3389–3402. https://doi.org/10.1093/nar/25.17.3389

Barahona-Palomo, M., 2014. Estimation of aquifers hydraulic parameters by three different tecniques: geostatistics, correlation and modeling. Universitat Politècnica de Catalunya.

Barbieri, M., 2011. Effect of redox conditions on the fate of emerging organic micropollutants during artificial recharge of groundwater: batch experiments. Universitat Politècnica de Catalunya.

Barbieri, M., Carrera, J., Ayora, C., Sanchez-Vila, X., Licha, T., Nodler, K., Osorio,

V., Perez, S., Kock-Schulmeyer, M., Lopez de Alda, M., Barcelo, D., 2012. Formation of diclofenac and sulfamethoxazole reversible transformation products in aquifer material under denitrifying conditions: batch experiments. Sci Total Env. 426, 256–263. https://doi.org/10.1016/j.scitotenv.2012.02.058

Barbieri, M., Carrera, J., Sanchez-Vila, X., Ayora, C., Cama, J., Köck-Schulmeyer, M., López de Alda, M., Barceló, D., Tobella Brunet, J., Hernández García, M., 2011. Microcosm experiments to control anaerobic redox conditions when studying the fate of organic micropollutants in aquifer material. J. Contam. Hydrol. 126, 330–345. https://doi.org/http://dx.doi.org/10.1016/j.jconhyd.2011.09.003

Bates, B.C., Z.W. Kundzewicz, S.Wu, J.P. Palutikof, 2008. Climate Change and Water. Technical Paper if the Intergovernmental Panel on Climate Change. Geneva.

Baveye, P., Vandevivere, P., Hoyle, B.L., DeLeo, P.C., Sanchez de Lozada, D., 1998. Environmental impact and mechanisms of the biological clogging of saturated soils and aquifer materials. Crit. Rev. Environ. Sci. Technol. 28, 123.

Bekele, E., Toze, S., Patterson, B., Higginson, S., 2011. Managed aquifer recharge of treated wastewater: Water quality changes resulting from infiltration through the vadose zone. Water Res. 45, 5764–5772. https://doi.org/10.1016/j.watres.2011.08.058

Bellini, M.I., Gutiérrez, L., Tarlera, S., Scavino, A.F., 2013. Isolation and functional analysis of denitrifiers in an aquifer with high potential for denitrification. Syst. Appl. Microbiol. 36, 505–16. https://doi.org/10.1016/j.syapm.2013.07.001

Bellini, M.I., Kumaresan, D., Tarlera, S., Murrell, J.C., Fernández-Scavino, A., 2018. Identification of active denitrifiers by DNA-stable isotope probing and amplicon sequencing reveals Betaproteobacteria as responsible for attenuation of nitrate contamination in a low impacted aquifer. FEMS Microbiol. Ecol. 94, fix181-fix181.

Betancourt, W.Q., Kitajima, M., Wing, A.D., Regnery, J., Drewes, J.E., Pepper, I.L., Gerba, C.P., 2014. Assessment of virus removal by managed aquifer recharge at three full-scale operations. J. Environ. Sci. Heal. Part A 49, 1685–1692. https://doi.org/10.1080/10934529.2014.951233

Bethke, C.M., Sanford, R.A., Kirk, M.F., Jin, Q., Flynn, T.M., 2011. The thermodynamic ladder in geomicrobiology. Am. J. Sci. 311, 183–210. https://doi.org/10.2475/03.2011.01

Bhatti, A.A., Haq, S., Bhat, R.A., 2017. Actinomycetes benefaction role in soil and plant health. Microb. Pathog. https://doi.org/10.1016/j.micpath.2017.09.036

Bouwer, H., 2002. Artificial recharge of groundwater: hydrogeology and engineering. Hydrogeol. J. 10, 121–142. https://doi.org/10.1007/s10040-001-0182-4

Braga, A., Horst, M., Traver, R.G., 2007. Temperature Effects on the Infiltration Rate through an Infiltration Basin BMP. J. Irrig. Drain. Eng. 133, 593–601. https://doi.org/10.1061/(ASCE)0733-9437(2007)133:6(593)

Bridgham, S.D., Cadillo-Quiroz, H., Keller, J.K., Zhuang, Q., 2013. Methane emissions from wetlands: biogeochemical, microbial, and modeling perspectives from local to global scales. Glob. Chang. Biol. 19, 1325–1346. https://doi.org/10.1111/gcb.12131

Brun, A., Engesgaard, P., 2002. Modelling of transport and biogeochemical processes in pollution plumes: literature review and model development. J. Hydrol. 256, 211–227. https://doi.org/10.1016/S0022-1694(01)00547-9

Burke, V., Greskowiak, J., Asmuß, T., Bremermann, R., Taute, T., Massmann, G., 2014. Temperature dependent redox zonation and attenuation of wastewater-derived organic micropollutants in the hyporheic zone. Sci. Total Environ. 482–483, 53–61. https://doi.org/10.1016/j.scitotenv.2014.02.098

Carles Brangarí, A., Sanchez-Vila, X., Freixa, A., M. Romaní, A., Rubol, S., Fernàndez-Garcia, D., 2017. A mechanistic model (BCC-PSSICO) to predict changes in the hydraulic properties for bio-amended variably saturated soils. Water Resour. Res. 53, 93–109. https://doi.org/10.1002/2015WR018517

Carrera, J., Vicent, T., Lafuente, F.J., 2003. Influence of temperature on denitrification of an industrial high-strength nitrogen wastewater in a two-sludge system. Water SA 29, 11–16. https://doi.org/10.4314/wsa.v29i1.4939

Casas-Ruiz, J.P., Tittel, J., von Schiller, D., Catalán, N., Obrador, B., Gómez-Gener, L., Zwirnmann, E., Sabater, S., Marcé, R., 2016. Drought-induced discontinuities in the source and degradation of dissolved organic matter in a Mediterranean river. Biogeochemistry 127, 125–139.

https://doi.org/10.1007/s10533-015-0173-5

Chau, J., Bagtzoglou, A., Willig, M., 2011. The effect of soil texture on richness and diversity of bacterial communities. Environ. Forensics 12, 333–341. https://doi.org/10.1080/15275922.2011.622348

Chellappa, N.T., Mederios Costa, M.A., 2003. Dominant and co-existing species of Cyanobacteria from a Eutrophicated reservoir of Rio Grande do Norte State, Brazil, in: Acta Oecologica. Elsevier Masson, pp. S3–S10. https://doi.org/10.1016/S1146-609X(03)00005-5

Chen, J., Wang, P.-F., Wang, C., Liu, J.-J., Gao, H., Wang, X., 2018. Spatial distribution and diversity of organohalide-respiring bacteria and their relationships with polybrominated diphenyl ether concentration in Taihu Lake sediments. Environ. Pollut. 232, 200–211. https://doi.org/10.1016/J.ENVPOL.2017.08.124

Chistoserdova, L., 2011. Methylotrophy in a lake: From metagenomics to single-organism physiology. Appl. Environ. Microbiol. https://doi.org/10.1128/AEM.00314-11

Chung, S. -O, Horton, R., 1987. Soil heat and water flow with a partial surface mulch. Water Resour. Res. 23, 2175–2186. https://doi.org/10.1029/WR023i012p02175

Connell, J.H., 1978. Diversity in Tropical Rain Forests and Coral Reefs. Science (80-.). 199, 1302–1310. https://doi.org/10.1126/science.199.4335.1302

Constantz, J., 1982. Temperature dependence of unsaturated hydraulic conductivity of two soils. Soil Sci. Soc. Am. J. 46, 466–470. https://doi.org/10.2136/sssaj1982.03615995004600030005x

Cory, R.M., Miller, M.P., McKnight, D.M., Guerard, J.J., Miller, P.L., 2010. Effect of instrument-specific response on the analysis of fulvic acid fluorescence spectra. Limnol. Oceanogr. Methods 8, 67–78. https://doi.org/10.4319/lom.2010.8.67

Curtis, T.P., Sloan, W.T., Scannell, J.W., 2002. Estimating prokaryotic diversity and its limits. Proc. Natl. Acad. Sci. 99, 10494–10499. https://doi.org/10.1073/pnas.142680199

Cycoń, M., Mrozik, A., Piotrowska-Seget, Z., 2017. Bioaugmentation as a strategy for the remediation of pesticide-polluted soil: A review. Chemosphere.

https://doi.org/10.1016/j.chemosphere.2016.12.129

D'Alessio, M., Yoneyama, B., Kirs, M., Kisand, V., Ray, C., 2015. Pharmaceutically active compounds: Their removal during slow sand filtration and their impact on slow sand filtration bacterial removal. Sci. Total Environ. 524–525, 124–135. https://doi.org/10.1016/j.scitotenv.2015.04.014

Daims, H., Nielsen, J.L., Nielsen, P.H., Schleifer, K.-H., Wagner, M., 2001. In Situ Characterization of Nitrospira-Like Nitrite-Oxidizing Bacteria Active in Wastewater Treatment Plants. Appl. Environ. Microbiol. 67, 5273–5284. https://doi.org/10.1128/AEM.67.11.5273-5284.2001

David, M.B., Gentry, L.E., Smith, K.M., Kovacic, D.A., 1997. Carbon, Plant, and Temperature Control of Nitrate Removal from Wetland Mesocosms. Trans. Illinois State Acad. Sci. 90, 103–112.

de-Bashan, L.E., Bashan, Y., 2010. Immobilized microalgae for removing pollutants: Review of practical aspects. Bioresour. Technol. 101, 1611–1627. https://doi.org/10.1016/j.biortech.2009.09.043

Dillehay, J.L., Bowman, K.S., Yan, J., Rainey, F.A., Moe, W.M., 2014. Substrate interactions in dehalogenation of 1,2-dichloroethane, 1,2-dichloropropane, and 1,1,2-trichloroethane mixtures by Dehalogenimonas spp. Biodegradation 25, 301–312. https://doi.org/10.1007/s10532-013-9661-2

Dillon, P., 2005. Future management of aquifer recharge. Hydrogeol. J. 13, 313–316. https://doi.org/10.1007/s10040-004-0413-6

Drewes, J.E., Li, D., Regnery, J., Alidina, M., Wing, A., Hoppe-Jones, C., 2014. Tuning the performance of a natural treatment process using metagenomics for improved trace organic chemical attenuation. Water Sci. Technol. 69, 628–633. https://doi.org/10.2166/wst.2013.750

Drewes, J.E., Reinhard, M., Fox, P., 2003. Comparing microfiltration-reverse osmosis and soil-aquifer treatment for indirect potable reuse of water. Water Res. 37, 3612–3621. https://doi.org/10.1016/S0043-1354(03)00230-6

Dutta, T., Carles-Brangarí, A., Fernàndez-Garcia, D., Rubol, S., Tirado-Conde, J., Sanchez-Vila, X., 2015. Vadose zone oxygen (O2) dynamics during drying and wetting cycles: An artificial recharge laboratory experiment. J. Hydrol. 527, 151–159. https://doi.org/10.1016/j.jhydrol.2015.04.048

Dwivedi, S., Tripathi, R.D., Rai, U.N., Srivastava, S., Mishra, S., Shukla, M.K., Gupta, A.K., Sinha, S., Baghel, V.S., Gupta, D.K., 2006. Dominance of algae in ganga water polluted through fly-ash leaching: Metal bioaccumulation potential of selected algal species. Bull. Environ. Contam. Toxicol. 77, 427–436. https://doi.org/10.1007/s00128-006-1083-y

Edgar, R.C., Haas, B.J., Clemente, J.C., Quince, C., Knight, R., 2011. UCHIME improves sensitivity and speed of chimera detection. Bioinformatics 27, 2194–2200.

El Alfy, M., Lashin, A., Abdalla, F., Al-Bassam, A., 2017. Assessing the hydrogeochemical processes affecting groundwater pollution in arid areas using an integration of geochemical equilibrium and multivariate statistical techniques. Environ. Pollut. 229, 760–770. https://doi.org/10.1016/j.envpol.2017.05.052

Eusuff, M.M., Lansey, K.E., 2004. Optimal operation of artificial groundwater recharge systems considering water quality transformations. Water Resour. Manag. 18, 379–405. https://doi.org/10.1023/B:WARM.0000048486.46046.ee

Fahrenfeld, N., Cozzarelli, I.M., Bailey, Z., Pruden, A., 2014. Insights into Biodegradation Through Depth-Resolved Microbial Community Functional and Structural Profiling of a Crude-Oil Contaminant Plume. Microb. Ecol. 68, 453–462. https://doi.org/10.1007/s00248-014-0421-6

Faulwetter, J.L., Gagnon, V., Sundberg, C., Chazarenc, F., Burr, M.D., Brisson, J., Camper, A.K., Stein, O.R., 2009. Microbial processes influencing performance of treatment wetlands: A review. Ecol. Eng. 35, 987–1004. https://doi.org/10.1016/j.ecoleng.2008.12.030

Frau, D., Pinto, P.D.T., Mayora, G., 2018. Are cyanobacteria total, specific and trait abundance regulated by the same environmental variables? Ann. Limnol. 54, 3. https://doi.org/10.1051/limn/2017030

Freixa, A., Rubol, S., Carles-Brangarí, A., Fernàndez-Garcia, D., Butturini, A., Sanchez-Vila, X., Romaní, A.M., 2015. The effects of sediment depth and oxygen concentration on the use of organic matter: An experimental study using an infiltration sediment tank. Sci. Total Environ. 540, 20–31. https://doi.org/10.1016/j.scitotenv.2015.04.007

Ghattas, A.-K., Fischer, F., Wick, A., Ternes, T.A., 2017. Anaerobic biodegradation of (emerging) organic contaminants in the aquatic environment. Water Res. 116, 268–295. https://doi.org/https://doi.org/10.1016/j.watres.2017.02.001

Ginige, M.P., Kaksonen, A.H., Morris, C., Shackelton, M., Patterson, B.M., 2013. Bacterial community and groundwater quality changes in an anaerobic aquifer during groundwater recharge with aerobic recycled water. FEMS Microbiol. Ecol. 85, 553–567. https://doi.org/10.1111/1574-6941.12137

Gisi, D., Willi, L., Traber, H., Leisinger, T., Vuilleumier, S., 1998. Effects of bacterial host and dichloromethane dehalogenase on the competitiveness of methylotrophic bacteria growing with dichloromethane. Appl. Environ. Microbiol. 64, 1194–1202.

Goren, O., Burg, A., Gavrieli, I., Negev, I., Guttman, J., Kraitzer, T., Kloppmann, W., Lazar, B., 2014. Biogeochemical processes in infiltration basins and their impact on the recharging effluent, the soil aquifer treatment (SAT) system of the Shafdan plant, Israel. Appl. Geochemistry 48, 58–69. https://doi.org/http://dx.doi.org/10.1016/j.apgeochem.2014.06.017

Grau-Martínez, A., Folch, A., Torrentó, C., Valhondo, C., Barba, C., Domènech, C., Soler, A., Otero, N., 2018. Monitoring induced denitrification during managed aquifer recharge in an infiltration pond. J. Hydrol. 561, 123–135. https://doi.org/10.1016/j.jhydrol.2018.03.044

Grau Martínez, A., 2018. Induced attenuation of nitrate pollution: multi-isotopic study at laboratory and field scale. Universitat de Barcelona.

Greskowiak, J., Hamann, E., Burke, V., Massmann, G., 2017. The uncertainty of biodegradation rate constants of emerging organic compounds in soil and groundwater – A compilation of literature values for 82 substances. Water Res. 126, 122–133. https://doi.org/10.1016/j.watres.2017.09.017

Greskowiak, J., Prommer, H., Massmann, G., Johnston, C.D., Nützmann, G., Pekdeger, A., 2005a. The impact of variably saturated conditions on hydrogeochemical changes during artificial recharge of groundwater. Appl. Geochemistry 20, 1409–1426. https://doi.org/http://dx.doi.org/10.1016/j.apgeochem.2005.03.002

Greskowiak, J., Prommer, H., Massmann, G., Nützmann, G., 2006. Modeling

Seasonal Redox Dynamics and the Corresponding Fate of the Pharmaceutical Residue Phenazone During Artificial Recharge of Groundwater. Environ. Sci. Technol. 40, 6615–6621. https://doi.org/10.1021/es052506t

Greskowiak, J., Prommer, H., Vanderzalm, J., Pavelic, P., Dillon, P., 2005b. Modeling of carbon cycling and biogeochemical changes during injection and recovery of reclaimed water at Bolivar, South Australia. Water Resour. Res. 41. https://doi.org/10.1029/2005WR004095

Griebler, C., Lueders, T., 2009. Microbial biodiversity in groundwater ecosystems. Freshw. Biol. 54, 649–677. https://doi.org/10.1111/j.1365-2427.2008.02013.x

Grimes, D.J., Woese, C.R., MacDonell, M.T., Colwell, R.R., 1997. Systematic study of the genus Vogesella gen. nov. and its type species, Vogesella indigofera comb. nov. Int. J. Syst. Bacteriol. 47, 19–27. https://doi.org/10.1099/00207713-47-1-19

Grimm, N.B., 1994. Disturbance, succession, and ecosystem processes in streams: a case study from the desert, in: P.S. Giller, A.G. Hildrew, and D.G.R. (Ed.), Joint Symposium of the British Ecological Society and the American Society of Lirrmologyand Oceanography. Blackwell Scientific, Oxford, pp. 93–112.

Haack, S.K., Fogarty, L.R., West, T.G., Alm, E.W., McGuire, J.T., Long, D.T., Hyndman, D.W., Forney, L.J., 2004. Spatial and temporal changes in microbial community structure associated with recharge-influenced chemical gradients in a contaminated aquifer. Env. Microbiol 6, 438–448. https://doi.org/10.1111/j.1462-2920.2003.00563.x

Hamann, E., Stuyfzand, P.J., Greskowiak, J., Timmer, H., Massmann, G., 2016. The fate of organic micropollutants during long-term/long-distance river bank filtration. Sci. Total Environ. 545–546, 629–640. https://doi.org/10.1016/j.scitotenv.2015.12.057

Hamersley, M.R., Howes, B.L., 2002. Control of denitrification in a septage-treating artificial wetland: The dual role of particulate organic carbon. Water Res. 36, 4415–4427. https://doi.org/10.1016/S0043-1354(02)00134-3

Hand, V.L., Lloyd, J.R., Vaughan, D.J., Wilkins, M.J., Boult, S., 2008. Experimental studies of the influence of grain size, oxygen availability and organic carbon availability on bioclogging in porous media. Env. Sci Technol 42, 1485–1491.

Heilweil, V.M., Solomon, D.K., Perkins, K.S., Ellett, K.M., 2004. Gas-partitioning

tracer test to quantify trapped gas during recharge. Ground Water 42, 589–600.

Hellauer, K., Karakurt, S., Sperlich, A., Burke, V., Massmann, G., Hübner, U., Drewes, J.E., 2017. Establishing sequential managed aquifer recharge technology (SMART) for enhanced removal of trace organic chemicals: Experiences from field studies in Berlin, Germany. J. Hydrol. https://doi.org/10.1016/j.jhydrol.2017.09.044

Henzler, A.F., Greskowiak, J., Massmann, G., 2016. Seasonality of temperatures and redox zonations during bank filtration - A modeling approach. J. Hydrol. 535, 282–292. https://doi.org/10.1016/j.jhydrol.2016.01.044

Huang, G., Liu, F., Yang, Y., Deng, W., Li, S., Huang, Y., Kong, X., 2015. Removal of ammonium-nitrogen from groundwater using a fully passive permeable reactive barrier with oxygen-releasing compound and clinoptilolite. J. Environ. Manage. 154, 1–7. https://doi.org/http://dx.doi.org/10.1016/j.jenvman.2015.02.012

Hudson, N., Baker, A., Reynolds, D., 2007. Fluorescence analysis of dissolved organic matter in natural, waste and polluted waters—a review. River Res. Appl. 23, 631–649. https://doi.org/10.1002/rra.1005

Huguet, A., Vacher, L., Relexans, S., Saubusse, S., Froidefond, J.M., Parlanti, E., 2009. Properties of fluorescent dissolved organic matter in the Gironde Estuary. Org. Geochem. 40, 706–719. https://doi.org/10.1016/j.orggeochem.2009.03.002

Jäckel, U., Schnell, S., Conrad, R., 2001. Effect of moisture, texture and aggregate size of paddy soil on production and consumption of CH4. Soil Biol. Biochem. 33, 965–971. https://doi.org/10.1016/S0038-0717(00)00248-0

Jacques, D., Simunek, J., 2005. User Manual of the Multicomponent Variably-Saturated Flow and Transport Model HP1, Univ. Calif.

Jurado, A., Vàzquez-Suñé, E., Carrera, J., López de Alda, M., Pujades, E., 2012. Emerging organic contaminants in groundwater in Spain: A review of sources, recent occurrence and fate in a European context. Sci. Total Environ. 440, 82–94. https://doi.org/10.1016/j.scitotenv.2012.08.029

Kalyuhznaya, M.G., Martens-Habbena, W., Wang, T., Hackett, M., Stolyar, S.M., Stahl, D.A., Lidstrom, M.E., Chistoserdova, L., 2009. Methylophilaceae link methanol oxidation to denitrification in freshwater lake sediment as suggested by stable isotope probing and pure culture analysis. Environ. Microbiol. Rep. 1,

385–392. https://doi.org/10.1111/j.1758-2229.2009.00046.x

Kalyuzhnaya, M.G., Bowerman, S., Lara, J.C., Lidstrom, M.E., Chistoserdova, L., 2006. Methylotenera mobilis gen. nov., sp. nov., an obligately methelamine-utilizing bacterium within the family Methylophilaceae. Int. J. Syst. Evol. Microbiol. 56, 2819–2823. https://doi.org/10.1099/ijs.0.64191-0

Kedziorek, M.A.M., Geoffriau, S., Bourg, A.C.M., 2008. Organic matter and modeling redox reactions during river bank filtration in an alluvial aquifer of the Lot River, France. Environ. Sci. Technol. 42, 2793–2798. https://doi.org/10.1021/es702411t

Kielak, A.M., Barreto, C.C., Kowalchuk, G.A., van Veen, J.A., Kuramae, E.E., 2016. The ecology of Acidobacteria: Moving beyond genes and genomes. Front. Microbiol. https://doi.org/10.3389/fmicb.2016.00744

Kirschbaum, M.U.F., 2000. Will changes in soil organic carbon act as a positive or negative feedback on global warming? Biogeochemistry 48, 21–51. https://doi.org/10.1023/A:1006238902976

Kirschbaum, M.U.F., 1995. The temperature dependence of soil organic matter decomposition, and the effect of global warming on soil organic C storage. Soil Biol. Biochem. 27, 753–760. https://doi.org/10.1016/0038-0717(94)00242-S

Knowles, R., 2005. Denitrifiers associated with methanotrophs and their potential impact on the nitrogen cycle. Ecol. Eng. 24, 441–446. https://doi.org/10.1016/J.ECOLENG.2005.01.001

Kolehmainen, R.E., Tiirola, M., Puhakka, J.A., 2008. Spatial and temporal changes in Actinobacterial dominance in experimental artificial groundwater recharge. Water Res. 42, 4525–4537. https://doi.org/10.1016/j.watres.2008.07.039

Kumaresan, D., Stephenson, J., Doxey, A.C., Bandukwala, H., Brooks, E., Hillebrand-Voiculescu, A., Whiteley, A.S., Murrell, J.C., 2018. Aerobic proteobacterial methylotrophs in Movile Cave: genomic and metagenomic analyses. Microbiome 6, 1. https://doi.org/10.1186/s40168-017-0383-2

Kung, K.-J.S., 1990. Preferential flow in a sandy vadose zone: 1. Field observation. Geoderma 46, 51–58. https://doi.org/10.1016/0016-7061(90)90006-U

Lapworth, D.J., Baran, N., Stuart, M.E., Ward, R.S., 2012. Emerging organic

contaminants in groundwater: A review of sources, fate and occurrence. Environ. Pollut. https://doi.org/10.1016/j.envpol.2011.12.034

Laws, B. V, Dickenson, E.R. V, Johnson, T.A., Snyder, S.A., Drewes, J.E., 2011. Attenuation of contaminants of emerging concern during surface-spreading aquifer recharge. Sci. Total Environ. 409, 1087–1094. https://doi.org/https://doi.org/10.1016/j.scitotenv.2010.11.021

Legendre, P., Gallagher, E.D., 2001. Ecologically meaningful transformations for ordination of species data. Oecologia 129, 271–280. https://doi.org/10.1007/s004420100716

Li, D., Alidina, M., Ouf, M., Sharp, J.O., Saikaly, P., Drewes, J.E., 2013. Microbial community evolution during simulated managed aquifer recharge in response to different biodegradable dissolved organic carbon (BDOC) concentrations. Water Res 47, 2421–2430. https://doi.org/10.1016/j.watres.2013.02.012

Li, D., Sharp, J.O., Saikaly, P.E., Ali, S., Alidina, M., Alarawi, M.S., Keller, S., Hoppe-Jones, C., Drewes, J.E., 2012. Dissolved organic carbon influences microbial community composition and diversity in managed aquifer recharge systems. Appl Env. Microbiol 78, 6819–6828. https://doi.org/10.1128/aem.01223-12

Li, J., Wen, Y., Zhou, Q., Xingjie, Z., Li, X., Yang, S., Lin, T., 2008. Influence of vegetation and substrate on the removal and transformation of dissolved organic matter in horizontal subsurface-flow constructed wetlands. Bioresour. Technol. 99, 4990–6. https://doi.org/10.1016/j.biortech.2007.09.012

Lin, C., Greenwald, D., Banin, A., 2003. Temperature dependence of infiltration rate during large scale water recharge into soils. Soil Sci. Soc. Am. J. 487–493.

Logue, J.B., Stedmon, C. a, Kellerman, A.M., Nielsen, N.J., Andersson, A.F., Laudon, H., Lindström, E.S., Kritzberg, E.S., 2015. Experimental insights into the importance of aquatic bacterial community composition to the degradation of dissolved organic matter. ISME J. 1–13.

Loos, R., Carvalho, R., António, D.C., Comero, S., Locoro, G., Tavazzi, S., Paracchini, B., Ghiani, M., Lettieri, T., Blaha, L., Jarosova, B., Voorspoels, S., Servaes, K., Haglund, P., Fick, J., Lindberg, R.H., Schwesig, D., Gawlik, B.M., 2013. EU-wide monitoring survey on emerging polar organic contaminants in wastewater

treatment plant effluents. Water Res. 47, 6475–6487. https://doi.org/10.1016/j.watres.2013.08.024

López-Serna, R., Postigo, C., Blanco, J., Pérez, S., Ginebreda, A., López De Alda, M., Petrović, M., Munné, A., Barceló, D., Ginebreda, A., De Alda, M.L., Petrović, : M, Barceló, D., Petrović, M., Munné, A., 2012. Assessing the effects of tertiary treated wastewater reuse on the presence emerging contaminants in a Mediterranean river (Llobregat, NE Spain). Env. Sci Pollut Res 19, 1000–1012. https://doi.org/10.1007/s11356-011-0596-z

Madhaiyan, M., Poonguzhali, S., Sa, T., 2007. Influence of plant species and environmental conditions on epiphytic and endophytic pink-pigmented facultative methylotrophic bacterial populations associated with field-grown rice cultivars. J. Microbiol. Biotechnol. 17, 1645–1654.

Maeng, S.K., Ameda, E., Sharma, S.K., Grützmacher, G., Amy, G.L., 2010. Organic micropollutant removal from wastewater effluent-impacted drinking water sources during bank filtration and artificial recharge. Water Res. 44, 4003–4014. https://doi.org/http://dx.doi.org/10.1016/j.watres.2010.03.035

Maeng, S.K., Sharma, S.K., Lekkerkerker-Teunissen, K., Amy, G.L., 2011. Occurrence and fate of bulk organic matter and pharmaceutically active compounds in managed aquifer recharge: A review. Water Res. 45, 3015–3033. https://doi.org/http://dx.doi.org/10.1016/j.watres.2011.02.017

Martín-González, L., Hatijah Mortan, S., Rosell, M., Parladé, E., Martínez-Alonso, M., Gaju, N., Caminal, G., Adrian, L., Marco-Urrea, E., 2015. Stable Carbon Isotope Fractionation During 1,2-Dichloropropane-to-Propene Transformation by an Enrichment Culture Containing Dehalogenimonas Strains and a dcpA Gene. Environ. Sci. Technol. 49, 8666–8674. https://doi.org/10.1021/acs.est.5b00929

Martín, S., López, N., 2001. Actualización hidrogeológica de la Cubeta de Sant Andreu (Martorell-Pallejà) (No. 35). Barcelona.

Martínez-Pascual, E., Jiménez, N., Vidal-Gavilan, G., Vinas, M., Solanas, A.M., 2010. Chemical and microbial community analysis during aerobic biostimulation assays of non-sulfonated alkyl-benzene-contaminated groundwater. Appl. Microbiol. Biotechnol. 88, 985–995.

https://doi.org/10.1007/s00253-010-2816-8

Massmann, G., Dünnbier, U., Heberer, T., Taute, T., 2008. Behaviour and redox sensitivity of antimicrobial residues during bank filtration– Investigation of residues of phenazone-type analgesics. Chemosphere 71, 1476–1485. https://doi.org/10.1016/j.chemosphere.2008.06.056

Massmann, G., Greskowiak, J., Dünnbier, U., Zuehlke, S., Knappe, A., Pekdeger, A., 2006. The impact of variable temperatures on the redox conditions and the behaviour of pharmaceutical residues during artificial recharge. J. Hydrol. 328, 141–156. https://doi.org/http://dx.doi.org/10.1016/j.jhydrol.2005.12.009

Mayer, K.U., Benner, S.G., Frind, E.O., Thornton, S.F., Lerner, D.N., 2001. Reactive transport modeling of processes controlling the distribution and natural attenuation of phenolic compounds in a deep sandstone aquifer. J. Contam. Hydrol. 53, 341–68.

McKnight, D.M., Boyer, E.W., Westerhoff, P.K., Doran, P.T., Kulbe, T., Andersen, D.T., 2001. Spectrofluorometric characterization of dissolved organic matter for indication of precursor organic material and aromaticity. Limnol. Oceanogr. 46, 38–48. https://doi.org/10.4319/lo.2001.46.1.0038

Meckenstock, R.U., Elsner, M., Griebler, C., Lueders, T., Stumpp, C., Aamand, J., Agathos, S.N., Albrechtsen, H.J., Bastiaens, L., Bjerg, P.L., Boon, N., Dejonghe, W., Huang, W.E., Schmidt, S.I., Smolders, E., Sørensen, S.R., Springael, D., Van Breukelen, B.M., 2015. Biodegradation: Updating the Concepts of Control for Microbial Cleanup in Contaminated Aquifers. Environ. Sci. Technol. 49, 7073–7081. https://doi.org/10.1021/acs.est.5b00715

Menció, A., Folch, A., Mas-Pla, J., 2012. Identifying key parameters to differentiate groundwater flow systems using multifactorial analysis. J. Hydrol. 472–473, 301–313. https://doi.org/10.1016/j.jhydrol.2012.09.030

Mermillod-Blondin, F., Simon, L., Maazouzi, C., Foulquier, A., Delolme, C., Marmonier, P., 2015. Dynamics of dissolved organic carbon (DOC) through stormwater basins designed for groundwater recharge in urban area: Assessment of retention efficiency. Water Res. 81, 27–37. https://doi.org/10.1016/j.watres.2015.05.031

Modin, O., Fukushi, K., Yamamoto, K., 2007. Denitrification with methane as

external carbon source. Water Res. 41, 2726–2738. https://doi.org/10.1016/j.watres.2007.02.053

Moe, W.M., Yan, J., Nobre, M.F., da Costa, M.S., Rainey, F.A., 2009. Dehalogenimonas lykanthroporepellens gen. nov., sp. nov., a reductively dehalogenating bacterium isolated from chlorinated solvent-contaminated groundwater. Int. J. Syst. Evol. Microbiol. 59, 2692–2697.

Mualem, Y., 1976. A new model for predicting the hydraulic conductivity of unsaturated porous media. Water Resour. Res. 12, 513–522. https://doi.org/10.1029/WR012i003p00513

Muyzer, G., De Waal, E.C., Uitterlinden, A.G., 1993. Profiling of complex microbial populations by denaturing gradient gel electrophoresis analysis of polymerase chain reaction-amplified genes coding for 16S rRNA. Appl. Environ. Microbiol. 59, 695–700. https://doi.org/0099-2240/93/030695-06$02.00/0

Nadav, I., Arye, G., Tarchitzky, J., Chen, Y., 2012. Enhanced infiltration regime for treated-wastewater purification in soil aquifer treatment (SAT). J. Hydrol. 420, 275–283. https://doi.org/10.1016/j.jhydrol.2011.12.013

Nijenhuis, I., Kuntze, K., 2016. Anaerobic microbial dehalogenation of organohalides—state of the art and remediation strategies. Curr. Opin. Biotechnol. 38, 33–38. https://doi.org/10.1016/j.copbio.2015.11.009

Nurk, K., Truu, J., Truu, M., Mander, Ü., 2005. Microbial Characteristics and Nitrogen Transformation in Planted Soil Filter for Domestic Wastewater Treatment. J. Environ. Sci. Heal. Part A 40, 1201–1214. https://doi.org/10.1081/ESE-200055659

O'Connell, A.M., 1990. Microbial decomposition (respiration) of litter in eucalypt forests of South-Western Australia: An empirical model based on laboratory incubations. Soil Biol. Biochem. 22, 153–160. https://doi.org/https://doi.org/10.1016/0038-0717(90)90080-J

Oksanen, J., Blanchet, F., Kindt, R., Legendre, P., Minchin, P., O'Hara, R., Simpson, G., Solymos, P., Stevens, M., Wagner, H., 2017. Vegan: Community Ecology Package. R package version 2.4–3. The R Project for Statistical Computing, Vienna, Austria.

Onesios-Barry, K.M., Berry, D., Proescher, J.B., Ashok Sivakumar, I.K., Bouwer,

E.J., 2014. Removal of pharmaceuticals and personal care products during water recycling: Microbial community structure and effects of substrate concentration. Appl. Environ. Microbiol. 80, 2440–2450. https://doi.org/10.1128/AEM.03693-13

Or, D., Phutane, S., Dechesne, A., 2007. Extracellular Polymeric Substances Affecting Pore-Scale Hydrologic Conditions for Bacterial Activity in Unsaturated Soils All rights reserved. No part of this periodical may be reproduced or transmitted in any form or by any means, electronic or mechanica. Vadose Zo. J. 298–305.

Or, D., Smets, B.F., Wraith, J.M., Dechesne, A., Friedman, S.P., 2007. Physical constraints affecting bacterial habitats and activity in unsaturated porous media – a review. Adv. Water Resour. 30, 1505–1527. https://doi.org/http://dx.doi.org/10.1016/j.advwatres.2006.05.025

Paliy, O., Shankar, V., 2016. Application of multivariate statistical techniques in microbial ecology. Mol. Ecol. https://doi.org/10.1111/mec.13536

Parkhurst, D.L., Appelo, C.A.J., 2013. Description of Input and Examples for PHREEQC Version 3—A Computer Program for Speciation, Batch-Reaction, One-Dimensional Transport, and Inverse Geochemical Calculations. Chapter 43 of Section A. Groundwater Book 6, Modeling Techniques.

Pedretti, D., 2012. Tools and analysis of spatio-temporal dynamics in heterogeneous aquifers : Applications to artificial recharge and forced-gradient solute transport by. Universitat Politècnica de Catalunya.

Pedretti, D., Barahona-Palomo, M., Bolster, D., Fernàndez-Garcia, D., Sanchez-Vila, X., Tartakovsky, D.M., 2012a. Probabilistic analysis of maintenance and operation of artificial recharge ponds. Adv. Water Resour. 36, 23–35. https://doi.org/http://dx.doi.org/10.1016/j.advwatres.2011.07.008

Pedretti, D., Barahona-Palomo, M., Bolster, D., Sanchez-Vila, X., Fernàndez-Garcia, D., 2012b. A quick and inexpensive method to quantify spatially variable infiltration capacity for artificial recharge ponds using photographic images. J. Hydrol. 430–431, 118–126. https://doi.org/http://dx.doi.org/10.1016/j.jhydrol.2012.02.008

Perujo, N., Romaní, A.M., Sanchez-Vila, X., 2018. Bilayer Infiltration System

Combines Benefits from Both Coarse and Fine Sands Promoting Nutrient Accumulation in Sediments and Increasing Removal Rates. Environ. Sci. Technol. 52, 5734–5743. https://doi.org/10.1021/acs.est.8b00771

Perujo, N., Sanchez-Vila, X., Proia, L., Romaní, A.M., 2017. Interaction between Physical Heterogeneity and Microbial Processes in Subsurface Sediments: A Laboratory-Scale Column Experiment. Environ. Sci. Technol. 51, 6110–6119. https://doi.org/10.1021/acs.est.6b06506

Pett-Ridge, J., Firestone, M.K., 2005. Redox fluctuation structures microbial communities in a wet tropical soil. Appl. Environ. Microbiol. 71, 6998–7007. https://doi.org/10.1128/AEM.71.11.6998-7007.2005

Pohlon, E., Fandino, A.O., Marxsen, J., 2013. Bacterial community composition and extracellular enzyme activity in temperate streambed sediment during drying and rewetting. PLoS One 8, e83365. https://doi.org/10.1371/journal.pone.0083365

Polkade, A. V, Mantri, S.S., Patwekar, U.J., Jangid, K., 2016. Quorum sensing: An under-explored phenomenon in the phylum Actinobacteria. Front. Microbiol. https://doi.org/10.3389/fmicb.2016.00131

Prommer, H., Barry, D.., Davis, G.., 2002. Modelling of physical and reactive processes during biodegradation of a hydrocarbon plume under transient groundwater flow conditions. J. Contam. Hydrol. 59, 113–131. https://doi.org/10.1016/S0169-7722(02)00078-5

Prommer, H., Stuyfzand, P.J., 2005. Identification of Temperature-Dependent Water Quality Changes during a Deep Well Injection Experiment in a Pyritic Aquifer. Environ. Sci. Technol. 39, 2200–2209. https://doi.org/10.1021/es0486768

Prommer, H., Tuxen, N., Bjerg, P.L., 2006. Fringe-controlled natural attenuation of phenoxy acids in a landfill plume: Integration of field-scale processes by reactive transport modeling. Environ. Sci. Technol. 40, 4732–4738. https://doi.org/10.1021/es0603002

Ragusa, S.R., McNevin, D., Qasem, S., Mitchell, C., 2004. Indicators of biofilm development and activity in constructed wetlands microcosms. Water Res. 38, 2865–2873. https://doi.org/10.1016/j.watres.2004.03.039

Rauch-Williams, T., Hoppe-Jones, C., Drewes, J.E., 2010. The role of organic matter

in the removal of emerging trace organic chemicals during managed aquifer recharge. Water Res. 44, 449–460. https://doi.org/10.1016/J.WATRES.2009.08.027

Reed, D.A., Toze, S., Chang, B., 2008. Spatial and temporal changes in sulphate-reducing groundwater bacterial community structure in response to Managed Aquifer Recharge. Water Sci. Technol. 57, 789. https://doi.org/10.2166/wst.2008.172

Regnery, J., Lee, J., Drumheller, Z.W., Drewes, J.E., Illangasekare, T.H., Kitanidis, P.K., McCray, J.E., Smits, K.M., 2017. Trace organic chemical attenuation during managed aquifer recharge: Insights from a variably saturated 2D tank experiment. J. Hydrol. 548, 641–651. https://doi.org/10.1016/j.jhydrol.2017.03.038

Regnery, J., Li, D., Roberts, S., Higgins, C., Sharp, J.O., Drewes, J.E., 2016. Linking Trace Organic Chemical Attenuation to Microbiome metabolic Capabilities: Insights from Laboratory- and Full-scale Managed Aquifer Recharge Systems, in: ACS Symposium Series. pp. 163–187. https://doi.org/10.1021/bk-2016-1241.ch011

Regnery, J., Wing, A.D., Alidina, M., Drewes, J.E., 2015. Biotransformation of trace organic chemicals during groundwater recharge: How useful are first-order rate constants? J. Contam. Hydrol. 179, 65–75. https://doi.org/10.1016/j.jconhyd.2015.05.008

Rezanezhad, F., Couture, R.M., Kovac, R., O'Connell, D., Van Cappellen, P., 2014. Water table fluctuations and soil biogeochemistry: An experimental approach using an automated soil column system. J. Hydrol. 509, 245–256. https://doi.org/10.1016/j.jhydrol.2013.11.036

Rivett, M.O., Buss, S.R., Morgan, P., Smith, J.W.N., Bemment, C.D., 2008. Nitrate attenuation in groundwater: A review of biogeochemical controlling processes. Water Res. 42, 4215–4232. https://doi.org/10.1016/j.watres.2008.07.020

Rodríguez-Escales, P., Canelles, A., Sanchez-Vila, X., Folch, A., Kurtzman, D., Rossetto, R., Fernández-Escalante, E., Lobo-Ferreira, J.-P., Sapiano, M., San-Sebastián, J., Schüth, C., 2018. A risk assessment methodology to evaluate the risk failure of managed aquifer recharge in the Mediterranean Basin. Hydrol.

Earth Syst. Sci. 22, 3213–3227. https://doi.org/10.5194/hess-22-3213-2018

Rodríguez-Escales, P., Fernàndez-Garcia, D., Drechsel, J., Folch, A., Sanchez-Vila, X., 2017. Improving degradation of emerging organic compounds by applying chaotic advection in Managed Aquifer Recharge in randomly heterogeneous porous media. Water Resour. Res. 53, 4376–4392. https://doi.org/10.1002/2016WR020333

Rodriguez-Escales, P., Folch, A., van Breukelen, B.M., Vidal-Gavilan, G., Sanchez-Vila, X., 2016. Modeling long term Enhanced in situ Biodenitrification and induced heterogeneity in column experiments under different feeding strategies. J. Hydrol. 538, 127–137. https://doi.org/10.1016/j.jhydrol.2016.04.012

Rodriguez-Escales, P., Sanchez-Vila, X., 2016. Fate of sulfamethoxazole in groundwater: Conceptualizing and modeling metabolite formation under different redox conditions. Water Res. 105, 540–550. https://doi.org/10.1016/j.watres.2016.09.034

Rodríguez Vicente, D., 2013. Análisis de la técnica de recarga artificial en la Cubeta de Sant Andreu de la Barca (Barcelona). Escuela Técnica Superior de Ingenieros de Minas.

Röling, W.F., van Breukelen, B.M., Braster, M., Lin, B., van Verseveld, H.W., 2001. Relationships between microbial community structure and hydrochemistry in a landfill leachate-polluted aquifer. Appl. Environ. Microbiol. 67, 4619–29.

Rolle, M., Clement, T.P., Sethi, R., Di Molfetta, A., 2008. A kinetic approach for simulating redox-controlled fringe and core biodegradation processes in groundwater: model development and application to a landfill site in Piedmont, Italy. Hydrol. Process. 22, 4905–4921. https://doi.org/10.1002/hyp.7113

Romera-Castillo, C., Sarmento, H., Álvarez-Salgado, X.A., Gasol, J.M., Marrasé, C., 2010. Erratum: Production of chromophoric dissolved organic matter by marine phytoplankton. Limnol. Oceanogr. 55, 1466–1466. https://doi.org/10.4319/lo.2010.55.3.1466

Ronan, A.D., Prudic, D.E., Thodal, C.E., Constantz, J., 1998. Field study and simulation of diurnal temperature effects on infiltration and variably saturated flow beneath an ephemeral stream. Water Resour. Res. 34, 2137–2153.

https://doi.org/10.1029/98WR01572

Rothschild, L.J., Mancinelli, R.L., 2001. Life in extreme environments (nature).PDF. Nature 409, 1092–1101. https://doi.org/10.1038/35059215

Rubol, S., Freixa, A., Carles-Brangarí, A., Fernàndez-Garcia, D., Romaní, A.M., Sanchez-Vila, X., 2014. Connecting bacterial colonization to physical and biochemical changes in a sand box infiltration experiment. J. Hydrol. 517, 317–327. https://doi.org/http://dx.doi.org/10.1016/j.jhydrol.2014.05.041

San-Sebastián-Sauto, J., Fernández-Escalante, E., Calero-Gil, R., Carvalho, T., Rodríguez-Escales, P., 2018. Characterization and benchmarking of seven managed aquifer recharge systems in south-western Europe. Sustain. Water Resour. Manag. 1–23. https://doi.org/10.1007/s40899-018-0232-x

Sanchez-Vila, X., Armenter, J.-L., Ortuño, F., Queralt, E., Fernàndez-Garcia, D., 2012. Managed Artificial Recharge in the Llobregat Aquifers: Quantitative Versus Qualitative Aspects, in: Sabater, S., Ginebreda, A., Barceló, D. (Eds.), The Llobregat. Springer Berlin Heidelberg, pp. 51–68. https://doi.org/10.1007/698_2012_154

Schaffer, M., Kröger, K.F., Nödler, K., Ayora, C., Carrera, J., Hernández, M., Licha, T., 2015. Influence of a compost layer on the attenuation of 28 selected organic micropollutants under realistic soil aquifer treatment conditions: Insights from a large scale column experiment. Water Res. 74, 110–121. https://doi.org/10.1016/j.watres.2015.02.010

Schloss, P.D., Westcott, S.L., Ryabin, T., Hall, J.R., Hartmann, M., Hollister, E.B., Lesniewski, R.A., Oakley, B.B., Parks, D.H., Robinson, C.J., Sahl, J.W., Stres, B., Thallinger, G.G., Van Horn, D.J., Weber, C.F., 2009. Introducing mothur: open-source, platform-independent, community-supported software for describing and comparing microbial communities. Appl. Environ. Microbiol. 75, 7537–41. https://doi.org/10.1128/AEM.01541-09

Schmidt, C.K., Lange, F.T., Brauch, H.-J., 2007. Characteristics and evaluation of natural attenuation processes for organic micropollutant removal during riverbank filtration. Water Sci. Technol. Water Supply 7.

Schütz, K., Nagel, P., Vetter, W., Kandeler, E., Ruess, L., 2009. Flooding forested groundwater recharge areas modifies microbial communities from top soil to

groundwater table. FEMS Microbiol. Ecol. 67, 171–182. https://doi.org/10.1111/j.1574-6941.2008.00608.x

Sendrós Brea-Iglesias, A., 2016. Using geophisical techniques in planning and management of groundwater resources. Application in Mediterranean aquifers. Institut de Recerca de l'Aigua. Universitat de Barcelona.

Shiklomanov, I.A., 1997. Comprehensive assessment of the freshwater resources of the World. World Meteorol. Organ. 88.

Sleytr, K., Tietz, A., Langergraber, G., Haberl, R., 2007. Investigation of bacterial removal during the filtration process in constructed wetlands. Sci. Total Environ. 380, 173–180. https://doi.org/10.1016/j.scitotenv.2007.03.001

Song, M., Jiang, L., Zhang, D., Luo, C., Wang, Y., Yu, Z., Yin, H., Zhang, G., 2016. Bacteria capable of degrading anthracene, phenanthrene, and fluoranthene as revealed by DNA based stable-isotope probing in a forest soil. J. Hazard. Mater. 308, 50–57. https://doi.org/10.1016/J.JHAZMAT.2016.01.009

Sprenger, C., Hartog, N., Hernández, M., Vilanova, E., Grützmacher, G., Scheibler, F., Hannappel, S., 2017. Inventory of managed aquifer recharge sites in Europe: historical development, current situation and perspectives. Hydrogeol. J. 25, 1909–1922. https://doi.org/10.1007/s10040-017-1554-8

Staats, M., Braster, M., Röling, W.F.M., 2011. Molecular diversity and distribution of aromatic hydrocarbon-degrading anaerobes across a landfill leachate plume. Environ. Microbiol. 13, 1216–1227. https://doi.org/10.1111/j.1462-2920.2010.02421.x

Stanier, R., Cohen-Bazire, G., 1977. Phototrophic prokaryotes: The cyanobacteria. Ann Rev Micriobiol. https://doi.org/10.1146/annurev.mi.31.100177.001301

Stein, H., Kellermann, C., Schmidt, S.I., Brielmann, H., Steube, C., Berkhoff, S.E., Fuchs, A., Hahn, H.J., Thulin, B., Griebler, C., 2010. The potential use of fauna and bacteria as ecological indicators for the assessment of groundwater quality. J. Environ. Monit. 12, 242–254. https://doi.org/10.1039/B913484K

Sun, Y., Shen, D., Zhou, X., Shi, N., Tian, Y., 2016. Microbial diversity and community structure of denitrifying biological filters operated with different carbon sources. Springerplus 5, 1752. https://doi.org/10.1186/s40064-016-3451-3

Terzaghi, K., Peck, R.B., Mesri, G., 1996. Soil mechanics in engineering practice, Third ed. ed. Wiley-Interscience.

Thullner, M., Zeyer, J., Kinzelbach, W., 2002. Influence of Microbial Growth on Hydraulic Properties of Pore Networks. Transp. Porous Media 49, 99–122. https://doi.org/10.1023/A:1016030112089

Tietz, A., Kirschner, A., Langergraber, G., Sleytr, K., Haberl, R., 2007. Characterisation of microbial biocoenosis in vertical subsurface flow constructed wetlands. Sci. Total Environ. 380, 163–172. https://doi.org/10.1016/j.scitotenv.2006.11.034

Torsvik, V., Øvreås, L., Thingstad, T.F., 2002. Prokaryotic diversity - Magnitude, dynamics, and controlling factors. Science (80-.). https://doi.org/10.1126/science.1071698

Truu, M., Juhanson, J., Truu, J., 2009. Microbial biomass, activity and community composition in constructed wetlands. Sci. Total Environ. 407, 3958–3971. https://doi.org/http://dx.doi.org/10.1016/j.scitotenv.2008.11.036

Turner, B.I., Clark, W., Kates, R., Richards, J., Mathews, J., Meyer, W., 1991. The Earth as Transformed by Human Action: Global and Regional Changes in the Biosphere over the Past 300 Years.

Valhondo, C., 2016. A reactive barrier to enhance the removal of emerging organic compounds during artificial recharge of aquifers through infiltration basins. Universitat Politècnica de Catalunya.

Valhondo, C., Carrera, J., Ayora, C., Barbieri, M., Nödler, K., Licha, T., Huerta, M., 2014. Behavior of nine selected emerging trace organic contaminants in an artificial recharge system supplemented with a reactive barrier. Environ. Sci. Pollut. Res. 21, 11832–11843.

Valhondo, C., Carrera, J., Ayora, C., Tubau, I., Martinez-Landa, L., Nödler, K., Licha, T., 2015. Characterizing redox conditions and monitoring attenuation of selected pharmaceuticals during artificial recharge through a reactive layer. Sci. Total Environ. 512–513, 240–50. https://doi.org/10.1016/j.scitotenv.2015.01.030

Valhondo, C., Martinez-Landa, L., Carrera, J., Ayora, C., Nödler, K., Licha, T., 2018. Evaluation of EOC removal processes during artificial recharge through a

reactive barrier. Sci. Total Environ. 612, 985–994. https://doi.org/10.1016/j.scitotenv.2017.08.054

Van Genuchten, M.T., 1980. A closed-form equation for predicting the hydraulic conductivity of unsaturated soils. Soil Sci. Soc. Am. J. 44, 892–898.

Vandenbohede, A., Van Houtte, E., 2012. Heat transport and temperature distribution during managed artificial recharge with surface ponds. J. Hydrol. 472–473, 77–89. https://doi.org/10.1016/j.jhydrol.2012.09.028

Vuilleumier, S., Chistoserdova, L., Lee, M.C., Bringel, F., Lajus, A., Yang, Z., Gourion, B., Barbe, V., Chang, J., Cruveiller, S., Dossat, C., Gillett, W., Gruffaz, C., Haugen, E., Hourcade, E., Levy, R., Mangenot, S., Muller, E., Nadalig, T., Pagni, M., Penny, C., Peyraud, R., Robinson, D.G., Roche, D., Rouy, Z., Saenempechek, C., Salvignol, G., Vallenet, D., Zaining, W., Marx, C.J., Vorholt, J.A., Olson, M. V, Kaul, R., Weissenbach, J., Médigue, C., Lidstrom, M.E., 2009. Methylobacterium genome sequences: A reference blueprint to investigate microbial metabolism of C1 compounds from natural and industrial sources. PLoS One 4. https://doi.org/10.1371/journal.pone.0005584

Wang, Z., Dai, Y., Zhao, Q., Li, N., Zhou, Q., Xie, S., 2015. Nonylphenol biodegradation, functional gene abundance and bacterial community in bioaugmented sediment: effect of external carbon source. Environ. Sci. Pollut. Res. 22, 12083–12091. https://doi.org/10.1007/s11356-015-4509-4

Ward, N.L., Challacombe, J.F., Janssen, P.H., Henrissat, B., Coutinho, P.M., Wu, M., Xie, G., Haft, D.H., Sait, M., Badger, J., Barabote, R.D., Bradley, B., Brettin, T.S., Brinkac, L.M., Bruce, D., Creasy, T., Daugherty, S.C., Davidsen, T.M., DeBoy, R.T., Detter, J.C., Dodson, R.J., Durkin, A.S., Ganapathy, A., Gwinn-Giglio, M., Han, C.S., Khouri, H., Kiss, H., Kothari, S.P., Madupu, R., Nelson, K.E., Nelson, W.C., Paulsen, I., Penn, K., Ren, Q., Rosovitz, M.J., Selengut, J.D., Shrivastava, S., Sullivan, S.A., Tapia, R., Thompson, S., Watkins, K.L., Yang, Q., Yu, C., Zafar, N., Zhou, L., Kuske, C.R., 2009. Three genomes from the phylum Acidobacteria provide insight into the lifestyles of these microorganisms in soils. Appl. Environ. Microbiol. 75, 2046–2056. https://doi.org/10.1128/AEM.02294-08

Weishaar, J.L., Aiken, G.R., Bergamaschi, B.A., Fram, M.S., Fujii, R., Mopper, K., 2003. Evaluation of Specific Ultraviolet Absorbance as an Indicator of the

Chemical Composition and Reactivity of Dissolved Organic Carbon. Environ. Sci. Technol. 37, 4702–4708. https://doi.org/10.1021/es030360x

Wright, J., Kirchner, V., Bernard, W., Ulrich, N., McLimans, C., Campa, M.F., Hazen, T., Macbeth, T., Marabello, D., McDermott, J., Mackelprang, R., Roth, K., Lamendella, R., 2017. Bacterial Community Dynamics in Dichloromethane-Contaminated Groundwater Undergoing Natural Attenuation. Front. Microbiol.

Yamashita, Y., Tanoue, E., 2003. Chemical characterization of protein-like fluorophores in DOM in relation to aromatic amino acids. Mar. Chem. 82, 255–271. https://doi.org/10.1016/S0304-4203(03)00073-2

Young, I.M., Crawford, J.W., 2004. Interactions and self-organization in the soil-microbe complex. Science (80-.). https://doi.org/10.1126/science.1097394

Zhang, Q., Katul, G., Oren, R., Daly, E., Manzoni, S., Yang, D., 2015. The hysteresis response of soil CO2 concentration and soil respiration to soil temperature. J. Geophys. Res. Biogeosciences 120, 1–14. https://doi.org/10.1002/2015JG003047.Received

Zhang, W., Huan, Y., Liu, D., Wang, H., Jiao, X., Wu, X., Du, S., 2016. Influences of microbial communities on groundwater component concentrations during managed artificial recharge. Environ. Earth Sci. 75, 1–8. https://doi.org/10.1007/s12665-015-4959-5

Zhang, Y., Sun, R., Zhou, A., Zhang, J., Luan, Y., Jia, J., Yue, X., Zhang, J., 2018. Microbial community response reveals underlying mechanism of industrial-scale manganese sand biofilters used for the simultaneous removal of iron, manganese and ammonia from groundwater. AMB Express 8, 2. https://doi.org/10.1186/s13568-017-0534-7

Zhou, Y., Kellermann, C., Griebler, C., 2012. Spatio-temporal patterns of microbial communities in a hydrologically dynamic pristine aquifer. FEMS Microbiol. Ecol. 81, 230–242. https://doi.org/10.1111/j.1574-6941.2012.01371.x

Zhu, B., Wang, X., Rioual, P., 2017. Multivariate indications between environment and ground water recharge in a sedimentary drainage basin in northwestern China. J. Hydrol. 549, 92–113. https://doi.org/10.1016/j.jhydrol.2017.03.058

Zsolnay, A., Baigar, E., Jimenez, M., Steinweg, B., Saccomandi, F., 1999.

Differentiating with fluorescence spectroscopy the sources of dissolved organic matter in soils subjected to drying. Chemosphere 38, 45–50. https://doi.org/10.1016/S0045-6535(98)00166-0

APPENDICES

APPENDIX A: HYDROCHEMICAL DATA IN SANT VICENÇ MAR SYSTEM

Table A1.1 – Summary of hydrochemical parameters at the Llobregat MAR site in both scenarios Dry and Wet.

Sampling location (depth-*masl*)	P1-*BG*(-0.6)		P8 (1)		P8 (-3)		P2 (3)		P2 (-2)		P2(-5)		P5 (2.3)		P5 (-2.2)		P3 (0.8)		P3 (-4.2)		P10 (-1)		Infiltration basin	
Scenario	W	D	W	D	W	D	W	D	W	D	W	D	W	D	W	D	W	D	W	D	W	D	W	D
pH	7.05	7.36	7.45	7.13	7.39	7.27	7.30		7.34		7.28		7.39	6.98	7.42		7.15	7.15	7.15		7.28	7.35	8.47	
DOC (mg/l)	1.63	1.93	13.65	3.96	8.02	1.652	3.17		1.80		4.70		3.61	1.53	3.76		3.22	2.33	3.15		2.57	1.61	6.6	
TOC (mg/L)	2.48	1.97	7.95	4.05	13.05	1.80	1.99		2.00		3.64		2.96	1.50	2.70		2.13	1.88	2.94		3.58	1.70		
HCO_3^- (mg/L)	354.3	382.6	241.3	379.3	253.8	408.1	261.2		314.2		272.6		256.1	408.1	255.2		399.0	294.3	385.8		327.1	396.4	144.5	
NO_3^- (mg/L)	5.02	17.79	2.75	2.82	2.88	15.49	3.13		12.9		3.64		3.41	17.7	4.08		6.06	18.2	8.73		5.88	16.28	6.14	
$SO4^{-2}$ (mg/L)	173.0	181.5	120.0	141.23	152.1	199.54	138.4		140.0		138.4		133.8	200.3	147.8		168.6	177.0	168.7		180.0	174.8	123.4	
Cl^- (mg/L)	224.8	212.4	267.5	186.1	262.8	193.5	267.0		211.8		212.0		274.6	191.7	269.7		241.0	193.2	241.7		265.5	189.1	245.9	
Ca (mg/L)	135.2	142.6	92.5	123.0	99.9	72.3	94.2		121.4		103.5		97.4	141.9	96.7		144.2	133.3	141.3		123.3	132.7	67.6	
Na (mg/L)	138.9	116.3	160.0	110.1	161.2	116.7	153.9		113.5		158.2		163.4	118.0	165.0		142.5	108.8	143.9		162.8	117.5	147.9	
K (mg/L)	19.6	23.7	30.0	23.0	29.4	20.7	30.2		22.9		31.0		38.6	24.4	31.9		24.2	23.9	24.4		26.3	27.5	28.0	
Mg (mg/L)	33.73	36.3	26.7	30.8	28.5	38.3	27.4		31.9		30.0		29.1	38.2	28.8		24.2	33.0	35.2		31.4	37.2	23.0	
S (mg/L)	52.2	63.5	40.5	51.2	47.2	64.3	41.7		58.1		42.6		42.9	63.4	42.7		47.7	58.7	47.9		51.4	59.9	42.2	
Fe (mg/L)	<0.2	<0.2	<0.2	<0.2	<0.2	<0.2	<0.2		<0.2		<0.2		<0.2	<0.2	<0.2		<0.2	<0.2	<0.2		<0.2	<0.2	<0.2	
Mn (ppb)	28.9	0.87	2.46	145.30	2.77	<0.8	10.79		5.507		8.94		2.17	<0.8	1.46		3.67	0.81	1.74		1.58	<0.8	4.76	

Table A1.2. Sequence information corresponding to the DGGE bands obtained from bacterial populations' fingerprints in Sant Vicenç MAR system

Phylotype		Phylogenetic affiliation		
Band code[a]	Accession number	Taxonomic lineage (Phylum, Class, Order, Family, Genus)[b]	Closest match (accession no.)[c]	Similarity (%)[d]
B1	MF47164	Firmicutes(100); Bacilli(100); Bacillales(100); Planococcaceae(100)	Chryseomicrobium sp. (KX889925)	98
B2	MF47164	Proteobacteria(100); Betaproteobacteria(100); Neisseriales(94); Neisseriaceae(94)	*Vogesella indigofer*a (KF951043)	100
B3	MF47164	Firmicutes(100); Bacilli(100); Bacillales(100); Planococcaceae(100)	*Chryseomicrobium* sp. (KX889925)	99
B4	MF47164	Proteobacteria(94); Betaproteobacteria(87); TRA3-20(54); TRA3-20_fa(54)	Uncultured beta proteobacterium (KF182906)	94
B5	MF47164	Chloroflexi(100); Dehalococcoidia(100); vadinBA26(61); vadinBA26_fa(61)	*Dehalogenimonas alkenigignens* (JQ994267)	100
B6	MF47164	Proteobacteria(100); Gammaproteobacteria(100); Xanthomonadales(100); Xanthomonadaceae(100); *Stenotrophomonas*(98)	*Stenotrophomonas* sp. (LC136883)	97
B7	MF47164	Nitrospirae(100); Nitrospira(100); Nitrospirales(100); Nitrospiraceae(100); *Nitrospira*(100)	Uncultured bacterium (HM445209)	97
B8	MF47164	Chloroflexi(100); Dehalococcoidia(100); vadinBA26(52); vadinBA26_fa(52)	*Dehalogenimonas alkenigignens* (JQ994267)	100
B9	MF47164	Firmicutes(100); Bacilli(100); Bacillales(100); Planococcaceae(100)	*Chryseomicrobium* sp. (KX889925)	99
B10	MF47165	Cyanobacteria(100); Cyanobacteria(100); SubsectionI(100); FamilyI(100)	Uncultured cyanobacterium (FJ916292)	99

B11	MF47165	Cyanobacteria(100); Cyanobacteria(100); SubsectionI(100); FamilyI(100)	Uncultured cyanobacterium (FJ916292)	97
B12	MF47165	Proteobacteria(97); Betaproteobacteria(86); Nitrosomonadales(38); Nitrosomonadaceae(34)	Uncultured Burkholderiaceae (AM935619)	94
B13	MF47165	Proteobacteria(100); Betaproteobacteria(100); Nitrosomonadales(89); Nitrosomonadaceae(89); uncultured(88)	Uncultured Burkholderiaceae (AM935619)	97
B14	MF47165	Proteobacteria(100); Betaproteobacteria(100); TRA3-20(100); TRA3-20_fa(100); TRA3-20_ge(100)	Uncultured beta proteobacterium (EU979071)	99
B15	MF47165	Proteobacteria(99); Betaproteobacteria(94); Hydrogenophilales(47); Hydrogenophilaceae(47)	Uncultured beta proteobacterium (JN868168)	92
B16	MF47165	Proteobacteria(82); Betaproteobacteria(56); Nitrosomonadales(20); Nitrosomonadaceae(20)	Uncultured beta proteobacterium (AM935274)	88
B17	MF47165	Nitrospirae(100); Nitrospira(100); Nitrospirales(100); Nitrospiraceae(100); *Nitrospira*(100)	Uncultured Nitrospiraceae (EU298577)	97
B18	MF47165	Bacteroidetes(100); Cytophagia(100); Cytophagales(100); Cytophagaceae(85); *Pontibacter*(84)	Uncultured Bacteroidetes (HF564274)	99
B19	MF47165	Chlorobi(80); Chlorobia(80); Chlorobiales(80); OPB56(80); OPB56_ge(80)	Uncultured bacterium (KC666711)	99
B20	MF47166	Actinobacteria(99); Actinobacteria(99); Frankiales(99); Sporichthyaceae(99); Sporichthyaceae_ge(99)	Uncultured actinobacterium (LC018957)	99
B21	MF47166	Actinobacteria(93); Actinobacteria(93); Micrococcales(86); Microbacteriaceae(77)	Uncultured actinobacterium (LC018957)	96
B22	MF47166	Acidobacteria(91); Solibacteres(91); Solibacterales(91); Solibacteraceae_(Subgroup_3)(91)	Uncultured Acidobacteria (KM016273)	97
B23	MF47166	Proteobacteria(100); Betaproteobacteria(100); Burkholderiales(99); Comamonadaceae(99)	Uncultured bacterium (EU465081)	95

B24	MF47166	Proteobacteria(100); Betaproteobacteria(100); Burkholderiales(94); Comamonadaceae(79)	Uncultured Comamonadaceae (LT679549)	94
B25	MF47166	Proteobacteria(96); Alphaproteobacteria(90); Rhizobiales(75); Rhizobiales_Incertae_Sedis(25)	Uncultured alpha proteobacterium (HF584680)	98
B26	MF47166	Proteobacteria(100); Betaproteobacteria(100); Burkholderiales(100); Comamonadaceae(100); *Aquabacterium*(100)	Uncultured bacterium (KF065163)	99
B27	MF47166	Bacteria(100); Proteobacteria(100); Betaproteobacteria(100); Methylophilales(100); Methylophilaceae(100); *Methylophilus*(100)	*Methylotenera mobilis* (AB698738)	99

[a] band numbers correspond to those presented in Figure 2.4

[b] taxonomic string with bootstrap values (in parentheses), generated in mothur using SILVA database reference file release 119

[c] closest relative according to INSA (International Nucleotide Sequence Database)

[d] percentage sequence similarity with closest INSA using BLAST tool

Table A1.3 Granulometric composition of sediments in Llobregat MAR site

Sampling location		*>12.7 mm*	*2-12.7 mm*	*0.3-2 mm*	*0.056-0.3 mm*	*<0.056 mm*
Pre-sed	End	*39.48*	*6.68*	*20.66*	*28.10*	*5.07*
Inf. pon	Entrance	54.05	25.43	12.93	6.91	0.68
	Midfield	40.35	30.36	20.90	7.62	0.76
	End	15.36	40.26	31.54	11.47	1.37

APPENDIX B

Hydrol. Earth Syst. Sci. Discuss., https://doi.org/10.5194/hess-2018-174
Manuscript under review for journal Hydrol. Earth Syst. Sci.
Discussion started: 17 April 2018

Hydrology and Earth System Sciences
Discussions

Microbial community changes induced by Managed Aquifer Recharge activities: Linking hydrogeological and biological processes

Carme Barba[1,2], Albert Folch[1,2], Núria Gaju[3], Xavier Sanchez-Vila[1,2], Marc Carrasquilla[3], Alba Grau-Martínez[4], and Maira Martínez-Alonso[3]

[1]Department of Civil and Environmental Engineering, Universitat Politècnica de Catalunya (UPC), C/Jordi Girona 1-3, 08034 Barcelona, Spain
[2]Associated Unit: Hydrogeology Group (UPC-CSIC)
[3]Department of Genetics and Microbiology, Universitat Autònoma de Barcelona (UAB), 08193 Bellaterra, Spain
[4]Grup de Mineralogia Aplicada i Geoquímica de Fluids, Departament de Mineralogia, Petrologia i Geologia Aplicada, Facultat de Ciències de la Terra, Universitat de Barcelona (UB), C/Martí i Franquès s/n, 08028 Barcelona, Spain

Correspondence: Carme Barba (carme.barba@upc.edu)

Abstract. Managed Aquifer Recharge (MAR) is a worldwide used technique to increase the availability of water resources. We study how MAR modifies microbial ecosystems, and its implications for enhancing biodegradation processes to eventually improve groundwater quality. We compare soil and groundwater samples taken from a MAR facility located in NE Spain during recharge (with the facility operating continuously for several months) and after four months of no recharge. The study demonstrates a strong correlation between soil and water microbial prints with respect to sampling location along the mapped infiltration path. In particular, managed recharge practices disrupt groundwater ecosystems by modifying diversity indices and the composition of microbial communities, indicating that infiltration favors the growth of certain populations. Analysis of the genetic profiles showed the presence of nine different bacterial phyla in the facility, revealing high biological diversity at the highest taxonomic range. In fact, the microbial population patterns under recharge conditions agree with the Intermediate Disturbance Hypothesis. Moreover, DNA sequence analysis of excised DGGE band patterns revealed the existence of indicator species linked to MAR, most notably *Dehalogenimonas sp*, *Nitrospira sp* and *Vogesella sp*. Our real facility multidisciplinary study (hydrological, geochemical and microbial), involving soil and groundwater samples, support that MAR is a naturally-based, passive, and efficient technique with broad implications for the biodegradation of pollutants dissolved in water.

1 Introduction

As the Intergovernmental Panel on Climate Change has stated for years, climate change is affecting and will continue to affect the availability and quality of freshwater resources, with severe consequences to humans and ecosystems. In particular, the

Hydrol. Earth Syst. Sci. Discuss., https://doi.org/10.5194/hess-2018-174
Manuscript under review for journal Hydrol. Earth Syst. Sci.
Discussion started: 17 April 2018

Hydrology and Earth System Sciences
Discussions

Mediterranean Basin is expected to become warmer and drier (Bates et al., 2008). Therefore, among other actions, claiming a secure water supply should increase groundwater storage of quality water as a strategic management tool in times of scarcity. Managed Aquifer Recharge (MAR) is a globally used, worldwide extended technology based on refilling aquifers with water from different sources (e.g., river, reclaimed, or opportunity water). MAR facilities are usually intended to recover groundwater levels or to become water reservoirs, but other objectives can be targeted. It is quite common to take advantage of the potential of soil as a biogeochemical reactor to enhance the quality of water infiltrating the vadose zone, especially in surface replenishment systems (Drewes et al., 2003; Nadav et al., 2012).

The Llobregat River (Catalonia, NE Spain) is fed by about a hundred Waste Water Treatment Plants. While nitrogen, phosphorous and organic matter (COD) are eliminated below the legal limits before treated wastewater is discharged to the river, emerging organic contaminants (EOCs) are not fully removed (Loos et al., 2013). Consequently, significant concentrations of many EOCs have been detected in the Llobregat River (López-Serna et al., 2012) and its associated groundwater bodies (Jurado et al., 2012).

Biodegradation of EOCs strongly depends on redox conditions (Barbieri et al., 2011; Maeng et al., 2010). In this regard, it has been shown that MAR is a feasible technique capable of partially degrading some of these contaminants (Hellauer et al., 2017; Massmann et al., 2008), particularly when bioprocesses are enhanced (Grau-Martínez et al., 2018; Schaffer et al., 2015). Infiltration through the soil intrinsically leads to two main consequences in groundwater recharge:

1. Development of different vertical and temporal redox zonations responding to organic matter availability as electron acceptors are consumed (Greskowiak et al., 2006).

2. Development of microbial communities according to the flow paths. Fingering below the surface of the recharge systems and preferential flow paths in the saturated zone can create anaerobic microsites (e.g. Bridgham et al., 2013) in which oxygen is consumed faster than it can be diffused from oxic zones.

Indeed, MAR implies groundwater quality modifications when compared to natural flow conditions. This includes several parameters such as organic matter, dissolved oxygen content, temperature, pH, electrical conductivity, and nutrients (Rivett et al., 2008; Zhang et al., 2016). Such disturbances have ecological implications, as all these parameters affect the growth and activity of microorganisms and the corresponding degradation of emerging contaminants (Barbieri et al., 2012; Regnery et al., 2017; Valhondo et al., 2018).

Microbial studies linked to MAR practices involve mostly laboratory experiments (Alidina et al., 2014b; Freixa et al., 2015; Li et al., 2013; Rubol et al., 2014). As for microbial MAR field studies, most relevant research is limited to well injection systems (Ginige et al., 2013; Reed et al., 2008; Zhang et al., 2016) or riverbank filtration conditions (Huang et al., 2015). Onesios-Barry et al. (2014) compared results from a column experiment and soil samples in a MAR site in the US, focusing on the microbial populations linked to pharmaceutical and personal care products removal, and concluded that microbial composition and structure of both systems were comparable. Regnery et al. (2016) went one step further by relating the relative abundance of functional genes involved in xenobiotic pathways with attenuation of some trace organic chemicals and their byproducts in a combination of laboratory experiments and a full-scale MAR facility. However, in our knowledge, there are no microbial fin-

Hydrol. Earth Syst. Sci. Discuss., https://doi.org/10.5194/hess-2018-174
Manuscript under review for journal Hydrol. Earth Syst. Sci.
Discussion started: 17 April 2018

Hydrology and Earth System Sciences
Open Access
Discussions

gerprinting studies of MAR surface infiltration basins, that integrate results from surface water, groundwater and soil samples and comparing them in two different operational periods.

The main goal of this study is to determine how MAR activities induce changes in the microbial communities in a real facility composed of a settling and infiltration pond adjacent to the Llobregat River. We evaluate changes on diversity indices and we incorporate results of the DNA sequence analysis of excised DGGE band patterns for samples taken from different environments and locations within the site and under conditions of recharge and non-recharge. Additionally, we link our results with ecological principles and potential biogeochemical processes (i.e. pollutants degradation) occurring due to MAR activities.

2 Material and Methods

2.1 The Llobregat MAR site

The Llobregat MAR system is located 15 km inland from the Mediterranean Sea, close to Barcelona city (Figure 1). The aquifer thickness in the vicinity is 10-15 m, with alternating sands and gravels. Non-continuous fine-grained sediments are widely present (Pedretti et al., 2012). The distance from the bottom of the pond to the water table oscillated from 9 m (July 2014) to 7 m (March 2015) in the period under study.

Water enters is diverted from upstream the river to a pre-sedimentation basin. After 2-4 days of residence time, it is diverted to an infiltration basin of 6500 m^2. The infiltration capacity has been estimated at 1 $m^3 m^{-2} d^{-1}$ on average, and the local transmissivity of the aquifer is estimated as 14000 $m^2 d^{-1}$ (unpublished).

In 2011, a reactive barrier was installed at the bottom of the infiltration basin to increase the organic load of the infiltration water, and thus promote biological processes through the soil and the vadose zone. The barrier was composed of organic compost (50% in volume) mixed with sand and gravel. Small amounts of clay and iron oxides were added to foster adsorption and ion exchange. Previous studies demonstrated that the reactive barrier enhanced the removal of some emergent contaminants, such as sulfamethoxazole or caffeine (Valhondo et al., 2014). More information about the site and the performance of the reactive barrier can be found in Valhondo et al. (2014).

There are six piezometers distributed in a 500 m transect across the study area (Figure 1). P1, P3, P2, P5 and P10 are fully screened. P8 is a multilevel piezometer drilled at three different depths. Water from piezometer P1 represents background conditions (not affected by recharge).

2.2 Hydrochemistry sampling surveys

Two recharge situations were compared to evaluate the effect of MAR on groundwater chemical signature. After six months of continuous recharge operation, a sampling campaign took place in July 2014 (wet campaign). Samples were collected from surface water in both basins and in the existing piezometers at different depths (from -5 to 3 masl, see diamonds in Figure 1).

Hydrol. Earth Syst. Sci. Discuss., https://doi.org/10.5194/hess-2018-174
Manuscript under review for journal Hydrol. Earth Syst. Sci.
Discussion started: 17 April 2018

Hydrology and Earth System Sciences
Discussions

The second sampling campaign was performed in March 2015 after recharge had been discontinued for four months. In this case, groundwater was also sampled.

Water was analyzed for cations, anions (Cl^-, NO_3^-, SO_4^{-2}, HCO_3^-), DOC and TOC. Analytical procedures are widely described in Supplementary Material section.

In both campaigns, temperature and electrical conductivity vertical profiles were mapped along the transect from data obtained at 50-cm intervals (MPS-D8, SEBA Hydrometrie).

2.3 Microbial community characterization

Water samples were extracted from the pre-sedimentation and infiltration basins at three locations (entrance, middle, and end) during recharge conditions (from now on, wet scenario). On the contrary, 3 soil samples were extracted at the same locations in the infiltration basin under non-recharge conditions (termed dry scenario). Soil samples were obtained from around 10 to 50cm in dept. The sampling procedure for soil was done taking into account Lombard et al. (2011) recommendations, especially regarding the variability of microbial communities along a field transect. Soil samples were taken by means of cores, individually disassembled and kept in a sterile bag. Groundwater samples were taken from -5 to 3 masl depending on the piezometers (10 samples for wet scenario and 7 for dry). All soil and groundwater samples were taken in duplicate, kept in sterile conditions, and preserved in dark at $-4°$C until being taken to the laboratory for molecular analyses.

Protocols for molecular analyses of liquid and soil samples are thoroughly described in the Supplementary Material.

Once the main microbial communities were characterized, three diversity indices were calculated. The first one is Richness (S), defined as the proportional number of microbial species present in a sample, i.e., equal to the total number of bands; the other two, Shannon (H), and Evenness (E), were calculated for each sample as follows:

$$H = \sum_{i=1}^{S} p_i ln(p_i) \tag{1}$$

$$E = \frac{H}{H_{max}} \qquad \text{; with } H_{max} = lnS \tag{2}$$

where p_i is the relative intensity of each band of the sample. Values reported correspond to the average of the two replicas.

2.4 Soil characterization

To complement the soil microbial community's characterization, particle size measurements of soil samples were taken according to the ASTM guidelines. The soil was sampled in the pre-sedimentation basin and at the entrance, middle, and end of infiltration basin. Soil sampling was performed close to the location where samples were taken for microbial analyses.

Hydrol. Earth Syst. Sci. Discuss., https://doi.org/10.5194/hess-2018-174
Manuscript under review for journal Hydrol. Earth Syst. Sci.
Discussion started: 17 April 2018

3 Results

3.1 Microbial differences in groundwater linked to recharge conditions

3.1.1 Closing the conceptual flow model

Understanding the flow pattern in MAR basins is essential to explain microbial community dynamics. In this regard, 2D transects of temperature and conductivity alterations obtained at the time of the sampling campaigns (Figure 2a and Figure 3a) based on vertical profiles indicate that: 1) the vertical flow gradient pushes the existing groundwater downwards and forms a shallow front that travels approximately 120 m downstream, eventually mixing with the background water; 2) the background water is mostly found near the recharge pond and at the deepest sampling points below the pond.

From this conceptual model, four main groups of groundwater can be defined under recharge conditions:

- Type I water represents the background environment of the aquifer, unaffected by MAR activities. Water sampled in P1 is an example of this type.
- Type II water, is the infiltrating one (best observed in P8 at both sampling depths). It flows vertically through the vadose zone to the aquifer, creating a small water mound that pushes down the Type I water.
- Type III water, characteristic of points P2(3), P5(2.3) and P5(-2.2), is a mixture between Types I and II waters, with a high proportion of the latter.
- Type IV water is again a mixture, but with a lower proportion of Type II water. It is present in piezometers P3(0.8), P3(-4.2), P2(-5) and P10(-1).

Apart from temperature and conductivity, major ions composition does not show any significant trend related with groundwater zonation below the pond (see Table S1 in Supplementary Material). The role of nitrate and DOC in microbial community patterns is discussed further below.

3.1.2 Clustering groundwater microbial communities according to presence and abundance

To characterize differences in microbial communities due the recharge, groundwater samples were subjected to molecular analysis. Post-processing of DGGE gels allowed for Non-Metric Multidimensional Scaling (NMDS), showing similarities among band patterns (Figure 4) and strong clustering of microbial communities. Samples from both scenarios were completely separated; blue squares (dry) and triangles (wet) represent groundwater samples, and are clearly clustered in top and bottom halves of the plot, respectively. Moreover, samples from the wet scenario grouped according to water types. Types I and II are displayed on opposite sides; Types III and IV (mixed) display in between. The two green triangles in the center of the plot correspond to groundwater samples from P10.

Discrete bands are also portrayed (circles), allowing linkage of the bands' contribution to sample assemblages. Filled circles

report the class and genus of the sequenced bands, whereas empty circles symbolize non-sequenced bands.

Figure 5 shows DGGE profiles and UPGMA clustering analysis of groundwater samples. The genetic fingerprints revealed high dissimilarities in the bacterial assemblage of about 70% and 80% during the active recharge period and the dry campaign, respectively (Figure 5). Moreover, most replicas grouped together, indicating sampling quality. Under active recharge (wet) conditions (Figure 5a), the dendrogram reproduces quite well the water types postulated by the conceptual flow model: in the first group, we can include four out of the five samples that were strongly influenced by recharge (P5(-2.2), P5(2.3), P8(1) and P8(-3)); while in the second group, P2(3), P3(-4.2) and P3(0.8) clustered together with P1 (non-affected by recharge). In the dry campaign (Figure 5b), although no infiltration occurred, P8 appears separated from the other piezometers, indicating the still marked influence of the water infiltrated during the wet period, which occurred over four months earlier.

3.1.3 Variations in microbial diversity indices in groundwater

The structure and processes of ecosystems change when a disturbance occurs (Grimm, 1994). Such changes in microbial communities have been quantified and described by means of diversity indices (Table 1). Such indices, grouped according to water types during wet conditions, were ordered along an imaginary line from low to highly perturbed as a consequence of water infiltration (Figure 6). The lowest diversity indices were obtained for the recharging water (Type II), indicating low species richness and a highly dissimilar proportion. In contrast, Type IV water, only slightly affected by water infiltration, displayed higher Shannon and Evenness indices, similar to Type I (unaffected by recharge).

3.1.4 Role of MAR activities for the microbial community structure

Prominent bands were recovered from the DGGE gels (Figure 5) and sequenced. Table S2 (Supplementary Material) shows the sequenced bands, their similarity values compared to the closest related GenBanK sequences, and their phylogenetic affiliations. Overall, sequences fell into nine different bacterial phyla and eleven classes: Proteobacteria (Alphaproteobacteria, Betaproteobacteria and Gammaproteobacteria), Cyanobacteria, Chloroflexi (Dehalococcoidia), Chlorobi (Chlorobia), Nitrospirae (Nitrospira), Acidobacteria, Actinobacteria, Firmicutes (Bacilli) and Bacteroidetes (Cytophagia) (Figure 7). The group designated as "Others" includes unclassified and non-sequenced fine bands.

The two main classes displaying the largest differences between the two scenarios are Betaproteobacteria and Dehalococcoidia, which were favored under recharge conditions. In particular, Dehalococcoidia is present in medium- and low-influenced waters, and it is absent in the high recharge-influenced groundwater (P8(1) and P8(-3)). This phylotype was identified at the genus level as *Dehalogenimonas sp* (Table S2). Similar behavior was found in the Nitrospira class, appearing in low-influenced groundwater in the wet scenario.

Patterns in the structure of microbial populations correlated with water types. For Type I, differences in the bacterial assemblage between both campaigns were attributed to seasonal changes (Table S1). Dehalococcoidia and Chlorobia were only detected in the wet scenario, while Cytophagia and Nitrospira could only be detected under dry conditions.

During the active recharge period and for Type IV water, Dehalococcoidia was found in three out of four sampling points and was the most abundant phylotype. For Type III water, significant differences were observed among in the samples analyzed. Populations with the highest relative abundance in P5 (2.3) were Betaproteobacteria and Bacilli. The former was also prominent in P5(–2.2), together with Cytophagia, while Dehalococcoidia were dominant in P2(3). Finally, in the case of groundwater Type II (recharge water), the bacterial assemblage was dominated by members of the Betaproteobacteria class. During the dry period, no clear distribution patterns in the bacterial relative abundances at the phylum and class level were observed, in part due to the DGGE profiles, mainly composed by fine bands (Figure 5); these were difficult to recover and purify, and thus could not be characterized. However, it should be mentioned that Betaproteobacteria were dominant in both P8 samples, contributing more than 50% to the relative abundance.

3.2 Microbial community indicators of MAR in soil and surface water

To study the impact of MAR on microbial community structure, recharge water from pre-sedimentation and infiltration basins, as well as soils, were analyzed. Figures 8 and 9 show the relative abundance of bacterial phylotypes at the taxonomical level of classes for surface water and soil samples. The results are displayed according to the distance to the recharge basin inlet.
Microbial richness in soil samples was controlled by water content. Non-recharge conditions had a primarily negative effect on the populations of Dehalococcoidia, Acidobacteria and Chlorobia, but favored the presence of Nitrospira, Cytophagia and Actinobacteria (Figure 8). Shannon and Evenness indices demonstrated that soils were more diverse under wet conditions than under dry ones (Table 1).
For surface water samples (Figure 9), there was a decreasing gradient in community complexity along the ponds. Acidobacteria, Betaproteobacteria and Cyanobacteria were the main phylotypes present.

4 Discussion

We contend that interdisciplinary analysis of geochemical characterization, recharge evaluation, and microbial fingerprinting, can provide relevant information about the fate of microbial ecosystems in soil and groundwater.

4.1 Matching groundwater model, ecological disturbance principle and microbial communities

Groundwater is a quite stable aquatic environment (Griebler and Lueders, 2009). One could expect that microbial communities in groundwater should also display low variability that could be reflected in the diversity indices. An example of this is P1, which is unaffected by recharge; the diversity indices remain constant regardless of the sampling campaign.

Hydrol. Earth Syst. Sci. Discuss., https://doi.org/10.5194/hess-2018-174
Manuscript under review for journal Hydrol. Earth Syst. Sci.
Discussion started: 17 April 2018

MAR is a passive treatment technique that can provide simultaneously oxic and anoxic conditions (Maeng et al., 2011). This has wide implications for the potential biological removal of selected emerging contaminants, as each micropollutant is most efficiently removed under specific redox conditions (Schmidt et al., 2007). Some can even be degraded by co-metabolism, involving different redox states in the process (Rodriguez-Escales and Sanchez-Vila, 2016). In this sense, MAR is an efficient remediation system. In addition, many sequenced phylotypes, such as *Nitrospira sp*, *Stenotrophomonas sp* and *Methylobacterium sp* have been associated with degradation capabilities (Cycoń et al., 2017; Daims et al., 2001; Wang et al., 2015). In short, the MAR microbial ecosystem studied in this work presents many more phylotypes than previous studies reported in groundwater systems (Logue et al., 2015), and thus, MAR can be considered an efficient remediation system.

We further tested the Intermediate Disturbance Hypothesis (IDH) for microbial communities in groundwater (Figure 6) related to MAR activities. IDH was originally proposed for tropical rain forests and coral reefs (Connell, 1978) and supports the idea that small perturbations create new access to resources for species which have overlapping niches, allowing their coexistence. This mechanism, known as a competition-colonization trade-off, can explain IDH in local communities, leading to an increase in diversity. However, when the degree of disturbance rises, only eurytolerant populations can survive and grow. Thus, an inverse correlation between diversity and the degree of disturbance (reflected in the temperature and conductivity profiles) was expected (see Table 1). Such correlations have also been reported in recharge wells and snowmelt-influenced aquifers (Ginige et al., 2013; Zhou et al., 2012).

In the Llobregat MAR system, the initial diversity in the microbial community increased with perturbation caused by recharge (Figure 6), with maximum diversity associated with Type IV water, and lowest for the most disturbed water (Type II). In ecological terms, Type III and Type IV waters represent different proportions of perturbation.

In the most altered groundwater zone (represented by P8 samples), Betaproteobacteria grew above 50% of the relative abundance (Figure 7). The main phylogenetic affiliation of this phylotype at the genus level is *Vogesella*. Strains of this genus are able to catabolize monosaccharides under aerobic conditions, but not under low-oxygen conditions. Furthermore, all *Vogesella* strains are denitrifiers (Grimes et al., 1997). Indeed, P8, located below the pond, receives oxygen-rich water during the recharge process, driven by fingering in the vadose zone. Although dissolved oxygen was not measured in the present study, data from other campaigns confirm this behavior for oxygen in P8 samples (data not shown). Moreover, nitrate concentration in the surface water was low (Table S1), and thus most denitrification is expected to occur under the pond. Grau-Martínez et al. (2018) recently confirmed that nitrate was consumed *via* denitrification pathway under the infiltration pond in the Llobregat MAR system, supporting the idea that *Vogesella sp* could be one of the genera involved in nitrate consumption. Likely, depending on the oxygen content, *Vogesella sp* will adapt its metabolic function in favor of aerobic oxidation of organic matter or by means of denitrification, thus becoming a good indicator of highly-disturbed MAR environments.

For Type III and Type IV waters, *Dehalogenimonas sp*, within the Dehalococcoidia class, is characteristic of medium-disturance groundwater (Figure 4 and Figure 7). *Dehalogenimonas sp* has been studied in recent years because some strains are associated with dechlorination in contaminated sites. This genus is strictly anaerobic and mesophilic, and some species can reductively dehalogenate polychlorinated aliphatic alkanes (Martín-González et al., 2015; Moe et al., 2009). As a result, recharge creates reducing conditions, likely indicating the existence of microzones or microsites (Bridgham et al., 2013; Hamersley and Howes,

2002), defined as local anoxic areas that coexist with fast-travelling oxygen-rich paths. Thus, microbial analysis can be used to unmask the apparent mishap of water samples that are oxic and display some typical anaerobic species. Moreover, some species of *Dehalogenimonas* can dechlorinate some Trichloroethane isomers (Dillehay et al., 2014), a pollutant reported in the Llobregat Lower Valley at levels as high as 300 $\mu g/L$ (Valhondo et al., 2014), thus opening the door for the development of enhanced remediation activities.

The Evenness index is an indicator of the equity of a community, and can be quite informative for observing perturbations to microbial communities. In the wet scenario, the lowest values of E were obtained for the samples most affected by recharge (Table 1), indicating that some species developed into predominant members of the microbial assemblage. Groundwater samples displayed the highest evenness values in the area less affected by recharge and in the dry scenario. in the latter case, values indicate the recovery of microbial communities from the disruption caused by recharge. In fact, P8(1) samples in dry scenario were not fully consistent with this conceptual model, with low evenness index and very low nitrate concentration. Furthermore, the presence of *Methylotenera mobilis* (Betaproteobacteria class) in both P8 sampling points was more than 40%, on average, of the relative abundance. *Methylotenera mobilis* is a methylotroph specie with denitrification abilities (Chistoserdova, 2011). These results suggest that P8 denitrification processes occur below the basin even when it is empty, indicating that four months is not enough time to revert back to natural conditions at this sampling point. This assumption is consistent with nitrate isotopic data presented in Grau-Martínez et al. (2018), and is also in agreement with the study of Rodriguez-Escales et al. (2016) in which biomass decay acted as an endogenous carbon source for respiration once the input carbon was reduced, maintaining denitrification rates.

4.2 Microbial community structure in soils and surface waters

We analyzed the heterogeneity of the microbial community structure in soil and surface water in terms of the distance to the infiltration basin entry point (Figure 9 and Table 1). Patterns in surface water microbial composition are linked to sequential sedimentation processes as revealed by granulometric analyses of soil samples (Table S3). The result was that surface water became poorer in terms of the presence of microbial communities between the pre-sedimentation basin and the end of the infiltration basin. The main reason could be the decrease in solids suspended throughout the system due to the sequential decantation of particles and their attached biomass. Furthermore, surface water displays relatively higher values of Cyanobacteria and Acidobacteria classes compared to groundwater. Cyanobacteria constitute the largest, most diverse, and most widely distributed group of photosynthetic prokaryotes, which are capable of conducting N fixation (Stanier and Bazine, 1977). However, members of the phylum Acidobacteria are physiologically diverse and ubiquitous in soils, degrade a wide range of carbon sources (from substances with a wide range of complexity), and are capable of reducing nitrates and nitrites (Kielak et al., 2016). This heterogeneous effect with distance to the entry point of the basin is also observed in the diversity indices, which lose diversity with distance and are inversely correlated to the proportion of fine particles. Similar behavior for richness correlated to soil texture was reported elsewhere (Chau et al., 2011).

Differences in the microbial communities in soils between the two basins were concentrated in the large organic matter content

provided by the reactive barrier present in the latter, being a source for the growth of bacterial communities and enhanced diversity under recharge conditions. The role of the humidity on microbial diversity is also significant, as was previously reported in horizontal subsurface constructed wetlands (Nurk et al., 2005). Furthermore, phylotypes distribution changes among scenarios. Whereas Dehaloccocoidia and Chlorobia classes appear in wet soils, Nitrospira, Cytophagia and Actinobacteria are favored under dry conditions.

The role of the reactive layer at the infiltration pond could be extrapolated as a system fed with a considerable organic carbon load. Laboratory experiments and constructed wetlands demonstrate that concentration of microbial activity and TOC degradation is concentrated in the first centimeters of the filter material (Ragusa et al., 2004; Sleytr et al., 2007; Tietz et al., 2007) in response to oxygen concentration vertical distribution. Although rapid oxygen depletion and consequent denitrification conditions have been evidenced in lab-scale MAR experiments (Alidina et al., 2014a; Dutta et al., 2015), this effect may not happen rapidly under real infiltration conditions, where entrapped gas (Heilweil et al., 2004) or fingering processes (Kung, 1990) may provide higher oxygen concentrations than in lower dimension systems (e.g., columns). Lab-experiments are doubtlessly useful to elucidate the behavior of microbial communities under controlled conditions. However, sometimes it could exist a difficulty of transferring conclusions obtained from lab samples to real sites.

5 Conclusions

This study aims at integrating different fields such as hydrogeology, ecology and microbiology applied to a real MAR facility, relating flow (infiltration) conditions, physicochemical water parameters, and microbial changes induced by managed recharge along vertical transect. We observed that infiltration ponds modify the hydrochemistry and ecology of the groundwater environment, especially in terms of microbial communities. Comparing recharge and non-recharge scenarios, we found that microbial diversity indices (Shannon) correlate inversely with the degree of perturbation caused by the induced recharge, substantiating an Intermediate Disturbance Hypothesis distribution. In fact, MAR (surface) basins operation can promote different levels of disturbance at the same time, and microbial community structures change accordingly. From microbial fingerprinting analysis, we observed the boosting of Betaproteobacteria and Dehalococcoidia classes correlate to recharge practices. Furthermore, genera such as *Dehalogenimonas*, *Nitrospira*, *Stenotrophomonas*, *Methylobacterium* were also detected, indicating a wide spectrum of biodegradation capabilities. Likewise, sequencing tasks revealed characteristic phylotypes from each water type, particularly *Vogesella sp* for highly perturbed water or *Dehalogenimonas sp* for medium-perturbed water. Microbial populations in soil are quite diverse when comparing wet with dry scenarios. Soil moisture and sediment grain size appear to be the key factors explaining diversity patterns. Furthermore, variation in recharge conditions do not translate immediately to changes in communities. All these results combined confirm the difficulty of extending laboratory experiment results to the field scale.

Competing interests. The authors declare that they have no conflict of interest.

Acknowledgements. This investigation was financially supported by the European Union project MARSOL grant agreement no. 619120, FP7-ENV-2013-WATER-INNO-DEMO, Generalitat de Catalunya via FI scholarship program (FI-DGR 2014) and the Spanish Government and EU (project ACWAPUR PCIN-2015-239). The authors would like to acknowledge Marc Vives for his help and Comunitat d'Usuaris d'Aigües de la Vall Baixa i del Delta del Riu Llobregat (CUADLL) for their cooperation.

References

Alidina, M., Hoppe-Jones, C., Yoon, M., Hamadeh, A. F., Li, D., and Drewes, J. E.: The occurrence of emerging trace organic chemicals in wastewater effluents in Saudi Arabia., The Science of the total environment, 478, 152–62, https://doi.org/10.1016/j.scitotenv.2014.01.093, http://www.sciencedirect.com/science/article/pii/S0048969714001211, 2014a.

Alidina, M., Li, D., Ouf, M., and Drewes, J. E.: Role of primary substrate composition and concentration on attenuation of trace organic chemicals in managed aquifer recharge systems., Journal of environmental management, 144, 58–66, https://doi.org/10.1016/j.jenvman.2014.04.032, http://www.sciencedirect.com/science/article/pii/S0301479714002552, 2014b.

Barbieri, M., Carrera, J., Sanchez-Vila, X., Ayora, C., Cama, J., Köck-Schulmeyer, M., López de Alda, M., Barceló, D., Tobella Brunet, J., and Hernández García, M.: Microcosm experiments to control anaerobic redox conditions when studying the fate of organic micropollutants in aquifer material, Journal of Contaminant Hydrology, 126, 330–345, https://doi.org/http://dx.doi.org/10.1016/j.jconhyd.2011.09.003, http://www.sciencedirect.com/science/article/pii/S0169772211000957, 2011.

Barbieri, M., Carrera, J., Ayora, C., Sanchez-Vila, X., Licha, T., Nodler, K., Osorio, V., Perez, S., Kock-Schulmeyer, M., Lopez de Alda, M., and Barcelo, D.: Formation of diclofenac and sulfamethoxazole reversible transformation products in aquifer material under denitrifying conditions: batch experiments, Sci Total Environ, 426, 256–263, https://doi.org/10.1016/j.scitotenv.2012.02.058, 2012.

Bates, B., Z.W. Kundzewicz, S.Wu, and J.P. Palutikof: Climate Change and Water. Technical Paper if the Intergovernmental Panel on Climate Change, Tech. rep., IPCC Secretariat, Geneva, https://www.ipcc.ch/publications{_}and{_}data/publications{_}and{_}data{_}technical{_}papers.shtml, 2008.

Bridgham, S. D., Cadillo-Quiroz, H., Keller, J. K., and Zhuang, Q.: Methane emissions from wetlands: biogeochemical, microbial, and modeling perspectives from local to global scales, Global Change Biology, 19, 1325–1346, https://doi.org/10.1111/gcb.12131, http://dx.doi.org/10.1111/gcb.12131, 2013.

Chau, J., Bagtzoglou, A., and Willig, M.: The effect of soil texture on richness and diversity of bacterial communities, Environmental Forensics, 12, 333–341, https://doi.org/10.1080/15275922.2011.622348, http://www.tandfonline.com/doi/abs/10.1080/15275922.2011.622348, 2011.

Chistoserdova, L.: Methylotrophy in a lake: From metagenomics to single-organism physiology, https://doi.org/10.1128/AEM.00314-11, http://www.ncbi.nlm.nih.gov/pubmed/21622781http://www.pubmedcentral.nih.gov/articlerender.fcgi?artid=PMC3147377, 2011.

Connell, J. H.: Diversity in Tropical Rain Forests and Coral Reefs, Science, 199, 1302–1310, https://doi.org/10.1126/science.199.4335.1302, http://www.sciencemag.org/cgi/doi/10.1126/science.199.4335.1302, 1978.

Cycoń, M., Mrozik, A., and Piotrowska-Seget, Z.: Bioaugmentation as a strategy for the remediation of pesticide-polluted soil: A review, https://doi.org/10.1016/j.chemosphere.2016.12.129, http://www.sciencedirect.com.recursos.biblioteca.upc.edu/science/article/pii/S0045653516318720, 2017.

Daims, H., Nielsen, J. L., Nielsen, P. H., Schleifer, K.-H., and Wagner, M.: In Situ Characterization of Nitrospira-Like Nitrite-Oxidizing Bacteria Active in Wastewater Treatment Plants, Applied and Environmental Microbiology, 67, 5273–5284, https://doi.org/10.1128/AEM.67.11.5273-5284.2001, http://www.ncbi.nlm.nih.gov/pmc/articles/PMC93301/, 2001.

Dillehay, J. L., Bowman, K. S., Yan, J., Rainey, F. A., and Moe, W. M.: Substrate interactions in dehalogenation of 1,2-dichloroethane, 1,2-dichloropropane, and 1,1,2-trichloroethane mixtures by Dehalogenimonas spp., Biodegradation, 25, 301–312, https://doi.org/10.1007/s10532-013-9661-2, http://www.ncbi.nlm.nih.gov/pubmed/23990262http://link.springer.com/10.1007/s10532-013-9661-2, 2014.

Drewes, J. E., Reinhard, M., and Fox, P.: Comparing microfiltration-reverse osmosis and soil-aquifer treatment for indirect potable reuse of water, Water Research, 37, 3612–3621, https://doi.org/10.1016/S0043-1354(03)00230-6, 2003.

Dutta, T., Carles-Brangarí, A., Fernàndez-Garcia, D., Rubol, S., Tirado-Conde, J., and Sanchez-Vila, X.: Vadose zone oxygen (O2) dynamics during drying and wetting cycles: An artificial recharge laboratory experiment, Journal of Hydrology, 527, 151–159, https://doi.org/10.1016/j.jhydrol.2015.04.048, http://www.sciencedirect.com/science/article/pii/S0022169415003078, 2015.

Freixa, A., Rubol, S., Carles-Brangarí, A., Fernàndez-Garcia, D., Butturini, A., Sanchez-Vila, X., and Romaní, A. M.: The effects of sediment depth and oxygen concentration on the use of organic matter: An experimental study using an infiltration sediment tank, Science of the Total Environment, 540, 20–31, https://doi.org/10.1016/j.scitotenv.2015.04.007, http://www.ncbi.nlm.nih.gov/pubmed/25900223http://linkinghub.elsevier.com/retrieve/pii/S004896971500443X, 2015.

Ginige, M. P., Kaksonen, A. H., Morris, C., Shackelton, M., and Patterson, B. M.: Bacterial community and groundwater quality changes in an anaerobic aquifer during groundwater recharge with aerobic recycled water, FEMS Microbiology Ecology, 85, 553–567, https://doi.org/10.1111/1574-6941.12137, 2013.

Grau-Martínez, A., Folch, A., Torrentó, C., Valhondo, C., Barba, C., Domènech, C., Otero, N., and Soler, A.: Monitoring induced denitrification during managed aquifer recharge in an infiltration pond, Journal of Hydrology, https://doi.org/10.1016/j.jhydrol.2018.03.044, http://linkinghub.elsevier.com/retrieve/pii/S0022169418302105, 2018.

Greskowiak, J., Prommer, H., Massmann, G., and Nützmann, G.: Modeling Seasonal Redox Dynamics and the Corresponding Fate of the Pharmaceutical Residue Phenazone During Artificial Recharge of Groundwater, Environmental Science & Technology, 40, 6615–6621, https://doi.org/10.1021/es052506t, http://pubs.acs.org/doi/abs/10.1021/es052506t, 2006.

Griebler, C. and Lueders, T.: Microbial biodiversity in groundwater ecosystems, Freshwater Biology, 54, 649–677, https://doi.org/10.1111/j.1365-2427.2008.02013.x, http://doi.wiley.com/10.1111/j.1365-2427.2008.02013.x, 2009.

Grimes, D. J., Woese, C. R., MacDonell, M. T., and Colwell, R. R.: Systematic study of the genus Vogesella gen. nov. and its type species, Vogesella indigofera comb. nov., International journal of systematic bacteriology, 47, 19–27, https://doi.org/10.1099/00207713-47-1-19, http://ijs.microbiologyresearch.org/content/view.action?itemId=http{%}3A{%}2F{%}2Fsgm.metastore.ingenta.com{%}2Fcontent{%}2Fjournal{%}2Fijsem{%}2F10.1099{%}2F00207713-47-1-19{&}view={&}itemType=http{%}3A{%}2F{%}2Fpub2web.metastore.ingenta.com{%}2Fns{%}2FArticle, 1997.

Grimm, N. B.: Disturbance, succession, and ecosystem processes in streams: a case study from the desert, in: Joint Symposium of the British Ecological Society and the American Society of Lirrmologyand Oceanography, edited by P.S. Giller, A.G. Hildrew and Raffaeli, D., pp. 93–112, Blackwell Scientific, Oxford, 1994.

Hamersley, M. R. and Howes, B. L.: Control of denitrification in a septage-treating artificial wetland: The dual role of particulate organic carbon, Water Research, 36, 4415–4427, https://doi.org/10.1016/S0043-1354(02)00134-3, 2002.

Heilweil, V. M., Solomon, D. K., Perkins, K. S., and Ellett, K. M.: Gas-partitioning tracer test to quantify trapped gas during recharge., Ground water, 42, 589–600, http://www.ncbi.nlm.nih.gov/pubmed/15318781, 2004.

Hellauer, K., Karakurt, S., Sperlich, A., Burke, V., Massmann, G., Hübner, U., and Drewes, J. E.: Establishing sequential managed aquifer recharge technology (SMART) for enhanced removal of trace organic chemicals: Experiences from field studies in Berlin, Germany, https://doi.org/10.1016/j.jhydrol.2017.09.044, https://www.sciencedirect.com/science/article/pii/S0022169417306480, 2017.

Huang, G., Liu, F., Yang, Y., Deng, W., Li, S., Huang, Y., and Kong, X.: Removal of ammonium-nitrogen from groundwater using a fully passive permeable reactive barrier with oxygen-releasing compound and clinoptilolite, Journal of Environmen-

tal Management, 154, 1–7, https://doi.org/http://dx.doi.org/10.1016/j.jenvman.2015.02.012, http://www.sciencedirect.com/science/article/pii/S0301479715000808, 2015.

Jurado, A., Vàzquez-Suñé, E., Carrera, J., López de Alda, M., and Pujades, E.: Emerging organic contaminants in groundwater in Spain: A review of sources, recent occurrence and fate in a European context, Science of The Total Environment, 440, 82–94, https://doi.org/10.1016/j.scitotenv.2012.08.029, 2012.

Kielak, A. M., Barreto, C. C., Kowalchuk, G. A., van Veen, J. A., and Kuramae, E. E.: The ecology of Acidobacteria: Moving beyond genes and genomes, https://doi.org/10.3389/fmicb.2016.00744, http://journal.frontiersin.org/Article/10.3389/fmicb.2016.00744/abstract, 2016.

Kung, K.-J.: Preferential flow in a sandy vadose zone: 1. Field observation, Geoderma, 46, 51–58, https://doi.org/10.1016/0016-7061(90)90006-U, http://linkinghub.elsevier.com/retrieve/pii/001670619090006U, 1990.

Li, D., Alidina, M., Ouf, M., Sharp, J. O., Saikaly, P., and Drewes, J. E.: Microbial community evolution during simulated managed aquifer recharge in response to different biodegradable dissolved organic carbon (BDOC) concentrations, Water Res, 47, 2421–2430, https://doi.org/10.1016/j.watres.2013.02.012, 2013.

Logue, J. B., Stedmon, C. a., Kellerman, A. M., Nielsen, N. J., Andersson, A. F., Laudon, H., Lindström, E. S., and Kritzberg, E. S.: Experimental insights into the importance of aquatic bacterial community composition to the degradation of dissolved organic matter, The ISME Journal, pp. 1–13, http://www.nature.com/doifinder/10.1038/ismej.2015.131, 2015.

Lombard, N., Prestat, E., van Elsas, J. D., and Simonet, P.: Soil-specific limitations for access and analysis of soil microbial communities by metagenomics, https://doi.org/10.1111/j.1574-6941.2011.01140.x, http://www.ncbi.nlm.nih.gov/pubmed/21631545https://academic.oup.com/femsec/article-lookup/doi/10.1111/j.1574-6941.2011.01140.x, 2011.

Loos, R., Carvalho, R., António, D. C., Comero, S., Locoro, G., Tavazzi, S., Paracchini, B., Ghiani, M., Lettieri, T., Blaha, L., Jarosova, B., Voorspoels, S., Servaes, K., Haglund, P., Fick, J., Lindberg, R. H., Schwesig, D., and Gawlik, B. M.: EU-wide monitoring survey on emerging polar organic contaminants in wastewater treatment plant effluents, Water Research, 47, 6475–6487, https://doi.org/10.1016/j.watres.2013.08.024, 2013.

López-Serna, R., Postigo, C., Blanco, J., Pérez, S., Ginebreda, A., López De Alda, M., Petrović, M., Munné, A., Barceló, D., Ginebreda, A., De Alda, M. L., Petrović, . M., Barceló, D., Petrović, M., and Munné, A.: Assessing the effects of tertiary treated wastewater reuse on the presence emerging contaminants in a Mediterranean river (Llobregat, NE Spain), Environ Sci Pollut Res, 19, 1000–1012, https://doi.org/10.1007/s11356-011-0596-z, 2012.

Maeng, S. K., Ameda, E., Sharma, S. K., Grützmacher, G., and Amy, G. L.: Organic micropollutant removal from wastewater effluent-impacted drinking water sources during bank filtration and artificial recharge, Water Research, 44, 4003–4014, https://doi.org/http://dx.doi.org/10.1016/j.watres.2010.03.035, http://www.sciencedirect.com/science/article/pii/S004313541000223X, 2010.

Maeng, S. K., Sharma, S. K., Lekkerkerker-Teunissen, K., and Amy, G. L.: Occurrence and fate of bulk organic matter and pharmaceutically active compounds in managed aquifer recharge: A review, Water Research, 45, 3015–3033, https://doi.org/http://dx.doi.org/10.1016/j.watres.2011.02.017, http://www.sciencedirect.com/science/article/pii/S004313541100073X, 2011.

Martín-González, L., Hatijah Mortan, S., Rosell, M., Parladé, E., Martínez-Alonso, M., Gaju, N., Caminal, G., Adrian, L., and Marco-Urrea, E.: Stable Carbon Isotope Fractionation During 1,2-Dichloropropane-to-Propene Transformation by an Enrichment Culture Containing Dehalogenimonas Strains and a dcpA Gene, Environmental Science & Technology, 49, 8666–8674, https://doi.org/10.1021/acs.est.5b00929, http://www.ncbi.nlm.nih.gov/pubmed/26111261, 2015.

Massmann, G., Dünnbier, U., Heberer, T., and Taute, T.: Behaviour and redox sensitivity of antimicrobial residues during bank filtration– Investigation of residues of phenazone-type analgesics, Chemosphere, 71, 1476–1485, https://doi.org/10.1016/j.chemosphere.2008.06.056, 2008.

Moe, W. M., Yan, J., Nobre, M. F., da Costa, M. S., and Rainey, F. A.: Dehalogenimonas lykanthroporepellens gen. nov., sp. nov., a reductively dehalogenating bacterium isolated from chlorinated solvent-contaminated groundwater, International Journal of Systematic and Evolutionary Microbiology, 59, 2692–2697, 2009.

Nadav, I., Arye, G., Tarchitzky, J., and Chen, Y.: Enhanced infiltration regime for treated-wastewater purification in soil aquifer treatment (SAT), Journal of Hydrology, 420, 275–283, https://doi.org/10.1016/j.jhydrol.2011.12.013, 2012.

Nurk, K., Truu, J., Truu, M., and Mander, Ü.: Microbial Characteristics and Nitrogen Transformation in Planted Soil Filter for Domestic Wastewater Treatment, Journal of Environmental Science and Health, Part A, 40, 1201–1214, https://doi.org/10.1081/ESE-200055659, http://www.tandfonline.com/doi/abs/10.1081/ESE-200055659{#}.V39pvVGAcWQ.mendeley, 2005.

Onesios-Barry, K. M., Berry, D., Proescher, J. B., Ashok Sivakumar, I. K., and Bouwer, E. J.: Removal of pharmaceuticals and personal care products during water recycling: Microbial community structure and effects of substrate concentration, Applied and Environmental Microbiology, 80, 2440–2450, https://doi.org/10.1128/AEM.03693-13, http://www.ncbi.nlm.nih.gov/pubmed/24509919http://www.pubmedcentral.nih.gov/articlerender.fcgi?artid=PMC3993184, 2014.

Pedretti, D., Barahona-Palomo, M., Bolster, D., Sanchez-Vila, X., and Fernàndez-Garcia, D.: A quick and inexpensive method to quantify spatially variable infiltration capacity for artificial recharge ponds using photographic images, Journal of Hydrology, 430–431, 118–126, https://doi.org/http://dx.doi.org/10.1016/j.jhydrol.2012.02.008, http://www.sciencedirect.com/science/article/pii/S0022169412001060, 2012.

Ragusa, S. R., McNevin, D., Qasem, S., and Mitchell, C.: Indicators of biofilm development and activity in constructed wetlands microcosms, Water Research, 38, 2865–2873, https://doi.org/10.1016/j.watres.2004.03.039, http://linkinghub.elsevier.com/retrieve/pii/S0043135404001757, 2004.

Reed, D. A., Toze, S., and Chang, B.: Spatial and temporal changes in sulphate-reducing groundwater bacterial community structure in response to Managed Aquifer Recharge, Water Science & Technology, 57, 789, https://doi.org/10.2166/wst.2008.172, http://wst.iwaponline.com/cgi/doi/10.2166/wst.2008.172, 2008.

Regnery, J., Li, D., Roberts, S., Higgins, C., Sharp, J. O., and Drewes, J. E.: Linking Trace Organic Chemical Attenuation to Microbiome metabolic Capabilities: Insights from Laboratory- and Full-scale Managed Aquifer Recharge Systems, in: ACS Symposium Series, vol. 1, chap. 2, pp. 163–187, https://doi.org/10.1021/bk-2016-1241.ch011, http://pubs.acs.org/doi/abs/10.1021/bk-2016-1241.ch011, 2016.

Regnery, J., Lee, J., Drumheller, Z. W., Drewes, J. E., Illangasekare, T. H., Kitanidis, P. K., McCray, J. E., and Smits, K. M.: Trace organic chemical attenuation during managed aquifer recharge: Insights from a variably saturated 2D tank experiment, Journal of Hydrology, 548, 641–651, https://doi.org/10.1016/j.jhydrol.2017.03.038, 2017.

Rivett, M. O., Buss, S. R., Morgan, P., Smith, J. W. N., and Bemment, C. D.: Nitrate attenuation in groundwater: A review of biogeochemical controlling processes, Water Research, 42, 4215–4232, https://doi.org/10.1016/j.watres.2008.07.020, 2008.

Rodriguez-Escales, P. and Sanchez-Vila, X.: Fate of sulfamethoxazole in groundwater: Conceptualizing and modeling metabolite formation under different redox conditions, Water Research, 105, 540–550, https://doi.org/10.1016/j.watres.2016.09.034, 2016.

Rodriguez-Escales, P., Folch, A., van Breukelen, B. M., Vidal-Gavilan, G., and Sanchez-Vila, X.: Modeling long term Enhanced in situ Biodenitrification and induced heterogeneity in column experiments under different feeding strategies, Journal of Hydrology, 538, 127–137, https://doi.org/10.1016/j.jhydrol.2016.04.012, http://linkinghub.elsevier.com/retrieve/pii/S0022169416301937, 2016.

Rubol, S., Freixa, A., Carles-Brangarí, A., Fernàndez-Garcia, D., Romaní, A. M., and Sanchez-Vila, X.: Connecting bacterial colonization to physical and biochemical changes in a sand box infiltration experiment, Journal of Hydrology, 517, 317–327, https://doi.org/http://dx.doi.org/10.1016/j.jhydrol.2014.05.041, http://www.sciencedirect.com/science/article/pii/S0022169414004053, 2014.

Schaffer, M., Kröger, K. F., Nödler, K., Ayora, C., Carrera, J., Hernández, M., and Licha, T.: Influence of a compost layer on the attenuation of 28 selected organic micropollutants under realistic soil aquifer treatment conditions: Insights from a large scale column experiment, Water Research, 74, 110–121, https://doi.org/10.1016/j.watres.2015.02.010, 2015.

Schmidt, C. K., Lange, F. T., and Brauch, H. J.: Characteristics and evaluation of natural attenuation processes for organic micropollutant removal during riverbank filtration, in: Water Science and Technology: Water Supply, vol. 7, pp. 1–7, https://doi.org/10.2166/ws.2007.060, 2007.

Sleytr, K., Tietz, A., Langergraber, G., and Haberl, R.: Investigation of bacterial removal during the filtration process in constructed wetlands, Science of the Total Environment, 380, 173–180, https://doi.org/10.1016/j.scitotenv.2007.03.001, http://linkinghub.elsevier.com/retrieve/pii/S0048969707003002, 2007.

Stanier, R. Y. and Bazine, G. C.: Phototrophic Prokaryotes: The Cyanobacteria, Annual Review of Microbiology, 31, 225–274, https://doi.org/10.1146/annurev.mi.31.100177.001301, http://www.annualreviews.org/doi/10.1146/annurev.mi.31.100177.001301, 1977.

Tietz, A., Kirschner, A., Langergraber, G., Sleytr, K., and Haberl, R.: Characterisation of microbial biocoenosis in vertical subsurface flow constructed wetlands, Science of the Total Environment, 380, 163–172, https://doi.org/10.1016/j.scitotenv.2006.11.034, http://linkinghub.elsevier.com/retrieve/pii/S0048969706009107, 2007.

Valhondo, C., Carrera, J., Ayora, C., Barbieri, M., Nödler, K., Licha, T., and Huerta, M.: Behavior of nine selected emerging trace organic contaminants in an artificial recharge system supplemented with a reactive barrier, Environmental Science and Pollution Research, 21, 11 832–11 843, 2014.

Valhondo, C., Martinez-Landa, L., Carrera, J., Ayora, C., Nödler, K., and Licha, T.: Evaluation of EOC removal processes during artificial recharge through a reactive barrier, Science of the Total Environment, 612, 985–994, https://doi.org/10.1016/j.scitotenv.2017.08.054, http://www.sciencedirect.com.recursos.biblioteca.upc.edu/science/article/pii/S0048969717320521, 2018.

Wang, Z., Dai, Y., Zhao, Q., Li, N., Zhou, Q., and Xie, S.: Nonylphenol biodegradation, functional gene abundance and bacterial community in bioaugmented sediment: effect of external carbon source, Environmental Science and Pollution Research, 22, 12 083–12 091, https://doi.org/10.1007/s11356-015-4509-4, http://www.ncbi.nlm.nih.gov/pubmed/25874439http://link.springer.com/10.1007/s11356-015-4509-4, 2015.

Zhang, W., Huan, Y., Liu, D., Wang, H., Jiao, X., Wu, X., and Du, S.: Influences of microbial communities on groundwater component concentrations during managed artificial recharge, Environmental Earth Sciences, 75, 1–8, https://doi.org/10.1007/s12665-015-4959-5, http://link.springer.com/10.1007/s12665-015-4959-5, 2016.

Zhou, Y., Kellermann, C., and Griebler, C.: Spatio-temporal patterns of microbial communities in a hydrologically dynamic pristine aquifer, FEMS Microbiology Ecology, 81, 230–242, https://doi.org/10.1111/j.1574-6941.2012.01371.x, http://dx.doi.org/10.1111/j.1574-6941.2012.01371.x, 2012.

Hydrol. Earth Syst. Sci. Discuss., https://doi.org/10.5194/hess-2018-174
Manuscript under review for journal Hydrol. Earth Syst. Sci.
Discussion started: 17 April 2018

Hydrology and Earth System Sciences
Discussions
Open Access
EGU

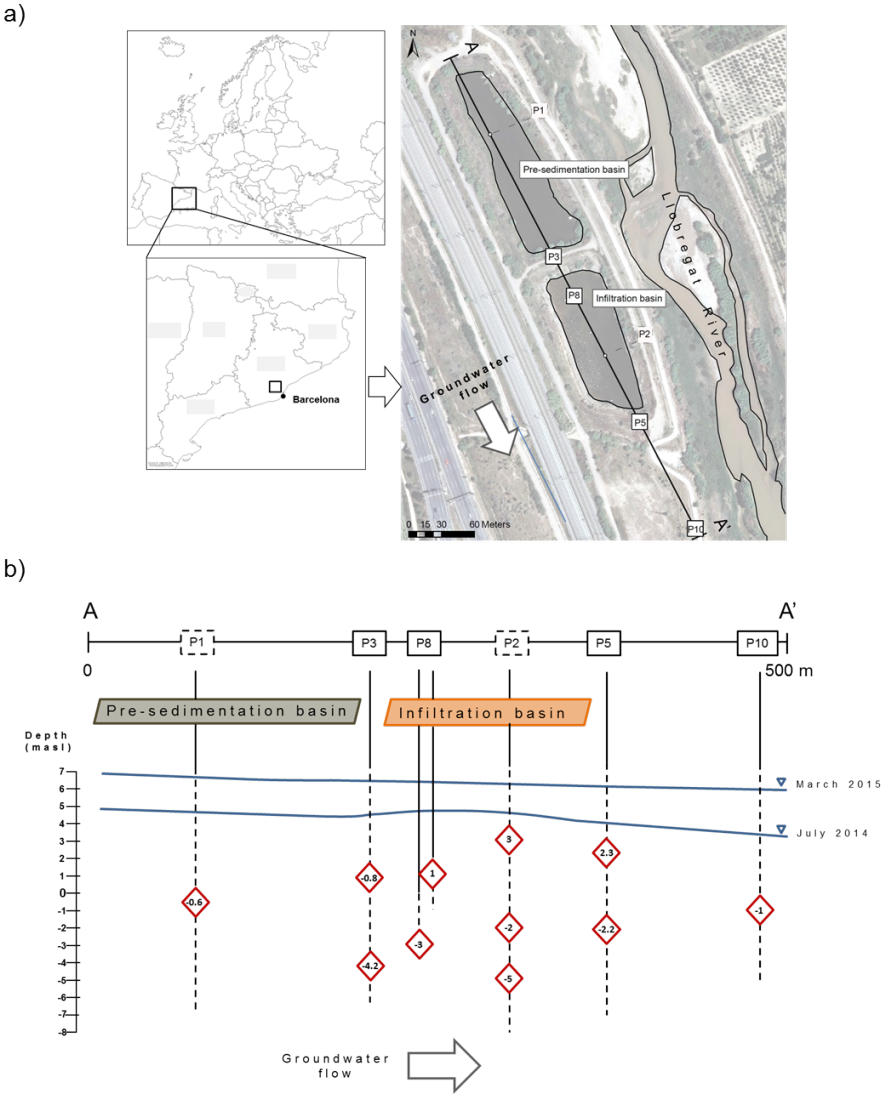

Figure 1. Geographical location of the Llobregat MAR system and location of the established transect (a) Transect section with piezometers (P1 and P2 are projected) and displaying sampling depths (red diamonds). (b) Blue line shows groundwater level in July 2014 (wet scenario - recharge) and March 2015 (dry scenario – non-recharge)

Hydrol. Earth Syst. Sci. Discuss., https://doi.org/10.5194/hess-2018-174
Manuscript under review for journal Hydrol. Earth Syst. Sci.
Discussion started: 17 April 2018

Hydrology and Earth System Sciences
Discussions
Open Access
EGU

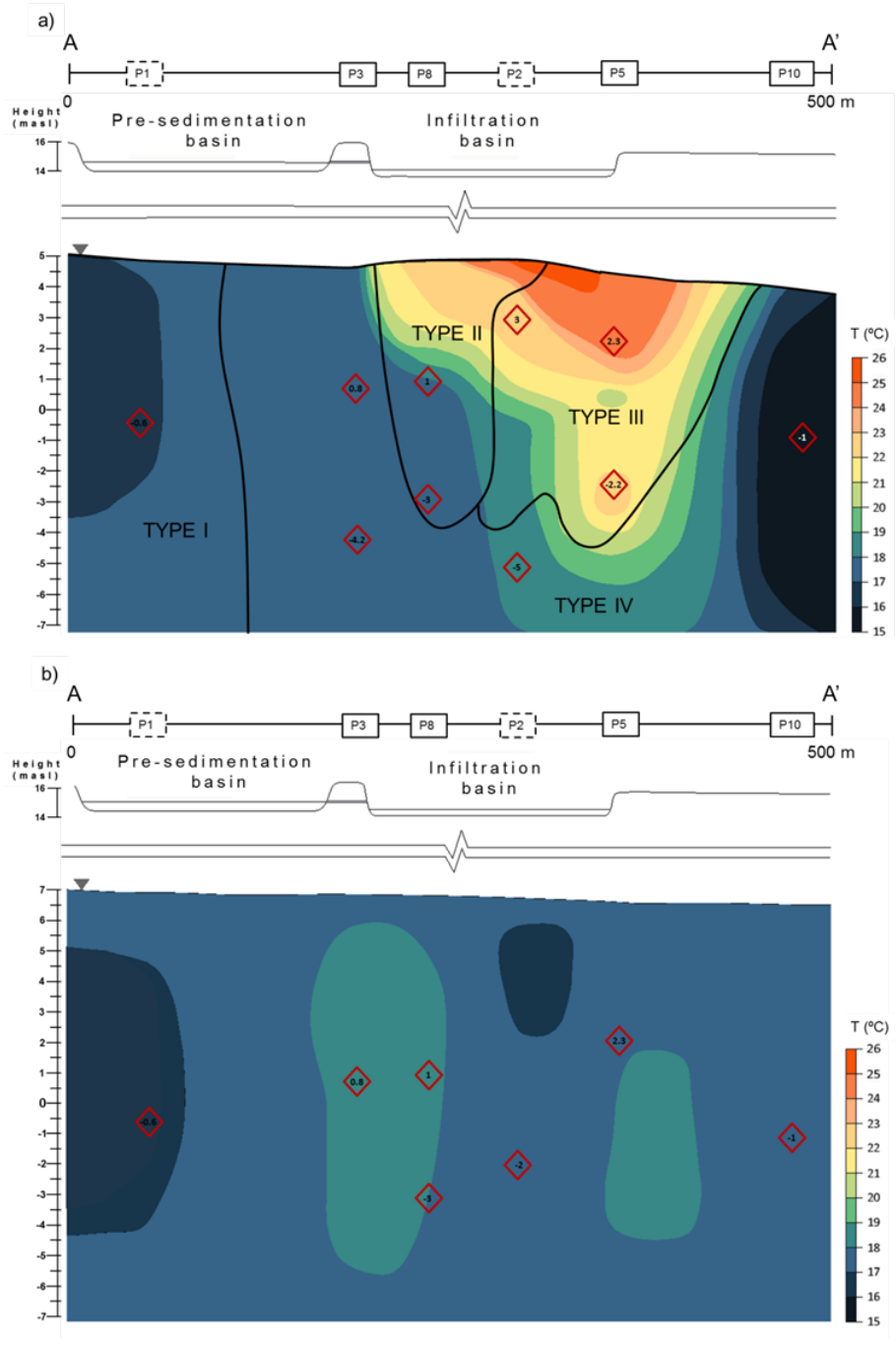

Figure 2. Temperature distribution at the local scale in (a) July 2014 (wet), and (b) March 2015 (dry). Red diamonds indicate sampling points for microbial and water analysis in each campaign

Hydrol. Earth Syst. Sci. Discuss., https://doi.org/10.5194/hess-2018-174
Manuscript under review for journal Hydrol. Earth Syst. Sci.
Discussion started: 17 April 2018

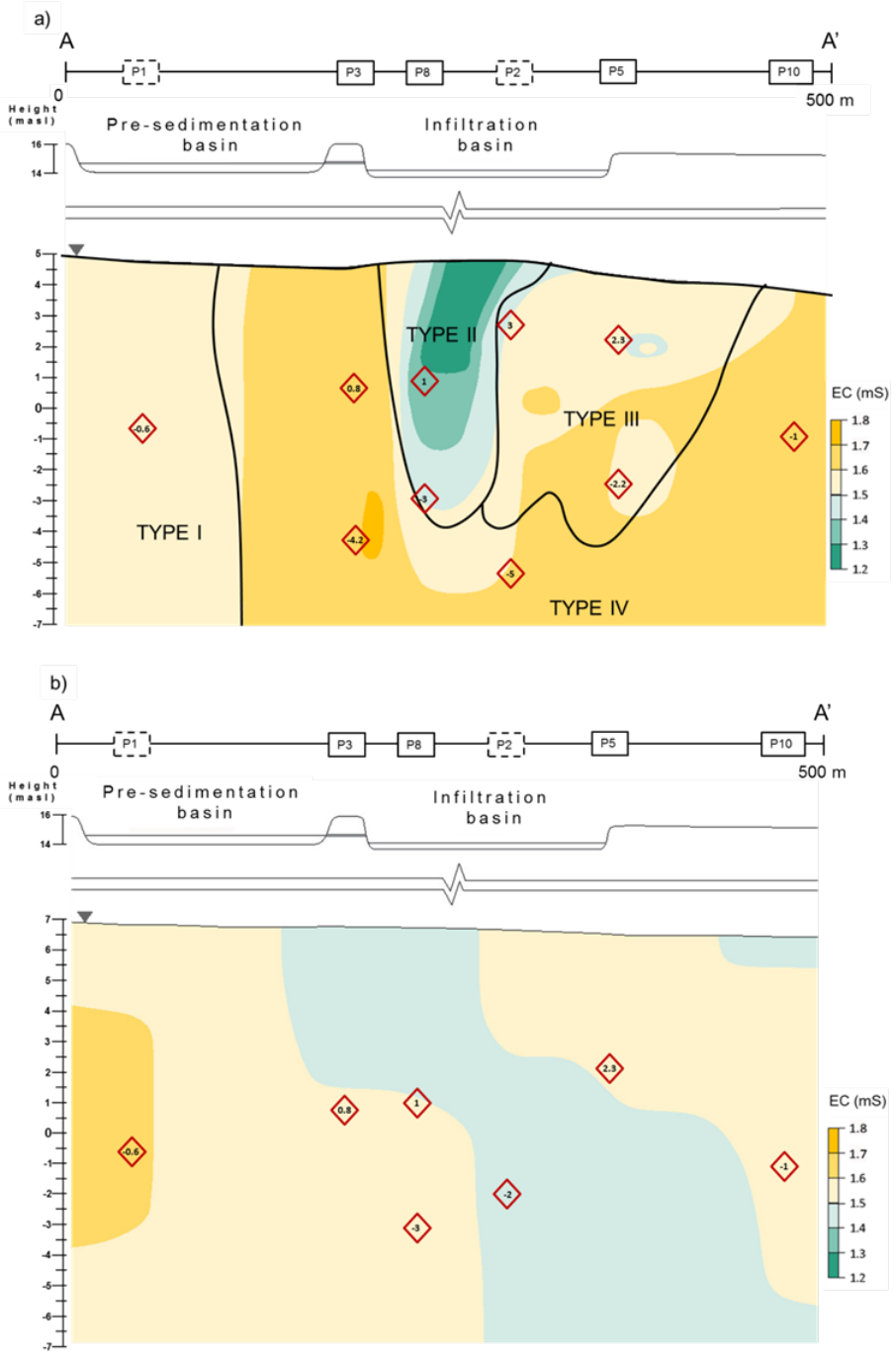

Figure 3. Electrical Conductivity distribution at the local scale in (a) July 2014 (wet), and (b) March 2015 (dry)

Hydrol. Earth Syst. Sci. Discuss., https://doi.org/10.5194/hess-2018-174
Manuscript under review for journal Hydrol. Earth Syst. Sci.
Discussion started: 17 April 2018

Hydrology and Earth System Sciences
Discussions
Open Access
EGU

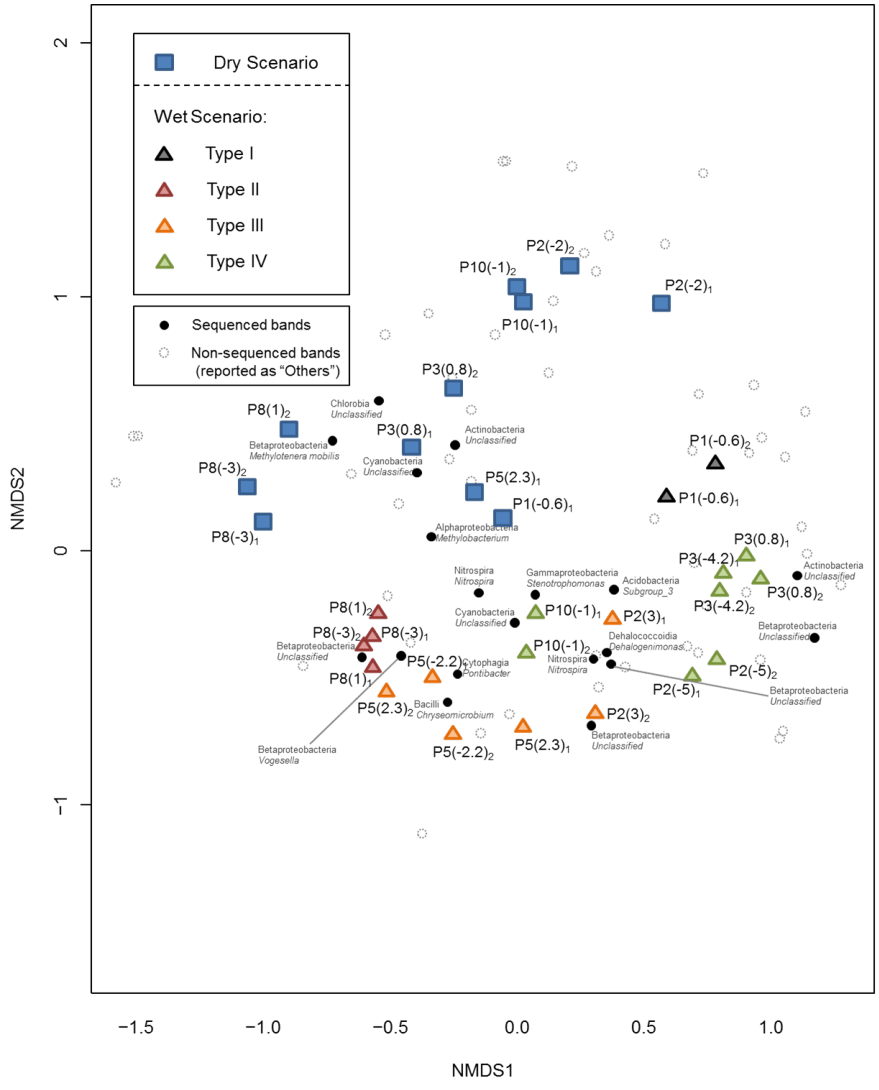

Figure 4. Non-metric Multidimensional Scaling clustering for all groundwater samples. Blue squares and triangles represent samples in dry and wet scenarios, respectively. Colors in triangles represent water types. Black circles correspond to band migration numbers in DGGE gels that were sequenced (phylogenetic affiliation corresponding to each black circle). Non-sequenced bands are also portrayed (empty circles)

Hydrol. Earth Syst. Sci. Discuss., https://doi.org/10.5194/hess-2018-174
Manuscript under review for journal Hydrol. Earth Syst. Sci.
Discussion started: 17 April 2018

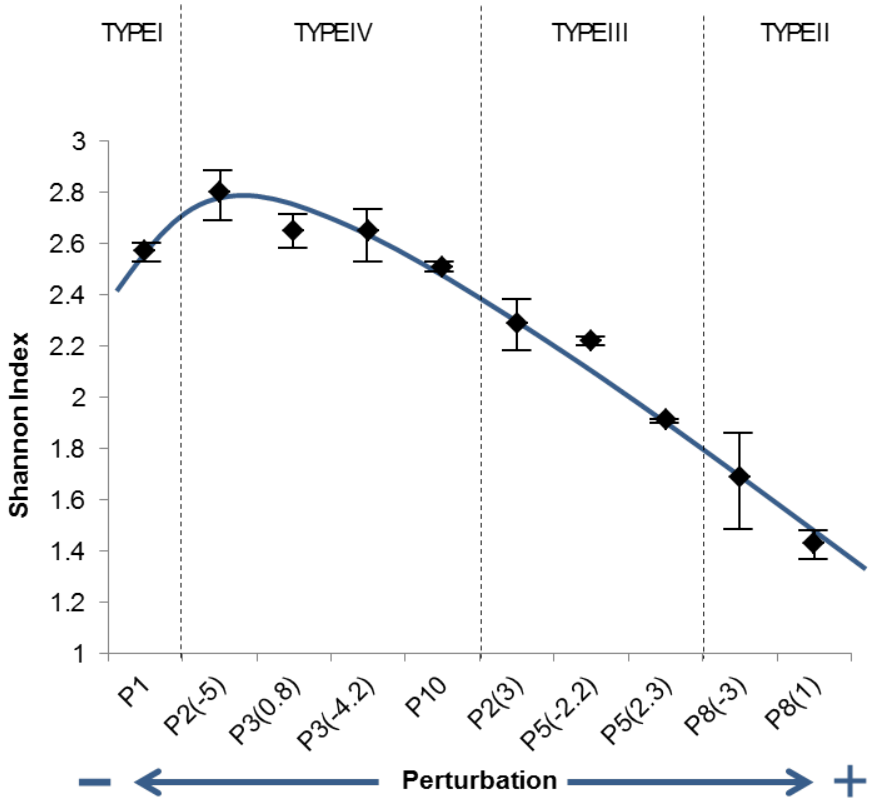

Figure 5. Average of Shannon Indices in piezometer samples under wet conditions. Standard deviation is shown in error bars. Horizontal axis reflects the degree of perturbation of original groundwater due to recharge

Hydrol. Earth Syst. Sci. Discuss., https://doi.org/10.5194/hess-2018-174
Manuscript under review for journal Hydrol. Earth Syst. Sci.
Discussion started: 17 April 2018

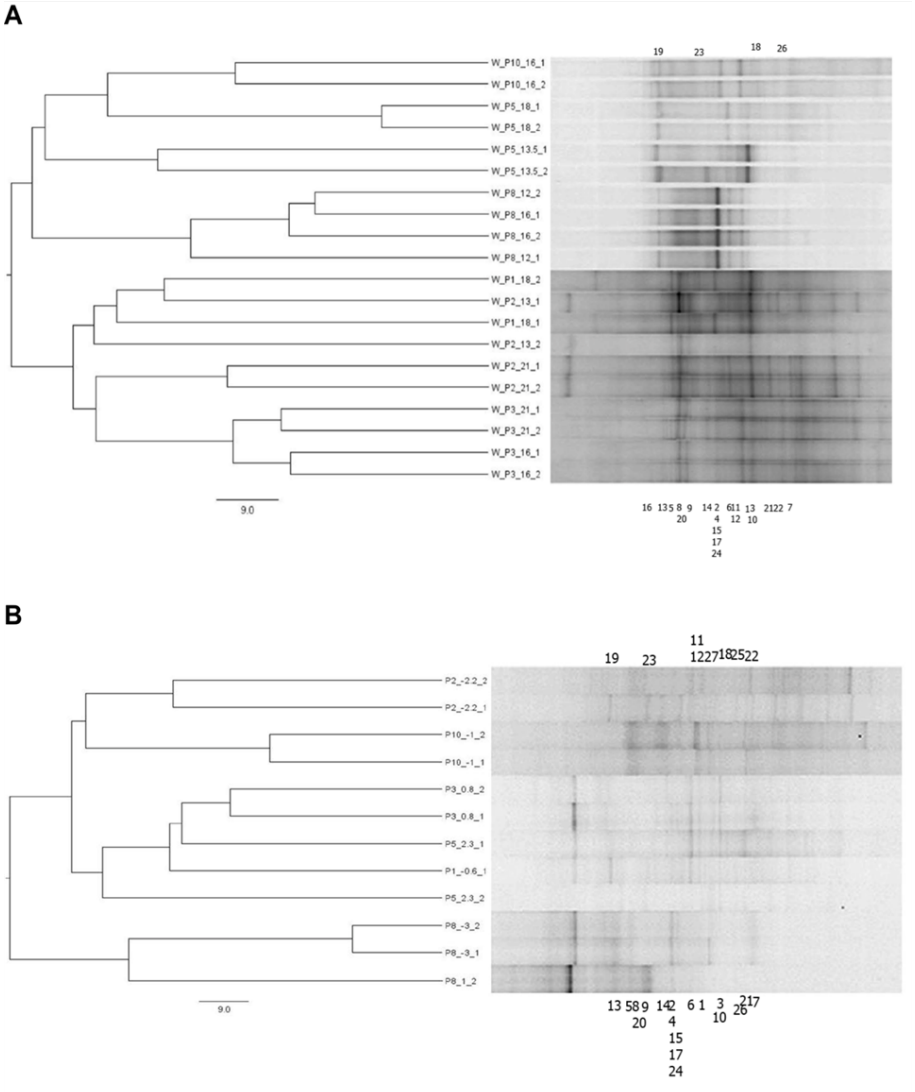

Figure 6. DGGE band patterns of bacterial 16S rRNA gene fragments and UPGMA cluster analysis for fingerprints obtained from wet (July 2014) (a) and dry (March 2015) (b) periods. Bar indicates 9% divergence. Each sample is defined by a code indicating piezometer number and sampling depth (see table 1). Black triangles indicate position of bands recovered and sequenced, and numbers correspond to their phylogenetic affiliation (see table S2 supplementary material)

Hydrol. Earth Syst. Sci. Discuss., https://doi.org/10.5194/hess-2018-174
Manuscript under review for journal Hydrol. Earth Syst. Sci.
Discussion started: 17 April 2018

Hydrology and Earth System Sciences
Discussions
Open Access
EGU

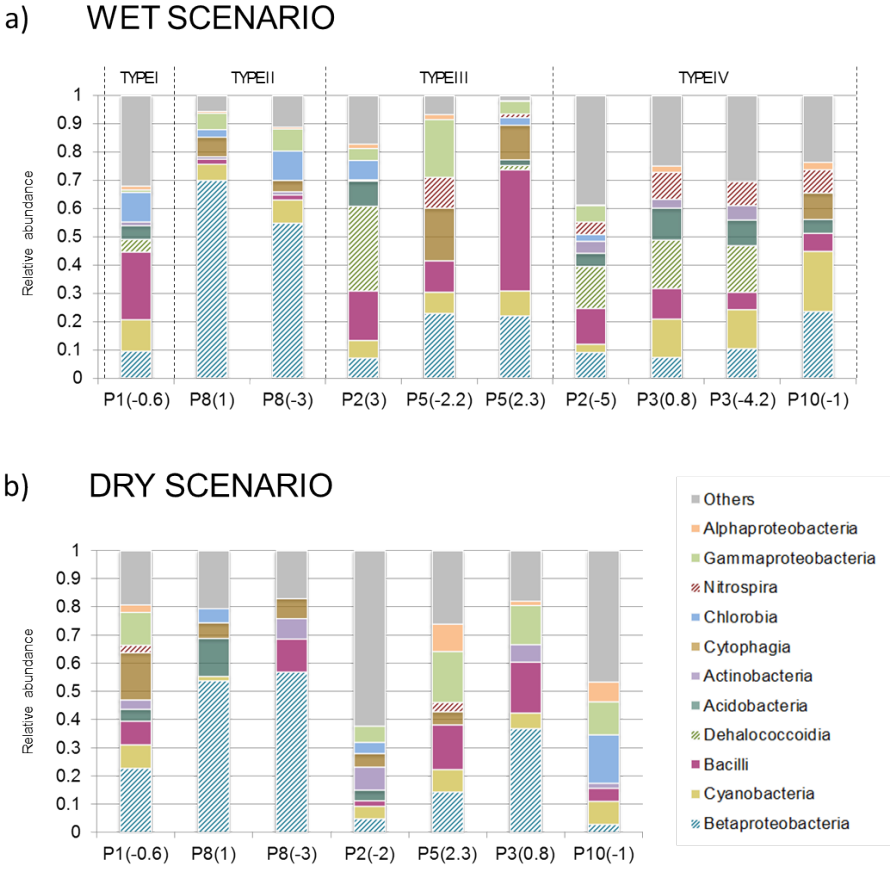

Figure 7. Bacterial community structure of groundwater samples. Class relative abundances calculated for wet (a) and dry (b) scenarios

Hydrol. Earth Syst. Sci. Discuss., https://doi.org/10.5194/hess-2018-174
Manuscript under review for journal Hydrol. Earth Syst. Sci.
Discussion started: 17 April 2018

Hydrology and Earth System Sciences
Discussions
Open Access
EGU

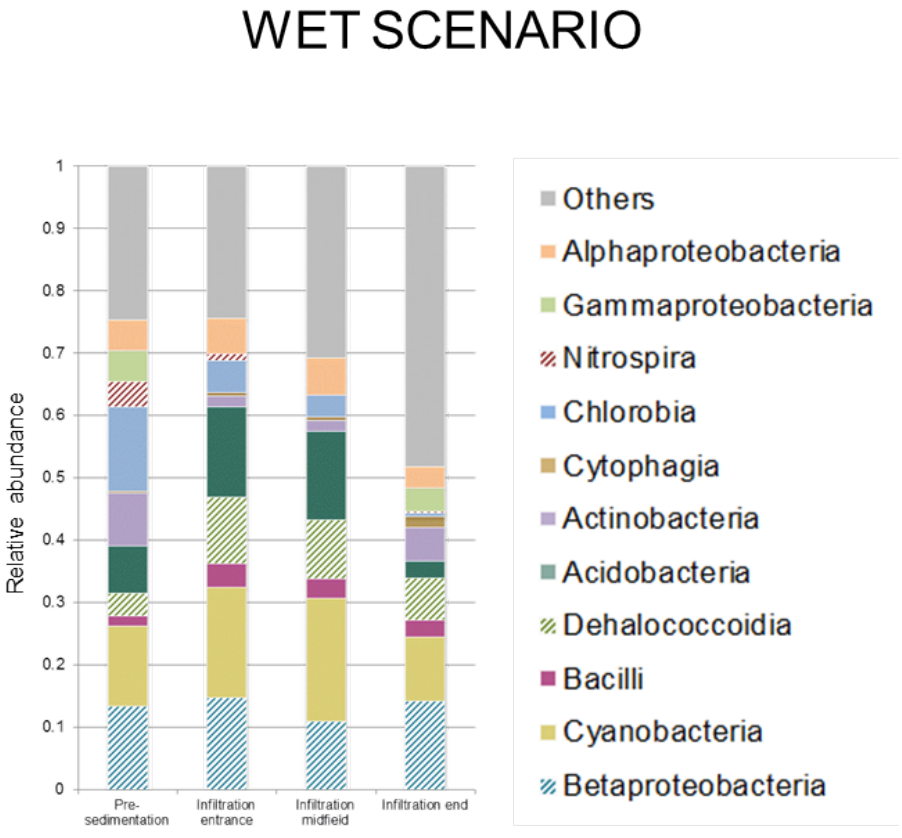

Figure 8. Bacterial community structure of soil samples from pre-sedimentation and infiltration basins. Class relative abundances calculated for wet (a) and dry (b) scenarios

Hydrol. Earth Syst. Sci. Discuss., https://doi.org/10.5194/hess-2018-174
Manuscript under review for journal Hydrol. Earth Syst. Sci.
Discussion started: 17 April 2018

Hydrology and Earth System Sciences
Discussions
Open Access
EGU

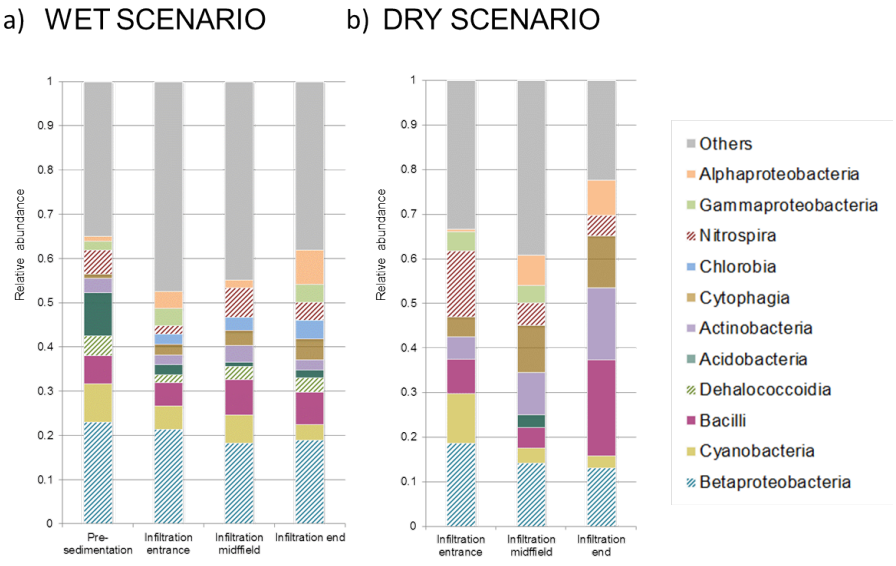

Figure 9. Bacterial community structure from water samples of pre-sedimentation and infiltration basins. Class relative abundance calculated for wet scenario

Hydrol. Earth Syst. Sci. Discuss., https://doi.org/10.5194/hess-2018-174
Manuscript under review for journal Hydrol. Earth Syst. Sci.
Discussion started: 17 April 2018

Hydrology and Earth System Sciences
Discussions
Open Access
EGU

Table 1. Summary of values of Shannon, Richness and Evenness indices at the Llobregat MAR site in different scenarios

Environment		Sampling location (**depth** *-masl-*)	Shannnon *(SD)**		Richness *(SD)**		E *(SD)**	
			WET	DRY	WET	DRY	WET	DRY
Groundwater	T.I	P1(**-0.6**)	2.57 *(0.04)*	2.73	22 *(4.1)*	19	0.61 *(0.01)*	0.64
	T.II	P8(**1**)	1.43 *(0.05)*	1.73	10 *(2.0)*	11	0.34 *(0.01)*	0.41
		P8(**-3**)	1.69 *(0.20)*	2.03 *(0.14)*	11	10 *(2.0)*	0.40 *(0.05)*	0.48 *(0.03)*
	T.III	P2(**3**)	2.29 *(0.13)*		18.5 *(7.2)*		0.54 *(0.03)*	
		P2(**-2**)		2.67 *(0.13)*		18 *(2.0)*		0.63 *(0.03)*
		P5(**2.3**)	1.91 *(0.01)*	2.41	14.5 *(1.0)*	14	0.45 *(1×10^{-3})*	0.56
		P5(**-2.2**)	2.22 *(0.01)*		12.5 *(1.0)*		0.52 *(2×10^{-3})*	
	T.IV	P3(**0.8**)	2.65 *(0.09)*	2.01 *(0.28)*	21	10.5 *(3.07)*	0.63 *(0.02)*	0.48 *(0.07)*
		P3(**-4.2**)	2.65 *(0.13)*		20		0.63 *(0.03)*	
		P2(**-5**)	2.80 *(0.12)*		23 *(4.1)*		0.66 *(0.12)*	
		P10(**-1**)	2.51 *(0.20)*	2.49 *(0.09)*	17	16 *(4.1)*	0.59 *(0.01)*	0.59 *(0.02)*
Water of basins		Pre-sedimentation	2.93 *(0.28)*		29 *(14.3)*		0.69 *(0.07)*	
		Infiltration entrance	2.78 *(0.53)*		28.5 *(17.4)*		0.66 *(0.12)*	
		Infiltration midfield	2.66 *(0.14)*		25.5 *(3.1)*		0.63 *(0.03)*	
		Infiltration end	2.58 *(0.08)*		24 *(2.0)*		0.61 *(0.02)*	
Soil of basins		Pre-sedimentation	2.89 *(0.16)*		25.5 *(7.2)*		0.68 *(0.04)*	
		Infiltration entrance	3.22 *(0.09)*	2.93 *(0.21)*	35.5 *(1.0)*	25 *(7.6)*	0.76 *(0.02)*	0.69 *(0.08)*
		Infiltration midfield	3.36 *(0.14)*	2.90 *(0.05)*	30.5 *(3.1)*	21	0.79 *(0.03)*	0.68 *(0.01)*
		Infiltration end	3.29 *(0.05)*	2.40 *(0.07)*	34 *(2.0)*	16	0.78 *(0.01)*	0.57 *(0.02)*

* Numbers in parenthesis after each index value indicate standard deviation, not reported whenever one replica was damaged.

Journal of Hydrology 561 (2018) 123–135

Contents lists available at ScienceDirect

Journal of Hydrology

journal homepage: www.elsevier.com/locate/jhydrol

Research papers

Monitoring induced denitrification during managed aquifer recharge in an infiltration pond

Alba Grau-Martínez [a,*], Albert Folch [b,c], Clara Torrentó [a,d], Cristina Valhondo [c,e], Carme Barba [b,c], Cristina Domènech [a], Albert Soler [a], Neus Otero [a,f]

[a] Grup de Mineralogia Aplicada i Geoquímica de Fluids, Departament de Mineralogia, Petrologia i Geologia Aplicada, SIMGEO UB-CSIC, Facultat de Ciències de la Terra, Universitat de Barcelona (UB), C/Martí i Franquès, s/n – 08028 Barcelona, Spain
[b] Department of Civil and Environmental Engineering (DECA), Universitat Politècnica de Catalunya (UPC), c/Jordi Girona 1-3, 08034 Barcelona, Spain
[c] Associated Unit: Hydrogeology Group (UPC-CSIC), Spain
[d] Centre for Hydrogeology and Geothermics, University of Neuchâtel, Rue Emile-Argand 11, 2000 Neuchâtel, Switzerland
[e] Institute of Environmental Assessment and Water Research (IDAEA), CSIC, c/Jordi Girona 18, 08034 Barcelona, Spain
[f] Serra Hunter Fellow, Generalitat de Catalunya, Spain

ARTICLE INFO

Article history:
Received 27 July 2017
Received in revised form 16 March 2018
Accepted 17 March 2018
Available online 28 March 2018
This manuscript was handled by "Corrado Corradini Editor-in-Chief, with the assistance of Jiin-Shuh Jean, Associate Editor

Keywords:
Nitrate reduction
Multi-isotope analysis
Reactive layer
Mixing zone
Artificial recharge
Field and laboratory experiments

ABSTRACT

Managed aquifer recharge (MAR) is a well-known technique for improving water quality and increasing groundwater resources. Denitrification (i.e. removal of nitrate) can be enhanced during MAR by coupling an artificial recharge pond with a permeable reactive layer (PRL). In this study, we examined the suitability of a multi-isotope approach for assessing the long-term effectiveness of enhancing denitrification in a PRL containing vegetal compost. Batch laboratory experiments confirmed that the PRL was still able to enhance denitrification two years after its installation in the infiltration pond. At the field scale, changes in redox indicators along a flow path and below the MAR-PRL system were monitored over 21 months during recharge and non-recharge periods. Results showed that the PRL was still releasing non-purgeable dissolved organic carbon five years after its installation. Nitrate concentration coupled with isotopic data collected from the piezometer network at the MAR system indicated that denitrification was occurring in the saturated zone immediately beneath the infiltration pond, where recharged water and native groundwater mix. Furthermore, longer operational periods of the MAR-PRL system increased denitrification extent. Multi-isotope analyses are therefore proved to be useful tools in identifying and quantifying denitrification in MAR-PRL systems.

1. Introduction

Increasing water demands with growing world population and potential water shortages require flexible management strategies to replenish aquifers. The artificial recharge of groundwater, commonly known as managed aquifer recharge (MAR), is becoming increasingly important all over the world as a sustainable way of protecting the quality and quantity of groundwater supplies (Bouwer, 2002; Dillon, 2004; Sprenger et al., 2017). Recharge ponds are one of the most commonly used approaches for MAR. This approach involves surface infiltration through spreading basins or ponds to introduce surface water into the subsurface environment (Bouwer, 2002; Miller et al., 2006).

Common sources of water for MAR in recharge ponds include wastewater effluents (after different stages of treatment) and effluent-receiving rivers (Díaz-Cruz and Barceló, 2008; Maeng et al., 2011), as well as river water and storm water runoff. These sources of water, mainly those from wastewater treatment plants (WWTPs), might contain high levels of ammonium (NH_4^+), whereas those resulting from agricultural activity might have high concentrations of nitrate (NO_3^-) (Schmidt et al., 2011). Furthermore, oxic conditions promote ammonium nitrification, transforming it to nitrate.

The chemical composition of the infiltrating water in MAR changes due to a combination of physical and biogeochemical processes as the water passes from unsaturated to saturated zones, where it mixes with native groundwater. In some circumstances, these changes can lead to an overall improvement in groundwater

* Corresponding author.
E-mail addresses: albagrau@ub.edu (A. Grau-Martínez), albert.folch.sancho@upc.edu (A. Folch), clara.torrento@ub.edu, clara.torrento@unine.ch (C. Torrentó), cristina.valhondo@upc.edu (C. Valhondo), carme.barba@upc.edu (C. Barba), cristina.domenech@ub.edu (C. Domènech), albertsoler@ub.edu (A. Soler), notero@ub.edu (N. Otero).

https://doi.org/10.1016/j.jhydrol.2018.03.044
0022-1694/

quality (Bouwer, 2002; Fox et al., 2006). Several studies have demonstrated that artificial recharge reduces the concentration of nutrients (Bekele et al., 2011), organic matter (Bekele et al., 2011; Vanderzalm et al., 2006), metals (Dillon et al., 2006; Bekele et al., 2011), pathogens (Dillon et al., 2006), organic contaminants (Dillon et al., 2006; Patterson et al., 2011) and pharmaceutically active compounds (PhACs) (Heberer et al. (2004); Valhondo et al., 2014, 2015). Massmann et al. (2006), investigated changes in redox conditions below an artificial recharge pond in Berlin, and found that the level of PhACs in groundwater was controlled by the transient hydraulic and hydrochemical conditions during artificial recharge. Thus, to increase the quality of recharge water and groundwater, the infiltration pond can be coupled to a permeable reactive layer (PRL), an organic reactive layer at the bottom of the pond (Valhondo et al., 2014, 2015, 2016) that promotes diverse redox conditions along the recharge path to enhance the degradation of pollutants.

NO_3^- is one of the most abundant pollutants in groundwater (Menció et al., 2016). Denitrification, a microbe-mediated process in which NO_3^- is converted into dinitrogen gas (N_2), is the main naturally occurring process that decreases NO_3^- concentration in groundwater. Dilution and dispersion also decrease groundwater nitrate concentration, but in contrast to denitrification, they do not lead to mass reduction of the contaminant within an aquifer. Denitrification is carried out by bacteria that use NO_3^- as the terminal electron acceptor when dissolved oxygen (DO), which is energetically more favorable, is unavailable (Knowles, 1982). Denitrification can be heterotrophic or autotrophic, depending on whether the substrate is organic or inorganic, respectively (Eqs. (1) and (2)).

$$5CH_2O + 4NO_3^- + 4H^+ \rightarrow 2N_2 + 5CO_2 + 7H_2O \quad (1)$$

$$5FeS_2 + 14NO_3^- + 4H^+ \rightarrow 7N_2 + 10SO_4^{2-} + 5Fe^{2+} + 2H_2O \quad (2)$$

Denitrification can be enhanced in MAR-PRL pond systems, since adequate residence time and the presence of easily degradable organic carbon promote the activity of heterotrophic denitrifying bacteria. Recent laboratory studies (Grau-Martínez et al., 2017; Gibert et al., 2008) have suggested that low-cost carbon-releasing materials like organic compost, palm tree leaves and wood by-products could induce denitrification. Promoting denitrification by using a reactive layer in a recharge pond requires control mechanisms to test the efficacy of the implemented materials at the field scale.

Multi-isotope analysis, coupled with chemical data, is useful for identifying and even quantifying denitrification processes in aquifers (Mariotti et al., 1988; Aravena and Robertson, 1998; Pauwels et al., 2000; among others). Denitrification affects the isotope composition of the residual nitrate, resulting in increased levels of the heavy isotopes ^{15}N and ^{18}O (Mariotti et al., 1988; Aravena and Robertson, 1998; Fukada et al., 2003; Kendall et al., 2007). This change in isotope composition, or isotope fractionation (ε), distinguishes denitrification at the field scale from other processes such as dilution, which can also decrease NO_3^- concentration, but without changing its isotopic value (Clark and Fritz, 1997; Kendall et al., 2007).

Isotopic studies coupled with chemical data are an effective tool to identify and describe denitrification (Aravena and Robertson, 1998; Pauwels et al., 1998, 2000, 2010; Kendall et al., 2007; Otero et al., 2009; among others). Furthermore, multi-isotopic studies of the solutes involved in denitrification reactions, such as $\delta^{34}S$ and $\delta^{18}O$ of dissolved sulfate and $\delta^{13}C$ of dissolved inorganic carbon, can help determining whether denitrification is promoted by heterotrophic or autotrophic bacteria and identifying the occurrence of secondary processes such as SO_4^{2-} reduction (Mariotti et al., 1988). Schmidt et al. (2011), Schmidt et al. (2012) used nitrate isotope ratios to demonstrate the occurrence of denitrification in the infiltrating water during its passage through the first meter of the soil beneath the base of a MAR pond in central coastal California.

In the present work, we monitored denitrification processes in a MAR-PRL system located at Sant Vicenç dels Horts, Barcelona, Spain (Valhondo et al., 2014, 2015, 2016, 2018), which has a layer of vegetal compost at the bottom of the infiltration pond. The aim of the present study is to test the usefulness of a combined isotope analysis and depth specific hydrochemical data to: (i) assess the long-term effectiveness of the reactive layer in promoting denitrification 5 years after its installation; (ii) identify the denitrification processes occurring at different aquifer depths and locations along the saturated zone below the infiltration pond (including the mixing zone between recharge and native groundwater). The methods tested here can be applied in other sites to assess the efficacy of MAR ponds coupled to reactive layer PRL in promoting denitrification.

2. Materials and methods

2.1. Study site description

The field site studied is located 15 km inland from the Mediterranean coast, in the lower valley of the Llobregat Delta (Catalonia, NE Spain). This area is characterized by a Mediterranean climate, with average annual precipitation around 590 mm. Precipitation is scarce in winter and summer (monthly average of 37 mm) and more frequent during spring (monthly average of 41 mm) and especially autumn (monthly average 77 mm). The aquifer consists of Quaternary alluvial sediments, mainly coarse gravel and sand with small clay lenses (Iribar et al., 1997). The minerals present include quartz, calcite and dolomite, and the solid phase fraction of organic carbon is less than 0.002 (g_{OC}/g_{soil}) (Barbieri et al., 2011). At this location, the aquifer extends to a depth of 23 to 27 m underground (Valhondo et al., 2014) and is located between 5 and 10 m below the Llobregat river bed, the river and aquifer thus being hydraulically disconnected (Vàzquez-Suñé et al., 2007). The regional groundwater flow direction is from NNW to SSE (Quevauviller et al., 2009), with a natural hydraulic gradient of 2.3‰. Previous pumping tests determined the hydraulic parameters to be 1.4×10^4 m^2 day^{-1} for transmissivity and 0.03 for storage coefficient (Barahona-Palomo et al., 2011).

Groundwater is artificially recharged by infiltrating water from the Llobregat River via a system of pipes and ponds. The river water is collected approximately 2 km upstream of the MAR system (Molins de Rei inlet) and flows by gravity through a concrete pipe to a decantation pond (≈4000 m^2). By the time the river reaches the capture point, it has received treated water from more than 50 wastewater treatment plants (Köck-Schulmeyer et al., 2011). In the decantation pond, the sediments are allowed to settle for approximately 2–4 days before the water is transferred by a concrete pipe to an infiltration pond (≈5000 m^2) (Fig. 1). The infiltration rate in the infiltration pond ranges from 0.5 to 2 m d^{-1}, whereas insignificant water infiltration occurs in the decantation pond (Valhondo et al., 2014).

A reactive layer was installed at the bottom of the infiltration pond in 2011 to create favorable conditions for the biodegradation of the contaminants present in the infiltration water. The reactive layer (≈65 cm thick) consists of aquifer sand (49.5% in volume), vegetal compost from gardens and scrap wood (49.5%), clay (≤1%) and iron oxide dust (≤0.1%). The components were mixed on site with an excavator until homogeneity was visually evident. The layer was covered with approximately 5 cm of sand to prevent the woody material from floating away. The compost in the

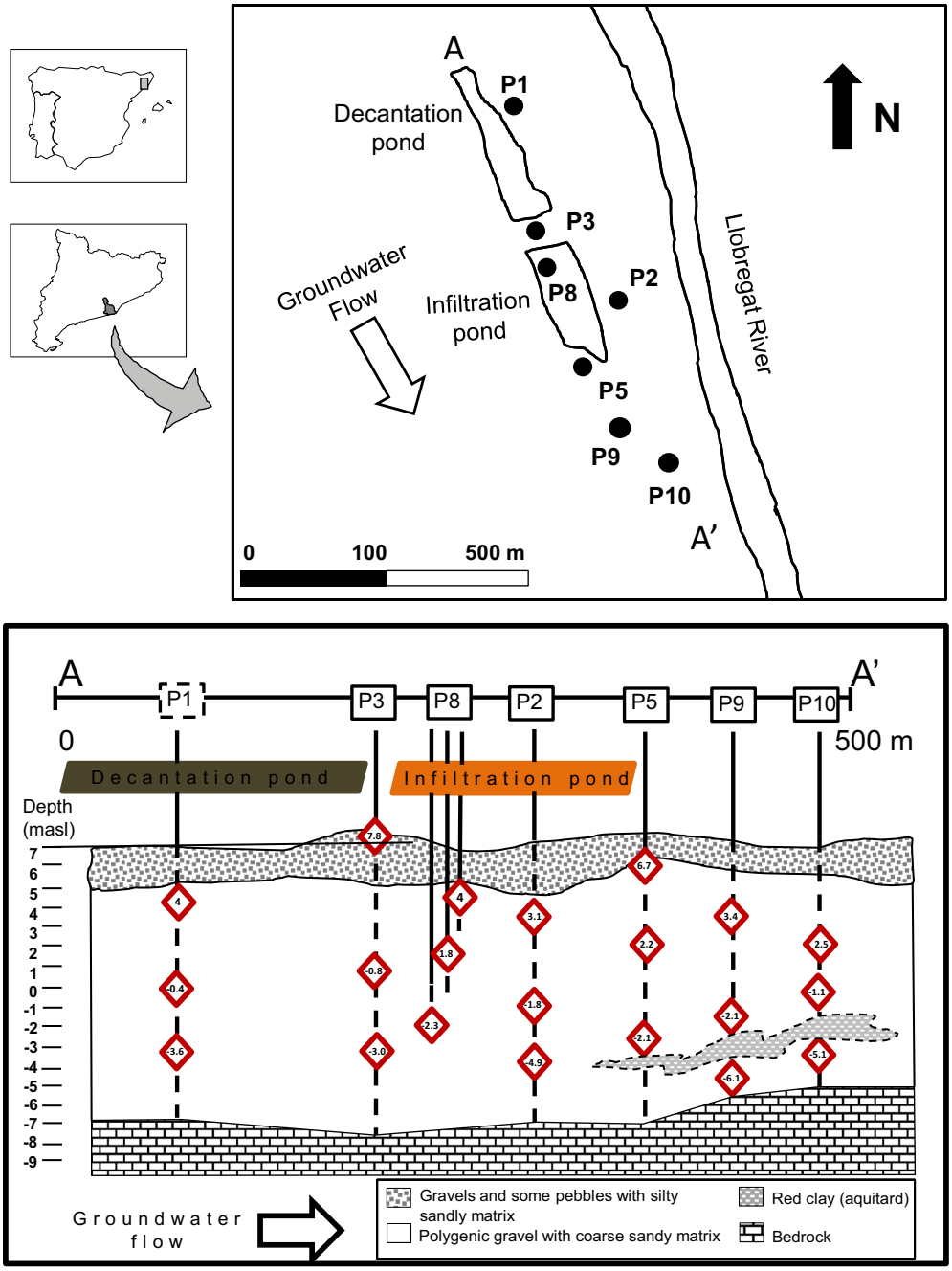

Fig. 1. Upper panel: Schematic location and plan view of the Sant Vicenç dels Horts recharge system. Lower panel: Cross-section of the transect A–A'. The red diamonds show the sampling depths. (For interpretation of the references to colour in this figure legend, the reader is referred to the web version of this article.)

reactive layer was added to promote microbial growth and redox conditions by providing organic matter to the infiltration water. The sand was added to provide structural integrity to the layer and guarantee high hydraulic conductivity. Finally, iron oxides and clay, consisting mainly of illite (33 wt%), smectite (16 wt%) and chlorite (9 wt%), were present to provide extra sorption capacity for cationic and anionic contaminants (Valhondo et al., 2014).

The MAR pond undergoes two main operational periods: (1) recharge periods (RPs), with continuous flow from the river to the pond (infiltration water is mainly river water with less than 1.5% contribution from precipitation on average) and (2) non-recharge periods (NRPs), when the pond is dried for operational redevelopment and/or when the infiltration is stopped because the quality of the river water is low. During recharge periods, total saturation conditions are not obtained (Valhondo et al., 2015, 2016).

NRPs are implemented when the control parameters of the infiltration water are exceeded, such as when NH_4^+ concentrations are higher than 1.5 mg L^{-1}, electrical conductivity (EC) is higher than 2000 μS cm^{-1}, river turbidity is greater than 100 NTU and input water turbidity exceeds 25 NTU. NRPs are also implemented when the clogged layer needs to be removed or the upper layer of sand has to be cleaned. During NRPs, the groundwater table declines and the bottom of the pond is exposed to the atmosphere.

A piezometric network consisting of seven piezometers was installed around the recharge MAR system (Fig. 1). Piezometer P1 (screened from 6 to 24 m) is located upstream of the infiltration pond and was used to monitor background groundwater. P3

(screened from 5 to 23 m) is located upstream of the infiltration pond, between the decantation and infiltration ponds, while P8 is located in the middle of the infiltration pond and is composed of three piezometers screened at different depths (P8.1 from 13 to 15 m, P8.2 from 10 to 12 m and P8.3 from 7 to 9 m). P8.3 was used to evaluate the behavior of the infiltration water through the vadose zone, while P8.1 was used to monitor the recharge at the deepest point of the saturated zone. P2 (completely screened from 6 to 24 m) and P5 (screened from 5 to 21 m) are situated downstream, at the edge of the infiltration pond. Additionally, P9 (screened from 9 to 24 m) and P10 (screened from 6 to 20 m) are located 190 m and 200 m downstream of the infiltration pond, respectively. Therefore, all the monitoring points, except P1 (native groundwater) and P8.3 (infiltration water just after crossing the vadose zone), represent different ratios of recharge water to native groundwater in the aquifer at different travel times. Travel time of the infiltration water from the pond to the piezometers is around 18 to 24 h for P8.3, nearly 2 days for P2 and P5, 10 days for P10 and P8.1, and more than 20 days for P9 (Valhondo et al., 2014, 2016).

2.2. Sampling surveys

To assess the long-term effectiveness of the PRL, four sampling campaigns were performed using the seven piezometers (Fig. 1) to evaluate nitrate removal under different operational conditions in June 2013, September 2013, July 2014 and March 2015. The monitored period started 5 years after the installation of the PRL. The June 2013 and July 2014 campaigns were performed during RPs, and the other two during NRPs. Fig. 2 shows the distribution along time of the operational periods and the sampling campaigns. The system was under RPs for a total of 222 days in 2013 and 213 days in 2014. In 2015, before the March 2015 campaign, the system was under NRPs for almost four months, whereas only two months of non-recharge had occurred before the September 2013 campaign.

Sampling was carried out using depth-specific samplers (bailers). Bailers are considered suitable for measuring groundwater nitrate concentration (Lasagna and De Luca, 2016). Each piezometer was sampled at three different depths (Fig. 1), which were selected according to the stratigraphic profiles. A layer with high transmissivity was identified in the middle depth of all the piezometers. This layer is composed of polygenic gravel and large-sized gravel with medium fine sandy matrix. Although some sampling protocols (ENSAT, 2012) do not deem it necessary to purge piezometers in aquifers with high transmissivity such as that of Sant Vicenç dels Horts (1.4×10^4 m^2 day^{-1}), we still purged the piezometers prior to sampling by removing well water three times at each specific depth. During the four sampling campaigns, samples from the Llobregat River were also collected, sometimes more than once on the same day.

Physicochemical parameters (pH, temperature (T) and EC) were measured *in situ*, using a Multi 3410 multi-parameter (WTW, Weilheim, Germany). Samples for measuring major cations were filtered through 0.2-μm Millipore® filters, preserved by the addition of 1% HNO_3^- and stored in polyethylene bottles at 4 °C until analysis. Samples for the analysis of major anions (Cl^-, NO_3^-, NO_2^- and SO_4^{2-}) and isotope ratios ($\delta^{15}N_{NO3}$, $\delta^{18}O_{NO3}$, $\delta^{34}S_{SO4}$, $\delta^{18}O_{SO4}$ and $\delta^{13}C_{HCO3}$) were filtered through 0.2-μm Millipore® filters and stored in polyethylene bottles. Samples for measuring NO_3^- isotopes were kept frozen until analysis, while those for $\delta^{18}O_{H2O}$ and $\delta^{2}H_{H2O}$ measurements were collected in glass flasks and filtered through 0.45-μm Millipore® filters. For isotope analyses, samples were taken only from the middle depth of each piezometer. Samples for the analysis of non-purgeable dissolved organic carbon (NPDOC) were collected in muffled (450 °C, 4.5 h) glass bottles, filtered through 0.45-μm Millipore® filters, acidified to pH 3 with hydrochloric acid and stored at 4 °C until analysis. To measure dissolved inorganic carbon (DIC), samples were collected in glass bottles, filtered through 0.45-μm Millipore® filters and analyzed within a day.

2.3. Laboratory experiments

Batch experiments were performed with material extracted in 2013 from the PRL of the MAR pond system. The substrate was used within a few hours after extraction without any pretreatment. Experiments were performed in triplicate, using 20 g of the PRL material and 400 mL of groundwater from the Llobregat aquifer (from P2) spiked with 0.80 mM of NO_3^- to evaluate the denitrification potential of the vegetal compost. The experiments were run in sterilized 500-mL glass bottles previously purged with N_2 for 15 min in a glove box in an argon atmosphere to minimize

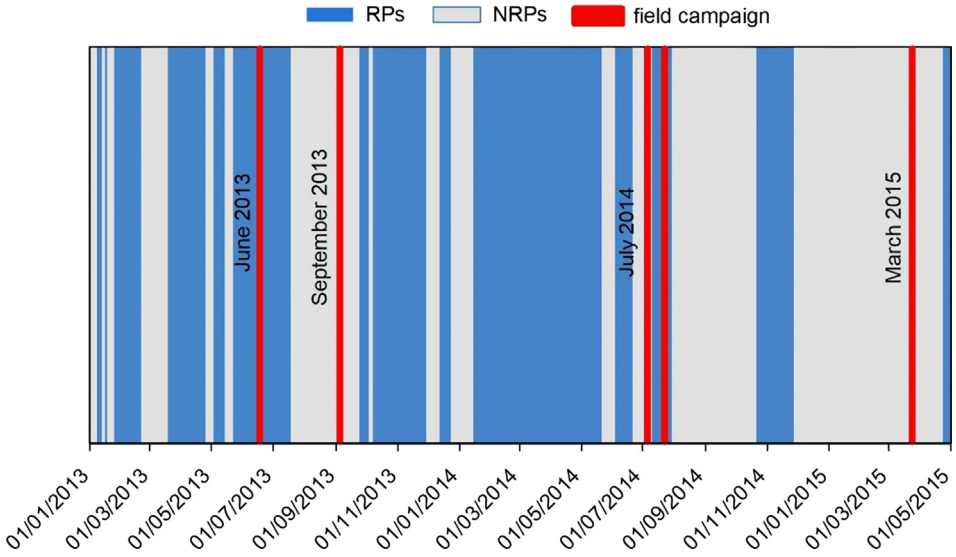

Fig. 2. Operational periods of the Sant Vicenç dels Horts MAR-PRL system between January 2013 and May 2015: recharge periods (RPs, blue) and non-recharge periods (NRPs, grey). The four sampling campaigns are also shown (red bars). (For interpretation of the references to colour in this figure legend, the reader is referred to the web version of this article.)

the O_2 level. Experimental oxygen partial pressure in the glove box was maintained between 0.1 and 0.3% O_2 and continuously monitored using an oxygen partial pressure detector (Sensotran, Gasvisor 6) with an accuracy of ±0.1% O_2. Batch experiments were manually shaken once a day and aqueous samples (5 mL) were collected daily using sterilized syringes. A ratio of solution/solid material at 90% of the initial value was maintained.

The experiments were performed to check the reactivity of the extracted material and also to estimate the isotopic fractionation (ε) of N and O.

The NO_3^- pseudo-first order degradation rate constants (k') were calculated using Eq. (3), where C_0 and C_t are the initial NO_3^- concentration and the NO_3^- concentration at time t, respectively.

$$C_t = C_0 e^{-kt} \quad (3)$$

Isotopic fractionation during denitrification can be expressed as a Rayleigh distillation process Eq. (4), from which the isotopic fractionation factor (α) can be obtained (Mariotti et al., 1988; Aravena and Robertson, 1998).

$$\ln\left(\frac{R_t}{R_0}\right) = (\alpha - 1) ln\left(\frac{C_t}{C_0}\right) \quad (4)$$

where C_0 and C_t are the initial and residual NO_3^- concentration, respectively (mmol L^{-1}), and R_o and R_t denote the ratios of heavy to light isotopes at the initial time and time t, respectively, which are calculated according to Eq. (5).

$$R = \left[\left(\frac{\delta}{1000}\right) + 1\right] \quad (5)$$

where δ is the isotopic composition of $\delta^{15}N$ and $\delta^{18}O$ (‰). The term (α -1) was calculated from the slope of the regression line in the double-logarithmic plots $[\ln(R_t/R_0)]$ vs. $[\ln(C_t/C_0)]$, according to Eq. (5), and converted into isotope fractionation (εN and εO) following Eq. (6).

$$\varepsilon = 1000 \times (\alpha - 1) \quad (6)$$

The Rayleigh equation applies to closed system conditions; therefore, isotopic fractionation is commonly calculated in laboratory experiments where conditions are wells constrained, no other sinks affect the NO_3^- pool and the concentration and isotopic composition of NO_3^- can be considered exclusively determined by NO_3^- reduction.

2.4. Analytical methods

Concentrations of major anions (Cl^-, NO_2^-, NO_3^-, and SO_4^{2-}) were determined by high performance liquid chromatography (HPLC) using a WATERS 515 HPLC pump, an IC-PAC anions column and a WATERS 432 detector. Cation concentrations were determined by inductively coupled plasma-optical emission spectrometry (ICP-OES, Perkin-Elmer Optima 3200 RL). NPDOC was measured by organic matter combustion using a MULTI N/C 3100 Analytik Jena carbon analyzer. DIC concentrations were analyzed by titration (METROHM 702 SM Titrino). Chemical analyses were conducted at the "Centres Científics i Tecnològics" of the University of Barcelona (CCiT-UB).

The $\delta^{15}N$ and $\delta^{18}O$ of dissolved NO_3^- were measured using a modified cadmium reduction method of McIlvin and Altabet (2005) and Ryabenko et al. (2009). Briefly, NO_3^- was converted into nitrite through a spongy cadmium reduction and then to nitrous oxide using sodium azide in an acetic acid buffer. Simultaneous $\delta^{15}N$ and $\delta^{18}O$ analysis of the N_2O produced was carried out with a PreCon system (Thermo Scientific) coupled to a Finnigan MAT-253 Isotope Ratio Mass Spectrometer (IRMS, Thermo Scientific). For $\delta^{34}S$ and $\delta^{18}O$ analyses, dissolved SO_4^{2-} was precipitated as $BaSO_4$ by adding $BaCl_2$ after acidifying the sample with HCl and boiling it to prevent $BaCO_3$ precipitation, following standard methods (Dogramaci et al., 2001). $\delta^{34}S$ was analyzed with a Carlo Erba elemental analyzer (EA)-Finnigan Delta C IRMS, while $\delta^{18}O$ was analyzed in duplicate with a ThermoQuest high temperature conversion EA (TC/EA) coupled in continuous flow with a Finnigan MAT Delta C IRMS. For $\delta^{13}C_{DIC}$ analysis, carbonates were precipitated by adding a NaOH-$BaCl_2$ solution and isotope ratio was measured on a Gas-Bench II-MAT-253 IRMS (Thermo Scientific). δ^2H_{H2O} and $\delta^{18}O_{H2O}$ were analyzed by Wavelength-Scanned Cavity Ring-down Spectroscopy (WS-CRDS) using L2120-i Picarro®. Total C, total N, $\delta^{15}N$ and $\delta^{13}C$ from the PRL material were measured using Carbo Erba EA-Finnigan Delta C IRMS. Isotope ratios were calculated using both international and internal laboratory standards. Notation was expressed in terms of δ relative to the international standards (V-SMOW for $\delta^{18}O$ and δ^2H, atmospheric N_2 for $\delta^{15}N$, V-CDT for $\delta^{34}S$ and V-PDB for $\delta^{13}C$). The reproducibility of the samples was ±1‰ for the $\delta^{15}N$ of NO_3, ±1.5‰ for the $\delta^{18}O$ of NO_3^-, ±0.2‰ for the $\delta^{34}S$ of SO_4^{2-}, ±0.5‰ for the $\delta^{18}O$ of SO_4^{2-}, ±0.2‰ for the $\delta^{13}C$ of DIC, ±0.2‰ for the $\delta^{18}O$ of H_2O and ±1‰ for the δ^2H of H_2O. Samples for isotopic analyses were prepared at the "Mineralogia Aplicada i Geoquímica de Fluids" laboratory and analyzed at CCiT-UB, except water isotopes, which were analyzed at the University of Málaga.

3. Results and discussion

3.1. Laboratory experiments

Total N and C content as well as the $\delta^{15}N$ and $\delta^{13}C$ of the reactive layer material are shown in the Supplementary Material (Table S1). Results of the chemical and isotopic characterization of the batch experiments are detailed in the Supplementary Material (Table S2).

Complete NO_3^- reduction was achieved within eleven days in the batch experiments (Fig. 3), with a slight transient increase in NO_2^- concentration (up to 0.07 mM). Nitrate reduction in previous batch experiments performed with fresh commercial compost was accompanied by a significant initial release of NO_3^- (up to 2.5 mM) and transient NO_2^- production (up to 0.12 mM) (Grau-Martínez et al., 2017). By comparison, the compost used in the present batch experiments, extracted from the PRL two years after its installation, did not release NO_3^- and produced a lower increase in NO_2^- concentration.

Denitrification in both sets of batch experiments followed pseudo-first-order kinetics and an initial lag phase of 6–7 days with a lower degradation rate was observed. The observed k' values were 0.21 ± 0.01 and 0.83 ± 0.06 d^{-1} with the PRL material and 0.17 ± 0.02 and 0.67 ± 0.01 d^{-1} with the fresh compost for the lag and main phases, respectively. Although highly similar, degradation rates were slightly higher for the PRL material than for the fresh compost. These results demonstrated that the compost from the PRL still had denitrification potential two years after its installation.

The isotopic fractionations obtained were −10.4‰ for εN and −13.8‰ for εO, with a εN/εO ratio of 0.75 (Fig. 4a and b). The εN and εO values obtained in this study were similar to those from previous laboratory experiments using fresh commercial compost (εN = −10.8‰ and εO = −9.0‰ Grau-Martínez et al., 2017), also falling within the range of laboratory values for heterotrophic denitrification reported in the literature (from -8.6‰ to -16.2‰ for εN and from −4‰ to −13.8‰ for εO (Knöller et al., 2011; Carrey et al., 2013)).

The obtained C and N isotope fractionations associated with denitrification induced by the two-year-old PRL material enables a more accurate quantification of the enhanced reduction in NO_3^- levels in the aquifer.

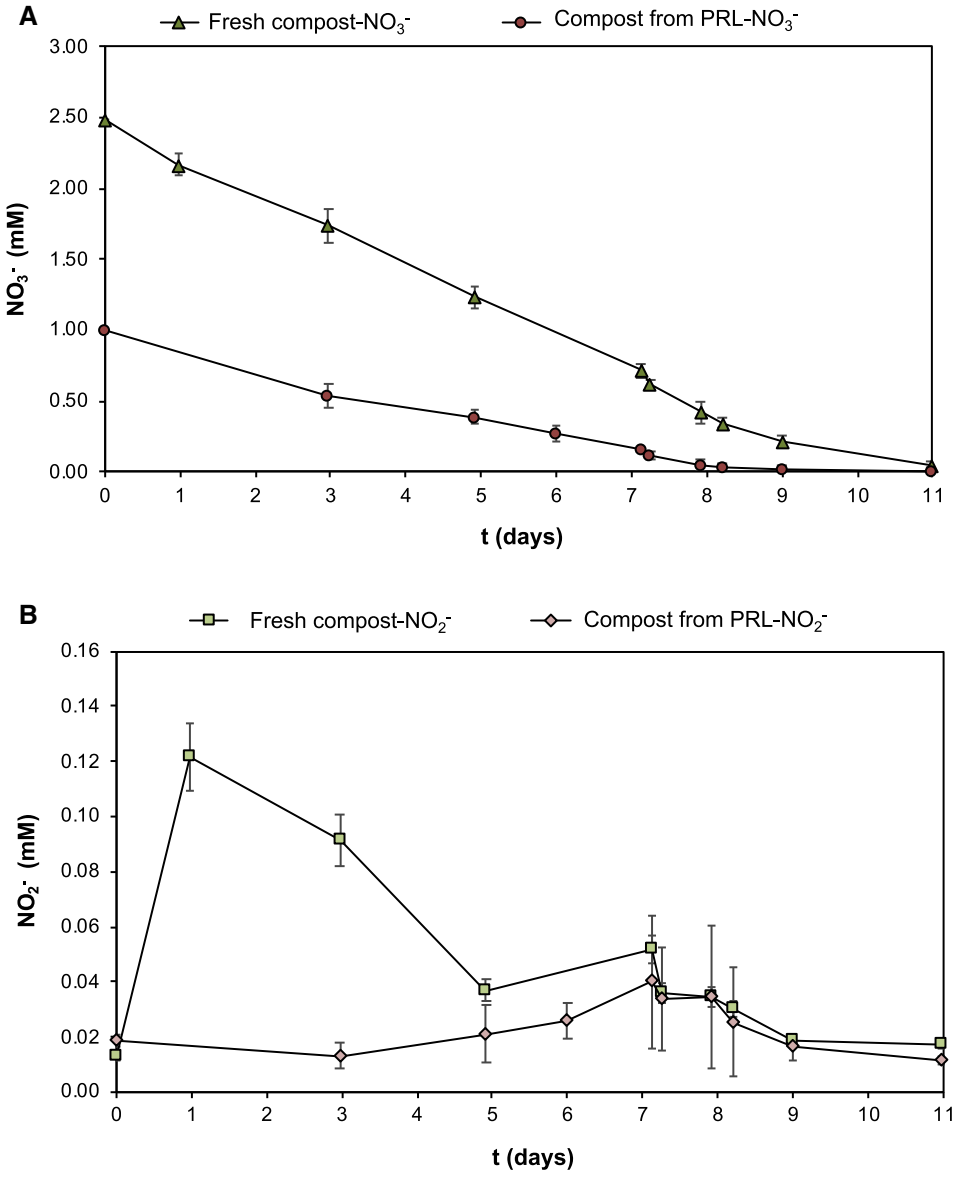

Fig. 3. Changes in NO_3^- (A) and NO_2^- (B) concentrations over time in the batch experiments with compost extracted from the PRL (two-year-old reactive layer). Results of previous batch experiments with fresh commercial compost (Grau-Martínez et al., 2017) are also shown for comparison. Values and error bars represent the mean and standard deviation, respectively, for the experiments performed in triplicate.

3.2. Field study

3.2.1. Hydrochemical characterisation

Results of the chemical characterization of the field samples are detailed in the Supplementary Material (Table S3). For all the analyzed samples, pH values ranged between 6.98 and 7.60, HCO_3^- concentrations between 223 and 408 mg L^{-1} and EC from 991 to 1653 µS cm^{-1}. There were no significant differences in the concentrations of major cations between the piezometers among the four sampling campaigns.

Groundwater underneath the infiltration pond can be considered a mixture of recharge water and native groundwater. Samples clustered in the HCO_3-Cl-Ca-Na hydrochemical facies, with negligible differences among the sampling campaigns (Fig. S1).

3.2.2. Sources of groundwater recharge

Results of the isotopic characterization of the field samples are detailed in the Supplementary Material (Table S4). δ^2H and $\delta^{18}O$ values of the infiltration water (river water) and groundwater sampled during RPs (June 2013 and July 2014) mostly plotted along the Local Meteoric Water Line (LMWL) (Fig. 5). The LMWL was calculated with data from the Global Network of Isotopes in Precipitation (GNIP) obtained from stations 0,818,001 and 0,818,002 in Barcelona (IAEA/WMO, 2017). Isotope ratios are lower than the weighted mean long-term isotopic composition of precipitation in Barcelona ($\delta^2H = -31.16‰$, $\delta^{18}O = -5.3‰$), but in agreement with the values obtained with the surface water of the Lower end of the Llobregat River (Otero et al., 2008) and samples from the Llobregat aquifer (Solà, 2009). The results confirmed that river water is the main source of recharge in the aquifer and indicate that evaporation is not an important process in the pond and/or the unsaturated zone. Lastly, the range of δ^2H and $\delta^{18}O$ values showed that only one recharge flow system is involved in the aquifer recharge. Accordingly, Valhondo et al. (2015) using electrical conductivity and 1,1,2-trichloroethane content as tracers, estimated the contribution of the infiltration water on the monitoring

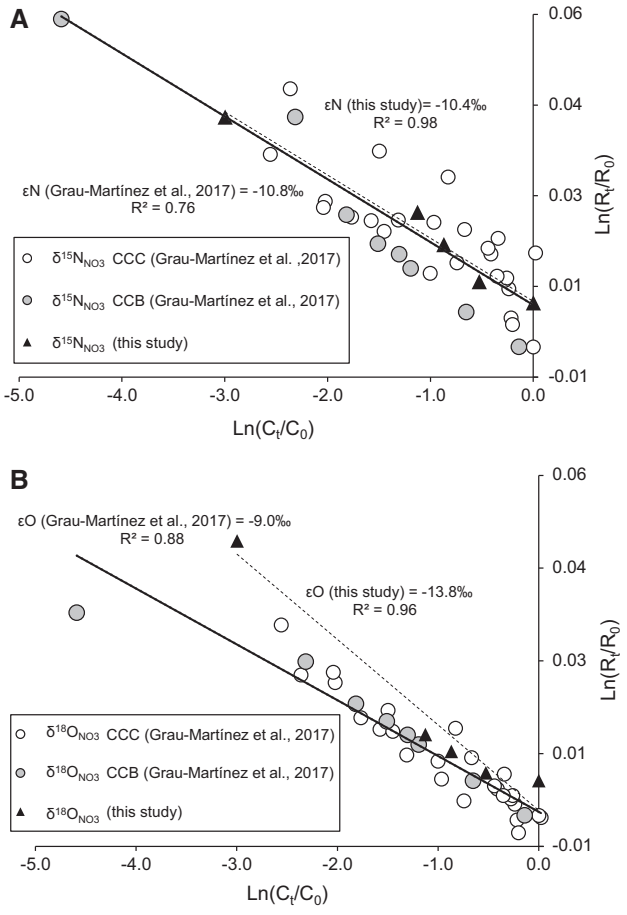

Fig. 4. N (A) and O (B) isotope results of the batch experiments performed with the two-year-old PRL material. Slopes of the regression lines represent (α-1) for N and O. Results of previous batch experiments with fresh commercial compost (Grau-Martínez et al., 2017) are also shown for comparison.

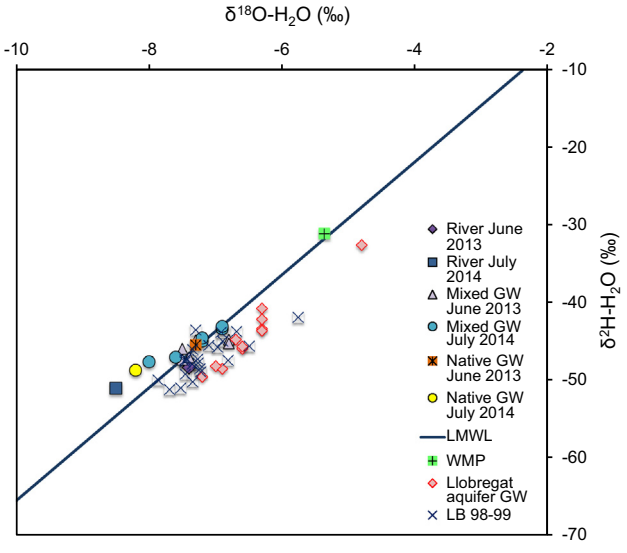

Fig. 5. $\delta^{18}O$-H_2O vs. $\delta^{2}H$-H_2O of samples collected in June 2013 (RP) and July 2014 (RP) from the Llobregat River, native groundwater (P1) and mixed groundwater (all the piezometers, except P1). The Local Meteoric Water Line (LMWL) and weighted mean precipitation (WMP) are also shown, as well as the groundwater samples from the Llobregat aquifer collected in an area close to the MAR pond ("Llobregat aquifer", Solà, 2009) and Llobregat river samples collected in 1998–1999 ("LB", Otero et al., 2008).

points and showed that samples collected in P2, P5, P8.3 and P10 comprised primarily infiltrated water, whereas wells P8.2, P8.1 and P9 displayed a mixture of infiltration water and local groundwater (P1), although the concentrations were closer to the infiltration water composition.

3.3. Changes in redox sensitive indicators

The evolution of the concentration of NO_3^- and NPDOC in the saturated zone along the flow path, during both RPs and NRPs, is shown in Fig.6. The results of major anions (Cl^-, SO_4^{2-}, HCO_3^-) are shown in the Supplementary Material (Fig. S2).

For assessing the effect of MAR, the chemical composition of groundwater collected upstream of the infiltration pond (P1, which represents native groundwater not affected by the recharge) was compared to that of the piezometers affected by recharge water. The concentrations of major anions in P1 samples remained almost constant with depth and time (Fig. S2). The influence of river water is clearly observed in the piezometers located closer to the infiltration pond (P8, P2 and P5) during RP and to a lesser extent during NRPs. Piezometers located furthest from the infiltration pond (P9 and P10) are less influenced by river water chemistry. Overall, no significant changes with depth were observed during both RP and NRPs.

NPDOC concentrations at the piezometers downstream of the infiltration pond generally ranged between those for native groundwater and those for river water (Fig.6) during both RP and NRP, being generally lower during NRPs. Higher NPDOC concentrations were detected in some samples (e.g. P2 in July 2014, P3 and P8 in September 2013, P8 in March 2015). These results suggest that the reactive layer was still releasing NPDOC five years after installation. Average higher NPDOC concentration was detected in September 2013 (two months of non-recharge before sampling) than in March 2015 (four months of non-recharge before sampling), indicating that the duration of recharge conditions had a significant effect.

NO_3^- concentration (measured as mg of NO_3^- L^{-1}) in native groundwater (P1) ranged from 4.2 to 9.8 mg L^{-1} with a median value of 5.6 (Table S3). Additional river water data show NO_3^- contents between 4.5 and 17.4 mg L^{-1} (Table S5). It should be noted that NO_3^- and NH_4^+ concentrations vary considerably in rivers with effluents from WWTPs, even among samples collected on the same day. During the RPs a significant decrease in NO_3^- concentration was observed in the piezometers located close to the infiltration pond (P2 and P5), especially in the June 2013 sampling, which showed complete NO_3^- reduction at some depths highlighting the ability of the MAR-PRL system to enhance nitrate reduction (Fig. 6). During the July 2014 RP, a decrease in NO_3^- concentration was also observed downstream of the pond but to a lesser extent. During NRPs, NO_3^- concentrations at the downstream piezometers were generally within native groundwater and river water samples, although slightly lower NO_3^- concentrations were seldom detected suggesting that NO_3^- reduction was maintained to some extent.

Fe concentrations in samples downstream of the infiltration pond were generally lower than that in the native groundwater (P1) (Table S3). No significant variations between the sampling campaigns were observed (values ranged from 0.2 to 1.0 μM), except for an important increase at P5 during the June 2013 RP (up to 3.7 μM) probably arising from more reducing conditions occurring. The solubility of Fe(III)-oxyhydroxides, which usually affects Fe concentration in groundwater, increases under more reducing conditions, thereby increasing aqueous Fe concentration.

Overall, the observed changes in redox indicators suggested that the PRL installed in 2011 was still releasing organic matter and promoting reducing conditions to varying extents below the infiltration pond.

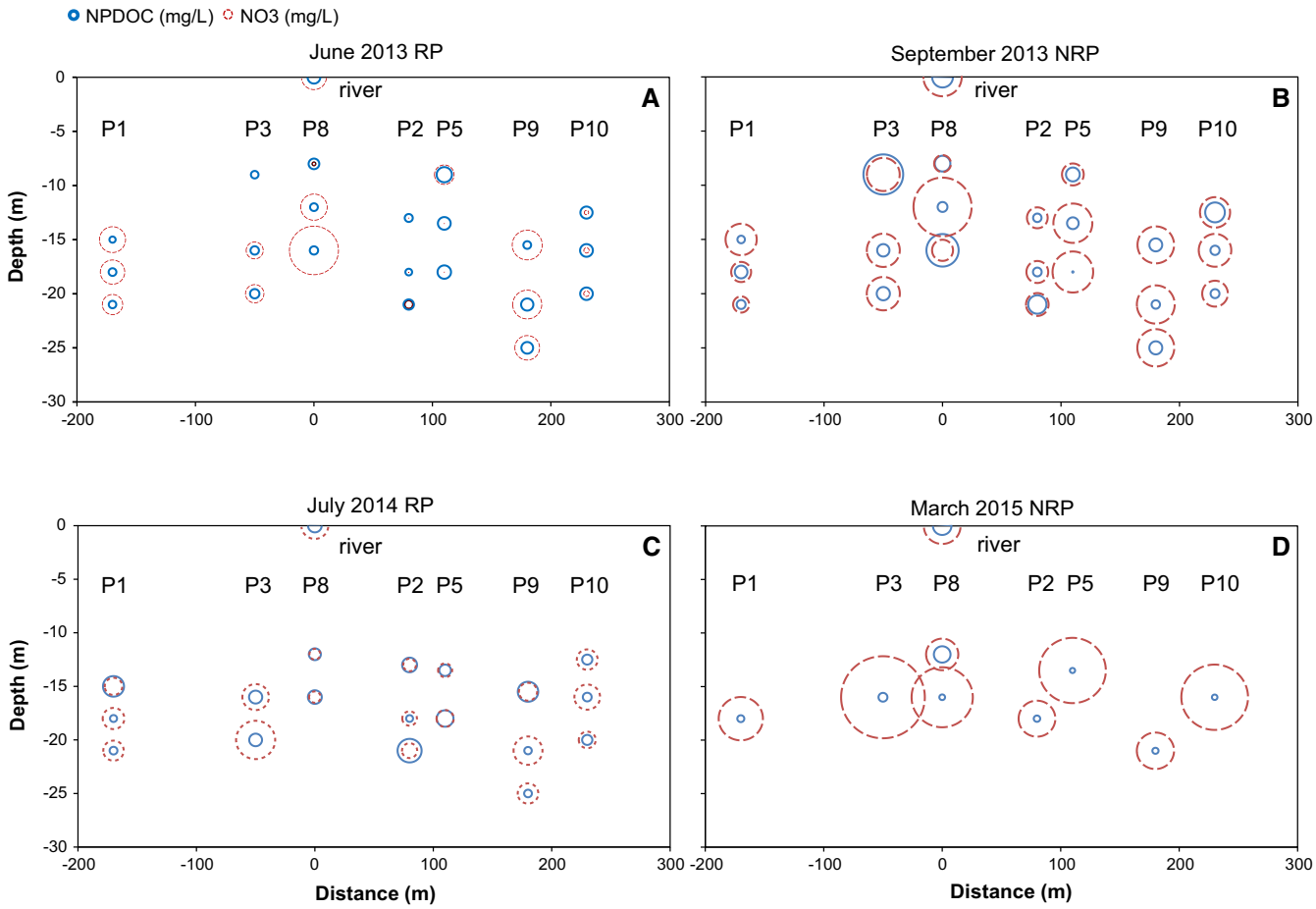

Fig. 6. Changes in the concentration of NPDOC and NO_3^- in depth-specific groundwater samples along the flow path under both RPs (a, c) and NRPs (b, d). Values for the Llobregat river samples are also shown. The size of the symbols is proportional to the corresponding concentration value. Concentrations ranged from 0.11 to 8.6 mg L^{-1} for NPDOC and from 0.01 to 19.4 mg L^{-1} for NO_3^-. Concentration values are given in the Supplementary Material (Table S3).

3.4. Denitrification during artificial recharge

Nitrate isotope composition was measured in a subset of these samples based on NO_3^- concentrations (Table S4). Fig. 7 shows the $\delta^{15}N_{NO3}$ and $\delta^{18}O_{NO3}$ values of dissolved nitrate at the piezometers, as well as the isotope composition of the main potential sources of nitrate: nitrate fertilizers, ammonium fertilizers, soil nitrate and animal manure or sewage (Vitòria et al., 2004; Kendall et al., 2007; Xue et al., 2009). The range of $\delta^{18}O$ of NO_3^- for ammonium fertilizers, soil nitrogen and manure/sewage plotted in Fig. 7 (+1.93‰ to + 3.13‰) was estimated according to Eq. (7) (Anderson and Hooper, 1983; Kendall et al., 2007), where $\delta^{18}O_{H2O}$ corresponds to the range measured in Sant Vicenç dels Horts groundwater samples and $\delta^{18}O_{O2}$ to atmospheric O_2 (+23.5‰ Horibe et al., 1973).

$$\delta^{18}O_{NO3} = \frac{2}{3}(\delta^{18}O_{H2O}) + \frac{1}{3}(\delta^{18}O_{O2}) \quad (7)$$

Native groundwater (P1) showed $\delta^{15}N$ and $\delta^{18}O$ values ranging from +13.0 to +17.5‰ and from +2.8 to +9.7‰, respectively. The nitrate isotope ratios of the samples from the piezometers located downstream of the pond ranged from +9.5 to +26.7‰ (averaging +18.4‰) for $\delta^{15}N$ and from +3.5 to +16.6‰ (averaging + 9.5‰) for $\delta^{18}O$ (Table S4). All samples presented isotope ratios compatible with those for soil organic nitrogen and sewage/manure. The mixed groundwater samples showed a positive correlation ($r^2 = 0.55$) between $\delta^{15}N_{NO3}$ and $\delta^{18}O_{NO3}$ and were aligned following a εN/εO ratio of 1.5 (Fig. 7), which is consistent with denitrification (Kendall et al., 2007). The εN/εO ratio reported in the literature for denitrification in groundwater ranges from 1.3 to 2.1 (Böttcher et al., 1990; Cey et al., 1999; Mengis et al., 1999; DeVito et al., 2000; Lehmann et al., 2003; Fukada et al., 2003).

Most samples collected during the RPs followed the denitrification trend, with higher $\delta^{15}N_{NO3}$ and $\delta^{18}O_{NO3}$ during the July 2014 sampling. During NRPs also a different behavior was observed in the two surveys, with lower isotopic values in March 2015 and high values in the September 2013 sampling. However, it should be noted that in both September 2013 and July 2014 samplings, high $\delta^{15}N$ and $\delta^{18}O$ values were also measured in river water. The high variability of NO_3^- contents in river water samples even on the same day (Table S5) could explain the particularly high isotope ratios measured in September 2013 and July 2014. Accordingly, Sine (2017) reported that NO_3^- isotopes values in a highly impacted river are not conservative, even when NO_3^- contents do not change. These authors studied the Grand River (south western Ontario, Canada), which receives high NO_3^- loading from point (urban WWTPs) and non-point sources (agricultural manure and fertilizer) and suggested that river metabolism influences rapid isotopic changes.

εN and εO values allow quantifying at field scale NO_3^- losses due to denitrification independently of dilution effects on NO_3^- concentrations (Mariotti et al., 1981; Böttcher et al., 1990; Fukada et al.,

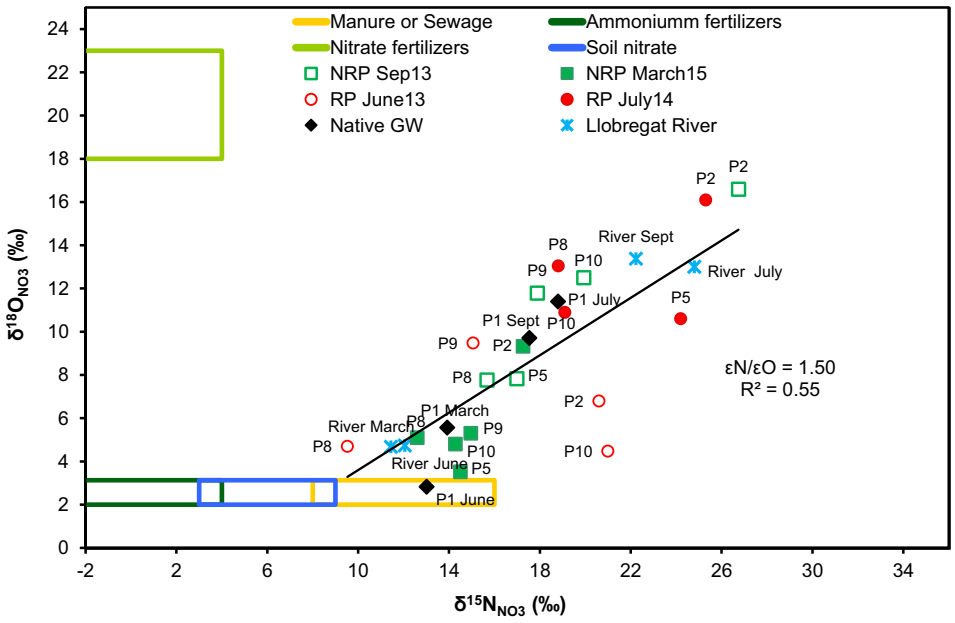

Fig. 7. $\delta^{15}N_{NO3}$ and $\delta^{18}O_{NO3}$ of dissolved NO_3^- in the collected samples, as well as the isotope composition of the main nitrate sources: fertilizers, soil nitrate and animal manure or sewage (Vitòria et al., 2004; Kendall et al., 2007; Xue et al., 2009).

2003; Otero et al., 2009; Torrentó et al., 2011). With the ε values obtained in laboratory experiments, the percentage of denitrification at the field scale can be calculated according to Eq. (8) using either εN or εO, or both.

$$\mathrm{DEN}(\%) = \left[1 - \frac{[NO_3]_{residual}}{[NO_3]_{initial}}\right] \times 100 = \left[1 - e^{\left(\frac{\delta(residual) - \delta(initial)}{\varepsilon}\right)}\right] \times 100 \quad (8)$$

The extent of denitrification enhanced by the MAR-PRL system was estimated for each sampling campaign. The isotope composition of the native groundwater (P1) for each campaign was used as the initial value, and the ε values were obtained from the batch experiments with the two-year-old PRL material (−10.4‰ for εN and −13.8‰ for εO, with an εN/εO ratio of 0.75) (Fig. 8).

This approximation shows that during both RPs, the NO_3^- reduction percentage was similar with a maximum value around 30% - 40%. Complete denitrification at some depths of P2 and P5 was observed in samples collected in June 2013 (Fig. 6), but isotopic values were not determined due to the low NO_3^- concentration. Denitrification was enhanced in the piezometers located closer to the infiltration pond (P2). In all campaigns, the isotope composition of P8.2 was very similar to that of P1, indicating that denitrification was not occurring. Since isotopes in samples at different depths were not determined, the cause of variations in NO_3^- concentration along depth at P8 could be either due to denitrification or other process (e.g., mixing). Comparing the two RP sampling campaigns, the June 2013 samples presented a slightly higher level of denitrification, most probably because the system was under almost continuous operation since January 2012 (except for 30 days in August 2012, 24 days in February-March 2013 and 5 days in April 2013). The MAR system was stopped from 22nd June to 1st July, 10 days before the July 2014 sampling campaign. The longer operational period before the June 2013 campaign could have induced a well-developed denitrifying microbial community, with the bacteria being more concentrated in the areas receiving more recharge water, such as P2 and P5. Li et al. (2013), simulating the infiltration zone of a MAR system, showed that microbial communities reached stability after 3–4 months of operation.

During NRPs, the percentage of denitrification was very low (less than 20%) in all the samples, except those from P2 (30–60%), which was one of the piezometers most affected by recharge water (Valhondo et al., 2014) (Fig. 8). All the samples collected in March 2015, including P2, showed the lowest percentage of denitrification among all the sampling campaigns. The September 2013 campaign was performed after a year of almost continuous recharge (Fig. 2) followed by less than two months of non-recharge, whereas the March 2015 campaign was undertaken after almost four months of non-recharge. Differences in the percentage of denitrification among the P2 samples collected from both NRPs indicate that the bacteria grow during RPs were still denitrifying even when the MAR pond was under non-recharge, but became less active with time in the absence of a carbon source (Rodríguez-Escales et al., 2016a,b).

Results indicate that time of operation is a key issue to enhance denitrification in the MAR-PRL system. However, in practical terms it is difficult to accomplish due to day by day management issues (low quality river water, maintenance, etc.). In this regard, chaotic advection could be a good technology to keep high denitrification rates as well as other pollutant degradation in both RPs and NRPs as stated in Rodríguez-Escales et al. (2017).

3.5. Additional isotope data

On the one hand, the redox conditions induced in a MAR-PRL system determine the degradation of different contaminants. In the case of mixtures of emerging organic contaminants, for example, increasing the variability of redox conditions is crucial since the individual degradation of these compounds depends on specific redox conditions (e.g. Barbieri et al., 2011; Liu et al., 2013). Characterizing the redox conditions achieved in the studied MAR-PRL system is thus critical.

Monitoring the redox sensitive indicators and the nitrate isotope data suggested that the organic matter released by the PRL was promoting reducing conditions to varying extents, at least to nitrate reduction conditions, and probably iron reductions conditions occasionally in P5. The isotope composition of SO_4^{2-} ($\delta^{34}S_{SO4}$ and $\delta^{18}O_{SO4}$) was analyzed to assess the occurrence of sulfate-

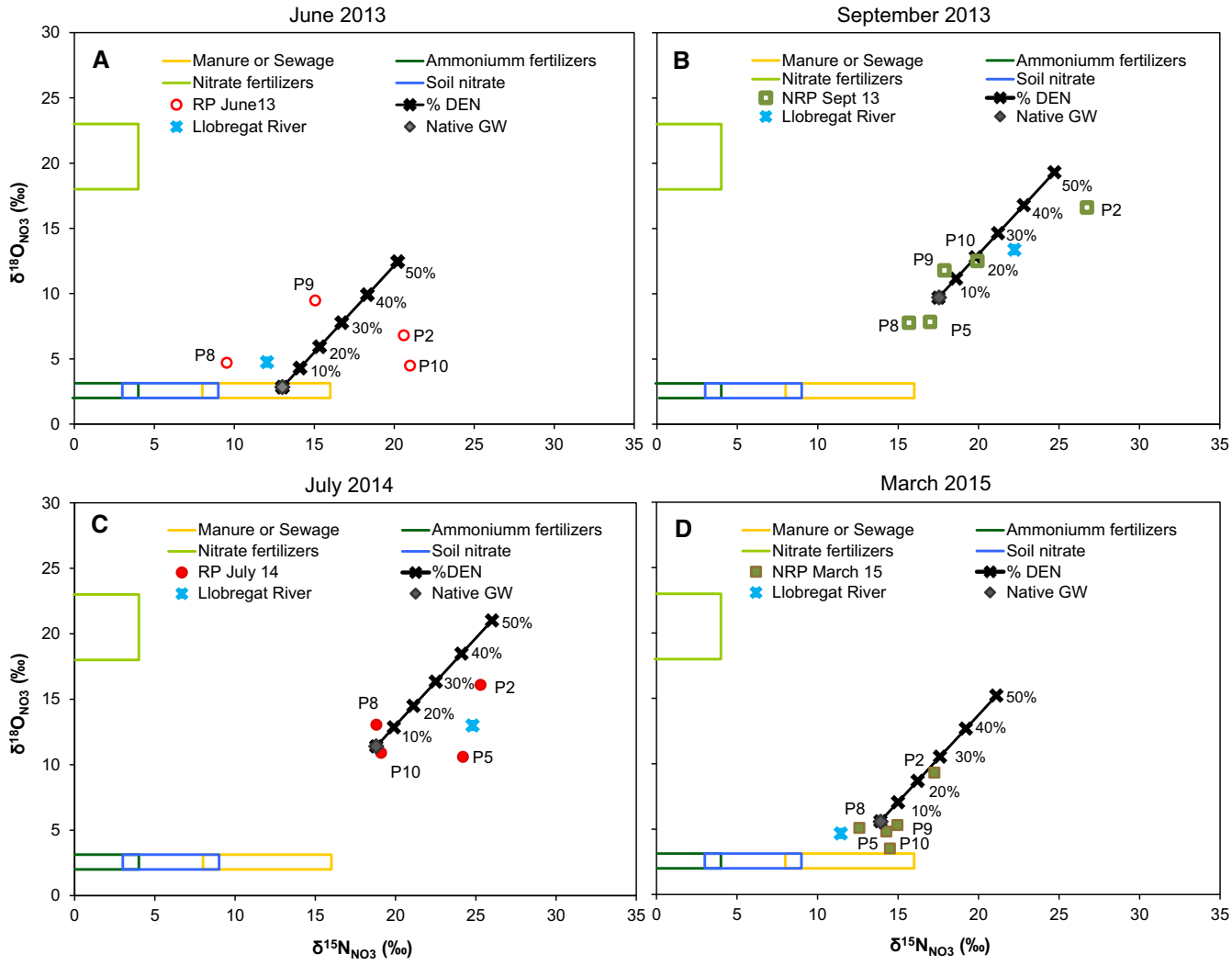

Fig. 8. Estimation of the extent of NO_3^- attenuation in all the sampling campaigns, using ε values obtained from the batch experiments with two-year-old PRL material. The isotope composition of the native groundwater was used as the initial value.

reducing conditions. Sulfate reduction should produce a decrease in the SO_4^{2-} concentration an increase in the $\delta^{34}S_{SO4}$ values of the dissolved SO_4^{2-}. The isotope composition of the dissolved SO_4^{2-} in mixed groundwater samples was only analyzed for the June 2013 and September 2013 campaigns. Values ranged from +6.7 to +10.6‰ for $\delta^{34}S$ and from +9.0 to +11.1‰ for $\delta^{18}O$ (Fig. 9). Similar values were obtained for the river water and native groundwater samples. Most of the mixed groundwater samples gave values within the range obtained for sewage (Otero et al., 2008) (Fig. 9), indicating that the vast majority of SO_4^{2-} came from sewage, which is consistent with the conclusions drawn from the NO_3^- isotope results regarding potential NO_3^- sources.

The narrow range of the $\delta^{34}S_{SO4}$ and $\delta^{18}O_{SO4}$ values obtained suggests a lack of SO_4^{2-} reduction. It can thus be concluded that the NPDOC released by the reactive layer produces variable redox conditions in the saturated zone along the flow path, leading mainly to the reduction of NO_3^-, as well as iron under certain conditions, but not of SO_4^{2-}. Results indicate that time of operation is a key issue to modify redox conditions as well as pollutant degradation in the MAR-PRL system.

On the other hand, the isotopic composition of dissolved inorganic carbon $\delta^{13}C_{HCO3}$ can provide information about the denitrification reaction (Aravena and Robertson, 1998). However, in the studied site, due to the aquifer lithology, groundwater contained high concentrations of bicarbonate (median value of 325 ± 25 mg L^{-1} in P1 for the four sampling campaigns) that could buffer any change in the $\delta^{13}C_{HCO3}$ isotope ratio linked to denitrification. The $\delta^{13}C_{HCO3}$ values in P1 samples (native groundwater) averaged −13.2 ± 1‰, which is in agreement with the known range of $\delta^{13}C_{HCO3}$ for groundwater (−16‰ to −11‰ Vogel and Ehhalt, 1963). Mixed groundwater samples displayed $\delta^{13}C_{HCO3}$ values close to that of P1 samples (between −13.8 and −12.0‰, with a median value of −12.7‰), except three samples collected in the June 2013 campaign (RP) (that had values ranging from −11.1 to −9.9‰) (Fig. 10). As expected, the role of organic matter oxidation in the observed denitrification processes was not evident from the $\delta^{13}C_{HCO3}$ data due to the buffering effect of the bicarbonate.

4. Conclusions

We evaluated the feasibility of a multi-isotope approach for assessing the efficacy of the MAR-PRL system of Sant Vicenç dels Horts in promoting denitrification in the groundwater below the infiltration pond. Similarities in the hydrochemical data (except for NO_3^- contents, which decreased during recharge periods in mixed groundwater) of river water, native groundwater and mixed groundwater demonstrated a unique recharge flow system.

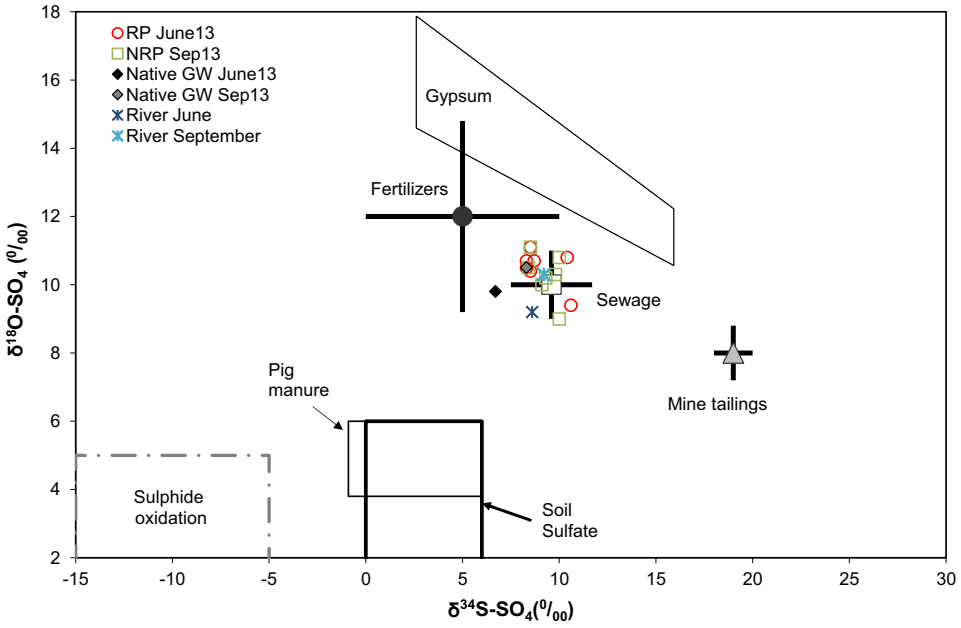

Fig. 9. $\delta^{18}O_{SO4}$ vs $\delta^{34}S_{SO4}$ for river, native groundwater and mixed groundwater samples collected in June 2013 and September 2013. The isotope composition of potential SO_4^{2-} sources is also shown. Values for SO_4^{2-} derived from sulfide oxidation are from Pierre et al. (1994) for disseminated pyrite in anoxic Tertiary marls that outcrop in the Llobregat River basin. Values for pig manure are taken from Otero et al. (2008) and Cravotta (1997). Soil SO_4^{2-} data are from Krouse and Mayer (2000) and fertilizer data from Vitòria et al. (2004). Gypsum values correspond to local gypsum outcrops (Utrilla et al., 1992). Sewage data are from the Igualada sewage plant (Otero et al., 2008).

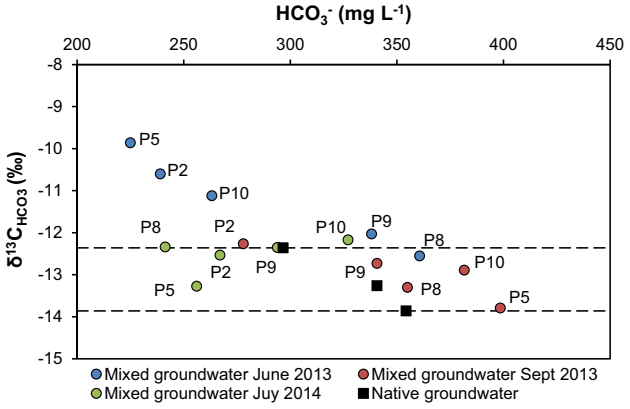

Fig. 10. $\delta^{13}C_{HCO3}$ vs HCO_3^- concentration for native and mixed groundwater samples collected in June 2013, September 2013 and July 2014. The dotted lines represent the range of the $\delta^{13}C_{HCO3}$ values for the native groundwater samples.

Changes in the redox indicators with depth and along the flow path during recharge and non-recharge periods confirmed that the reactive layer was still releasing NPDOC five years after installation. NO_3^- concentrations decreased during recharge periods especially in the piezometers closest to the infiltration pond, while aqueous Fe concentrations increased in the piezometers with lower NO_3^- concentrations, however, SO_4^{2-} reduction was not observed.

Isotope data revealed that denitrification mainly occurred in the area under the infiltration pond. The piezometers closest to the MAR-PRL, P2 and P5, showed higher levels of denitrification than the other piezometers. Importantly, denitrification was enhanced by a more continuous recharge of the MAR-PRL system, probably because microbial communities become stable after 3–4 months of continuous operation. Although a more detailed field sampling survey is needed to determine the real extent of denitrification at the field scale, the results of this study show the usefulness of a multi-isotope approach in identifying denitrification in MAR-PRL systems.

Acknowledgements

This study was funded by the projects REMEDIATION [ref. CGL2014-57215-C4-1-R] and ISOTEC [CGL2017-87216-C4-1-R], financed by the Spanish Ministry of Economy (Agencia Estatal de Investigación/Fondo Europeo de Desarrollo Regional/Unión Europea, AEI/FEDER, EU), the project MAG [Catalan Government, ref. 2014SGR-1456] and the European Union projects WADIS-MAR [European Commission, ref. ENPI/2011/280-008] and MARSOL [European Commission, FP7-ENV-2013-WATER-INNO-DEMO]. We thank the editor and three anonymous reviewers for comments that improved the quality of the manuscript.

Appendix A. Supplementary data

Supplementary data associated with this article can be found, in the online version, at https://doi.org/10.1016/j.jhydrol.2018.03.044.

References

Anderson, K.K., Hooper, A.B., 1983. O_2 and H_2O are each the source of O in NO_2 produced from NH_3 by Nitrosomas ^{15}N-NMR evidence. FEBS Lett. 64, 236–240.
Aravena, R., Robertson, W.D., 1998. Use of multiple isotope tracers to evaluate denitrification in ground water: study of nitrate from a large-flux septic system plume. Ground Water 36, 975–982.
Barahona-Palomo, M., Barbieri, M., Fernàndez-Garcia, D., Pedretti, D., Sanchez-Vila, X., Valhondo, C., Queralt, E., Massana, J., Hernández, M., Tobella, J., 2011. Caracterització del Sistema de Recàrrega de Sant Vicenç dels Horts: Projecte RASA, Informe Fase 2. CUADLL, Barcelona.
Barbieri, M., Carrera, J., Sanchez-Vila, X., Ayora, C., Cama, J., Köck-Schulmeyer, M., López de Alda, M., Barceló, D., Tobella Brunet, J., Hernández García, M., 2011. Microcosm experiments to control anaerobic redox conditions when studying the fate of organic micropollutants in aquifer material. J. Contam. Hydrol. 126 (3–4), 330–345.
Bekele, E., Toze, S., Patterson, B., Higginson, S., 2011. Managed aquifer recharge of treated wastewater: water quality changes resulting from infiltration through the vadose zone. Water Res. 45 (17), 5764–5772.

Böttcher, J., Strebel, O., Voerkelius, S., Schmidt, H.L., 1990. Using isotope fractionation of nitrate-nitrogen and nitrate-oxigen for evaluation of microbial denitrification in sandy aquifer. J. Hydrol. 114, 413–424.
Bouwer, H., 2002. Artificial recharge of groundwater: hydrogeology and engineering. Hydrogeol. J. 10, 121–142.
Carrey, R., Otero, N., Soler, A., Gomez-Alday, J.J., Ayora, C., 2013. The role of Lower Cretaceous sediments in groundwater nitrate attenuation in central Spain: column experiments. Appl. Geochem. 32, 142–152.
Cey, E.E., Rudolph, D.L., Aravena, R., Parkin, G., 1999. Role of the riparian zone in controllingthe distribution and fate of agricultural nitrogen near a small stream in southern Ontario. J. Contam. Hydrol. 37, 45–67.
Clark, I.D., Fritz, P., 1997. Environmental Isotopes in Hydrogeology. Lewis Publishers, New York, pp. 352.
Cravotta, C.A., (1997). Use of stable isotopes of carbon, nitrogen and Sulphur to identify sources of nitrogen in surface waters in the lower Susquehanna River Basin, Pennsylvania. U.S. Geological Survey Water-Supply Paper. 2497.
Devito, K.J., Fitzgerald, D., Hill, A.R., Aravena, R., 2000. Nitrate dynamics in relation to lithology and hydrologic flow path in a river riparian zone. J. Environ. Qual. 29, 1075–1084.
Díaz-Cruz, M.S., Barceló, D., 2008. Trace organic chemicals contamination in ground water recharge. Chemosphere 72 (3), 333–342.
Dillon, P.J., 2004. Future management of aquifer recharge. Hydro. Geol. J. 13 (1), 313–316.
Dillon, P., Pavelic, P., Toze, S., Rinck-Pfeiffer, S., Martin, R., Knapton, A., Pidsley, D., 2006. Role of aquifer storage in water reuse. Desalination 188 (1–3), 123–134.
Dogramaci, S.S., Herczeg, A.L., Schi, S.L., Bone, Y., 2001. Controls on δ34S and δ18O of dissolved sulfate in aquifers of the Murray Basin, Australia and their use as indicators of flow processes. Appl. Geochem. 16, 475–488.
ENSAT (Enhancement of Soil Aquifer Treatment), 2012. Modelo hidrogeológico: Modelo conceptual de flujo en el sistema de recarga de Sant Vicenç dels Horts. ENSAT, Barcelona.
Fox, P. et al., 2006. Advances in Soil Aquifer Treatment Research for Sustainable Water Reuse. Denver, Awwa Research Foundation, p. 200.
Fukada, T., Hiscock, K., Dennis, P.F., Grischek, T., 2003. A dual isotope approach to identify denitrifaction in groundwater at river-bank infiltration site. Water Res. 37, 3070–3078.
Gibert, O., Pomierny, S., Rowe, I., Kalin, R.M., 2008. Selection of organic substrates as potential reactive materials for use in a denitrification permeable reactive barrier (PRB). Bioresour. Technol. 99, 7587–7596.
Grau-Martínez, A., Torrentó, C., Carrey, R., Rodríguez-Escales, P., Domènech, C., Ghiglieri, G., Soler, A., Otero, N., 2017. Feasibility of two low-cost organic substrates for inducing denitrification in artificial recharge ponds: batch and flow-through experiments. J. Contam. Hydrol. 198, 48–58.
Heberer, T., Mechlinski, A., Franck, B., Knappe, A., Massmann, G., Pekdeger, A., Fritz, B., 2004. Field studies on the fate and transport of pharmaceutical residues in bank filtration. Ground Water Monit. Remediat. 24 (2), 70–77.
Horibe, Y., Shigehara, K., Takakuwa, Y., 1973. Isotope separation factors of carbon dioxide water system and isotopic composition of atmospheric oxygen. J. Geophys. Res. 78, 2625–2629.
IAEA/WMO (2017). Global Network of Isotopes in Precipitation. The GNIP Database. Accessible at: http://www.iaea.org/water
Iribar, V., Carrera, J., Custodio, E., Medina, A., 1997. Inverse modelling of seawater intrusion in the Llobregat delta deep aquifer. J. Hydrol. 198 (1–4), 226–244.
Kendall, C., Elliott, E.M., Wankel, S.D., 2007. Tracing anthropogenic inputs of nitrogen to ecosystems Chapter 12. In: Michener, R.H., Lajtha, K. (Eds.), Stable isotopes in Ecology and Environmental Science. second ed. Blackwell Publishing, pp. 375–449.
Knöller, K., Vogt, C., Haupt, M., Feisthauer, S., Richnow, H.H., 2011. Experimental investigation of nitrogen and oxygen isotope fractionation in nitrate and nitrite during denitrification. Biogeochemistry 103, 371–384.
Knowles, R., 1982. Denitrification. Microbiol. Rev. 46, 43–70.
Köck-Schulmeyer, M., Ginebreda, A., Postigo, C., López-Serna, R., Pérez, S., Brix, R., Llorca, M., Alda, MLd, Petrovic, M., Munné, A., Tirapu, L., Barceló, D., 2011. Wastewater reuse in Mediterranean semi-arid areas: the impact of discharges of tertiary treated sewage on the load of polar micro pollutants in the Llobregat River (NE Spain). Chemosphere 82 (5), 670–678.
Krouse, H.R., Mayer, B., 2000. Sulphur and oxygen isotopes in sulphate. In: Cook, P. G., Hercseg, A.L. (Eds.), Environmnetal Tracers in Subsurface Hydrology. Kluwer Academic Press, Boston, pp. 195–231.
Lasagna, M., De Luca, D.A., 2016. The use of multilevel sampling techniques for determining shallow aquifer nitrate profiles. Environ. Sci. Pollut. Res. 23 (20), 20431–20448.
Lehmann, M.F., Reichert, P., Bernasconi, S.M., Barbieri, A., McKenzie, J.A., 2003. Modelling nitrogen and oxygen isotope fractionation during denitrification in a lacustrine redox-transition zone. Geochim. Cosmochim. Acta 67, 2529–2542.
Li, D., Alidina, M., Ouf, M., Sharp, J.O., Saikaly, P., Drewes, J.E., 2013. Microbial community evolution during simulated managed aquifer recharge in response to different biodegradable dissolved organic carbon (BDOC) concentrations. Water Res. 47 (7), 2421–2430.
Liu, Y.-S., Ying, G.-G., Shareef, A., Kookana, R.S., 2013. Biodegradation of three selected benzotriazoles in aquifer materials under aerobic and anaerobic conditions. J. Contam. Hydrol. 151, 131–139.
Maeng, S.K., Sharma, S.K., Lekkerkerker-Teunissen, K., Amy, G.L., 2011. Occurrence and fate of bulk organic matter and pharmaceutically active compounds in managed aquifer recharge: a review. Water Res. 45 (10), 3015–3033.
Mariotti, A., Germon, J.C., Hubert, P., Kaiser, P., Letolle, R., Tardieux, P., 1981. Experimental determination of nitrogen kinetic isotope fractionation: some principles, illustration for the denitrification and nitrification processes. Plant Soil 62, 413–430.
Mariotti, A., Landreau, A., Simon, B., 1988. 15N isotope biogeochemistry and natural denitrification process in groundwater application to the chalk aquifer of northern France. Geochim. Cosmochim. Acta 52, 1869–1878.
Massmann, G., Greskowiak, J., Dunnbier, U., Zuehlke, S., Knappe, A., Pekdeger, A., 2006. The impact of variable temperatures on the redox conditions and the behaviour of pharmaceutical residues during artificial recharge. J. Hydrol. 328 (1–2), 141–156.
McIlvin, M.R., Altabet, M.A., 2005. Chemical conversion of nitrate and nitrite to nitrous oxide for nitrogen and oxygen isotopic analysis in freshwater and seawater. Anal. Chem. 77, 5589–5595.
Menció, A., Mas-Pla, J., Soler, A., Regàs, O., Boy-Roure, M., Puig, R., Bach, J., Domènech, C., Folch, A., Zamarona, M., Brusi, D., 2016. Nitrate pollution of groundwater; all right, but nothing else? Sci. Total Environ. 539C, 241–251.
Mengis, M., Schif, S.L., Harris, M., English, M.C., Aravena, R., Elgood, R.J., MacLean, A., 1999. Multiple geochemical and isotopic approaches for assessing ground water NO_3 elimination in a riparian zone. Ground Water 37, 448–457.
Miller, J.H., Ela, W.P., Lansey, K.E., Chipello, P.L., Arnold, R.G., 2006. Nitrogen transformations during soil-aquifer treatment of wastewater effluent-oxygen effects in field studies. J. Environ. Eng. Asce 132 (10), 1298–1306.
Otero, N., Soler, A., Canals, A., 2008. Controls of δ34S and δ18O in dissolved sulphate: learning from a detailed survey in the Llobregat River (Spain). Appl. Geochm. 23, 1166–1185.
Otero, N., Torrentó, C., Soler, A., Menció, A., Mas-Pla, J., 2009. Monitoring groundwater nitrate attenuation in a regional system coupling hydrogeology with multi-isotopic methods: the case of Plana de Vic (Osona, Spain). Agric. Ecosyst. Environ. 133 (1–2), 103–113.
Pauwels, H., Foucher, J.C., Kloppmann, W., 2000. Denitrification and mixing in a schist aquifer: influence on water chemistry and isotopes. Chem. Geol. 168, 307–324.
Pauwels, H., Ayraud-Vergnaud, V., Aquilina, L., Molénat, J., 2010. The fate of nitrogen and sulfur in hard-rock aquifers as shown by sulfate-isotope tracing. Appl. Geochem. 25, 105–115.
Pauwels, H., Kloppmann, W., Foucher, J.C., Martelat, A., Fritsche, V., 1998. Field tracer test for denitrification in a pyrite-bearing schist aquifer. Appl. Geochem. 13, 284–292.
Patterson, B., Shackleton, M., Furness, A., Bekele, E., Pearce, J., Linge, K., Busetti, F., Spadek, T., Toze, S., 2011. Behaviour and fate on nine recycled water trace organics during managed aquifer recharge in aerobic aquifer. J. Contam. Hydrol. 122 (1–4), 53–62.
Pierre, C., Taberner, C., Urquiola, M.M., Pueyo, J.J., 1994. Sulphur and oxygen isotope composition of sulphates in hypersaline environments, as markers of redox depositional versus diagenetic changes. Mineral Mag. 58, 724–725.
Quevauviller, P.P., Fouillac, A.M., Grath, J., Ward, R., 2009. Groundwater Monitoring. Wiley, New York.
Rodríguez-Escales, P., Folch, A., van Breukelen, B.M., Vidal-Gavilan, G., Sanchez-Vila, X., 2016a. Modeling long term enhanced in situ biodenitrification and induced heterogeneity in column experiments under different feeding strategies. J. Hydrol. 538, 127–137.
Rodríguez-Escales, P., Folch, A., Vidal-Gavilan, G., van Breukelen, B.M., 2016b. Modeling biogeochemical processes and isotope fractionation of enhanced in situ biodenitrification in a fractured aquifer. Chem. Geol. 425, 52–64.
Rodríguez-Escales, P., Fernàndez-Garcia, D., Drechsel, J., Folch, A., Sanchez-Vila, X., 2017. Improving degradation of emerging organic compounds by applying chaotic advection in Managed Aquifer Recharge in randomly heterogeneous porous media. Water Resour. Res. 53 (5), 4376–4392.
Ryabenko, E., Altabet, M.A., Wallace, D.W.R., 2009. Effect of chloride on the chemical conversion of nitrate to nitrous oxide for δ15N analysis. Limnol. Oceanogr. 7, 545–552.
Schmidt, C.M., Fisher, A.T., Racz, A., Wheat, C.G., Los Huertos, M., Lockwood, B., 2012. Rapid nutrient load reduction during infiltration of managed aquifer recharge in an agricultural groundwater basin: Pajaro Valley, California. Hydrol. Process. 26, 2235–2247.
Schmidt, C.S., Richardson, D.J., Baggs, E.M., 2011. Constraining the conditions conducive to dissimilatory nitrate reduction to ammonium in temperate arable soils. Soil Biol. Biochem. 43, 1607–1611.
Sine S.E., (2017) Paradigm shift: does river metabolism mask the isotopic signal of nitrate sources? MSc. Thesis. University of Waterloo. pp. 118.
Solà, V., (2009). Actualització hidroquímica I isotòpica dels aqüífers del Baix Llobregat per a la determinació de la intrusió marina, amb consideració de la isotopia del sulfat. Tesi de Màster en Hidrologia Subterrània.
Sprenger, C., Hartog, N., Hernández, M., Vilanova, E., Grützmacher, G., Scheibler, F., Hannappel, S., 2017. Inventory of managed aquifer recharge sites in Europe: historical development, current situation and perspectives. Hydrogeol. J. 25, 1909–1922.
Torrentó, C., Urmeneta, J., Otero, N., Soler, A., Viñas, M., Cama, J., 2011. Enhanced denitrification in groundwater and sediments from a nitrate-contaminated aquifer after addition of pyrite. Chem. Geol. 287, 90–101.
Utrilla, R., Pierre, C., Orti, F., Pueyo, J.J., 1992. Oxygen and sulphur isotope compositions as indicators of the origin of Mesozoic and Cenozoic evaporites from Spain. Chem. Geol. Isot. Geosci. 102, 229–244.
Valhondo, C., Carrera, J., Ayora, C., Barbieri, M., Noedler, K., Licha, T., Huerta, M., 2014. Behavior of nine selected emerging trace organic contaminants in an

artificial recharge system supplemented with a reactive barrier. Environ. Sci. Pollut. R. 21, 11832–11843.
Valhondo, C., Carrera, J., Ayora, Tubau, I., Martinez-Landa, L., Nödler, K., Licha, T., 2015. Characterizing redox conditions and monitoring attenuation of selected pharmaceuticals during artificial recharge through a reactive layer. Sci. Total Environ. 512–513, 240–250.
Valhondo, C., Martinez-Landa, L., Carrera, J., Hidalgo, J.J., Tubau, I., De Pourcq, K., Grau-Martínez, A., Ayora, C., 2016. Tracer test modeling for local scale residence time distribution characterization in an artificial recharge site. Hydrol. Earth Syst. Sci. 20, 4209–4221.
Valhondo, C., Martinez-Landa, L., Carrera, J., Ayora, c., Nödler, K., Licha, T., 2018. Evaluation of EOC removal processes during artificial recharge through a reactive barrier. Sci. Total Environ. 612, 985–994.
Vanderzalm, J., Salle, C.L.G.L., Dillon, P., 2006. Fate of organic matter during aquifer storage and recovery (ASR) of reclaimed water in a carbonate aquifer. Appl. Geochem. 21 (7), 1204–1215.
Vàzquez-Suñé, E., Capino, B., Abarca, E., Carrera, J., 2007. Estimation of recharge from floods in disconnected stream-aquifer systems. Ground Water 45 (5), 579–589.
Vitòria, L., Otero, N., Canals, A., Soler, A., 2004. Fertilizer characterization: isotopic data (N, S, O, C and Sr). Environ. Sci. Technol. 38, 3254–3262.
Vogel, J.C., Ehhalt, D.H., 1963. The use of carbon isotopes in groundwater studies. In: Radioisotopes in Hydrology. International Atomic Energy Agency, Vienna, pp. 338–396.
Xue, D., Botte, J., De Baets, B., Accoe, F., Nestler, A., Taylor, P., Van Cleemput, O., Berglund, M., Boeckkx, P., 2009. Present limitations and future prospects of stable isotopes methods for nitrate source identification in surface and groundwater. Water Res. 43, 1159–1170.